Developing an induced pluripotent stem cell model of pulmonary arterial hypertension to understand the contribution of *BMPR2* mutations to disease-associated phenotypes in smooth muscle cells

Fedir Kiskin

July 2018

St Catharine's College Cambridge

This dissertation is submitted for the degree of Doctor of Philosophy

Fedir Kiskin

Developing an induced pluripotent stem cell model of pulmonary arterial hypertension to understand the contribution of *BMPR2* mutations to disease-associated phenotypes in smooth muscle cells

Mutations in the gene encoding the bone morphogenetic protein type 2 receptor (*BMPR2*) are the most common genetic cause of heritable pulmonary arterial hypertension (PAH). However, given the reduced penetrance of *BMPR2* mutations in affected families, a major outstanding question is the identity of additional factors or pathways that are responsible for the manifestation of clinical disease. Furthermore, limited human tissue is available for study and usually only from patients with end-stage disease, making it difficult to understand how PAH is established and progresses. Alternative human models of PAH are therefore required.

This thesis describes the characterisation of the first human iPSC-derived smooth muscle cell (iPSC-SMC) model of PAH and elucidates the role of *BMPR2* deficiency in establishing PAH-associated phenotypes in iPSC-derived SMCs. To achieve this, I used CRISPR-Cas9 gene editing to generate wild-type and *BMPR2*$^{+/-}$ iPSC lines with isogenic backgrounds which were subsequently differentiated into lineage-specific iPSC-SMCs that displayed a gene expression profile and responses to BMP signalling akin to those present in distal pulmonary artery smooth muscle cells (PASMCs).

Using these cells, I found that the introduction of a single *BMPR2* mutation in iPSC-SMCs was sufficient to recapitulate the pro-proliferative and anti-apoptotic phenotype of patient-derived *BMPR2*$^{+/-}$ PASMCs. However, acquisition of the mitochondrial hyperpolarisation phenotype was enhanced by inflammatory signalling and required an interaction between *BMPR2* mutations and environmental stimuli provided by exposure to serum over time. Furthermore, I showed that *BMPR2*$^{+/-}$ iPSC-SMCs had an altered differentiation state and were less contractile compared to wild-type iPSC-SMCs, phenotypes which have not been observed previously in PAH-derived PASMCs. Finally, RNA sequencing analysis identified genes that were differentially expressed between wild-type and *BMPR2*$^{+/-}$ iPSC-SMCs and may hence provide further insights into PAH pathobiology.

The iPSC-SMC model described in this study will be useful for identifying additional factors involved in disease penetrance and for validating therapeutic approaches that target *BMPR2*.

Declaration

I hereby declare that this dissertation is the result of my own work and includes nothing which is the outcome of work done in collaboration except as declared in the Preface and specified in the text.

I also declare that it is not substantially the same as any that I have submitted, or, is being concurrently submitted for a degree or diploma or other qualification at the University of Cambridge or any other University or similar institution except as declared in the Preface and specified in the text. I further state that no substantial part of my dissertation has already been submitted, or, is being concurrently submitted for any such degree, diploma or other qualification at the University of Cambridge or any other University or similar institution except as declared in the Preface and specified in the text.

I confirm that it does not exceed the prescribed word limit as specified by the Clinical Medicine and Clinical Veterinary Medicine Degree Committee.

Fedir Kiskin

Acknowledgements

First and foremost, I would like to thank my primary supervisor Dr Amer 'Moo' Rana for supervising this PhD project and for providing me with help, support, advice and motivation throughout my time in the lab. A great big thank you also goes to Professor Nicholas Morrell who co-supervised this project and provided further help and support. It has truly been a great pleasure to work with you both and I am going to miss my time in the Rana/Morrell lab!

I would also like to thank my fellow friends and colleagues Baraa Kwieder, Dr C-Hong Chang, Christopher J.Z. Huang and Kim Lachani for helping out with extensive stem cell maintenance, looking after my precious cells during rotating weekends, helping out when a large experiment required an extra pair of hands, providing advice and, most importantly, for creating a fun, friendly and supportive environment to work in. I would also like to thank Dr Mattia Frontini and Dr Frances Burden from the Department of Haematology for generating RNA-Seq libraries and sequencing my iPSC-SMC samples, as well as Dr Stefan Gräf, Dr Matthias Haimel and Dr Marta Bleda for analysing the raw RNA-Seq data.

A special thank you also goes to Dr Felipe Serrano and Dr Sanjay Sinha for performing microarray SMC gene expression analysis, and to Dr Ian Horan for efficiently ordering the countless laboratory reagents required for this project and for making sure that the reagents were delivered on time. Thank you also to Dr Elizabet Ferrer, Dr Benjamin Dunmore, Dr Paul Upton, Dr Mark Toshner, Dr Xudong Yang, Ms Sarah Chantler, and everyone else in the Morrell Group for their help and support throughout this project. I would also like to thank the staff at the NIHR Cambridge BRC Cell Phenotyping Hub for assistance with flow cytometry.

In addition, I am also extremely grateful to Professor Martin Bennett, Dr Anthony Davenport and Ms Suzanne Diston for accepting me on the British Heart Foundation (BHF) 4-Year PhD Programme here at Cambridge and overseeing my progress throughout the programme.

This project was generously supported by BHF PhD Studentship grant FS/13/51/30636, with work in the lab also being funded by BHF project grant PG/14/31/30786 and programme grant RG/13/4/30107, the Dinosaur Trust, Fondation Leducq, the Medical Research Council, Pulmonary Hypertension Association UK and Fight for Sight and the Robert McAlpine Foundation.

I would also like to thank my PhD thesis examiners for dedicating their valuable time to examine this thesis and for their helpful comments and feedback during my *viva voce*. I am also grateful to friends and staff at St Catharine's College Cambridge which has become my 'second home' and provided me with lasting memories, great food, a wonderful library to work in, and also supported me through a travel grant to help cover the costs associated with attending an international scientific conference in the USA. I would also like to acknowledge Selwyn College Cambridge for providing me with delicious food during Christmas Formals and during college meetings with Dr Rana!

Finally, I would like to thank my parents Nikolai and Natalia, my brother Ivan and my girlfriend Yuze for always being there for me and for their unwavering love and support.

List of Abbreviations

2-DG – 2-deoxyglucose

5-HTT – 5-hydroxytryptamine (serotonin) transporter

ACTB – beta-actin

ActR-IIA – activin receptor type IIA

AEC – alveolar epithelial cell

ALK – activin receptor-like kinase

ANOVA – analysis of variance

APC – adenomatous polyposis coli

AQP1 – aquaporin 1

ATP13A3 – adenylpyrophosphatase (ATPase) 13A3

AV – arteriovenous

AXIN2 – Axin 2

BAMBI – BMP and activin membrane bound inhibitor

BHF – British Heart Foundation

BIRC3 – baculoviral IAP repeat containing 3

BK – CDM-BSA/KSR feeder-free iPSC culture medium

BLAST – Basic Local Alignment Search Tool

BMP – bone morphogenetic protein

BMPER – BMP binding endothelial regulator

BMPR-1A – bone morphogenetic protein receptor type 1A

BMPR-1B – bone morphogenetic protein receptor type 1B

BMPR2 – bone morphogenetic protein receptor 2

BOEC – blood outgrowth endothelial cell

bp – base pair

BRC – Biomedical Research Centre

BSA – bovine serum albumin

C-Myc – Myc proto-oncogene, basic helix-loop-helix transcription factor

cAMP – cyclic adenosine monophosphate

CAV1 – caveolin 1

CBP – cAMP-response element binding protein (CREB-binding protein)

CD – cluster of differentiation

CDM – Chemically-defined medium

cDNA – complementary DNA

CES1 – carboxylesterase 1

cGMP – cyclic guanosine monophosphate

CLC – cardiotrophin-like cytokine

CLF1 – cytokine-like factor 1

CMV – cytomegalovirus

CNV – copy number variation

CO_2 – carbon dioxide

COMPERA – Comparative, Prospective Registry of Newly Initiated Therapies for Pulmonary Hypertension

CPP – cardiopulmonary progenitor

CRISPR-Cas9 – clustered regularly interspaced short palindromic repeats CRISPR-associated protein 9

CRLF1 – cytokine receptor like factor 1

C_t – cycle threshold

CTEPH – chronic thromboembolic pulmonary hypertension

DAN – differential screening-selected gene in neuroblastoma

DAPI – 4′,6-diamidino-2-phenylindole

DCA – dichloroacetate

DLL – Delta-like canonical Notch ligand

DMEM – Dulbecco's Modified Eagle Medium

DNA – deoxyribonucleic acid

DTA – diphtheria toxin A

DUOX2 – dual oxidase 2

Dvl – Dishevelled

EC – endothelial cell

ECAR – extracellular acidification rate

ECL – enhanced chemiluminescence

ECM – extracellular matrix

EDTA – ethylenediaminetetraacetic acid

EGLN1 – Egl-9 family hypoxia inducible factor 1

ELISA – enzyme-linked immunosorbent assay

ENG – endoglin

EPAS1 – endothelial PAS domain protein 1

ER – endoplasmic reticulum

ESC – embryonic stem cell

FACS – fluorescence-activated cell sorting

FBS – foetal bovine serum

FCCP – carbonyl cyanide 4-trifluoromethoxyphenylhydrazone

FDR – false discovery rate

FGF-2 – fibroblast growth factor 2

FIH – factor inhibiting HIF

FITC – fluorescein isothiocyanate

FKBP12 – 12 kilodalton (kDa) FK506-binding protein

FPAH – familial pulmonary arterial hypertension

FZD – Frizzled class receptor

GCN5 – general control of amino acid synthesis 5

GDF2 – growth differentiation factor 2

GFP – green fluorescent protein

GPI – glycosylphosphatidylinositol

GSK3β – glycogen synthase kinase-3 beta

GTPase – guanosine triphosphatase

H_2O_2 – hydrogen peroxide

H_2S – hydrogen sulphide

HBSS – Hank's Balanced Salt Solution

HES1 – Hes family basic helix-loop-helix transcription factor 1

hESC – human embryonic stem cell

HEY1 – Hes related family basic helix-loop-helix transcription factor with YRPW motif 1

Hh – Hedgehog

HIF-1α – hypoxia inducible factor-1alpha

HIV – human immunodeficiency virus

HMBS – hydroxymethylbilane synthase [also known as porphobilinogen deaminase (PBGD)]

HPAH – hereditary pulmonary arterial hypertension

HPRT – hypoxanthine phosphoribosyltransferase 1

HPSC – haematopoietic stem cell

hPSC – human pluripotent stem cell

HPV – hypoxic pulmonary vasoconstriction

HRP – horseradish peroxidase

ID – inhibitor of differentiation/DNA binding

IL – interleukin

IMDM – Iscove's Modified Dulbecco's Medium

iMEF – irradiated mouse embryonic fibroblast

IMM – inner mitochondrial membrane

IP – prostacyclin receptor

IPAH – idiopathic pulmonary arterial hypertension

iPSC – induced pluripotent stem cell

iPSC-EC(L) – induced pluripotent stem cell-derived endothelial cell-like cell

iPSC-MSC – induced pluripotent stem cell-derived mesenchymal stromal cell

iPSC-SMC – induced pluripotent stem cell-derived smooth muscle-like cell

JAG – Jagged

JNK – c-Jun amino-terminal kinase

K(O)SR – KnockOut Serum Replacement

KCNK3 – potassium two pore domain channel subfamily K member 3

KCP – kielin/chordin-like protein

KISS1 – kisspeptin 1

KLF4 – Krüppel like factor 4

L-EPC – late-outgrowth endothelial progenitor cell

LEF – lymphoid enhancer binding factor

LM – lateral plate mesoderm

LPS – lipopolysaccharide

MAPK – mitogen-activated protein kinase

MC1 – polyoma enhancer/herpes simplex virus thymidine kinase

MCT – monocrotaline

MEM – Minimum Essential Medium

miRNA – microRNA (ribonucleic acid)

MMP – matrix metalloproteinase

MnSOD – manganese superoxide dismutase

mPAP – mean pulmonary arterial pressure

MPTP – mitochondrial permeability transition pore

MRC – Medical Research Council

mRNA – messenger ribonucleic acid

MSC – mesenchymal stem cell

MYH11 – myosin heavy chain 11

NADPH – nicotinamide adenine dinucleotide phosphate

NANOG – Nanog homeobox

NCBI – National Center for Biotechnology Information

NE – neuroectoderm (neural ectoderm)

NF-κB – nuclear factor kappaB

NICD – Notch intracellular domain

NIH – National Institutes of Health

NIHR – National Institute for Health Research

NO – nitric oxide

NOX – nicotinamide adenine dinucleotide phosphate oxidase

OCT4 – octamer-binding transcription factor 4

OFP – orange fluorescent protein

OKSM – Oct4, Sox2, Klf4 and c-Myc

OP – osteogenic protein

PAAF – pulmonary artery adventitial fibroblast

PAH – pulmonary arterial hypertension

PAM – protospacer adjacent motif

PASMC – pulmonary artery smooth muscle cell

PBS – phosphate-buffered saline

PCA – principal component analysis

PCH – pulmonary capillary hemangiomatosis

PCP – planar cell polarity

PCR – polymerase chain reaction

PCWP – pulmonary capillary wedge pressure

PDGF – platelet-derived growth factor

PE – phycoerythrin

PES – polyethersulfone

PFA – Paraformaldehyde

PGK-Neo – phosphoglycerate kinase promoter-driven neomycin resistance

PH – pulmonary hypertension

PHD – prolyl hydroxylase domain

PI – propidium iodide

PI3K – phosphatidylinositol 3-kinase

PM – paraxial mesoderm

PPAR-γ – peroxisome proliferator-activated receptor gamma

PPHN – persistent pulmonary hypertension of the newborn

PT – PDGF-BB + TGF-β1

PTB – PDGF-BB + TGF-β1 + BMP4

PTC – papillary thyroid carcinoma

PVA – polyvinyl alcohol

PVDF – polyvinylidene difluoride

PVOD – pulmonary veno-occlusive disease

qPCR – quantitative polymerase chain reaction

R-SMAD – receptor-regulated SMAD

REVEAL – Registry to Evaluate Early and Long-term PAH Disease Management

RGM – repulsive guidance molecule

RGS5 – regulator of G-protein synthesis 5

RHOA – ras homolog gene family A

RNA-Seq – RNA Sequencing

ROCK – Rho-associated protein kinase

ROS – reactive oxygen species

RUNX2 – Runt-related transcription factor 2

RV – right ventricle

RVSP – right ventricular systolic pressure

s.e.m. – standard error of the mean

SDM – site-directed mutagenesis

SDS-PAGE – sodium dodecyl sulphate polyacrylamide agarose gel electrophoresis

SFRP – secreted Frizzled related protein

SIP1 – Smad interacting protein 1

siRNA – small interfering ribonucleic acid

SIRT3 – sirtuin-3

sJag1 – soluble Jagged 1

SLIT3 – split guidance ligand 3

SM22 – smooth muscle-specific 22 kDa protein (transgelin)

SMA – smooth muscle actin

SMAD – Sma Mothers against decapentaplegic

SMC – smooth muscle cell

SMTN – smoothelin

SMURF1 – SMAD-specific E3 ubiquitin protein ligase 1

SnoN – Ski novel gene N

SOD3 – superoxide dismutase 3 (extracellular)

SOX – sex determining region Y (SRY)-box

SP-C – surfactant protein C

SSEA3 – stage-specific embryonic antigen 3

SST – somatostatin

SSTR – somatostatin receptor

T_3 – triiodothyronine

TALEN – transcription activator-like effector nuclease

TBX4 – T-Box 4

TCF7 – transcription factor 7

TGF-β – transforming growth factor-beta

TIE2 – protein tyrosine kinase Tie2

TMRE – tetramethylrhodamine ethyl ester

TNFα – tumour necrosis factor alpha

TRA-1-60/81 – podocalyxin antigens

UCP – mitochondrial uncoupling protein

UK – United Kingdom

USA – United States of America

UMC – unaffected mutation carrier

UV – ultraviolet

VDAC – voltage-dependent anion channel

VEGF – vascular endothelial growth factor

VGR1 – vegetal related growth factor 1

VIP – vasoactive intestinal peptide

VSMC – vascular smooth muscle cell

WHO – World Health Organisation

WT1 – Wilms' tumour 1

ZFN – zinc-finger nuclease

TABLE OF CONTENTS

List of figures

List of tables

CHAPTER 1 – INTRODUCTION

1.1 – Pulmonary hypertension

The term pulmonary hypertension (PH) describes a range of conditions that can be devastating and often fatal, characterised by high blood pressure in the pulmonary artery, with clinical symptoms including fatigue, dyspnea (shortness of breath) and presyncope/syncope (lightheadedness/fainting) (Lai et al., 2014). For a positive diagnosis of PH, the mean pulmonary arterial pressure (mPAP) at rest should be greater than or equal to 25 mm Hg as measured using right heart catheterisation (Hoeper et al., 2013a).

1.1.1 – Classification of pulmonary hypertension

Pulmonary hypertension is classified into five main categories based on the underlying cause, pathology and haemodynamic profile (**Table 1.1**): pulmonary arterial hypertension (PAH) (Group 1); pulmonary hypertension due to left heart disease (Group 2); pulmonary hypertension due to lung diseases and/or hypoxia (Group 3); chronic thromboembolic pulmonary hypertension (CTEPH) (Group 4); and pulmonary hypertension with unclear multifactorial mechanisms (Group 5) (Simonneau et al., 2013). Pulmonary veno-occlusive disease (PVOD) and/or pulmonary capillary hemangiomatosis (PCH), as well as persistent pulmonary hypertension of the newborn (PPHN), were previously classified as subcategories of PAH (Simonneau et al., 2009). However, because PVOD/PCH and PPHN are thought to carry more differences than similarities compared to other PAH subgroups, they are currently classified into distinct categories (Groups 1' and 1", respectively), although these are not completely separated from PAH (Simonneau et al., 2009; 2013). A modification of the existing classification is expected in late 2018.

Table 1.1. Classification of pulmonary hypertension (taken from Simonneau et al., 2013)

Group	Cause
1	**Pulmonary arterial hypertension (PAH)** 1.1 Idiopathic PAH 1.2 Heritable PAH 1.2.1 BMPR2 1.2.2 ALK1, ENG, SMAD9, CAV1, KCNK3 1.2.3 Unknown 1.3 Drug and toxin induced 1.4 Associated with: 1.4.1 Connective tissue disease 1.4.2 HIV infection 1.4.3 Portal hypertension 1.4.4 Congenital heart diseases 1.4.5 Schistosomiasis
1'	**Pulmonary veno-occlusive disease and/or pulmonary capillary hemangiomatosis**
1''	**Persistent pulmonary hypertension of the newborn (PPHN)**
2	**Pulmonary hypertension due to left heart disease** 2.1 Left ventricular systolic dysfunction 2.2 Left ventricular diastolic dysfunction 2.3 Valvular disease 2.4 Congenital/acquired left heart inflow/outflow tract obstruction and congenital cardiomyopathies
3	**Pulmonary hypertension due to lung diseases and/or hypoxia** 3.1 Chronic obstructive pulmonary disease 3.2 Interstitial lung disease 3.3 Other pulmonary diseases with mixed restrictive and obstructive pattern 3.4 Sleep-disordered breathing 3.5 Alveolar hypoventilation disorders 3.6 Chronic exposure to high altitude 3.7 Developmental lung diseases
4	**Chronic thromboembolic pulmonary hypertension (CTEPH)**
5	**Pulmonary hypertension with unclear multifactorial mechanisms** 5.1 Hematologic disorders: chronic haemolytic anaemia, myeloproliferative disorders, splenectomy 5.2 Systemic disorders: sarcoidosis, pulmonary histiocytosis, lymphangioleiomyomatosis 5.3 Metabolic disorders: glycogen storage disease, Gaucher disease, thyroid disorders 5.4 Others: tumoral obstruction, fibrosing mediastinitis, chronic renal failure, segmental PH

Source: 5th World Symposium on Pulmonary Hypertension (Nice, 2013)

1.1.2 – Pulmonary arterial hypertension

The term PAH describes a subgroup of PH patients characterised haemodynamically by having a pulmonary capillary wedge pressure (PCWP) ≤ 15 mm Hg and a pulmonary vascular resistance (PVR) greater than 3 Wood units in the absence of left heart disease, lung diseases, CTEPH or other rare diseases (Hoeper et al., 2013a). PAH can be classified as being either idiopathic (IPAH, where the cause of the disease is unknown), heritable (HPAH, defined as present in at least two members of the same family or by the presence of a pathogenic mutation), drug- and toxin-induced, or associated with other conditions such as human immunodeficiency virus (HIV) infection, congenital heart disease, connective tissue disease, or schistosomiasis (**Table 1.1**) (Simonneau et al., 2013).

In the Western world, IPAH is thought to be the most common form of PAH (30 – 50% of PAH cases), whereas HPAH patients with a family history of the disease account for approximately 6% of PAH cases (Lane et al., 2000; Humbert et al., 2006; Badesch et al., 2010).
The incidence of PAH is estimated to be between 2.0 and 7.6 cases per million adults per year, with a prevalence ranging from 11 to 26 cases per million adults (Humbert et al., 2006; Peacock et al., 2007; Badesch et al., 2010; Ling et al., 2012). In patient registries (**Table 1.2**), PAH is approximately twice as common in females than in males and is increasingly being diagnosed in older patients (Simonneau et al., 2009; Hoeper and Gibbs, 2014). Symptoms may develop at any age, with an estimated 5-year mortality rate of 30% (Humbert et al., 2006; Badesch et al., 2010).

Currently available therapies target three main signalling pathways which play a key role in regulating vascular cell proliferation and pulmonary vascular tone (Humbert et al., 2014; Humbert & Ghofrani, 2016; Lau et al., 2017). Prostaglandin analogues such as iloprost (Olschewski et al., 2002) and the prostacyclin IP receptor agonist selexipag (Sitbon et al., 2015) target the prostacyclin pathway, stimulating the production of cyclic adenosine monophosphate (cAMP) which induces vadodilation (Murray, 1990). Phosphodiesterase type V inhibitors such as sildenafil and the soluble guanylate cyclase stimulator riociguat target the nitric oxide signalling pathway, promoting vasodilation by boosting the levels of cyclic guanosine monophosphate (cGMP) (Galie et al., 2005; Ghofrani et al., 2013). By contrast, endothelin-1 receptor antagonists such as bosentan reduce vasoconstriction by targeting endothelin receptors (Rubin et al., 2002). However, although these therapies have contributed to improved life

expectancy, they probably do not change the underlying pathology. Patients with end-stage PAH require a heart and/or lung transplantation to survive (Lai et al., 2014).

Registry	Time period	Sample size	Mean age (years)	Females (%)	1-year survival (%)	5-year survival (%)	References
NIH registry	1981-1988	187	36 ± 15	63	68	34	Rich et al., 1987 D'Alonzo et al., 1991
French registry	2002-2003	674	52 ± 15	62	89	NA	Humbert et al., 2006 Humbert et al., 2010
REVEAL	2006-2009	2525	50 ± 15	80	88	63	Frost et al., 2011 Benza et al., 2010 Benza et al., 2012
UK and Ireland	2001-2009	482	50 ± 17	70	93	60	Ling et al., 2012
COMPERA	2007-2011	587	65 ± 15	60	92	NA	Hoeper et al., 2013b
New Chinese Registry	2008-2011	956	38 ± 13	70	92	NA	Zhang et al., 2011
Czech registry	2000-2007	191	52 ± 17	65	89	NA	Jansa et al., 2014

Table 1.2. Characteristics of pulmonary arterial hypertension registries. NIH: National Institutes of Health; REVEAL: Registry to Evaluate Early and Long-term PAH Disease Management; UK: United Kingdom; COMPERA: Comparative, Prospective Registry of Newly Initiated Therapies for Pulmonary Hypertension (adapted from Hoeper & Gibbs, 2014 and Thenappan et al., 2018)

1.1.3 – Cellular phenotypes associated with pulmonary arterial hypertension

At the cellular level, pulmonary arterial hypertension is characterised by extensive vascular remodelling due to abnormal proliferation, migration and apoptosis of pulmonary artery smooth muscle cells (PASMCs), endothelial cells (ECs), and pulmonary artery adventitial fibroblasts (PAAFs) (Humbert et al., 2004) (**Figure 1.1**). During this process, abnormal ECs may release factors such as fibroblast growth factor 2 (FGF-2) which promote smooth muscle cell (SMC) proliferation or fail to produce agents which inhibit SMC proliferation and induce vasodilation (Thompson & Rabinovitch, 1996; Alastalo et al., 2011; Lai et al., 2014). Increased EC apoptosis during the early stages of PAH is thought to lead to a loss of smaller pulmonary arteries, whilst SMC dedifferentiation, migration, proliferation and clonal expansion result in progressive muscularisation of normally non-muscularised distal pulmonary vessels (Rabinovitch, 2008; Sheikh et al., 2015).

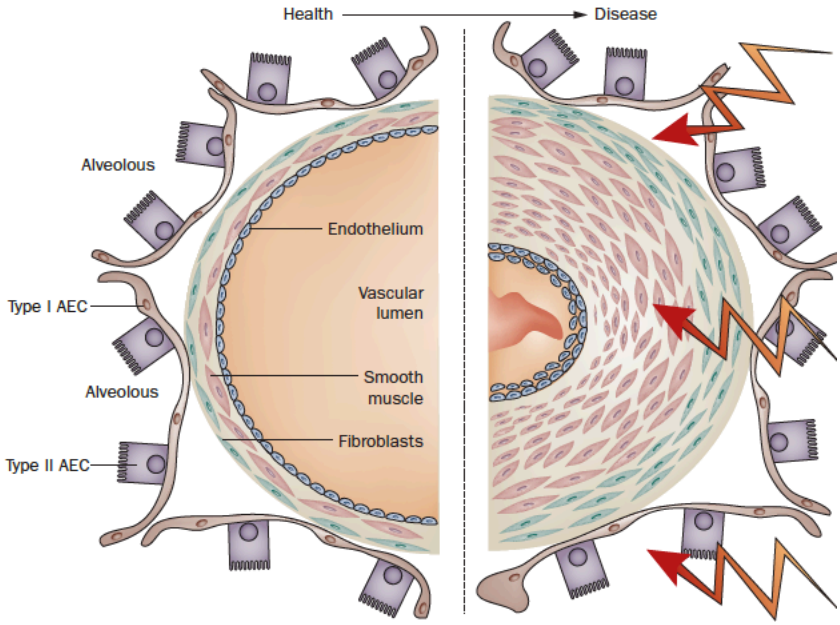

Figure 1.1. Vascular remodelling in pulmonary arterial hypertension. Vascular remodelling is characterised by increased proliferation of smooth muscle cells, endothelial cells and fibroblasts within the pulmonary artery which causes narrowing of the vascular lumen, thus impeding blood flow and resulting in elevated pulmonary arterial pressure. AEC, alveolar epithelial cell (from Schermuly et al., 2011).

Furthermore, PAH is associated with metabolic dysfunction such as increased glycolysis and mitochondrial abnormalities such hyperpolarisation of the inner mitochondrial membrane (Paulin & Michelakis, 2014). In addition, increased elastase and matrix metalloproteinase (MMP) activity lead to extracellular matrix degradation and fragmentation of the internal elastic lamina (Rabinovitch, 2001; Zaidi et al., 2002; Tuder et al., 2013), whilst platelet activation and *in situ* thrombus formation further obstruct blood flow within pulmonary vessels (Lannan et al., 2014). Complex, lumen-obliterating plexiform lesions are often found in patients with end-stage PAH (Tuder et al., 1994) (**Figure 1.2**). Taken together, these changes ultimately lead to the development of right heart failure, which may further be accelerated by increased inflammation and formation of reactive oxygen species (Bogaard et al., 2009).

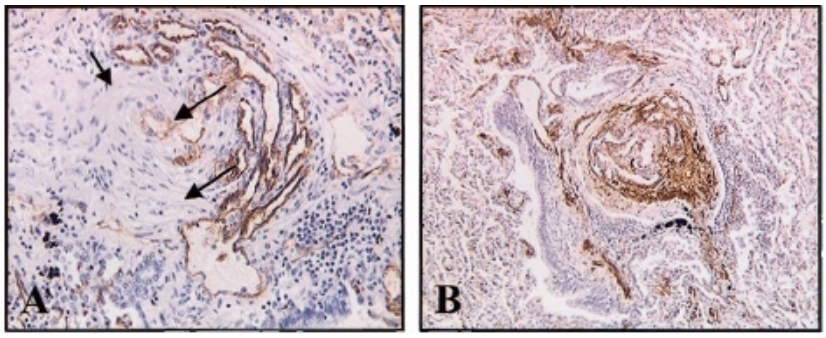

Figure 1.2. Photomicrographs of lung sections from PAH patients showing the histological appearance of plexiform lesions. (**A)** Plexiform lesions immunostained for the endothelial marker CD31 on a single layer of cells lining endothelial channels (arrows) (**B**) Stromal cells stain positively for α-smooth muscle actin (brown). Images taken at approximately 200x magnification (from Atkinson et al., 2002).

1.1.4 – The genetic basis of pulmonary arterial hypertension

In the year 2000, heterozygous germline mutations in the bone morphogenetic protein receptor type 2 (*BMPR2*) gene were identified as the main genetic cause of heritable PAH (Deng et al., 2000; Lane et al., 2000). Although mutations in several other genes have also been detected in PAH patients (**Table 1.3**), these are estimated to be present in approximately 8% of PAH cases (Gräf et al., 2018). Furthermore, the observation that BMPR2 protein expression is reduced in most PAH patients regardless of whether they have *BMPR2* mutations (Atkinson et al., 2002) highlights the central role of BMPR2 signalling in the pathogenesis of PAH.

To date, over 400 different PAH-associated *BMPR2* mutations have been identified, of which over 75% were detected in families with PAH (Soubrier et al., 2013; Best et al., 2014; Machado et al., 2015). PAH-associated *BMPR2* mutations have been detected in almost all exons within the gene, including the ligand binding domain, the serine-threonine kinase domain and the cytoplasmic tail (Machado et al., 2006). Approximately 70% of *BMPR2* mutations are nonsense or frame-shift mutations which cause haploinsufficiency due to degradation of the mutant transcripts by nonsense-mediated mRNA decay, whereas the remaining 30% result in impaired BMPR2 trafficking to the plasma membrane or have reduced kinase activity (Machado et al., 2006).

Although *BMPR2* mutations are present in approximately 82% of HPAH patients (Evans et al., 2016), only approximately 20% of people carrying *BMPR2* mutations go on to develop the disease, meaning there may be no history of disease in multiple generations within affected families (Lai et al., 2014). Moreover, penetrance of *BMPR2* mutations is higher in females than in males, with 43% of female versus 14% of male *BMPR2* mutation carriers developing PAH during their lifetime (Larkin et al., 2012). In addition, BMPR2 expression in HPAH patients is considerably lower than the 50% reduction expected due to haploinsufficiency alone (Atkinson et al., 2002). Together with the reduced penetrance of *BMPR2* mutations, this suggests that additional environmental or genetic ‘second hits’ are required to further reduce BMPR2 expression or signalling to a level that is sufficient to initiate the development of PAH (Morrell et al., 2009). However, a major unaddressed question is precisely how reduced BMPR2 signalling, either alone or via interaction with ‘second hits’, contributes to the development and progression of PAH.

Gene Symbol	Gene Name	References
BMPR2	Bone Morphogenetic Protein Receptor Type 2	Deng et al., 2000 Lane et al., 2000
ENG	Endoglin	Harrison et al., 2003
ALK1	Activin receptor-like kinase 1	Chaouat et al., 2004
BMPR1B (*ALK6*)	Bone Morphogenetic Protein Receptor Type 1B	Chida et al., 2012
SMAD4	SMAD Family Member 4	Nasim et al., 2011
SMAD9	SMAD Family Member 9	Nasim et al., 2011
GDF2 (*BMP9*)	Growth Differentiation Factor 2	Wang et al., 2016 Gräf et al., 2018
CAV1	Caveolin-1	Austin et al., 2012
KCNK3	Potassium Two Pore Domain Channel Subfamily K Member 3	Ma et al., 2013
TBX4	T-Box 4	Kerstjens-Frederikse et al., 2013
EIF2AK4	Eukaryotic initiation translation factor 2 alpha kinase 4	Best et al., 2017
ATP13A3	ATPase 13A3	Gräf et al., 2018
AQP1	Aquaporin 1	Gräf et al., 2018
SOX17	SRY-Box 17	Gräf et al., 2018

Table 1.3. List of mutated genes identified to date in patients with pulmonary arterial hypertension.

1.2 – Bone morphogenetic protein signalling

1.2.1 – Bone morphogenetic proteins

Bone morphogenetic proteins (BMPs) are members of the transforming growth factor β (TGF-β) superfamily of ligands. Originally identified as proteins that induce bone and cartilage formation (Urist, 1965; Wang et al., 1988), it is now evident that BMPs also play important roles in regulating many other biological functions including morphogenesis, cell differentiation, proliferation, and apoptosis (Katagiri & Watabe, 2016). To date, over twenty different BMP isoforms have been identified (Bragdon et al., 2011) (**Table 1.4**). They have highly conserved structures that are shared by other members of the TGF-β family, and can be classified into several sub-groups, including the BMP-2/4 group, BMP-5/6/7/8 group, BMP-9/10 group and BMP12/13/14 group (Bubnoff & Cho, 2001; Mazerbourg & Hsueh, 2006). BMP-1 is a metalloproteinase which cleaves the C-terminus of type I collagen and is therefore not a member of the TGF-β family (Kessler et al., 1996).

BMP family member	Tissue expression in humans	Biological function(s) in humans
BMP2	Lung, kidney, pancreas, spleen	Heart formation, skeletal repair/ regeneration
BMP4	Heart, lung, skeletal muscle, thymus, bone marrow, spleen, brain, spinal cord, liver, kidney, pancreas, prostate	Skeletal repair and regeneration, kidney formation
BMP5	Heart, lung, skeletal muscle, thymus, bone marrow, spleen, brain, spinal cord, kidney, pancreas, prostate	Bone and cartilage morphogenesis, limb development, connecting soft tissues
BMP6 (VGR1)	Heart, lung, skeletal muscle, liver, kidney, thymus, bone marrow, spleen, brain, spinal cord, pancreas, prostate	Bone morphogenesis, nervous system development, cartilage hypertrophy
BMP7 (OP1)	Heart, lung, skeletal muscle, liver, kidney, thymus, bone marrow, spleen, brain, spinal cord, pancreas, prostate	Skeletal repair and regeneration, nervous system development, kidney and eye formation

BMP8A (OP2)	Heart, lung, kidney, thymus, bone marrow, spleen, brain, spinal cord, pancreas, prostate	Bone morphogenesis, spermatogenesis
BMP8B	Heart, skeletal muscle, bone marrow, spleen, brain, spinal cord, liver, kidney, pancreas	Spermatogenesis
BMP9 (GDF-2)	Liver	Bone morphogenesis, glucose metabolism, anti-angiogenesis, development of cholinergic neurons
BMP10	Heart, lung, skeletal muscle, liver, thymus, bone marrow, spleen, brain, spinal cord, pancreas, prostate	Heart morphogenesis
BMP11 (GDF-11)	Thymus, bone marrow, spleen, brain, spinal cord, pancreas	Patterning mesodermal and neural tissues, dentin formation
BMP12 (GDF-7)	?	Ligament and tendon development, sensory neuron development
BMP13 (GDF-6)	?	Skeletal morphogenesis, normal formation of bones and joints, chondrogenesis
BMP14 (GDF-5)	Heart, bone marrow, liver, kidney	Skeletal repair and regeneration
BMP15 (GDF-9B)	None	Oocyte and follicular development
BMP3 (Osteogenin)	Heart, skeletal muscle, thymus, bone marrow, spleen, brain, pancreas, prostate	Negative regulator of bone morphogenesis
BMP3B (GDF-10)	Skeletal muscle, brain, spinal cord, pancreas, prostate	Regulation of cell differentiation, skeletal morphogenesis

Table 1.4. Overview of bone morphogenetic proteins, their functions and expression (adapted from Bragdon et al., 2011)

Most BMPs are expressed in a variety of tissues during development, where they often play crucial roles, as evidenced by the embryonic lethal phenotype of knock-out animals that are homozygous for null mutations in BMPs 2, 4, 8b and 10 (Winnier, 1995; Zhang & Bradley, 1996; Zhao & Hogan, 1996; Chen et al., 2004). The embryonic lethal phenotype of these animals therefore suggests that these bone morphogenetic proteins are necessary for development, including vascular development.

1.2.2 – Bone morphogenetic protein receptor signalling

BMPs elicit their effects by binding to type I and type II transmembrane receptors (Shi & Massague, 2003; de Caestecker, 2004) **(Figure 1.3)**, which consist of a short extracellular domain, a single transmembrane domain, one intracellular domain with serine/threonine kinase activity and a C-terminal cytoplasmic tail region (Miyazono et al., 2010). Unlike TGF-β proteins, BMPs can bind to type I receptors in the absence of type II receptors, although their binding affinities are higher when both receptor types are present (Rosenzweig et al., 1995).

There are three type II receptors - bone morphogenetic protein receptor type II (BMPR2), activin receptor type IIA (ActR-IIA) and activin receptor type IIB (ActRIIB). BMPR2 specifically binds BMPs, whereas ActR-IIA and ActRIIB also act as receptors for activin and myostatin (Yu et al., 2005). Activin receptor-like kinases ALK1, ALK2, ALK3 (BMPR-1A) and ALK6 (BMPR-1B) serve as type I receptors for most BMPs, whereas TGF-β signals via ALK5 (Shi & Massague, 2003). Whilst ALK2 and ALK3 are expressed in many different cell types, ALK6 is less widely expressed, and ALK1 is mainly expressed in endothelial cells and certain other cell types (Katagiri & Watabe, 2016).

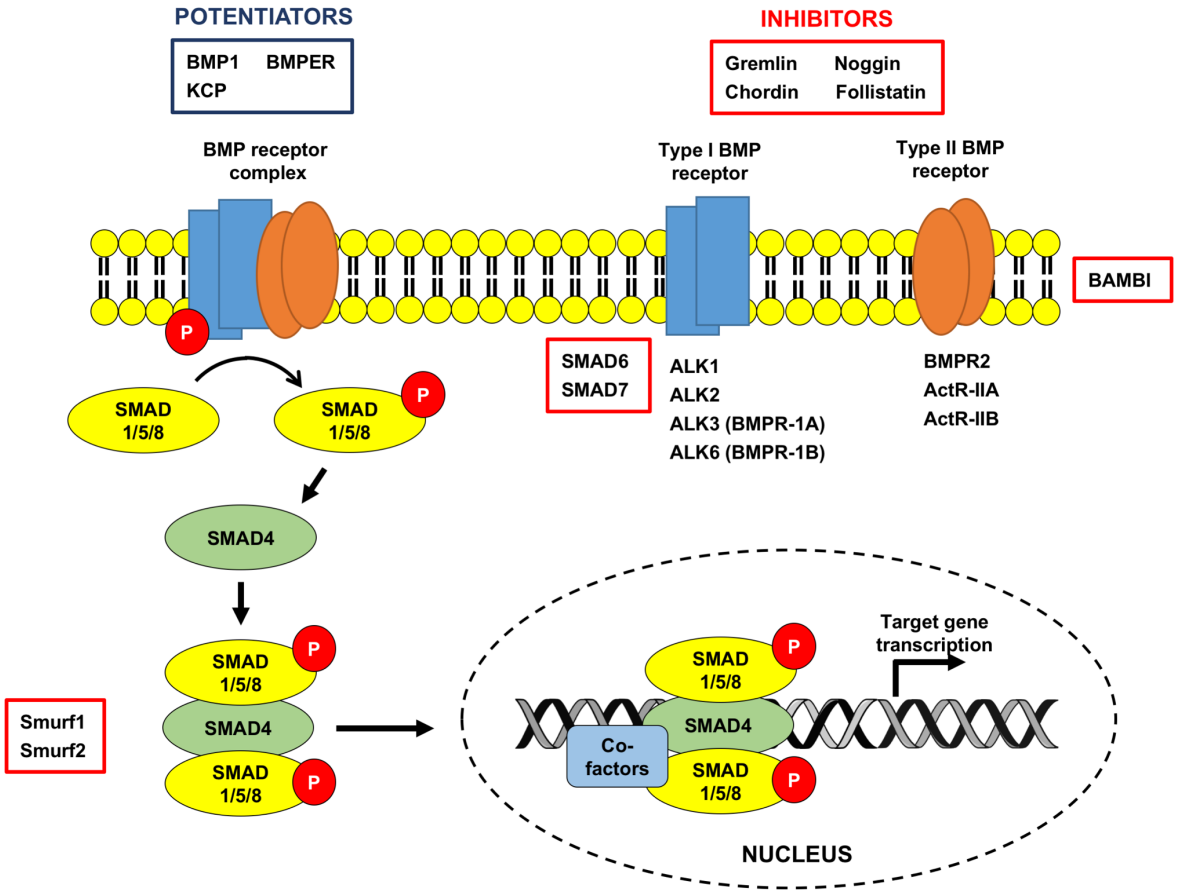

Figure 1.3. Overview of bone morphogenetic protein receptor signalling. Activators of BMP signalling are listed in the blue box, whereas BMP signalling inhibitors are shown in red boxes. BMP, bone morphogenetic protein; ALK, activin receptor-like kinase; BMPR; bone morphogenetic protein receptor; ActR, activin receptor; BMPER, BMP binding endothelial regulator; BAMBI, BMP and activin membrane bound inhibitor; KCP, kielin/chordin-like protein.

BMP2 and BMP4 bind to ALK3 and ALK6, recruiting type II receptors to form an active receptor complex (ten Dijke et al., 1994; Macias-Silva et al., 1998). By contrast, BMP6 and BMP7 bind to ActR-IIA in a complex with ALK2 or ALK3 (ten Dijke et al., 1994; Yamashita et al., 1995; Ebisawa et al., 1999). BMP9 and BMP10 bind to BMPR2 together with ALK1 or ALK2 (Brown et al., 2005; David et al., 2007), but can also signal via ActR-IIA or endoglin, a co-receptor for TGF-β/BMP signalling (Alt et al., 2012). These signalling combinations are summarised in **Figure 1.4** below.

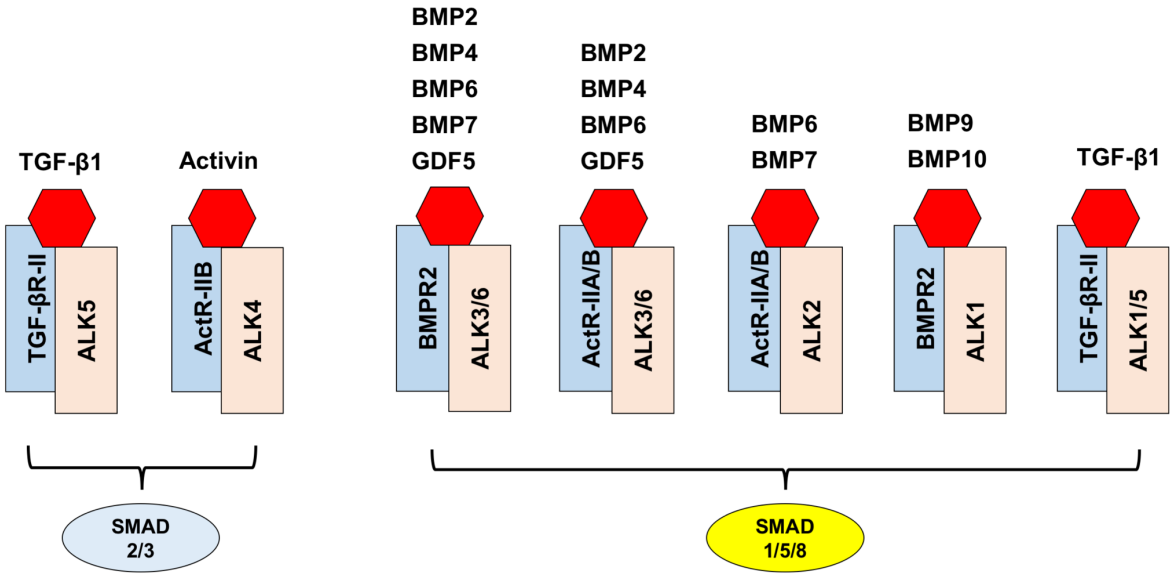

Figure 1.4. Summary of interactions between BMP and TGF-β proteins and their receptors. Different receptor complexes preferentially bind particular BMP ligands, with TGF-β1 and activin predominantly signalling via Smad2/3, whereas bone morphogenetic proteins mainly signal via Smad1/5/8 (adapted from Upton & Morrell, 2009).

Upon binding of the BMP ligand, type II receptors phosphorylate and activate type I receptors. In turn, the activated type I receptor phosphorylates at least one of the receptor-regulated Smads (Smad1, Smad5 and Smad8). These BMP-specific R-Smads are then able to form a complex with the co-Smad, Smad4, followed by translocation of the resulting Smad complex to the nucleus where it can activate or inhibit gene transcription by binding to DNA and interacting with transcriptional co-activators (p300, CBP, Runx2, and/or GCN5) or co-repressors (c-Ski, SnoN, Tob or SIP1) (Shi and Massague, 2003; Massague et al., 2005; Katagiri & Watabe, 2016). By contrast, TGF-β ligands signal via Smad2 and Smad3, although TGF-β can also signal via ALK1 and ALK2 to activate Smad1 and Smad5 in endothelial cells and some other cells (Goumans et al., 2003; Daly et al., 2008).

Downstream targets of BMPR2 signalling include the inhibitor of DNA binding/differentiation (ID) proteins which control PASMC proliferation by inhibiting the cell cycle (Yang et al., 2013), as well as the transcription factors Hey1 and Tcf7 which are involved in Notch and Wnt signalling, respectively (Miyazono et al., 2010).

1.2.2.1 – Regulation of BMP signalling

BMP signalling is temporally and spatially regulated at multiple levels via interactions with many different intracellular and extracellular signals (Shi & Massague, 2003; Guo & Wang, 2009) **(Figure 1.3)**. Extracellular BMP antagonists include gremlin, noggin, chordin, follistatin and differential screening-selected gene in neuroblastoma (DAN) family members (Katagiri & Watabe, 2016), some of which can be up-regulated by BMPs, thus forming negative feedback loops (Kameda et al., 1999; Pereira et al., 2000). By contrast, BMP1, kielin/chordin-like protein (KCP) and BMP binding endothelial regulator (BMPER) can potentiate BMP signalling (Marques et al., 1997; Piccolo et al., 1997; Moser et al., 2003).

At the cell membrane, BMP signalling is inhibited by BAMBI (BMP and activin membrane-bound inhibitor), which prevents the formation of signal receptor complexes. On the other hand, glycosylphosphatidylinositol (GPI)-anchored membrane proteins of the repulsive guidance molecule (RGM) family enhance BMP signalling by forming complexes with BMP type I receptors (Halbrooks et al., 2007).

Intracellularly, Smad6 and Smad7 act as inhibitory Smads by binding to BMP type I receptors, thus preventing downstream Smad1/5 activation, thereby negatively regulating BMP signalling (Imamura et al., 1997; Heldin & Moustakas, 2012).

Furthermore, BMP signalling is modulated by ubiquitin-mediated proteasomal degradation of Smad1 and Smad5 by the E3 ubiquitin ligase Smurf1, which also interacts with Smad6 to mediate degradation of type I BMP receptors (Zhu et al., 1999; Murakami et al., 2003).

Additional regulation of BMP signalling is achieved by several different microRNAs (miRNAs) such as miR-21 and miR-302 (Ahmed et al., 2011; Kang et al., 2012), as well as by proteins such as the 12-kDa FK506-binding protein (FKBP12) which binds to and inhibits the activation of type I BMP receptors (Spiekerkoetter et al., 2013).

1.2.3 – Cross-talk of BMP signalling with other signalling pathways

In addition to signalling via the Smad-dependent pathways described above, BMPs can also signal via mitogen-activated protein kinases (MAPKs), Akt, phosphatidylinositol 3-kinase (PI3K), c-Jun amino-terminal kinase (JNK), and small GTPases. These Smad-independent pathways interact with Smad-dependent pathways to modulate various cellular responses (Katagiri & Watabe, 2016). For example, interactions between TGF-β/BMP, Notch, Wnt, Hedgehog (Hh) and other signalling pathways **(Figure 1.5)** regulate stem cell maintenance, organogenesis, and cell fate specification during embryonic development, whilst also being important for modulating cell growth in adult tissues (Attisano & Labbe, 2004; Sumi et al., 2008). Dysregulated Notch and Wnt signalling have also been implicated in pulmonary arterial hypertension, as discussed below.

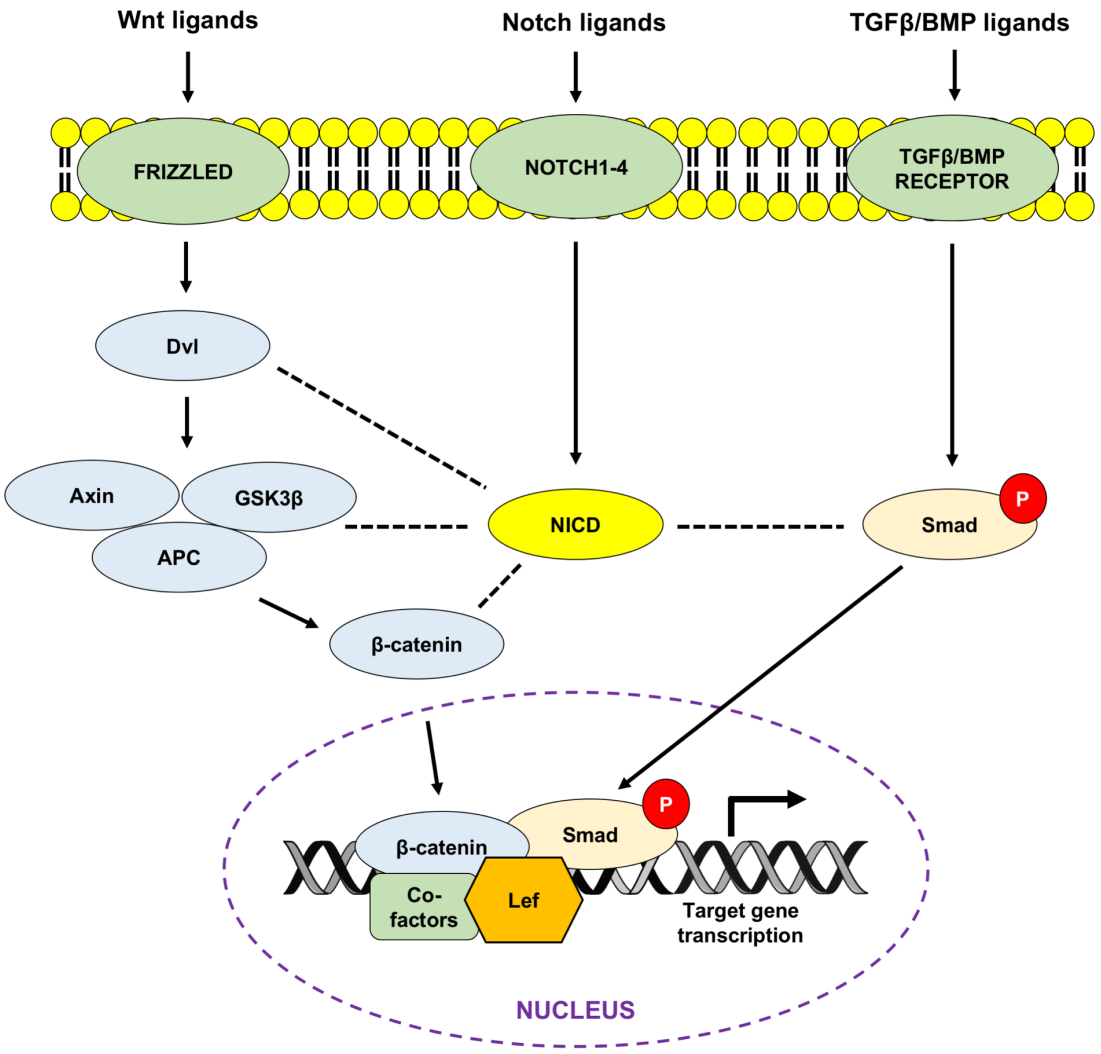

Figure 1.5. Simplified schematic summarising some of the main interactions between the Notch, Wnt and TGF-β/BMP signalling pathways. Cross-talk between the TGF-β and Notch signalling pathways most commonly occurs in the nucleus where the Smad/β-catenin-Lef protein complex regulates the transcription of a shared set of target genes. Multiple context-specific protein interactions (dashed black lines) between Notch, Wnt and TGF-β signalling also occur in the cell cytoplasm. Dvl, Dishevelled; GSK3β, glycogen synthase kinase-3 beta; APC, adenomatous polyposis coli; NICD, Notch intracellular domain; TGF-β, transforming growth factor beta; BMP, bone morphogenetic protein; Lef, lymphoid enhancer binding factor (adapted from Guo & Wang, 2009 and Andersson et al., 2011).

1.2.3.1 – Wnt signalling in pulmonary arterial hypertension

Wnt proteins are secreted molecules which signal via canonical and non-canonical pathways to regulate a variety of biological functions. The canonical pathway involves Wnt signalling via cytoplasmic β-catenin, which can translocate to the nucleus to regulate the expression of genes involved in processes such as cell proliferation, differentiation and survival (Papkoff et al., 1996). By contrast, the non-canonical Wnt/planar cell polarity (PCP) pathway does not require β-catenin accumulation and regulates more specialised functions such as cell motility and polarity (Shulman et al., 1998; Veeman et al., 2003).

Several genes involved in the PCP pathway, such as those encoding ras homolog gene family A (RHOA), WNT11, and Dishevelled (DVL), were found to be upregulated in laser-microdissected pulmonary arterial resistance vessels from patients with IPAH (Laumanns et al., 2009). Furthermore, overexpression of the soluble Wnt receptor Secreted Frizzled Related Protein 2 (SFRP2) was detected in HPAH patient-derived fibroblasts and lung tissue, as well as in the lungs of R899X *Bmpr2*$^{+/-}$ mice (West et al., 2014). Taken together, these findings suggest that reduced BMPR2 signalling in PAH is associated with increased Wnt signalling, which may contribute to increased proliferation and migration of pulmonary vascular cells in PAH (de Jesus Perez et al., 2009; Takahashi et al., 2016). However, whether this is indeed the case is yet to be confirmed.

1.2.3.2 – Notch signalling in pulmonary arterial hypertension

To date, four different Notch receptors (Notch1 – Notch4) and five cell-bound Notch ligands of the Jagged (Jag1 and Jag2) and Delta-like (Dll1, Dll3 and Dll4)) families have been characterised in mammals (Alva & Iruela-Arispe, 2004). Aberrant Notch signalling has also been implicated in the pathogenesis of PAH, although there is controversy as to whether this is due to changes in Notch2 or Notch3 expression (Li et al., 2009; Xiao et al., 2013; Yu et al., 2013; Hurst et al., 2017). For example, Notch1, Notch3 and Jagged 1 were found to be highly expressed in animal models of PAH, whilst adenoviral transfection of soluble Jagged 1 (sJag1) resulted in significantly reduced proliferation and increased apoptosis of PASMCs from pulmonary hypertensive rats (Xiao et al., 2013). Similarly, increased Notch3 expression has also been detected in human patient-derived PASMCs (Li et al., 2009); however, Notch3 and its downstream target HES1 were found to be decreased in tumour necrosis factor-alpha (TNFα)-treated HPAH PASMCs (Hurst et al., 2017). Interestingly, Hurst *et al.* found that TNFα stimulation in HPAH PASMCs induced post-translational cleavage and shedding of

BMPR2 at the cell surface, thus diverting BMP signalling via ActR-IIA which promoted PASMC proliferation via downstream activation of Notch2 and Src kinases (Hurst et al., 2017). This suggests that Notch2 rather than Notch3 signalling contributes to the increased proliferation of PASMCs observed in PAH.

1.2.4 – Bone morphogenetic protein signalling in vascular smooth muscle cells

In the lung, BMPR2 is predominantly expressed in pulmonary artery endothelial cells (PAECs) and PASMCs (Atkinson et al., 2002). Under normal conditions, BMP2, BMP4 and BMP7 inhibit the proliferation of vascular smooth muscle cells isolated from the proximal pulmonary artery (Farber & Loscalzo, 2004). Disruption of BMPR2 signalling in these cells results in the loss of the anti-proliferative effects of BMP4, reduced BMP6 and BMP7 signalling, as well as increased PASMC proliferation in response to TGF-β1 (Yu et al., 2005; Dewachter et al., 2009). Furthermore, depending on their anatomical and potentially also their developmental origin, adult PASMCs may have different responses to the same BMP molecules. For example, PASMCs in the proximal vascular branch tend to be growth-suppressed by BMPs 2, 4 and 7 and may even undergo apoptosis in response to these ligands, whereas BMP2 and BMP4 stimulate proliferation in PASMCs isolated from smaller pulmonary arteries in the distal vascular branches (Yang et al., 2005). This difference in BMP responsiveness between proximal and distal PASMCs is an important consideration for developing disease models and PAH therapies, as it is predominantly the smaller, more distal vessels that are the site of disease initiation (Thenappan et al., 2016).

1.3 – Molecular pathogenesis of pulmonary arterial hypertension

1.3.1 – Hypoxia and PAH

The acute response of the pulmonary vasculature to hypoxia involves the constriction of precapillary pulmonary arteries in a process known as hypoxic pulmonary vasoconstriction (HPV) (von Euler & Liljestrand, 1946) which increases pulmonary vascular resistance and pulmonary arterial pressure. By contrast, chronic exposure to hypoxia leads to vascular remodelling characterised by the muscularisation of previously non-muscularised pulmonary arteries, an increase in the extent of muscularisation of already muscularised arteries, and the pruning of smaller peripheral arteries (Arias-Stella & Saldana, 1963; Hislop & Reid, 1976; Stenmark et al., 2006). At the cellular level, these structural changes are caused by increased proliferation and reduced apoptosis of PASMCs which has been linked to increased expression of hypoxia inducible factor-1alpha (HIF-1α) (Ball et al., 2014).

The amount of pulmonary vascular remodelling in response to chronic hypoxia varies both between and within species (Grünig et al., 2000; Zhao et al., 2001; Rhodes, 2005; Swenson, 2013), suggesting that susceptibility to hypoxia-induced pulmonary hypertension is affected by genetic background. For example, Tibetan highlanders are less prone to develop pulmonary hypertension compared to more recent migrants to high altitude, partly due to natural selection of non-coding variants of the HIF pathway genes *EPAS1* and *EGLN1* (Beall et al., 2010; Simonson et al., 2010). Furthermore, *Bmpr2*$^{+/-}$ mice might be more susceptible to hypoxia-induced PH compared to wild-type mice (Frank et al., 2008). However, previous work from our group has shown that *Bmpr2*$^{+/-}$ mice exposed to chronic hypoxia for 2-3 weeks display similar pulmonary haemodynamics and vascular morphometry compared to wild-type littermates (Long et al., 2006). By comparison, targeted delivery of an adenoviral vector containing the *Bmpr2* gene to the pulmonary vascular endothelium of hypoxic rats significantly reduced pulmonary arterial and right ventricular (RV) pressures, RV hypertrophy and muscularisation of distal pulmonary arterioles (Reynolds et al., 2007).

However, in most forms of human hypoxic PH [World Health Organisation (WHO) Group 3], the pathological changes are less severe compared to those found in PAH patients with *BMPR2* mutations (Pugliese et al., 2015). In contrast to Group 3 pulmonary hypertension in which hypoxia is the primary stimulus, PAH is characterised by the normoxic activation of HIF-1α signalling in the absence of alveolar hypoxia (Bonnet et al., 2006), although cellular hypoxia may contribute to pulmonary vascular remodelling as the disease progresses (Farber & Loscalzo, 2005).

1.3.2 – Inflammation and metabolic dysfunction in PAH

Immune dysfunction is a central feature of PAH associated with connective tissue diseases and infections, with schistosomiasis probably being the single largest cause of PAH (Graham et al., 2010; Rabinovitch et al., 2014). In patients with pulmonary hypertension, inflammation is also an early consequence of exposure to hypoxia and is one of the proposed "second hits" that are thought to be required to trigger PAH establishment and progression (Rabinovitch et al., 2014). Hypoxia may promote inflammation by inducing the transcription of HIF target genes such as nuclear factor kappaB (NF-κB), a transcription factor which regulates the production of inflammatory cytokines (Cummins et al., 2016). In turn, activation of NF-κB can increase HIF expression (Eltzschig & Carmeliet, 2011; Fröhlich et al., 2013), thus creating a potential feedforward loop between hypoxia, HIF and inflammation (**Figure 1.6**).

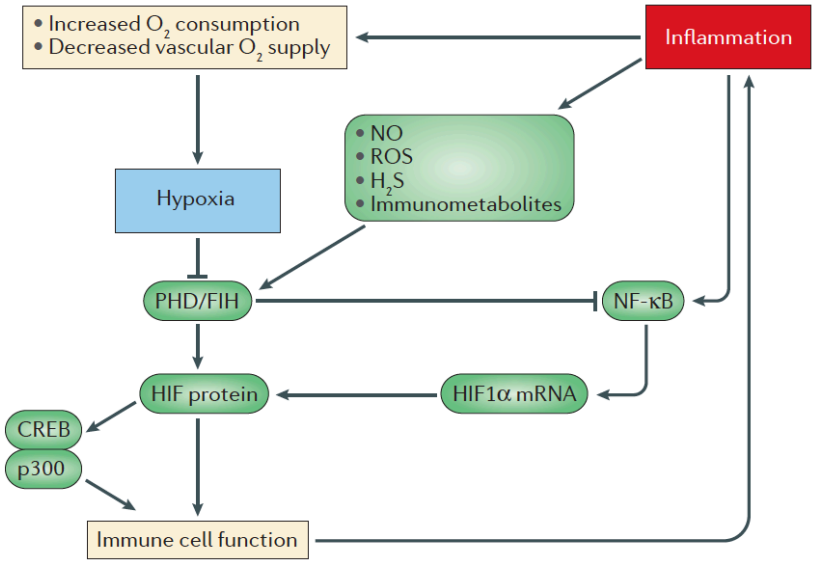

Figure 1.6. Signalling crosstalk between inflammation and hypoxia. In addition to increasing HIF protein expression, hypoxia also induces the production of inflammatory cytokines which activate nuclear factor kappaB (NF-κB), a key transcriptional regulator of cellular immune responses. In turn, NF-κB promotes the transcription of HIF-1α, thus creating a potential feedforward loop between hypoxia, HIF and inflammation. Inflammation also promotes the production of immunometabolites, gasotransmitters such as hydrogen sulphide (H_2S) and nitric oxide (NO), and reactive oxygen species (ROS) which regulate HIF activity and metabolic processes in immune cells. CREB, cyclic AMP-response element binding protein; FIH, factor inhibiting HIF; p300, histone acetyltransferase p300; PHD, prolyl hydroxylase domain (from Taylor & Colgan, 2017).

Furthermore, HIF can also modulate inflammatory immune responses by controlling cellular metabolism (Corcoran & O'Neill, 2016). For example, HIF expression can promote glycolysis by increasing the transcription of glycolytic genes (Semenza et al., 1994), which in turn can activate a number of immune cell types such as macrophages, dendritic cells, T cells and B cells (Corcoran & O'Neill, 2016). Conversely, inflammatory cytokines and ROS influence the activity of the HIF pathway, resulting in complex crosstalk between hypoxia, inflammation and metabolism (Halligan et al., 2016).

Such crosstalk is evident in pulmonary arterial hypertension, where hypoxia increases IL-6 expression in human PASMCs (Savale et al., 2009) and a range of pro-inflammatory cytokines and chemokines in pulmonary adventitial fibroblasts (Li et al., 2011). Consistent with these observations, increased levels of IL-1β, IL-6, IL-8 and TNFα are detected in IPAH patients (Humbert et al., 1995; Soon et al., 2010), with increased levels of several of these cytokines correlating with increased mortality (Cracowski et al., 2014).

Furthermore, prolonged exposure to hypoxia may impair mitochondrial function (Ye et al., 2016) and increase oxidative stress (Takahashi et al., 2006), which might further exacerbate inflammation. Cytokines and HIF-1α are thought to contribute to the hyperglycolytic phenotype of PASMCs and pulmonary artery endothelial cells (PAECs) in PAH, even in the absence of alveolar hypoxia (Archer et al., 2010). In support of this concept, the pyruvate dehydrogenase kinase inhibitor dichloroacetate (DCA) reduced glycolysis and reversed the activation of HIF-1α in Fawn-hooded rats which spontaneously develop pulmonary hypertension (Bonnet et al., 2006). Taken together, these findings suggest that hypoxic signalling and inflammation contribute to the metabolic dysfunction associated with PAH.

The hyperglycolytic phenotype of the vasculature in PH has been compared the phenotype of cancer cells which display a metabolic shift from glucose oxidation to glycolysis under aerobic conditions (Archer et al., 2010; Tuder et al., 2013). This phenomenon, termed "the Warburg effect", has been observed in SMCs, ECs and fibroblasts from PAH patients and animal models of PH (Freund-Michel et al., 2014; Paulin & Michelakis, 2014), and is associated with a more highly proliferative phenotype, apoptosis resistance, increased mitochondrial membrane polarisation, dysregulation of calcium dynamics and endoplasmic reticulum (ER) stress (Michelakis et al., 2002; Vander Heiden et al., 2009; Archer et al., 2010; Semenza, 2011; Stenmark et al., 2011; Fessel et al., 2013).

The anti-apoptotic phenotype of PASMCs in PAH can be partially attributed to a failure of pro-apoptotic mediators to be released from mitochondria via the mitochondrial permeability transition pore (MPTP), a voltage- and redox-sensitive channel that closes when the inner mitochondrial membrane becomes hyperpolarised (Zamzami et al., 1996; Zamzami & Kroemer, 2001; Pastorino et al., 2005). The glycolytic phenotype of PAH has been linked to increased activity of the glycolytic enzyme hexokinase 2, which inhibits a portion of the MPTP known as the voltage-dependent anion channel (VDAC) (Pastorino et al., 2005). Inhibition of the VDAC results in the accumulation of anions within the intermembrane space, thus leading to mitochondrial membrane hyperpolarisation, which further prevents MPTP opening and induces a relative state of apoptosis resistance (Camara et al., 2010).

Mitochondrial membrane hyperpolarisation has been reported in PASMCs from PAH patients and in animal models of PH (McMurtry et al., 2004; Bonnet et al., 2006; Sutendra et al., 2011; Dromparis et al., 2013; Pak et al., 2013), as well as in *BMPR2*$^{+/-}$ PAECs which also display mitochondrial fission, increased glycolysis and a pro-inflammatory state characterised by increased expression of IL-6 and IL-8 (Diebold et al., 2015). Under certain conditions, these changes may result in the increased production of reactive oxygen species (ROS) which are thought to promote PASMC proliferation (Sanders & Hoidal, 2007), vascular remodelling (Liu et al., 2006; Hoshikawa et al., 2001) and contribute to pulmonary vasoconstriction or vasodilation (Archer et al., 1986, 2008). However, whether mitochondrial ROS is increased or decreased in PAH remains controversial (Aggarwal et al., 2013; Bonnet & Boucherat, 2018).

Furthermore, it is also unclear whether reduction in *BMPR2* promotes inflammation directly, or whether inflammatory events precede the development of pulmonary hypertension. TNFα reduces *BMPR2* expression in distal PASMCs and PAECs, stimulates the proliferation of *BMPR2*$^{+/-}$ PASMCs via preferential ActR-IIA signalling, and can promote endothelial cell apoptosis (Courboulin et al., 2011; Cracowski et al., 2014; Hurst et al., 2017). The soluble TNFα inhibitor etanercept reversed PH progression in rats, which was associated with restored *Bmpr2* expression (Zhang et al., 2016; Hurst et al., 2017). Similarly, the immunosuppressant FK506 (Tacrolimus) restored BMPR2 signalling and reversed severe PH in rats (Spiekerkoetter et al., 2013). Taken together, these findings suggest that inflammation contributes to the pathogenesis of PAH by reducing *BMPR2* expression.

Currently available PAH therapies in humans have been shown to reduce inflammation by decreasing the expression of endothelial cell adhesion molecules (Verma et al., 2002; Zardi et al., 2005), inhibiting pro-inflammatory cytokine secretion (Finsnes et al., 2001; Zhou et al., 2007) and by preventing the activation of lymphocytes and dendritic cells (Guruli et al., 2004). However, none of these therapeutics specifically target inflammation, and immunosuppression *per se* does not appear to be effective at treating PAH in humans, except in isolated cases where PAH has been linked to connective tissue diseases (Jais et al., 2008). This suggests that inflammation on its own is not sufficient to initiate the development of pulmonary hypertension and that multiple signalling pathways will need to be targeted to develop more effective treatments for PAH.

1.3.3 – Animal models of pulmonary hypertension

Studying the role of inflammation, hypoxia and metabolic dysfunction in diseased human tissues from PAH patients is hampered by their limited availability. As PAH is a rare disease, these tissues can only be obtained from patients at the time of heart/lung transplantation. Furthermore, patient-derived primary cells have a limited proliferative capacity *in vitro*, meaning that repeated biopsies are often required to study individual mutations. As a result, several rodent models of PAH have been developed in an attempt to gain a better understanding of the molecular pathogenesis of PAH, as described below.

1.3.3.1 – Monocrotaline injury

Monocrotaline injury in rats is the most commonly used animal model of Group 1 pulmonary arterial hypertension (Sztuka & Jasinska-Stroschein, 2017). A single subcutaneous or intraperitoneal injection (typically 60 mg/kg) of the pyrrolizidine alkaloid monocrotaline (MCT) is sufficient to trigger progressive development of severe PH in rats (Lalich & Mercow, 1961; Kay et al., 1967). Although the exact mechanism through which MCT triggers PH development is poorly understood, it is thought to involve direct damage to the endothelium (Jasmin et al., 2001). Rats appear normal during the first two weeks after MCT injection, but subsequently develop muscularisation of previously non-muscularised arteries and adventitial remodelling which leads to an increase in pulmonary vascular resistance (Pak et al., 2010). Furthermore, metabolomic profiling of rat lungs after 14 days of exposure to monocrotaline revealed metabolic changes similar to those associated with human PH (Rafikova et al., 2016). Taken together, monocrotaline causes right ventricular systolic pressure (RVSP) to increase from approximately 25 to 80 mm Hg, with rats dying due to right heart failure after 6-8 weeks (Schermuly et al., 2005; Pak et al., 2010).

The MCT model of PH is associated with the accumulation of many inflammatory cell types and is therefore useful for studying the contribution of inflammation to pulmonary vascular remodelling (West & Hemnes, 2011). Furthermore, MCT-induced PH has been widely used as a preclinical model of PAH to test potential therapeutic agents, with over 30 compounds shown to be effective at preventing or reversing monocrotaline-induced pulmonary hypertension (Stenmark et al., 2009). However, only a few of these experimental agents went on to be tested in human subjects (Hill et al., 2017).

There are multiple reasons why the MCT model of PH is poor at predicting treatment outcomes in any human form of pulmonary hypertension. For example, monocrotaline injury does not recapitulate the neointima formation and vascular obliteration of small pulmonary arterioles that is observed in human PAH (Yi et al., 2000). Furthermore, PAH is not caused by a single trigger and develops more slowly compared to the rapid disease progression observed in MCT-induced PH (Hill et al., 2017). In addition, monocrotaline may cause off-targets effects such as myocarditis, which is not normally observed in human PAH, thus potentially confounding the study of right ventricular hypertrophy commonly associated with end-stage disease (Miyauchi et al., 1993). Monocrotaline can also have different effects in different species, strains and even individual animals due to differences in its hepatic metabolism by cytochrome P450 enzymes (reviewed in Stenmark et al., 2009). Futhermore, monocrotaline may damage the liver by causing hepatic veno-occlusive disease which is not normally observed in PAH and may hence confound the study of PAH-associated phenotypes in MCT rats (Roth et al., 1981; DeLeve et al., 1999).

1.3.3.2 – Chronic hypoxia

Unlike monocrotaline, chronic hypoxia is a physiological stimulus that can lead to or accelerate the development of pulmonary hypertension in humans (Vender, 1994). Chronic hypoxia is a model of Group 3 pulmonary hypertension and usually involves exposing mice and rats to normobaric or hypobaric hypoxia for 2 to 4 weeks (West & Hemnes, 2011). The response to chronic hypoxia is very predictable and reproducible within a specific animal strain, with most of these changes occurring within the first 3 to 4 weeks before stabilising (West & Hemnes, 2011). Whilst mice display only modest vascular remodelling following exposure to chronic hypoxia, exposure to chronic hypoxia in rats causes several PH-associated phenotypes such as muscularisation of previously non-muscularised arteries, medial thickening, and increased proliferation of PASMCs and adventitial fibroblasts (Stenmark et al., 2009; Pak et al., 2010).

However, there is minimal evidence of vascular obstruction or plexiform lesions, with most hypoxia-induced structural changes gradually reversing following removal of the hypoxic stimulus (Meyrick & Reid, 1980). Furthermore, it is unclear whether the loss of smaller pulmonary vessels that is thought to be associated with human PAH is also present in hypoxic rats (Stenmark et al., 2009). There is also a lot of variation in the response to hypoxia with age and sex, as well as between and within species (Aguirre et al., 2000). In addition, hypoxic pulmonary vasoconstriction is weaker in humans than in rats (Reeves et al., 1979). Therefore,

the chronic hypoxia model of PH is more representative of less severe PH, whereas the MCT model may have more relevance to advanced stages of PH.

1.3.3.3 – Refinement of the MCT and chronic hypoxia models of pulmonary hypertension

A systematic review and meta-analysis of studies reporting the use of animal models of PH revealed that nearly all (94.6%) of the studies reviewed used the MCT and chronic hypoxia models (Sztuka & Jasinska-Stroschein, 2017). However, these models do not recapitulate more complex phenotypes such as neointimal and plexiform lesions that are often associated with advanced PAH in humans (Stenmark et al., 2009). As a result, attempts have been made to refine these animal models of PH in order to more closely model the human disease state.

For example, monocrotaline injury in combination with one-sided pneumonectomy in rats induces intimal remodelling in distal pulmonary arteries, which is not observed following MCT injection alone (Yi et al., 2000), although this model still could not recapitulate the complex plexiform lesions found in humans.

Furthermore, unlike exposure to chronic hypoxia alone, the vascular endothelial growth factor (VEGF) receptor inhibitor Sugen-5416 in combination with chronic hypoxia causes severe PH in rats which persists and progresses after removal of the hypoxic stimulus (Taraseviciene-Stewart et al., 2001). In addition, Sugen/hypoxic rats display minimal responses to vasodilators such as iloprost (Oka et al., 2007) and sometimes develop complex plexiform-like lesions (Abe et al., 2010). As a result, whilst the chronic hypoxia model is more representative of Group 3 PH, the Sugen-5416/hypoxia model is considered to more closely resemble the irreversible nature of severe Group 1 PAH in humans. In addition, unlike MCT, Sugen-5416 only affects the lungs, where it promotes the selection of apoptosis-resistant ECs which subsequently proliferate (Sakao et al., 2005). Moreover, the Sugen-hypoxia model is associated with an inflammatory cytokine profile that is similar to that of PAH patients (Taraseviciene-Stewart et al., 2001).

1.3.3.4 – Transgenic mouse models of pulmonary hypertension

In addition to the MCT and the Sugen/hypoxia models of PH, gene overexpression, knockout and knock-in strategies in mice have led to the development of several transgenic mouse models of pulmonary hypertension. For example, whilst heterozygous *Bmpr2* knockout (*Bmpr2*$^{+/-}$)

mice (Beppu et al., 2005) do not develop pulmonary hypertension in the absence of additional triggers, chronic administration of the bacterial endotoxin lipopolysaccharide (LPS) induced pulmonary hypertension in *Bmpr2*$^{+/-}$ mice, where it was associated with increased IL-6 and KC (an analogue of IL-8) expression in PASMCs (Soon et al., 2015). *Bmpr2* deficiency in these mice was also linked to reduced expression of extracellular superoxide dismutase (SOD3) which scavenges superoxide radicals by converting them into the diffusible second messenger hydrogen peroxide (H_2O_2) (Soon et al., 2015). In line with these findings, the superoxide dismutase mimetic tempol reduced inflammation and prevented PH development in *Bmpr2*$^{+/-}$ mice (Soon et al., 2015), whereas lung-specific SOD3 overexpression attenuated pulmonary hypertension in hypoxic mice (Nozik-Grayck et al., 2008).

Another *Bmpr2*$^{+/-}$ mouse model of Group 1 PH was developed by West et al. (2008), who generated doxycycline-inducible transgenic mice in which a known, pathogenic heterozygous R899X mutation in *BMPR2* was placed under the control of the smooth muscle-specific SM22 promoter. Smooth muscle-specific overexpression of the R899X mutation in these mice resulted in the infiltration of inflammatory cells into the perivascular region but only elevated RVSPs in about one-third of animals, with some mice developing complex vascular lesions (West et al., 2008). By comparison, similar histological changes were observed when West et al. used the universal Rosa26 promoter to drive expression of the R899X mutation in all cell types, but this time 75% of mice developed increased RVSP after 8 weeks (West & Hemnes, 2011). By contrast, *Bmpr2*$^{+/R899X}$ knock-in mice harbouring a heterozygous R899X mutation in exon 12 of the endogenous *Bmpr2* locus did not display increased RVSP at 3 months of age (Long et al., 2015). However, these mice developed elevated RVSP and displayed increased muscularisation of distal pulmonary arteries by 6 months of age, although no right ventricular hypertrophy was observed (Long et al., 2015).

Furthermore, lung-specific overexpression of the pro-inflammatory cytokine IL-6 in mice promoted inflammatory events in distal pulmonary vessels together with the formation of neointimal lesions after exposure to chronic hypoxia (Steiner et al., 2009). Conversely, *Il-6*$^{-/-}$ mice exposed to hypoxia for two weeks displayed reduced recruitment of inflammatory cells as well as reduced RVSP, RV hypertrophy and medial thickness of muscular pulmonary vessels in comparison to wild-type littermates (Savale et al., 2009). Moreover, lung-specific overexpression of TNFα, achieved by placing TNFα under the control of the surfactant protein C (SP-C) promoter, stimulated the development of severe PH and RV hypertrophy in mice (Fujita et al., 2001).

Other transgenic mouse models of PH include (i) *Tie2* Cre-mediated disruption of *Egln1* which results in the spontaneous development of progressive PH (Dai et al., 2016), (ii) overexpression of the serotonin plasma membrane transporter 5-HTT (Guignabert et al., 2006) and (iii) vasoactive intestinal peptide (VIP) knockout (Said et al., 2007). However, these models also do not recapitulate the diverse aetiology and complex pathology of human forms of pulmonary hypertension.

1.3.3.5 – Other animal models of pulmonary hypertension

Attempts have also been made to generate a mouse model of schistosomiasis infection, which is thought to be the single largest cause of PAH worldwide (Graham et al., 2010; Rabinovitch et al., 2014). Chronic infection of female C57BL/6 mice with *Schistosoma mansoni* resulted in profound pulmonary vascular remodelling, infiltration of inflammatory cells into the perivascular region, severe thickening of the media of small pulmonary arteries, and the formation of plexiform-like lesions (Crosby et al., 2010). Furthermore, these mice developed significantly increased RVSP and right ventricular hypertrophy at 25 weeks after infection (Crosby et al., 2011).

Other animal models of PH include the use of fawn-hooded rats which spontaneously develop PH (Sato et al., 1992), as well as ligation of the ductus arteriosus or graft placement between the ascending aorta and the main pulmonary artery in fetal lambs (Morin, 1989; Abman et al., 1989; Belik et al., 1993; Black et al., 1998) to model the development of persistent pulmonary hypertension of the newborn (PPHN).

By contrast, there are no animal models of PH secondary to left heart disease (Group 2), and there are also no rodent models of CTEPH (Group 4). Although several large animal models of chronic CTEPH have been described, they are difficult to create, requiring repetitive embolisation of venous thrombi in addition to the use of fibrinolytic inhibitors (Mercier & Fadel, 2013). Similarly, animal models of pulmonary hypertension due to multifactorial reasons (Group 5) have provided little insight into the pathogenesis of this disease (Ryan et al., 2011).

1.3.4 – Challenges associated with studying pulmonary arterial hypertension

Our understanding of PAH is hampered by the limited availability of human tissue which can only be obtained from patients with end-stage disease, thus making it difficult to determine how PAH is established and how it progresses. Furthermore, these cells have a limited proliferative capacity, meaning that repeated biopsies are required to study individual *BMPR2* mutations. Moreover, as described above, currently available animal models of PAH are associated with several limitations and are unable to recapitulate the complex aetiology and pathology observed in patients with pulmonary hypertension.

Therefore, alternative human disease models of PAH are required to gain a better understanding of PAH establishment and progression. One way in which this could be achieved is through the use of induced pluripotent stem cells (iPSCs), which have been used to model a number of human diseases, including PAH (West et al., 2014; Sa et al., 2017; Gu et al., 2017; Kiskin et al., 2018), as described below.

1.4 – Disease modelling using induced pluripotent stem cells

1.4.1 – Introduction to induced pluripotent stem cells

Embryonic stem cells (ESCs) are derived from the inner cell mass of blastocyst stage embryos and are able to limitlessly self-renew whilst having the potential to differentiate into any cell type within the human body (Thomson et al., 1998; Kiskinis & Eggan, 2010). However, the expansion and differentiation of human ESCs is associated with ethical concerns (Grskovic et al., 2011). By contrast, induced pluripotent stem cells are highly similar to ESCs, but are generated by reprogramming the nuclei of somatic cells via the ectopic expression of a select group of transcription factors (Takahashi & Yamanaka, 2006).

The first iPSCs were generated by retroviral vector-mediated delivery of the transcription factors Oct4, Sox2, Klf4 and c-Myc (OKSM) into mouse skin fibroblasts (Takahashi & Yamanaka, 2006). This was soon followed by the generation of human iPSCs from skin fibroblasts (Takahashi et al., 2007; Yu et al., 2007; Lowry et al., 2008), human peripheral blood (Loh et al., 2009; Loh et al., 2010), and other somatic cell types.

Although skin fibroblasts are the most common cell type used for generating iPSCs, the genomes of many fibroblast-derived iPSC lines carry copy number variations (CNVs) which

could potentially affect their phenotypic behaviour (Hussein et al., 2011; Yusa et al., 2011; Martins-Taylor & Xu, 2012). By contrast, previous work in our laboratory has shown that human iPSC lines generated by retroviral-based reprogramming of human blood outgrowth endothelial cells [BOECs, also known as late-outgrowth endothelial progenitor cells (L-EPCs)] display normal karyotypes compared to the genomes of donor-matched circulating monocytes (Geti et al., 2012). The majority (>80%) of these BOEC-derived iPSC lines did not acquire any CNVs during reprogramming and displayed a reprogramming efficiency that was approximately 10-fold higher compared to the two fibroblast lines tested (Geti et al., 2012). Furthermore, BOECs are isolated from human peripheral blood (Lin et al., 2000; Medina et al., 2010) which is less invasive than performing skin biopsies to isolate skin fibroblasts. Taken together, these observations highlight some of the advantages of using BOECs to generate human iPSC lines.

iPSCs are characterised by their ability to differentiate into the three embryonic germ layers (ectoderm, mesoderm and endoderm) (**Figure 1.7**) and form teratomas after subcutaneous or intramuscular injection into immunodeficient mice (Lensch et al., 2007; Takahashi et al., 2007; Yu et al., 2007; Park et al., 2008). At the molecular level, iPSCs must (i) express key pluripotency genes including *OCT4*, *SOX2* and *NANOG* (Stadtfeld et al., 2008), (ii) stain positively for the embryonic antigens SSEA3, TRA-1-60, and TRA-1-81 (Chan et al., 2009), (iii) display functional telomerase expression (Wolf & Goff, 2007), and (iv) lack expression of the delivered reprogramming factors with concomitant downregulation of lineage-specific genes associated with the adult cell that the iPSCs were derived from (Robinton & Daley, 2012). In culture, iPSC colonies can be identified by their cobblestone morphology, prominent nucleoli and well-defined individual cell borders (Robinton & Daley, 2012).

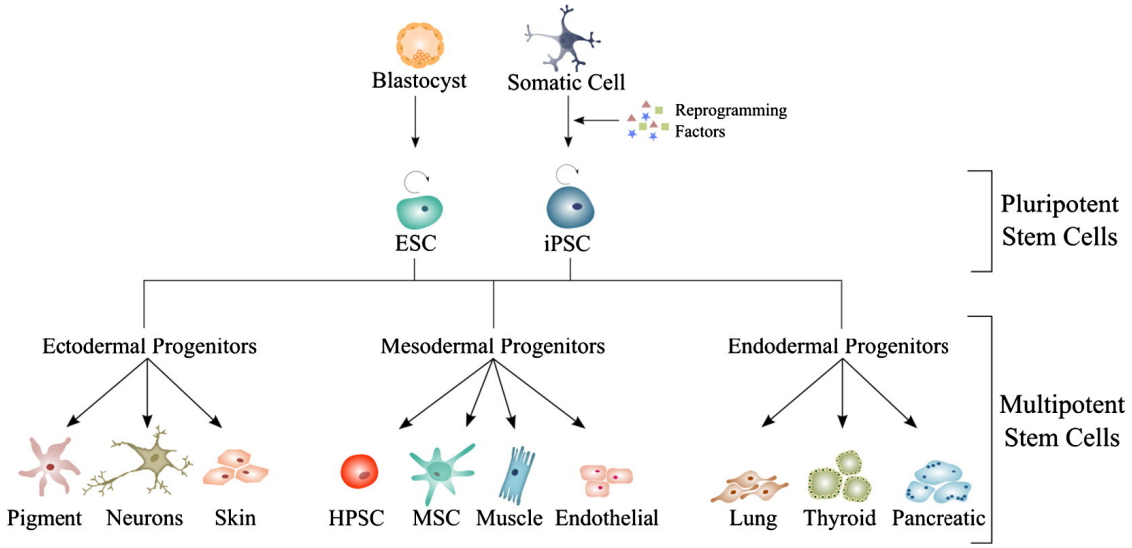

Figure 1.7. Differentiation potential of pluripotent stem cells. Embryonic stem cells (ESCs) and induced pluripotent stem cells (iPSCs) are able to limitlessly self-renew and differentiate into all cell types of the three embryonic germ layers (ectoderm, mesoderm and endoderm). ESCs are derived from the inner cell mass of blastocyst stage embryos, whereas iPSCs are derived by nuclear reprogramming of somatic cells via the ectopic expression of a select group of transcription factors, typically Oct4, Sox2, Klf4 and c-Myc. HPSC, haematopoietic stem cell; MSC, mesenchymal stem cell (from Kaebisch et al., 2015)

1.4.2 – Utility of induced pluripotent stem cells for disease modelling

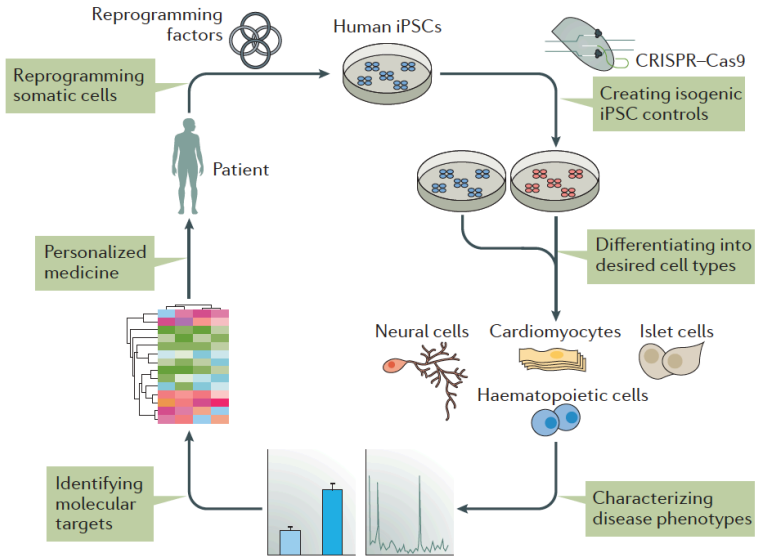

Figure 1.8. Disease modelling using induced pluripotent stem cells. iPSC-based disease modelling typically involves isolating patient-derived iPSCs, introducing disease-associated mutations into control iPSCs using CRISPR-Cas9 gene editing to generate cells with isogenic backgrounds, and differentiating these cells into the cell types implicated in the disease being modelled. The iPSC-derived cells are then used to study mechanisms contributing to the establishment of disease-associated cellular phenotypes and identify molecular targets that could be used for drug screening and personalised medicine (from Shi et al., 2017).

Human induced pluripotent stem cells offer an invaluable model system for studying the molecular pathogenesis of human diseases which have strong genetic components. Unlike non-human animal models, patient-derived iPSCs are genetically matched to the individual they were derived from. Furthermore, whilst patient-derived primary cells are difficult to isolate and are of limited supply, iPSCs can be differentiated into virtually any disease-relevant cell type, thus providing a potentially limitless supply of patient-specific cells which can be used for drug screening and personalised medicine (**Figure 1.8**).

Since their discovery, iPSCs have been successfully differentiated into a number of different cell types, including neurons (Dimos et al., 2008; Ebert et al., 2009; Soldner et al., 2009), blood cells (Choi et al., 2009; Ye et al., 2009), adipocytes (Taura et al., 2009), fibroblasts (Hockemeyer et al., 2008; Maherali et al., 2008), endothelial cells (Choi et al., 2009; Patsch et al., 2015; Sa et al., 2017, Kiskin et al., 2018), and smooth muscle cells (Cheung et al., 2012;

Patsch et al., 2015; Kiskin et al., 2018). iPSCs have also been isolated from individuals with different diseases and were shown to retain the genetic characteristics of their donor cells (Park et al., 2008). This makes patient-specific iPSCs especially useful for studying monogenic diseases or diseases with strong genetic components such as HPAH (Ebert et al., 2009; Lee et al., 2009). Furthermore, patient-specific iPSCs can be differentiated into large numbers of disease-relevant cells which were previously difficult to obtain, such as neurons and cardiomyocytes (Shi et al., 2017). This approach would therefore be extremely useful for generating pulmonary vascular-like cells to model PAH, as pulmonary artery smooth muscle and endothelial cells can only be obtained from patients at the time of transplantation or death.

Another advantage of using iPSCs for disease modelling is their amenability to genetic manipulation (Hockemeyer & Jaenisch, 2016). Gene editing efficiency can be improved by using zinc-finger nucleases (ZFN) (Hockemeyer et al., 2009; Zou et al., 2009), transcription activator-like effector nucleases (TALENs) (Christian et al., 2010; Hockemeyer et al., 2011; Sanjana et al., 2012) and the CRISPR-Cas9 (Clustered Regularly Interspaced Short Palindromic Repeats CRISPR-associated protein 9) system (Jinek et al., 2012; Cong et al., 2013; Perez-Pinera et al., 2013; Shalem et al., 2014) to induce double-stranded DNA breaks at sites of gene modification.

Owing to its relatively low cost and ease of use, the CRISPR-Cas9 system has become the most commonly used gene editing strategy. CRISPR-Cas9 gene editing has been used to introduce disease-associated mutations into wild-type iPSCs (Wen et al., 2014; Murai et al., 2016) and to correct such mutations in patient-derived iPSCs (Hotta & Yamanaka, 2015; Seah et al., 2015; Deleidi & Yu, 2016; Orqueda et al., 2016; Gu et al., 2017), thus allowing comparisons to be made between isogenic lines that are genetically identical apart from the introduced mutation. This approach avoids potential confounding effects of inter-line variability on the phenotypes being studied and has great utility in investigating the contributions of specific mutations to the establishment of disease-associated phenotypes. Given the reduced penetrance of *BMPR2* mutations in PAH (Machado et al., 2009), genetically matched wild-type iPSCs and their gene-edited counterparts could therefore be very useful for studying the precise role of *BMPR2* mutations in establishing PAH-associated disease phenotypes.

1.4.3 – Developing induced pluripotent stem cell models of pulmonary arterial hypertension

Owing to the limited availability of diseased pulmonary vascular cells from PAH patients, attempts have been made to generate iPSC-derived cells that could serve as surrogates for adult cells and be used to study PAH.

West et al. (2014) differentiated two wild-type and two PAH patient-derived iPSC lines (derived from skin fibroblasts) into vascular mesenchymal stromal cells (iPSC-MSC) and subsequently into EC-like cells (iPSC-ECL), using microarrays to compare their gene expression profiles with control and IPAH patient-derived PAECs, as well as with skin fibroblasts from IPAH and HPAH patients (West et al., 2014). The authors looked at the effect of decreased BMPR2 signalling on gene expression at various stages of differentiation of iPSC-MSCs and iPSC-ECLs and identified 33 developmental genes and 18 genes related to cell death that were specifically upregulated in *BMPR2* mutants during differentiation. Among these, the Wnt receptors *FZD4* and *FZD5* and secreted Wnt modulators *SFRP1* and *SFRP2* were upregulated in *BMPR2* mutants compared to controls, leading the authors to conclude that aberrant BMPR2 signalling may result in increased canonical Wnt/β-catenin signalling in PAH (West et al., 2014). In support of these observations, increased expression of the Wnt pathway genes *FZD4*, *FZD10* and *AXIN2* was detected in lung tissue samples from 22 IPAH patients compared to 22 control subjects (Wu et al., 2016), although none of these IPAH patients carried *BMPR2* mutations. Furthermore, non-canonical Wnt signalling has been associated with vasoconstriction and vascular remodelling in IPAH patients (Laumanns et al., 2009).

However, the iPSC model of PAH developed by West et al. (2014) was limited to the analysis of just two iPSC-ECL and iPSC-MSC lines that were not genetically matched, and the authors also did not characterise iPSC-ECLs in terms of their proliferative and apoptotic responses. Furthermore, although *BMPR2* mutant iPSC-MSCs were less apoptotic compared to control iPSC-MSCs, they were not more proliferative (West et al., 2014). Therefore, further work will be required to clarify whether reduced BMPR2 signalling contributes to increased Wnt signalling in PAH.

In addition to the iPSC model of PAH developed by West and colleagues, iPSC-derived endothelial cells were used in two subsequent studies as surrogates for PAECs to model PAH (Sa et al., 2017; Gu et al., 2017). Sa et al. (2017) derived iPSCs from skin fibroblasts of HPAH and IPAH patients, differentiated these into iPSC-ECs and compared these iPSC-ECs to PAECs obtained from the same patients in terms of their ability to recapitulate several PAH-associated disease phenotypes (Sa et al., 2017). However, the iPSC-ECs generated by Sa et al. did not recapitulate increased proliferation, mitochondrial hyperpolarisation and DNA damage that have previously been reported in IPAH and HPAH-derived PAECs (Diebold et al., 2015; Sa et al., 2017).

Nevertheless, Sa et al. showed that matched patient-derived iPSC-ECs and PAECs displayed similar susceptibility to apoptosis and reduction in BMPR2 signalling, cell adhesion and tube formation compared to iPSC-ECs and PAECs from control individuals (Sa et al., 2017). RNA-Seq analysis of these cells suggested that impaired migration and survival were attributed to increased expression of kisspeptin 1 (*KISS1*) and downregulation of carboxylesterase 1 (*CES1*), respectively (Sa et al., 2017). Furthermore, IPAH/HPAH-derived PAECs and iPSC-ECs displayed similar responses to the immunosuppressant FK506 and the neutrophil elastase inhibitor, elafin, both of which improved angiogenesis in two patient-derived iPSC-EC and PAEC lines. In addition, the authors showed that the lack of a response to FK506 and elafin in the other five cell lines was at least partly due to increased expression of the anti-migratory factor split guidance ligand 3 (*SLIT3*), suggesting that *SLIT3* might act as a potential genetic modifier in PAH (Sa et al., 2017).

The same group subsequently went on to look for other possible genetic modifiers in three families with FPAH patients and unaffected mutation carriers (UMCs) (Gu et al., 2017). UMC iPSC-ECs displayed increased cell adhesion and survival compared to FPAH-derived iPSC-ECs harbouring the same *BMPR2* mutation, which the authors attributed to increased expression of BMPR2 activators and a reduced expression of BMPR2 inhibitors in UMC iPSC-ECs relative to FPAH iPSC-ECs (Gu et al., 2017). However, preserved UMC iPSC–EC survival was not found to be regulated by the BMPR2 pathway (Gu et al., 2017). Instead, baculoviral IAP repeat containing 3 (*BIRC3*), a gene encoding a protein that is thought to protect ECs against apoptosis, was upregulated in UMC- relative to FPAH-derived iPSC-ECs in all three families. Whilst CRISPR-Cas9-mediated repair of the C118W *BMPR2* mutation in FPAH iPSC-ECs restored cell adhesion, cell survival and the expression of BMPR2 target genes to control levels, *BIRC3* expression remained upregulated, suggesting that BIRC3 expression is

not regulated by BMPR2 signalling (Gu et al., 2017). siRNA-mediated knock-down of *BIRC3* increased apoptosis in UMC iPSC-ECs, leading the authors to conclude that *BIRC3* is responsible for the preserved cell survival in UMC iPSC-ECs and may hence act as a protective genetic modifier in PAH (Gu et al., 2017). These findings agree with previous work showing that reduced BMPR2 signalling in PAECs is associated with increased apoptosis in response to injury (de Jesus Perez et al., 2009) and with impaired adhesion and migration (de Jesus Perez et al., 2012; Rhodes et al., 2015).

1.4.4 – Limitations of currently available iPSC models of pulmonary arterial hypertension

Whilst the studies described above successfully generated iPSC-derived ECs and MSCs that could recapitulate several PAH-associated disease phenotypes and could be used to gain insight into some of the genes which may be dysregulated in PAH, these studies are associated with several limitations. For instance, neither *BMPR2* mutant iPSC-MSCs or iPSC-ECs were able to recapitulate the hallmark pro-proliferative phenotype of patient-derived *BMPR2*$^{+/-}$ PASMCs and PAECs. Furthermore, most cells used in these studies did not have isogenic backgrounds, thus making it very difficult to discern whether the introduction of a specific *BMPR2* mutation is sufficient to result in the acquisition of PAH-associated cellular phenotypes. Finally, whilst Sa et al. (2017), Gu et al. (2017) and West et al. (2014) showed that iPSC-ECs can be used as surrogates for PAECs for studying PAH, no iPSC-derived SMCs have yet been described that recapitulate PAH-associated PASMC phenotypes.

Therefore, developing protocols for differentiating iPSCs into vascular smooth muscle-like cells which could be used as surrogates for PASMCs would provide another critical source of cells that could further aid the study of the molecular mechanisms implicated in PAH establishment and progression.

1.5 – Vascular smooth muscle cell differentiation

1.5.1 – Embryonic origins of vascular smooth muscle cells

When developing protocols for differentiating iPSCs into vascular smooth muscle-like cells, the ultimate goal is to generate cells that are akin to the adult cell types being modelled or at least that these display functional responses akin to the specific type of primary cell they are trying to mimic.

Vascular smooth muscle is a mosaic tissue, with specific vascular beds being derived from one or more possible embryonic origins (reviewed in Majesky, 2007). Furthermore, individual vessels or even vessel segments may consist of multiple SMC populations that arise from distinct progenitor populations which themselves have unique developmental histories (Majesky, 2007). For example, lineage tracing has shown that four major embryonic lineages contribute to the pulmonary vasculature: (i) $Wnt1^+$ neural crest, which contributes to the SMCs at the root of the pulmonary artery (Jiang et al., 2000), (ii) cardiopulmonary progenitors (CPPs), which contribute ECs and SMCs to the proximal pulmonary artery and vein (Peng et al., 2013), (iii) Wilms' tumour 1-positive ($WT1^+$) mesothelium, which surrounds the lung and contributes widely to both ECs and SMCs throughout the vasculature (Que et al., 2008), and (iv) lateral plate mesoderm, which contributes to the PASMCs in peripheral pulmonary arteries (Hall et al., 2000).

The ability to recapitulate specific lineages and their vascular derivatives is likely to be critical for generating a high-fidelity model of PAH. This is because these SMC populations may display distinct, lineage-specific responses to the same stimuli, even under identical experimental conditions (Rosenquist et al., 1989; Topouzis & Majesky, 1996). Specific SMC subpopulations may also respond to injury in unique ways and may therefore contribute differently to the vascular remodelling process (Frid et al., 1997). Furthermore, depending on their anatomical origin, SMCs may display opposite responses to hypoxia. Systemic arteries relax in response to tissue hypoxia in order to improve blood flow and oxygen supply in hypoxic tissues (Detar, 1980; Gupte & Wolin, 2008). By contrast, pulmonary arteries respond by contracting, thereby diverting blood flow from poorly ventilated regions towards the more oxygenated areas of the lungs – a process termed hypoxic pulmonary vasoconstriction (HPV) (von Euler & Liljestrand, 1946).

Mammalian lung development begins with the ventral budding of the primordium from the foregut to form the lung bud (Perl & Whitsett, 1999). Pulmonary SMCs develop from local mesenchymal cells at the distal end of the growing lung bud, with the mesenchymal precursor cells gradually migrating in a distal to proximal fashion along the bronchial tree, whereas bronchial smooth muscle cells migrate in the opposite direction (Badri et al., 2008). As lung development proceeds, BMP4 becomes most highly expressed at the tips of the distal buds, suggesting that it plays a role in bronchial branching (Bellusci et al., 1996). Moreover, BMP4 differentially affects the proliferation and apoptosis of PASMCs depending on their location along the bronchial tree. For example, proximal PASMCs are growth-suppressed by BMP4, whereas distal PASMCs are not growth-suppressed by BMP4 (Yang et al., 2005). This is an important consideration in developing iPSC-SMC models of PAH, as it is the distal PASMCs that are thought to be predominantly affected in this disease (Humbert et al., 2004).

1.5.2 – Arterial and venous smooth muscle cells have different functions and identities

In addition to embryonic origin, it is important to consider arteriovenous (AV) specification when developing protocols for differentiating iPSCs into distal PASMC-like cells. This is because PAH predominantly affects arteries, with arterial and venous SMCs having distinct functions and identities (Wong et al., 2005; Deng et al., 2006). For example, arterial SMCs isolated from carotid arteries of male rabbits displayed elevated levels of the inhibitory proteoglycan decorin compared to SMCs isolated from the jugular vein (Wong et al., 2005). By contrast, jugular vein SMCs are more dedifferentiated, displaying reduced adhesion to collagen and fibronectin, and are associated with increased activity of the matrix metalloproteases MMP2 and MMP9 (Wong et al., 2005).

Furthermore, *Notch3* expression in mice was shown to be required for the maturation of arterial SMCs, with vascular smooth muscle cells (VSMCs) from *Notch3*$^{-/-}$ mice potentially being more venous in nature (Domenga et al., 2004). In addition, Li et al. (2011) showed that human arterial and venous SMCs differed in terms of their proliferative responses to the platelet-derived growth factor (PDGF) isoforms PDGF-AA and PDGF-BB (Li et al., 2011). The authors showed that PDGF-AA stimulated the proliferation of arterial but not venous SMCs, whilst human saphenous vein SMCs were more proliferative compared to arterial SMCs following stimulation with PDGF-BB (Li et al., 2011). Other genes that have been shown to be upregulated in arterial versus venous SMCs include regulator of G-protein synthesis 5 (*RGS5*), elastin and vimentin (Adams et al., 2000).

However, our current understanding of AV identity in SMCs, unlike in ECs, is very limited and modelling AV identity is a major challenge.

1.5.3 – Phenotypic plasticity of vascular smooth muscle cells

Another challenge of developing iPSC-SMC differentiation protocols is the ability to produce mature, fully differentiated SMCs. This is important because unlike skeletal or cardiac muscle, VSMCs are not terminally differentiated and are able to undergo transient changes between contractile, synthetic and intermediate phenotypic states in response to changes in signalling within their local environment (Wolinsky & Glagov, 1967; Owens, 1995). Mature, fully developed VSMCs are normally quiescent and have a contractile phenotype characterised by an elongated, spindle-shaped morphology, the presence of contractile filaments and the expression of contractile protein markers myosin heavy chain 11 (*MYH11*) and smoothelin (*SMTN*) (Sobue et al., 1999; Owens et al., 2004). However, in response to vascular injury, contractile VSMCs undergo phenotypic switching by becoming more proliferative and starting to secrete components of the extracellular matrix (ECM) such as collagen, elastin, fibronectin, laminin and proteoglycans (Stiemer et al., 1993; Kane et al., 2011). These dedifferentiated VSMCs have a 'synthetic' phenotype characterised by increased expression of proteolytic enzymes such as matrix metalloproteinases (MMPs) and serine elastases (Chelladurai et al., 2012), reduced *MYH11* expression (Owens, 1995) and a less elongated, cobblestone-like morphology referred to as an epithelioid (Chamley-Campbell et al., 1979; Hao et al., 2003).
Phenotypic switching plays an important role in pulmonary arterial hypertension, where increased degradation and reduced synthesis of the ECM contributes to vascular remodelling (Stenmark & Mecham, 1997; Vieillard-Baron et al., 2003). For example, the matrix-degrading enzymes MMP2 and MMP9 were found to be upregulated in PAH-derived PASMCs and patient-derived plasma samples, respectively (Lepetit et al., 2005). Furthermore, increased MMP expression has also been detected in the lungs of MCT rats (Schermuly et al., 2004; Pullamsetti et al., 2005), as well in cultured SMCs in response to TNFα treatment (Rajavashisth et al., 1999).

1.5.4 – Developing differentiation protocols for generating iPSC-derived SMCs

The directed *in vitro* differentiation of iPSCs into different cell types can be achieved by using specific concentrations, combinations and sequences of agonists and antagonists of a number of different signalling pathways to mimic the signalling events which occur during embryonic development (Murry & Keller, 2008; Cheung et al., 2012).

For example, Patsch et al. (2015) developed a chemically-defined differentiation protocol which involved using BMP4 treatment and glycogen synthase kinase 3 (GSK3) inhibition to differentiate pluripotent cells into mesoderm and subsequently into iPSC-derived ECs or SMCs via exposure to vascular endothelial growth factor A (VEGF-A) or PDGF-BB, respectively (Patsch et al., 2015). However, although metabolomic and transcriptome-wide expression analysis showed that these iPSC-derived ECs and VSMCs displayed a high degree of similarity to their respective primary cells (Patsch et al., 2015), these cells were not embryonic lineage-specific. Therefore, these cells are limited in terms of their ability to model specific SMC populations in distinct vascular regions which may display different signalling responses and disease susceptibility compared to SMC populations derived from other lineages (Haimovici & Maier, 1964; VanderLaan et al., 2004; Yang et al., 2005).

By contrast, by exploiting the principle that a posterior-anterior BMP concentration gradient along the primitive streak determines lateral plate mesoderm (LM) and paraxial mesoderm (PM) specification during embryogenesis (Dosch et al., 1997), Cheung et al. (2012) used varying concentrations of BMP4 to show that origin-specific smooth muscle cells can be generated from iPSCs via these two intermediate lineages (Cheung et al., 2012). Using this lineage-specific approach together with chemically-defined conditions, the authors showed that high BMP4 concentrations inhibit the development of paraxial mesoderm but promote LM specification. Once formed, the LM cells could subsequently be stimulated to differentiate into iPSC-SMCs by culturing the cells for 12 days in chemically defined medium containing PDGF-BB and TGF-β1. At the end of the differentiation protocol, over 80% of iPSC-SMCs derived from these intermediate populations expressed smooth muscle myosin heavy chain (MYH11), a marker which is only thought to be selectively expressed in mature, fully differentiated SMCs (Owens et al., 2004). Furthermore, these iPSC-SMCs displayed contractility and calcium transients when stimulated with carbachol, thus suggesting that these cells exhibit functional responses that are characteristic of adult vascular smooth muscle cells in general (Cheung et

al., 2012). However, it was not shown whether these iPSC-SMCs display functional responses akin to more specific types of VSMCs such as distal PASMCs.

1.6 – Aims and hypothesis

1.6.1. – Aims and objectives

The overarching aim of this thesis is to develop a human induced pluripotent stem cell-derived smooth muscle cell model of PAH associated with mutations in *BMPR2*.

To achieve this, the specific aims and objectives of this thesis are as follows:

1) To use CRISPR-Cas9 gene editing to introduce a known disease-associated *BMPR2* mutation into a human control iPSC line to generate wild-type and *BMPR2*$^{+/-}$ iPSCs with an isogenic background

2) To differentiate control and *BMPR2*$^{+/-}$ iPSCs into lineage-specific iPSC-derived smooth muscle-like cells and show that these iPSC-SMCs can be used as surrogates for distal PASMCs for studying PAH establishment and progression.

3) To determine the extent to which *BMPR2*$^{+/-}$ iPSC-SMCs recapitulate PAH-associated disease phenotypes observed in PASMCs and thus whether the introduction of a single *BMPR2* mutation is necessary and sufficient to establish PAH-associated cellular phenotypes in iPSC-SMCs

1.6.2. – Hypothesis

My hypothesis is that the introduction of a single *BMPR2* mutation is necessary but not sufficient to establish PAH-associated cellular phenotypes in iPSC-SMCs, with additional factors being required to fully recapitulate PAH-associated cellular phenotypes observed in PASMCs from PAH patients.

CHAPTER 2 – MATERIALS AND METHODS

2.1 – Characteristics of human iPSC and PASMC lines

The characteristics of the human induced pluripotent stem cell (iPSC) and pulmonary artery smooth muscle cell (PASMC) lines used in this investigation are summarised in **Table 2.1** and **Table 2.2** below. Prior to the start of this study, human iPSC lines were generated by reprogramming late blood outgrowth endothelial cells (BOECs) isolated from human peripheral blood as previously described (Geti et al., 2012; Ormiston et al., 2015). All blood donors provided informed written consent in accordance with human study 07/H0306/134 (Cambridgeshire 3 Research Ethics Committee, UK). For PASMC isolation, the Papworth Hospital ethical review committee (Papworth Everard, Cambridge, UK) approved the study, and subjects or relatives gave informed written consent.

iPSC line	Sex	Age	Disease status	*BMPR2* status
C2	M	20	No disease	Wild-type
C6	F	40	No disease	Wild-type
C10	M	28	No disease	Wild-type
C2 W9X$^{+/-}$	M	20	No disease	W9X
C2 ΔExon1	M	20	No disease	Deletion of *BMPR2* Exon 1
B3	M	27	No disease	C347R
B4	F	37	Hereditary PAH	W9X
B11	M	32	Hereditary PAH	Del in 5'UTR
IPAH1	M	62	Idiopathic PAH	Wild-type

Table 2.1. Characteristics of human iPSC lines. Prior to the start of this thesis project, human iPSC lines were generated from late blood outgrowth endothelial cells from three control subjects (C2, C6 and C10), three heterozygous *BMPR2* mutation carriers (B3, B4 and B11) and one idiopathic PAH patient (IPAH1), as described in Geti et al. (2012). The isogenic C2 W9X$^{+/-}$ and C2 ΔExon1 iPSC lines were generated as part of this thesis project, as described in *Section 2.4* and in *Chapter 3, Section 3.1*.

PASMC line	Sex	Age	Disease status	BMPR2 status
32 MP	F	58	Centrilobular emphysema	Wild-type
79 MP	M	60	Squamous cell carcinoma	Wild-type
82 MP	F	71	Adenocarcinoma	Wild-type
83 MP	F	56	Unknown donor control	Wild-type
84 MP	F	59	Differential adenocarcinoma	Wild-type
56 MP	M	58	Hereditary PAH	C347R
67 MP	M	22	Hereditary PAH	W9X
73 MP	F	30	Hereditary PAH	R899X

Table 2.2. Characteristics of human pulmonary artery smooth muscle cell lines

2.2 – Non-commercial cell culture media recipes

All cell culture media were supplemented with antibiotic-antimycotic solution (Thermo Fisher Scientific) (1% v/v) containing penicillin (10,000 Units/mL), streptomycin (10,000 µg/mL) and amphotericin B (25 µg/mL). Where non-sterile components were added, media were sterile-filtered through a polyethersulfone (PES) membrane with a pore size of 0.2 µm.

Chemically-defined medium (CDM): IMDM (49.5% v/v), Ham's F-12 Nutrient Mixture (49.5% v/v), chemically defined lipid concentrate (1% v/v) (all from Thermo Fisher Scientific), transferrin from human serum (15 µg/ml, Roche), recombinant human insulin (7 µg/ml, Roche), and 1-thioglycerol (450 µM, Sigma) (Vallier et al., 2009)

CDM-BSA: Chemically-defined medium (CDM) supplemented with bovine serum albumin (BSA) Cohn fraction V (5 mg/ml, Europa Bioproducts) (Brons et al., 2007)

CDM-PVA: Chemically-defined medium (CDM) supplemented with polyvinyl alcohol (1.2 mg/ml, Sigma)

KnockOut Serum Replacement (KSR) medium: DMEM/F12 (79.5% v/v), Gibco KnockOut Serum Replacement (KOSR) (19.5% v/v), MEM Non-Essential Amino Acids Solution (1% v/v), L-glutamine (2 mM) (all from Thermo Fisher Scientific) and fibroblast growth factor 2 (FGF-2) (10 ng/ml, Wellcome Trust – MRC Cambridge Stem Cell Institute, Cambridge, UK)

CDM-BSA/KSR ('BK') feeder-free iPSC culture medium: CDM-BSA (50% v/v), KSR (50% v/v), activin A (12.5 ng/ml), FGF-2 (15 ng/ml) (Wellcome Trust – MRC Cambridge Stem Cell Institute, Cambridge, UK) and L-ascorbic acid (50 ng/ml, Sigma).

Feeder-dependent iPSC culture medium: CDM-BSA (25% v/v), KSR (50% v/v) and filtered conditioned medium (25% v/v) from irradiated, mitotically inactive mouse embryonic fibroblasts (iMEFs) (Wellcome Trust – MRC Cambridge Stem Cell Institute, Cambridge, UK) cultured for 24 hours in CDM-BSA + FGF-2 (4 ng/ml). Feeder-dependent iPSC culture medium also contains activin A (12.5 ng/ml), FGF-2 (15 ng/ml) and L-ascorbic acid (50 ng/ml).

2.3 – Human pluripotent stem cell and PASMC culture

To aid attachment of human pluripotent stem cells (hPSCs), empty cell culture plates were incubated for one hour at 37°C in a 0.2% w/v solution of porcine gelatine (Sigma) in HyClone cell culture grade water (GE Healthcare Life Sciences) followed by incubation in DMEM supplemented with 10% FBS and 2-mercaptoethanol (55 μM, Sigma) for at least 2 hours at 37°C. Prior to laying down cells, this medium was aspirated and the plates washed once with PBS before laying down cells in their respective cell culture media.

Feeder-free human iPSCs were cultured in BK medium, whereas feeder-dependent iPSCs growing on top of a 25% confluent layer of irradiated mouse embryonic fibroblasts (iMEFs) were cultured in feeder-dependent iPSC culture medium (*See Section 2.2*). Feeder-free H9 human embryonic stem cells (hESCs) were cultured in CDM-BSA supplemented with activin A (10 ng/ml) and FGF-2 (12 ng/ml) (Vallier et al., 2009).

Human pulmonary artery smooth muscle cells (PASMCs) from PAH patients carrying heterozygous *BMPR2* mutations, or from unaffected donor control subjects at the time of heart/lung transplantation (**Table 2.2**), were cultured in high glucose (4.5 g/L) DMEM (Thermo Fisher Scientific) supplemented with 10% heat-inactivated foetal bovine serum (FBS) (Sigma) and antibiotic-antimycotic solution (1% v/v) (Thermo Fisher Scientific). All cells were incubated at 37°C in a humidified atmosphere containing 5% CO_2.

2.4 – Generation of *BMPR2*$^{+/-}$ iPSC lines with isogenic backgrounds

2.4.1 – Site-directed mutagenesis

The generation of the W9X targeting construct and the CRISPR-Cas9 targeting strategy used to introduce the W9X mutation into exon 1 of the *BMPR2* gene are described in *Section 3.1* in *Chapter 3*. The W9X mutation was created by site-directed mutagenesis by following the QuikChange II Site-Directed Mutagenesis (SDM) kit protocol (Agilent Technologies). The polymerase chain reaction (PCR) cycling parameters used for site-directed mutagenesis are shown in **Table 2.3**.

Stage	Number of Cycles	Temperature	Time
1	1	95°C	5 minutes
2	18	95°C	30 seconds
		55°C	1 minute
		68°C	5 minutes 30 seconds

Table 2.3. PCR cycling parameters used for site-directed mutagenesis to insert the W9X *BMPR2* mutation into the targeting construct.

2.4.2 – Generation of the ΔExon1 targeting construct

The targeting strategy used to delete exon1 of the *BMPR2* gene is presented in **Figure 3.3** in *Chapter 3*. Genomic DNA, extracted from C2 iPSCs using the DNeasy Blood and Tissue kit (Qiagen), was used to PCR amplify the left and right homology arms using Pfx50 DNA polymerase (Thermo Fisher Scientific) and the primers listed in **Table 2.6**. The 5' homology arm spans the region chr2: 202,376,583-202,377,403, 883 base pairs upstream of *BMPR2* exon 1, and the 3' homology arms spans the region chr2: 202,377,511-202,378,844. Each PCR-amplified product was then TOPO cloned using Zero Blunt TOPO PCR cloning kit according to the manufacturer's instructions (Thermo Fisher Scientific) and used to finalise the construct. Using the QuikChange II Site-Directed Mutagenesis kit (Agilent Technologies) protocol, a point base pair mutation changing a *Sty1* restriction endonuclease site to a *PvuI* site was created 285bp downstream of the region where the left homology starts. The GeneArt® CRISPR Nuclease Vector (Thermo Fisher Scientific) used for W9X targeting was also used for ΔExon1 targeting, and successful introduction of the ΔExon1 mutation into C2 iPSCs was confirmed by Sanger sequencing (performed by Source Bioscience, Cambridge, UK).

2.4.3 – Cell electroporation

The W9X and ΔExon1 DNA targeting vectors (*see Section 3.1*) were linearised by digestion with NotI-HF restriction enzyme (New England Biolabs) at 37°C overnight, followed by DNA precipitation to purify DNA from the reaction mixture. DNA precipitation was performed by adding 10% by volume of sodium acetate (3M, pH 5.2) to the digestion reaction, vortexing for 1 minute, adding 2x volume of ice-cold (-20°C) absolute molecular biology grade ethanol (Sigma), vortexing for a further 2 minutes and then placing the sample in a -80°C freezer for at least 1 hour. Subsequently, the sample was centrifuged at maximum speed (≤17,000 x *g*) for 20 minutes at 4°C before discarding the supernatant, washing the pellet with 70% ethanol, centrifuging at full speed for 5 minutes, air drying the pellet and finally re-suspending the pellet in 12 µl of EB elution buffer (Qiagen).

The linearised targeting vector (2 µg) and CRISPR vector (2 µg) were subsequently co-transfected into C2 wild-type iPSCs by electroporation using Human Stem Cell Nucleofector Kit 1 according to the manufacturer's guidelines (Lonza). To achieve this, C2 iPSCs growing in 6-well plates were washed with 1.5 ml of PBS, trypsinised for 5 minutes at 37 °C using 0.5 ml of 1x TrypLE Select (Thermo Fisher Scientific) supplemented with 2 mM EDTA (Thermo Fisher Scientific) and neutralised using 1 ml of BK medium per well. Cells in the resulting cell suspension were then counted before transferring 8 x 10^5 cells to a separate 1.5 ml centrifuge tube and centrifuging these cells at 150 x *g* for 3 minutes at room temperature prior to gently re-suspending the cell pellet in 100 µl of Nucleofector® Solution (Lonza). 2 µg of linearised targeting vector and 2 µg of CRISPR vector were then added prior to transferring the cell/DNA suspension to a cuvette without introducing any bubbles. The cuvette containing the cell/DNA suspension was subsequently inserted into the Amaxa Nuleofector machine (Lonza) and electroporated using Nucleofector Program B-016. A separate set of C2 iPSCs were electroporated with 2 µg of pmaxGFP vector (Lonza) as a positive control. Subsequently, 500 µl of warm BK culture medium supplemented with Rho-associated protein kinase (ROCK) inhibitor Y-27632 dihydrochloride (1 µM, Tocris Bioscience) was gently added to the cuvette before using a supplied pipette (Lonza) to gently transfer the sample into a gelatine-coated 24-well plate containing 500 µl of warm BK culture medium per well (to achieve a final volume of 1 ml of media per well).

2.4.4 – Analysis of electroporation efficiency

To determine whether electroporation was successful, the cells were assessed for orange fluorescence [indicative of orange fluorescent protein (OFP) expression] and/or green fluorescence (indicative of pmaxGFP expression) by flow cytometry approximately 24 hours post-transfection. Flow cytometric analysis of OFP and pmaxGFP expression was performed by staff at the NIHR Cambridge BRC Cell Phenotyping Hub at the Department of Medicine, University of Cambridge using a BD FACSCanto flow cytometer and BD FACSDiva software (version 6.1.3). In addition, transfection efficiency was visually assessed 48 hours after electroporation using a Leica DMI3000 B manual inverted microscope equipped with a Leica EL6000 external light source for fluorescence excitation.

2.4.5 – Genomic cleavage detection

The efficiency with which the CRISPR construct produced targeted double strand breaks at the locus of interest after electroporation was determined using the GeneArt® Genomic Cleavage Detection Kit according to manufacturer's guidelines (Thermo Fisher Scientific). Loci at which CRISPR/Cas9 produced targeted double-strand breaks and resulted in insertions/deletions (indels) being created by cellular repair mechanisms were amplified by PCR using the CRISPR cleavage detection primers listed in **Table 2.6**. The PCR product was then denatured and re-annealed in order to enable strands with indels to re-anneal with strands without indels or with different indels, thus creating mismatches. These mismatches were subsequently detected and cleaved by Detection Enzyme (Thermo Fisher Scientific), with the resultant bands being analysed by running a 2% agarose gel with a 2-log DNA ladder (0.1 – 10 kb, New England Biolabs) and performing band densitometry using ImageJ software.

2.4.6 – Geneticin selection of electroporated iPSCs

Wild-type C2 iPSCs co-transfected with the CRISPR vector and the W9X or ΔExon1 targeting construct were trypsinised 48 hours after electroporation, plated in gelatine-coated 6-cm diameter cell culture dishes (Corning) and cultured for at least 5 days in BK medium containing Geneticin (G418) (50 ng/ml, Thermo Fisher Scientific). Individual Geneticin-resistant iPSC colonies were manually picked using a P1000 pipette tip, trypsinised using 50 µl of 1x TrypLE Select (Thermo Fisher Scientific) supplemented with 2 mM EDTA (Thermo Fisher Scientific), neutralised with 100 µl of BK medium and laid down in separate wells of a gelatine-coated 24-well plate containing 400 µl BK medium supplemented with Y-27632 dihydrochloride (1 µM, Tocris Bioscience). When confluent, cells in each well were trypsinised and passaged, with a proportion of the cells from each passage being pelleted for subsequent genotyping.

2.4.7 – Genotyping

To assess whether the CRISPR targeting strategy resulted in the creation of the desired *BMPR2* mutation, and if so, whether the mutation was heterozygous or homozygous, a pair of genotyping primers (**Table 2.6**) were designed to amplify the homology arm containing the W9X or ΔExon1 site by PCR using the cycling parameters shown in **Table 2.4**. To determine whether targeting was successful, 300 ng of the amplified PCR product was digested for 1 hour at 37°C by *AatII* (for W9X) or *PvuI* (for ΔExon1) restriction enzyme (New England Biolabs) and subsequently run on a 2% agarose gel with a 2-log DNA ladder. Successful targeting should yield 750 bp and 350 bp bands for W9X, or 547 bp and 293 bp bands for ΔExon1 and was further verified by sending the samples off for Sanger sequencing (Source Bioscience, Cambridge, UK).

Stage	Number of Cycles	Temperature	Time
1	1	95°C	5 minutes
2	35	95°C	15 seconds
		60°C	30 seconds
		68°C	1 minute 15 seconds
3	1	68°C	5 minutes

Table 2.4. PCR cycling parameters used for genotyping of CRISPR/Cas9-targeted C2 control iPSCs.

2.5 – Generation of lineage-specific iPSC-derived smooth muscle-like cells

Human iPSCs were differentiated into iPSC-derived smooth muscle-like cells (iPSC-SMCs) via lateral plate mesoderm (LM), paraxial mesoderm (PM) or neural ectoderm (NE) intermediate populations, as previously described (Cheung et al., 2012), with modifications. To generate LM- and PM-iPSC-SMCs, early mesoderm formation was induced by culturing iPSCs in gelatine-coated T-25 flasks for 36 hours in CDM-PVA supplemented with FGF-2 (20 ng/ml, Wellcome Trust - MRC Centre for Stem Cell Research, Cambridge, UK), LY294002 (10 ng/ml, Sigma) and BMP4 (10 ng/ml, Thermo Fisher Scientific). Subsequently, lateral plate mesoderm formation was induced by culturing the early mesoderm cell population for a further 3.5 days in CDM-PVA + FGF-2 (20 ng/ml) and BMP4 (50 ng/ml), whereas paraxial mesoderm formation was induced by culturing the early mesoderm cell population for 3.5 days in CDM-PVA supplemented with FGF-2 (20ng/ml) and LY294002 (10 ng/ml). By contrast, neuroectoderm specification was induced by culturing iPSCs for 7 days in CDM-PVA supplemented with FGF-2 (12 ng/ml) and the ALK4/5/7 inhibitor SB-431542 (10 μM, Tocris Bioscience).

Upon formation of these three intermediate lineages, the cells were subsequently trypsinised and SMC differentiation was induced by culturing the cells for at least 12 days in gelatine-coated T-25 flasks containing CDM-PVA supplemented with PDGF-BB (10 ng/ml, Thermo Fisher Scientific) and TGF-β1 (2 ng/ml, Thermo Fisher Scientific) (hereafter referred to as 'PT'). In addition to differentiation in PT, lateral plate mesoderm-derived iPSC-SMCs (LM-iPSC-SMCs) were also differentiated in PT medium supplemented with BMP4 (50 ng/ml) (hereafter referred to as 'PTB'). Where relevant, the iPSC-SMCs at the end of the serum-free differentiation protocol were then further matured for 7-14 days in DMEM supplemented with 10% FBS.

2.6 – Microarray hybridisation and analysis

RNA isolated from PASMCs, LM-SMCs, PM-SMCs, NE-SMCs and cDNA libraries were hybridised to the Illumina Human HT-12 BeadChip (Illumina Inc., San Diego, http://www.illumina.com). All data processing and analysis were performed using the algorithms included with the Bioconductor packages beadarray and lumi implemented in R software environment for statistical computing and graphics (R Foundation for Statistical Computing, Vienna, Austria, http://www.r-project.org). Principal component analysis (PCA) and hierarchical clustering was performed and plotted with Perseus software, which used complete linkage and Euclidean distance metric to generate the heat maps.

2.7 – RNA extraction

Cell pellets for RNA extraction were either frozen directly or stored in TRIzol Reagent (Thermo Fisher Scientific) at -80°C. After homogenisation of the cell pellet, RNA was extracted from TRIzol suspension or using the RNeasy Plus Mini Kit (Qiagen) as per the manufacturers' instructions.

2.8 – Reverse Transcription and Real-Time Quantitative Polymerase Chain Reaction (RT-qPCR)

1 µg of total RNA per sample, quantified using a NanoDrop Lite UV spectrophotometer, was treated with DNase I (Amplification Grade) and subsequently reverse transcribed into cDNA using the High-Capacity cDNA Reverse Transcription Kit and a Veriti 96-Well Thermal Cycler (all from Thermo Fisher Scientific) by following the manufacturer's protocol. The PCR thermocycler settings were: 25˚C for 10 min, followed by 37˚C for 2 hours and then 85˚C for 5 min. qPCR reactions were set up in triplicates in MicroAmp Optical 384-Well Reaction Plate with Barcode (Thermo Fisher Scientific) PCR plates using SYBR® Green JumpStart™ *Taq* ReadyMix™ (5 µl per well, Sigma), ROX Reference Dye (0.2 µl per well, Thermo Fisher Scientific), cDNA made from 10 ng of total RNA, as well as 167 nM of sense and antisense primers (sequences listed in **Table 2.6**). Primers were tested for amplification efficiency by assessing cDNA amplification over a 4-log scale using 10-fold serial dilutions of cDNA (from 1:10 to 1:10,000). Primer efficiencies were calculated from a linear regression line plotted for cycle threshold (C_t) against the DNA dilution. Only primers with amplification efficiencies between 90% and 110% were used.

Quantitative PCR (qPCR) amplification was performed using a QuantStudio 6 Flex Real-time PCR System (Thermo Fisher Scientific) using the following thermal cycling parameters: initial denaturation at 95°C for 2 minutes, 50 cycles of denaturation at 95°C for 30 seconds, annealing at 55°C for 30 seconds, extension at 72°C for 30 seconds, followed by a step at 55°C for 2 minutes, and then 95°C for 15 seconds, 55°C for 60 seconds, followed by 95°C for 15 seconds to generate a melt curve, with a ramp rate of ±1.6°C/s between each step. Data were analysed using Life Technologies QuantStudio Software V1.1 and Microsoft Excel by the comparative $2^{-(\Delta\Delta Ct)}$ method (Livak & Schmittgen, 2001), with gene expression normalised to *HPRT* or *HMBS* (PBGD) as the internal housekeeping reference gene.

2.9 – Immunocytochemistry

iPSC-SMCs cultured in 24-well cell culture plates were washed with phosphate-buffered saline (PBS) (0.5 ml/well) at room temperature and fixed at 4°C overnight with 4% paraformaldehyde (PFA, Sigma) in PBS. Cells were subsequently washed for 3 × 5 min in PBS, permeabilised for 3 × 10 minutes with 0.2% Tween-20 (Sigma) in PBS and blocked for at least 1 hour at room temperature with 10% FBS in PBS. Cells were then stained at 4°C overnight with the following primary antibodies diluted in 0.1% BSA (Sigma) in PBS: monoclonal mouse anti-myosin (smooth) (1:200, M7786, Sigma), monoclonal mouse anti-smooth muscle myosin heavy chain 11 (1:400, ab683, Abcam), mouse anti-human smooth muscle actin (1:300, M0851, Dako), monoclonal mouse anti-calponin (1:5000, C2687, Sigma). Subsequently, cells were washed for 5 × 5 minutes in PBS at room temperature prior to incubation for 1 hour at room temperature with donkey anti-mouse Alexa Fluor 488 fluorochrome-conjugated secondary antibody (1:300, Thermo Fisher Scientific). Cells were then washed with PBS for 5 × 5 minutes, incubated with 4′,6-diamidino-2-phenylindole (DAPI) (1 μg/ml, D9542, Sigma) for 5 minutes at room temperature, and washed for 3 × 5 minutes in PBS prior to imaging using a Leica DMI3000 B manual inverted microscope with a Leica EL6000 external light source for fluorescence excitation. Uncompressed TIFF colour images were captured with a Pixera Penguin 600CL digital camera using Image-Pro Plus software (MediaCybernetics).

2.10 – Western blotting

Western blotting for Smad1/5 was performed by Dr Liam Hurst prior to the start of this thesis project. Proteins were separated by sodium dodecyl sulphate polyacrylamide agarose gel electrophoresis (SDS-PAGE) and transferred electrophoretically from the gel to an Amersham Hybond P polyvinylidene difluoride (PVDF) membrane (GE Healthcare) via semi-dry transfer. After transfer, membranes were blocked in 5% non-fat milk powder (Marvel) in TBS-Tween 20 for 1 hour and then incubated at 4ºC overnight with primary antibodies directed against pSmad1/5 or total Smad1 (1:1000, Cell Signaling Technology) in 5% BSA (Sigma). The next day, membranes were washed and then incubated for 1 hour at room temperature with secondary antibody (anti-rabbit horseradish peroxidase (HRP), 1:2000) in 5% milk. Membranes were visualised by chemiluminescence using Amersham ECL Western Blotting Detection Reagent (GE Healthcare).

2.11 – Cell proliferation assays

2.11.1 – Assessing iPSC-SMC proliferation using cell counts

iPSC-SMCs were laid down in triplicates in gelatine-coated 24-well plates at a density of 2 x 10^4 cells per well and cultured for 7 days in either CDM-PVA + PT, CDM-PVA + PTB, DMEM + 5% FBS, DMEM + 2% FBS or DMEM + 2% FBS + BMP4 (50 ng/ml). On Day 7, the cells in each well were trypsinised for 5 minutes at 37 ºC with 200 µl of TrypLE Select + EDTA (2 mM), neutralised with 100 µl of PBS + EDTA (2 mM) and counted manually using disposable haemocytometer counting grids (Kova International). Proliferation rates were assessed by calculating and comparing fold changes in cell number after 7 days in culture for each cell line.

2.11.2 – Assessing proliferation by measuring cellular DNA content

LM-iPSC-SMCs were laid down in triplicates in gelatine-coated 6-well plates at a density of 5 x 10^5 cells per well and cultured for 48 hours in CDM-PVA + PT or CDM-PVA + PTB. The cells in each well were then trypsinised for 5 minutes at 37 ºC using 0.5 ml of 1x TrypLE Select + EDTA (2 mM), neutralised with 1 ml of CDM-PVA and counted manually using disposable haemocytometer counting grids. 2 x 10^5 cells from each suspension were then transferred into separate 5 ml round-bottom polystyrene tubes (BD Biosciences), centrifuged at 300 x *g* for 5 minutes and re-suspended in 400 µl of CDM-PVA. 0.8 µl of Vybrant DyeCycle Ruby Stain (ThermoFisher Scientific) was then added to the re-suspended cells in each sample before

incubating the cells in the dark for 15 minutes at 37ºC and subsequently measuring the percentage of cells in each sample which displayed red fluorescence by running the samples on a BD Accuri C6 flow cytometer (BD Biosciences) using 488 nm excitation and >670 nm emission. An unstained sample containing 2 x 10^5 C2 control LM-iPSC-SMCs served as a negative control.

2.11.3 – Somatostatin proliferation assays

PAH patient-derived *BMPR2*$^{+/-}$ PASMCs and isogenic iPSC-SMCs differentiated in PTB were laid down in triplicates in gelatine-coated 24-well plates at a density of 2 x 10^4 cells per well and cultured for 7 days in CDM-PVA + 5% FBS (for iPSC-SMCs) or DMEM + 5% FBS (for PASMCs) in the presence or absence of somatostatin-14 (1 µM, Sigma) or the somatostatin analogues lanreotide (1 µM, Sigma), octreotide (100 nM – 1 µM, Sigma) or CH-275 (100 nM – 1 µM, Tocris Bioscience). After 7 days in culture, the cells in each well were trypsinised for 5 minutes at 37 ºC with 200 µl of TrypLE Select + EDTA (2 mM), neutralised with 100 µl of PBS + EDTA (2 mM) and counted manually using disposable haemocytometer counting grids (Kova International).

2.12 – Apoptosis assays

2.12.1 – Annexin-V-FITC/propidium iodide apoptosis assay

Serum-free LM-iPSC-SMCs were laid down in triplicates in 6-well plates at a density of 2 x 10^5 cells per well and cultured for 48 hours in CDM-PVA + PT or CDM-PVA + PTB. Subsequently, cells were washed once with PBS and apoptosis was induced for 2.5 hours by replacing the growth medium with serum-free DMEM. For the unstained negative control, the medium was replaced with fresh CDM-PVA + PT or CDM-PVA + PTB. As a positive control for apoptosis, wild-type iPSC-SMCs were treated with staurosporine (50 nM, Enzo Life Sciences) during the 2.5-hour serum-free incubation period. Subsequently, all cell samples were washed once with PBS, trypsinised for 5 minutes at 37 ºC using 0.5 ml of 1x TrypLE Select + EDTA (2 mM), neutralised with 1 ml of CDM-PVA and collected in 5 ml round-bottom polystyrene tubes (BD Biosciences). The cells were then centrifuged at room temperature for 5 minutes at 300 x *g* before removing the supernatant, adding 1.5 ml of PBS to each cell pellet and centrifuging the samples again for 5 minutes at 300 x *g*. The cells in each tube were then re-suspended in 100 µl of Annexin V Binding Buffer (BD Biosciences) before adding 5 µl of

fluorescein isothiocyanate (FITC)-conjugated annexin V and 5 µl of propidium iodide (PI) (supplied as part of the BD Biosciences FITC Annexin V Apoptosis Detection Kit I) to each sample, gently vortexing and then incubating the cells in the dark for 15 minutes at room temperature. 400 µl of Annexin V Binding Buffer was then added to each sample to quench the reaction before measuring the percentage of cells that were positive for FITC Annexin V staining whilst being negative for PI staining by running the samples on a BD Accuri C6 flow cytometer. FITC fluorescence was detected in the FL1 channel (533/30 band pass filter), whereas PI fluorescence was detected in the FL2 channel (585/40 band pass filter). Unstained C2 iPSC-SMCs and C2 iPSC-SMCs stained with either FITC Annexin V or PI (single-stained controls) were used for fluorescence compensation and gating.

2.12.2 – Caspase 3/7 cleavage assay

Serum-free LM-iPSC-SMCs were laid down in triplicates in a gelatine-coated 96-well tissue culture plate (CELLSTAR, Greiner Bio-one) at a density of 2 x 10^4 cells per well and cultured for 48 hours in 100 µl of CDM-PVA + PT (for cells differentiated in PT) or CDM-PVA + PTB (for cells differentiated in PTB) per well. The cells were then cultured for a further 1 hour in 100 µl of their respective media (to assess basal apoptosis) or switched to 100 µl of serum-free DMEM or serum-free DMEM supplemented with staurosporine (50 nM) (to assess induced apoptosis). Subsequently, 100 µl of Caspase-Glo 3/7 reagent (Promega) was added to each well before mixing the contents of the wells using a plate shaker at 400 rpm for 30 seconds and incubating the plate at room temperature in the dark for 1 hour. The contents of each well were then transferred to a 96-well white polystyrene microplate (BRAND) and the luminescence of each sample measured using a Centro LB 960 microplate luminometer (Berthold Technologies).

2.13 – iPSC-SMC and PASMC contractility assay

Wild-type and *BMPR2*$^{+/-}$ LM-iPSC-SMCs matured for 7 days in DMEM + 10% FBS post-differentiation in PTB, and human wild-type and *BMPR2*$^{+/-}$ PASMCs, were laid down in triplicates at a density of 5 x 10^4 cells per well in 12-well plates and cultured for 48 hours in DMEM + 10% FBS. The cells were then washed for 2 x 3 minutes with warm PBS containing 0.1% w/v bovine serum albumin (BSA), and subsequently incubated at 37°C for 15 minutes in 0.1% w/v BSA + carbachol (300 μM, Sigma) in PBS. Carbachol-induced cell contraction was assessed by taking time-lapse images of the cells every 30 seconds over a period of 15 minutes and using ImageJ software (https://imagej.nih.gov/ij/) to measure percentage changes in individual cell surface areas (for n = 10-11 cells per cell line) between t = 0 and t = 15 minutes.

2.14 – Mitochondrial membrane potential assay

The polarisation state of the inner mitochondrial membrane in wild-type and *BMPR2*$^{+/-}$ LM-iPSC-SMCs was assessed at three different time points – immediately after the cells finished differentiating in serum-free conditions, after the cells had been cultured for one week in DMEM + 10% FBS in the presence or absence of exogenous recombinant human TNFα (1 ng/ml, R&D Systems), as well as after these untreated and TNFα-treated iPSC-SMCs were cultured for a further week in DMEM + 10% FBS only (i.e. after a total of two weeks in serum). At the end of each time-point, iPSC-SMCs were plated in triplicates at a density of 5 x 10^4 cells per well in gelatine-coated 12-well cell culture plates and cultured at 37°C for 48 hours in their respective media, after which the cells were loaded for 30 minutes with tetramethylrhodamine ethyl ester (TMRE) (30 nM, Enzo Life Sciences). Subsequently, the cells were incubated for 30 minutes at 37°C in fresh cell culture medium containing 30 nM TMRE, washed with PBS, trypsinised for 5 minutes at 37 ºC using 0.25 ml of 1x TrypLE Select + EDTA (2 mM), neutralised with 0.5 ml of CDM-PVA and collected in 5 ml round-bottom polystyrene tubes (BD Biosciences) prior to measuring the mean fluorescence intensity of the stained cell population in the FL2 channel (585/40 band pass filter) on a BD Accuri C6 flow cytometer (BD Biosciences).

To confirm that changes in TMRE staining intensity correctly reflected changes in mitochondrial membrane potential, wild-type iPSC-SMCs and PASMCs were incubated for 20 minutes in DMEM + 10% FBS in the presence or absence of carbonyl cyanide 4-trifluoromethoxyphenylhydrazone (FCCP, 5 μM), after which the cells were loaded for 30

minutes with TMRE (30 nM) in the continuing presence or absence of FCCP (5 μM) prior to analysis by flow cytometry.

2.15 – Mitochondrial superoxide staining

Isogenic C2 and C2 W9X$^{+/-}$ LM-iPSC-SMCs were differentiated in PT and laid down in triplicates in gelatine-coated 24-well cell culture plates at a density of 7.5 x 10^4 cells per well (for C2 iPSC-SMCs) or 1 x 10^5 cells per well (for C2 W9X$^{+/-}$ LM-iPSC-SMCs). The cells in each well were then cultured for 48 hours in DMEM supplemented with 10% FBS, washed with 0.5 ml of Hank's balanced salt solution containing calcium and magnesium (HBSS/Ca/Mg, Thermo Fisher Scientific) and incubated for 30 min at 37 ºC in 500 μl of HBSS/Ca/Mg containing MitoSOX Red mitochondrial superoxide indicator (5 μM, Thermo Fisher Scientific). Unstained C2 LM-iPSC-SMCs were incubated in HBSS/Ca/Mg as a negative control. The cells were then washed three times with warm HBSS/Ca/Mg (500 μl/well) before taking representative immunofluorescence images of the cells in each well at 200x magnification using a Leica DMI3000 B manual inverted microscope equipped with a Leica EL6000 external light source for fluorescence excitation. The level of MitoSOX staining was assessed by measuring average image intensities using the "Measure" tool in ImageJ.

2.16 – Seahorse XF glycolysis stress test assay

Glucose-stimulated glycolytic rates in wild-type and *BMPR2*$^{+/-}$ iPSC-SMCs were assessed using the Seahorse XF Glycolysis Stress Test assay according to the manufacturer's guidelines (Agilent Technologies), with modifications. To determine optimal cell densities for plating LM-iPSC-SMCs, wild-type and *BMPR2*$^{+/-}$ iPSC-SMCs were plated in triplicates at cell densities of 1 x 10^4, 2 x 10^4 or 3 x 10^4 cells per well in 96-well XF96 V3 PS cell culture microplates (Agilent Technologies), and cultured for 14 hours overnight in DMEM supplemented with 10% FBS. Cell confluency was then visually assessed by inspecting the cells under an inverted light microscope, after which the cells in each well were trypsinised using 50 μl of 1x TrypLE Select + EDTA (2 mM), neutralised with 100 μl of DMEM supplemented with 10% FBS and counted manually using disposable haemocytometer counting grids to assess cell attachment. A plating density of 3 x 10^4 cells per well resulted in optimal (95-99%) cell confluency for wild-type iPSC-SMCs, and the percentage of *BMPR2*$^{+/-}$ iPSC-SMCs which attached was found to be approximately 50% lower relative to wild-type iPSC-SMCs across the plating densities trialled. As a result, plating densities of 3 x 10^4 cells/well for

C2 iPSC-SMCs and 6 x 10^4 cells/well for isogenic *BMPR2*$^{+/-}$ iPSC-SMCs were chosen to ensure that the glycolysis stress test assay was performed on approximately equal numbers of confluent wild-type and *BMPR2*$^{+/-}$ iPSC-SMCs.

On the day of the assay, XF Base Medium (Agilent Technologies) was supplemented with L-glutamine (1 mM, Thermo Fisher Scientific), adjusted to pH 7.4, sterile-filtered through a 0.2 µm PES membrane and then used to wash the attached iPSC-SMCs two times (200 µl per well per wash) prior to incubating the iPSC-SMCs in 180 µl of this XF assay medium at 37 ºC in a non-CO_2 buffered incubator for 1 hour. During this time, the XF sensor cartridge, previously hydrated overnight according to the manufacturer's guidelines (Agilent Technologies), was loaded with the injection compounds (all dissolved in XF assay medium, pH-adjusted to pH 7.4 and pre-warmed to 37 ºC) listed in **Table 2.5**.

Injection compound	Stock concentration	Stock volume	Media volume	10X concentration (port)	Add to port	Final concentration (per well)
Port A Glucose	2.5 M	200 µl	4800 µl	100 mM	20 µl	10 mM
Port B Oligomycin A	2.5 mM	20 µl	4980 µl	10 µM	22 µl	1 µM
Port C 2-deoxy-D-glucose	1 M	2000 µl	2000 µl	500 mM	25 µl	50 mM

Table 2.5. Compounds used for loading Seahorse XF sensor cartridge ports

The hydrated sensor cartridge with the added compounds was then loaded into a Seahorse XF96 analyser (Agilent Technologies). After automated calibration, the utility plate used for calibration was replaced with the XF96 V3 PS cell culture microplate containing the iPSC-SMCs immediately prior to the start of the glycolysis stress test assay.

Glycolysis was assessed by measuring the extracellular acidification rate (ECAR), which was automatically performed by the XF96 analyser four times for 3 minutes (with a 3-minute mixing step between each ECAR measurement) both before and after sequential injection of glucose (10 mM, Sigma) to stimulate glycolysis, oligomycin A (1 µM, Tocris Bioscience) to maximise the glycolytic rate, and 2-deoxy-D-glucose (50 mM, Thermo Fisher Scientific) to inhibit glycolysis. The rate of glycolysis was calculated by subtracting the last rate measurement taken prior to glucose injection from the maximum rate measurement before oligomycin injection.

2.17 – RNA sequencing (RNA-Seq)

2.17.1 – RNA-Seq library preparation

Three wild-type (C2, C6 and C10) and five *BMPR2*$^{+/-}$ (C2 W9X$^{+/-}$, C2 ΔExon1, B3, B4 and B11) LM-iPSC-SMC lines (see **Table 2.1** for characteristics) were submitted for RNA sequencing immediately after being differentiated under serum-free, chemically defined conditions in PTB.

After harvesting and extracting RNA from these cells using the RNeasy Plus Mini Kit (Qiagen), the RNA concentration of each sample was determined using a Qubit Fluorometer (Thermo Fisher Scientific) and RNA integrity was assessed by running each RNA sample on a Bioanalyzer (Agilent Technologies) (performed by Dr Frances Burden, Department of Haematology, University of Cambridge, UK).

RNA-Seq libraries were generated by Dr Frances Burden and Dr Mattia Frontini as previously described (Petersen et al., 2017) by using 1 μg of DNase-treated RNA to generate ribosomal RNA-depleted libraries with a TruSeq Stranded Total RNA Library Prep Kit (with Ribo-Zero Human/Mouse/Rat, RS-122-2201, Illumina). Libraries were quantified using a qPCR Library Quantification Kit (Kapa Biosystems), pooled and sequenced using paired-end 76 bp sequencing on a HiSeq 2000 Sequencing System (Illumina).

2.17.2 – RNA-Seq analysis

RNA-Seq analysis was performed by Dr Matthias Haimel and Dr Marta Bleda in Dr Stefan Gräf's group in the Department of Medicine, University of Cambridge. Trim Galore 0.3.7 (http://www.bioinformatics.babraham.ac.uk/projects/trim_galore/) with parameters '-q 15 --stringency 3 --paired' was used to trim PCR and sequencing adapters. Trimmed reads were aligned to the Ensembl v70 (Flicek et al., 2013) human transcriptome with Bowtie 1.0.1 (Langmead et al., 2009), with parameters '-a --best --strata -S -m 100 -X 500 --chunkmbs 256 --nofw -fr'. MMSEQ 1.0.8a (Turro et al., 2011; Turro et al., 2014) was used with default parameters to calculate fragment counts and DESeq2 (Love et al., 2014) was applied with regularised log transformation to quantify gene expression. Genes with an adjusted false discovery rate (FDR) P value < 0.05 were considered differentially expressed.

2.18 – Isolation of *Bmpr2*$^{+/R899X}$ mouse lung tissue

Lung tissue was isolated from *Bmpr2*$^{+/R899X}$ mice by Dr Xudong Yang and Dr Lu Long as previously described (Long et al., 2015). Animal work was conducted in accordance with the UK Animals (Scientific Procedures) Act 1986 and approved under Home Office project licence number PPL 70/8850.

2.19 - Statistical analysis

Statistical analysis was performed using GraphPad Prism 6 software. Statistical analysis of iPSC-SMC data was based on either (i) the number of technical replicates (independent experiments performed on the same cells from the same iPSC-SMC differentiation), or (ii) on the number of experimental replicates where each experiment was performed using cells from independent iPSC-SMC differentiations. When the results from *n* independent iPSC-SMC differentiations were analysed, statistical tests were based on a sample size of *n*. Similarly, when data from *n* technical replicates were tested for statistical significance, the sample size was *n*. Where statistical analysis was performed, the type of statistical analysis used is stated in the corresponding figure legends.

Data were tested for statistical significance using an unpaired two-tailed Student's *t*-test, by one-way or two-way analysis of variance (ANOVA), or by performing false discovery rate (FDR) analysis (for RNA-Seq data). When performing ANOVA analysis, multiple comparisons were corrected for using Tukey's, Dunnett's or Sidak's post-hoc tests. Results were deemed statistically significant when the Probability (*P*) value was less than 0.05. For FDR analysis, genes were deemed to be differentially expressed when the adjusted *P* value (P_{adj}) was less than 0.05.

2.20 – PCR primer sequences

The nucleotide sequences and sources of the PCR primers used in this thesis project are listed in **Table 2.6** below.

Table 2.6. List of PCR primer sequences and their sources

Primer name/ target gene	Forward primer (5' – 3')	Reverse primer (5' – 3')	Source/ Reference
Homology arm primers used to amplify a 1 kb region of *BMPR2* Exon1			
BMPR2 W9X left homology arm	AAGGAAAAAGCGGCCG CGATCCAGTCAAGGAA GAGG	TTGGCGCGCCTCGTTGCA TTACCTCACAGC	Designed using Primer3Plus
BMPR2 W9X right homology arm	GGGAATTCCATATGTAA TCACCAGTGAACAGTG C	AAGGAAAAAGGCCAATTA GGCCATCTGGTGCTATGC AATACC	Designed using Primer3Plus
BMPR2 ΔExon1 left homology arm	TTAATTAATCACAGGAG CCATTGACGGG	CGGCCCTAGGAGGCTCGT CTTCTCTCCCGT	Designed using Primer3Plus
BMPR2 ΔExon1 right homology arm	GGGAATTCCATATGTGG CTACCATGGACCATCC	GGGAATTCCATATGGGAA CCACATGGCTTATGGC	Designed using Primer3Plus
CRISPR cleavage detection primers			
BMPR2 W9X cleavage detection	CTGTATTGTGATACGGG C	TGTCAAGATACCACACCC	Designed using Primer3Plus
CRISPR genotyping primers			
BMPR2 W9X genotyping	TCTCACGGTTGTTCTGC G	TATGGAAGTGGGGATAGG	Designed using Primer3Plus
BMPR2 ΔExon1 genotyping	CAGAGCTGCGGGAGAA CGAG	AGGCTCGTCTTCTCTCCC GT	Designed using Primer3Plus
Site-directed mutagenesis primers used to introduce the W9X mutation			
BMPR2 W9X SDM	GGGATGACgTCgTCGCT aCAaCGGCCCTGaCGG	CCGtCAGGGCCGtTGtAGC GAcGAcGTCATCCC	Designed using Primer3Plus
Mouse qPCR primers			
Sst	Proprietary	Proprietary	QIAGEN QuantiTect Primer Assay QT00239295
Duox2	ACATATCCTTCCGGGAG TTC	TGAAGAACTCGTCCTTGG AG	Designed using Primer3Plus
Ucp2	ATGTGGTAAAGGTCCG CTTC	CAATGGTCTTGTAGGCTTC G	Designed using Primer3Plus
Crlf1	CCCCTGAGAAGCCTTTT AAC	TAAGAATGTCTCCCCGTGT G	Designed using Primer3Plus
Actb	AGTGTGACGTTGACATC CGT	TGCTAGGAGCCCAGAGCAG TA	Designed using Primer3Plus

Human qPCR primers			
SST	Proprietary	Proprietary	QIAGEN QuantiTect Primer Assay QT00004277
DUOX2	Proprietary	Proprietary	QIAGEN QuantiTect Primer Assay QT00012236
UCP2	TGTGGTAAAGGTCCGATTCC	TGGTCTTGTAGGCATTGACG	Designed using Primer3Plus
CRLF1	ACCTTCCTCCACACCAACTAC	TCCTCACATGTGTTGTCCTG	Designed using Primer3Plus
BMPR2	CAAATCTGTGAGCCCAACAGTCAA	GAGGAAGAATAATCTGGATAAGGACCAAT	Upton et al. (2009)
ID1	GACGGCCGAGGCGGCATG	GGGGAGACCCACAGAGCACG	Yang et al. (2008)
ID2	GACCCGATGAGCCTGCTATAC	GGTGCTGCAGGATTTCCATCT	Upton et al. (2009)
IL6	Proprietary	Proprietary	QIAGEN QuantiTect Primer Assay QT00083720
MYH11	AGATGGTTCTGAGGAGGAAACG	AAAACTGTAGAAAGTTGCTTATTCACT	Cheung et al. (2012)
HPRT1	GCTATAAATTCTTTGCTGACCTGCTG	AATTACTTTTATGTCCCCTGTTGACTGG	Larson Gedman et al. (2009)
HMBS (PBGD)	ATTACCCCGGGAGACTGAAC	GGCTGTTGCTTGGACTTCTC	Designed using NCBI Primer-BLAST
SST (Somatostatin)	Proprietary	Proprietary	QIAGEN QuantiTect Primer Assay QT00004277
SSTR1	ACTGACAGCCTTTGATGGAG	AGTGGGAGACCCAGAAAAAG	Designed using Primer3Plus
SSTR2	Proprietary	Proprietary	QIAGEN QuantiTect Primer Assay QT00081179
SSTR3	ACCCATATTCTCCCTTCCTG	TTCAGACACTCTGCCTTTCC	Designed using Primer3Plus
SSTR4	TCTGCTGGATGCCTTTCTAC	AGCCATAGAGAATGGGGTTG	Designed using Primer3Plus
SSTR5	Proprietary	Proprietary	QIAGEN QuantiTect Primer Assay QT00228277

CHAPTER 3 – RESULTS (I)

Generating the tools to model PAH using induced pluripotent stem cells

3.1 – Generation of *BMPR2*$^{+/-}$ iPSC lines with isogenic backgrounds

Reduced BMPR2 signalling is central to the pathobiology of pulmonary arterial hypertension. However, an important observation in heritable PAH is that *BMPR2* mutations exhibit reduced penetrance (Rosenzweig et al., 2008; van der Bruggen et al., 2016; Gu et al., 2017). Clinically, unaffected *BMPR2* mutation carriers appear healthy and yet have a massively increased risk of developing PAH (Sztrymf et al., 2008). Furthermore, penetrance is higher in females (45%) than in males (15%) (Evans et al., 2016). These observations suggest a requirement for additional environmental or genetic triggers for disease initiation and progression. To date, it has proved difficult to elucidate these factors due to the lack of appropriate models. Therefore, alternative human disease models of PAH are required to gain a better understanding of PAH establishment and progression.

Patient-specific iPSCs can be differentiated into disease-relevant cell types and have been used to model a number of human diseases, including PAH (West et al., 2014; Sa et al., 2017; Gu et al., 2017). However, previous studies have predominantly focused on using patient-derived iPSCs with different genetic backgrounds, thus making it difficult to delineate the precise contribution of individual *BMPR2* mutations to the establishment of PAH-associated cellular phenotypes.

To remove the effects that different genetic modifiers may have on the penetrance of cellular phenotypes, I therefore commenced this thesis project by generating wild-type and *BMPR2*$^{+/-}$ iPSC lines with an isogenic background. To achieve this, I used CRISPR-Cas9-mediated homologous recombination (Cong et al., 2013) to introduce a single pathogenic *BMPR2* mutation (W9X) into a control iPSC line (C2) which was previously derived from a disease-free individual with no family history of PAH or cardiovascular disease (see **Table 2.1** for characteristics) (Geti et al., 2012).

3.1.1 – CRISPR design

CRISPR-Cas9 genome editing was used to artificially introduce a known, disease-associated *BMPR2* mutation (W9X) into the C2 iPSC line originating from a wild-type individual with no family history of PAH (see **Table 2.1**).

Prior to the start of this thesis project, a CRISPR-Cas9 system was designed by Dr Amer Rana so that the protospacer adjacent motif (PAM) sequence, fused to the 3' end of a 20 bp guide RNA sequence, recognises the PAM sequence constituting the arginine (R7) position within exon 1 of the *BMPR2* gene. The resulting CRISPR-Cas9 complex is therefore able to introduce a double-strand DNA break 2-3 bp upstream of the PAM sequence, resulting in the disruption of an endogenous *PstI* restriction site within the targeted allele (**Figure 3.1**).

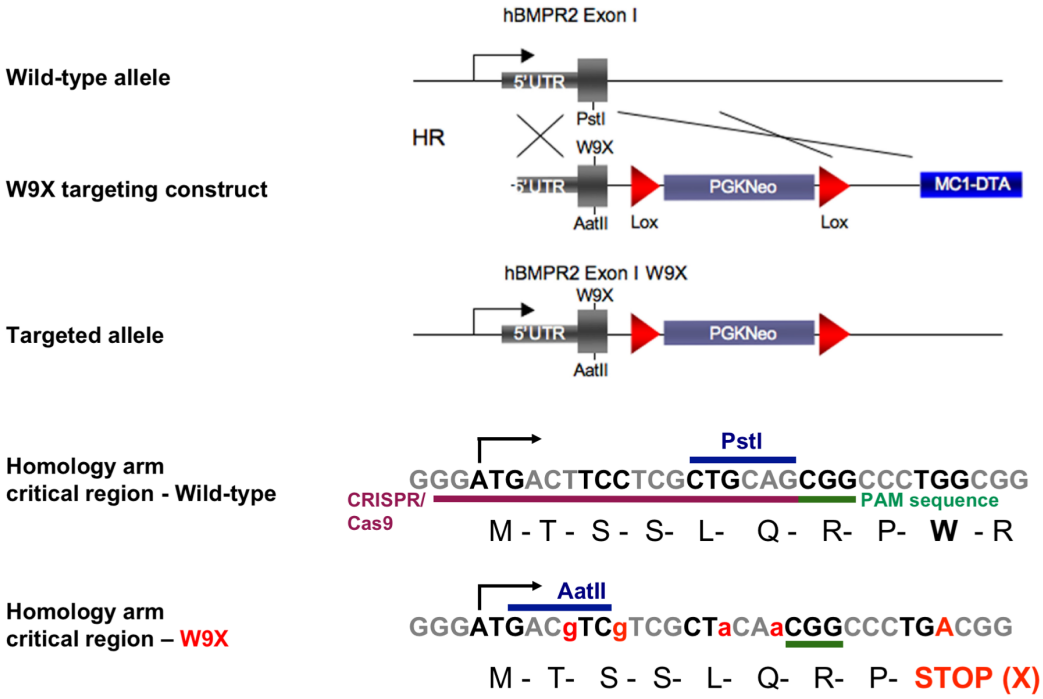

Figure 3.1. CRISPR-Cas9 genome editing strategy used to introduce a heterozygous W9X mutation into the *BMPR2* gene in the C2 control iPSC line. The engineered CRISPR-Cas9 complex contains a synthetic guide RNA (gRNA) which recognises a sequence of three nucleotides known as the protospacer adjacent motif (PAM) sequence (underlined in green) and interacts with the adjacent 20 bases immediately upstream of this sequence (underlined in magenta). The Cas9 nuclease introduces a double-strand DNA break just upstream of the PAM sequence, thus increasing the efficiency of homologous recombination of the W9X targeting construct with the genomic locus. Successful targeting would result in the destruction of an endogenous *PstI* restriction enzyme site and introduction of a new *AatII* site (highlighted in dark blue). Furthermore, a total of 4 silent mutations (lower case nucleotides highlighted in red), in addition to the single point mutation (upper case nucleotide highlighted in red) required to generate the W9X mutation, were introduced to prevent the CRISPR from directing the cutting of the targeting construct and to aid the genotyping of correctly targeted clones. The completed targeting vector contains a 2 kilobase pair phosphoglycerate kinase promoter-driven neomycin resistance (PGK-Neo) and MC1-DTA (diphtheria toxin A) cassettes to enable positive and negative selection of the targeted iPSCs, respectively.

To create this CRISPR-Cas9 complex, prior to the start of this thesis project, double-stranded DNA sequences encoding the desired CRISPR RNA targets (5'-GGATGACTTCCTCGCTGCAGgtttt-3' and 3'-gtggcCCTACTGAAGGAGCGACGTC-5') were cloned into the GeneArt® CRISPR Nuclease Vector (Thermo Fisher Scientific) (**Figure 3.2**) which contains an orange fluorescent protein (OFP) reporter to enable assessment of transfection efficiency.

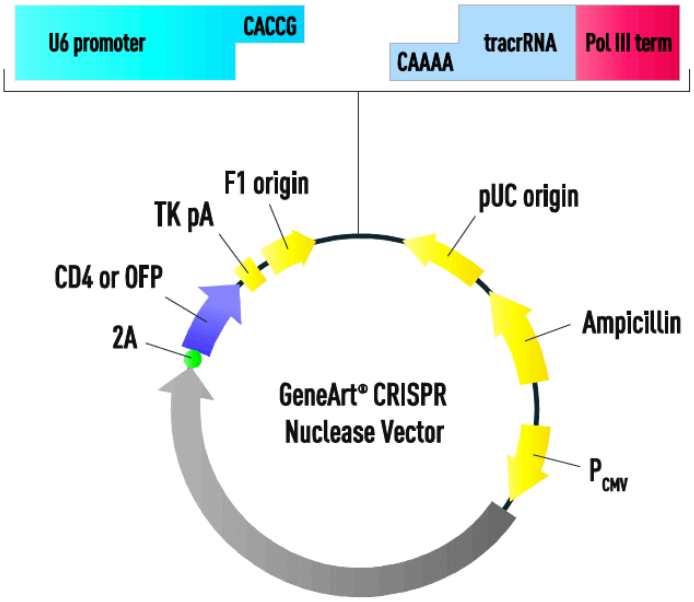

Figure 3.2. GeneArt® CRISPR Nuclease Vector map. The GeneArt® CRISPR Nuclease Vector with orange fluorescent protein (OFP) is 9219 bp in size. Double-stranded oligonucleotide sequences encoding the desired CRISPR RNA targets are cloned into the vector where the 3' overhangs are located. The auxiliary trans-activating CRISPR RNA (tracrRNA) allows the Cas9 nuclease to be loaded onto the guide RNA, the expression of which is driven by the human U6 promoter. Cas9 nuclease and OFP expression are driven by the cytomegalovirus (CMV) promoter. The vector also contains a TK pA polyadenylation signal, a self-cleaving 2A peptide linker, F1 and pUC origins of replication, an ampicillin resistance gene and a Pol III terminator that helps to stop RNA Polymerase III-mediated transcription. Image reproduced from the GeneArt® CRISPR Nuclease Vector kit manual (Thermo Fisher Scientific).

3.1.2 – Generation of the W9X targeting construct

To insert a W9X mutation into exon 1 of *BMPR2* by CRISPR-mediated homologous recombination, a 1 kb genomic fragment including exon 1 (Chromosome 2: 202,376,889 - 202,377,848) was cloned from the iPSC line C2 using the *BMPR2* W9X left and right homology arm primer sequences listed in **Table 2.6** and by following the Zero Blunt TOPO PCR cloning kit protocol (Thermo Fisher Scientific). The W9X mutation was introduced into exon 1 by site-directed mutagenesis by using 50 ng of genomic DNA (gDNA) template to replace the TGG sequence encoding the tryptophan at position 9 in the coding region with a TGA sequence encoding a stop codon (**Figure 3.1**). The SDM primers (sequences listed in **Table 2.6**) were designed in a way that would enable an *AatII* restriction site to be introduced 22 bp upstream of the W9X site within the left homology arm of the targeting construct. Introduction of this *AatII* restriction site would destroy an endogenous *PstI* site after homologous recombination with the targeted allele. Furthermore, a total of 4 silent mutations, in addition to the single point mutation required to generate the W9X mutation, were introduced to prevent the CRISPR from directing the cutting of the targeting construct and to aid the genotyping of correctly targeted clones.

To complete the targeting construct, this engineered 1 kb fragment was cloned into a vector upstream of a 2 kb phosphoglycerate kinase promoter-driven neomycin resistance (PGK-Neo) positive selection cassette, a second 1.3 kb homology arm corresponding to intron 1 of *BMPR2* (Chromosome 2: 202,377,863 - 202,379,154), and an MC1-DTA (diphtheria toxin A) negative selection cassette). In addition to performing test digestion reactions using *PstI* and *AatII* restriction enzymes, samples were sent for Sanger sequencing (Source Bioscience, Cambridge, UK) to verify that the W9X mutation was successfully introduced and that the targeting construct was cloned correctly.

3.1.3 – Generation of the ΔExon1 targeting construct

The targeting vector used to generate the W9X targeting construct was also used to generate a targeting vector that would result in the deletion of exon 1 of the *BMPR2* gene (ΔExon1) (**Figure 3.3**). This work was performed by Dr C-Hong Chang and is described in *Section 2.4.2*.

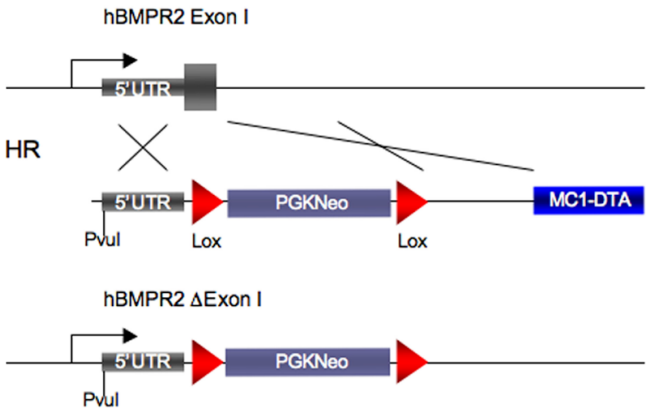

Figure 3.3. Targeting strategy used to delete exon 1 of the *BMPR2* gene. The targeting construct consists of a 1.1 kb homology region containing a single *PvuI* restriction enzyme site, a 2 kb phosphoglycerate kinase promoter-driven neomycin resistance (PGK-Neo) positive selection cassette, a second 1.3 kb homology arm corresponding to intron 1 of *BMPR2,* and an MC1-DTA (diphtheria toxin A) negative selection cassette. Successful CRISPR-Cas9-mediated homologous recombination would result in the introduction of the *PvuI* site and the insertion of the PGK-Neo cassette into the targeted *BMPR2* locus. The MC1-DTA expression cassette contains a constitutively active hybrid polyoma virus enhancer/herpes simplex virus thymidine kinase (HSVtk) promoter and prevents the survival of cells in which random integration has occurred.

3.1.4 – CRISPR validation

Having generated the W9X and ΔExon1 targeting constructs, I next set out to confirm whether the CRISPR nuclease vector containing double-stranded DNA sequences encoding the desired CRISPR RNA targets and an orange fluorescent protein (OFP) reporter (**Figure 3.2**) can be successfully introduced into control C2 iPSCs by electroporation. Transfected C2 iPSCs displayed orange fluorescence when visualised under a fluorescence microscope 48 hours post-transfection (**Figure 3.4 A**), indicating successful expression of the transfected CRISPR vector. Furthermore, flow cytometric analysis of C2 iPSCs 24 hours post-transfection (performed by staff at the NIHR Cambridge BRC Cell Phenotyping Hub) revealed that 86.3% of cells transfected with the pmaxGFP control vector displayed green fluorescence (**Figure 3.4 B**) and that 22.5% of the iPSCs transfected with the CRISPR vector displayed orange fluorescence indicative of OFP expression (**Figure 3.4 C**).

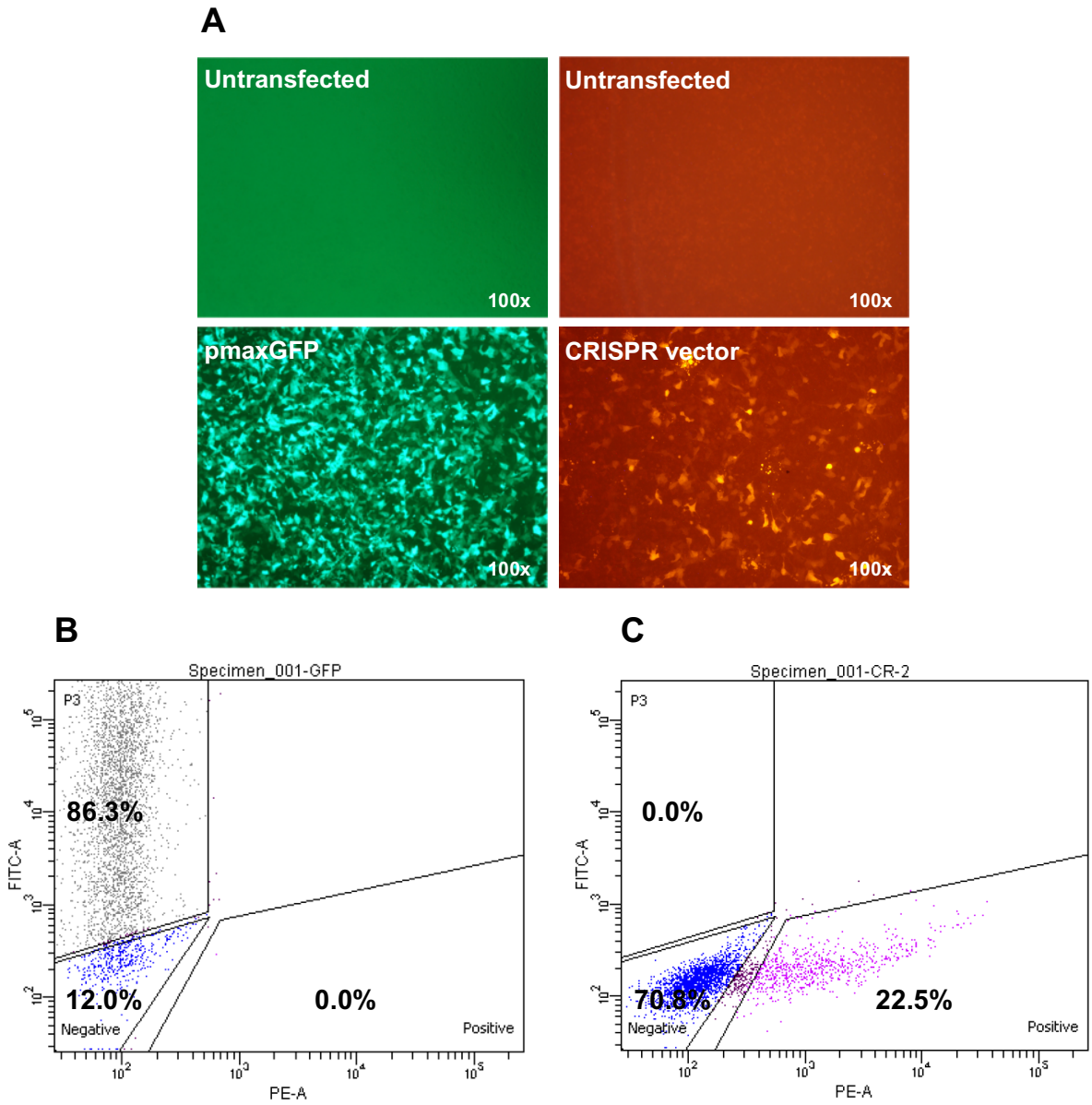

Figure 3.4. Functional expression of the CRISPR nuclease vector in control C2 iPSCs. (**A**) Representative immunofluorescence images (100x magnification) of control C2 iPSCs transfected by electroporation with a GeneArt CRISPR Nuclease Vector containing the desired CRISPR target sequences and an orange fluorescent protein (OFP) reporter. Transfection with pmaxGFP vector served as a positive control. Transfected C2 iPSCs displayed orange fluorescence, indicating successful expression of the transfected CRISPR vector, albeit with a lower transfection efficiency compared to the pmaxGFP control vector. (**B** and **C**) Flow cytometric analysis of C2 iPSCs approximately 24 hours post-transfection revealed that 86.3% of cells were successfully transfected with the pmaxGFP control plasmid (**B**), whereas 22.5% of cells transfected with the CRISPR vector displayed orange fluorescence indicative of OFP expression (**C**). Flow cytometric analysis was performed by staff at the NIHR Cambridge BRC Cell Phenotyping Hub at the Department of Medicine, University of Cambridge. PE-A, phycoerythrin amplitude; FITC-A, fluorescein isothiocyanate amplitude.

In addition, I followed the GeneArt Genomic Cleavage Detection Kit protocol (Thermo Fisher Scientific) to estimate the efficiency with which the CRISPR construct cleaved genomic DNA at the *BMPR2* locus in transfected C2 iPSCs. To do this, loci at which CRISPR-Cas9 produced targeted double-strand breaks and resulted in insertions/deletions (indels) being created by cellular repair mechanisms were amplified by PCR. The PCR product was then denatured and re-annealed in order to enable strands with indels to re-anneal with strands without indels or with different indels, thus creating mismatches. These mismatches were subsequently detected and cleaved by Detection Enzyme, with the resultant bands being analysed on a 2% agarose gel (**Figure 3.5**). CRISPR cleavage efficiency was calculated by performing band densitometry and inputting the calculated band intensities into the following formulae:

$$Cleavage\ Efficiency = 1 - [(1\text{-}fraction\ cleaved)^{1/2}]$$

where

$$Fraction\ Cleaved = Sum\ of\ cleaved\ band\ intensities/(sum\ of\ cleaved\ and\ parental\ band\ intensities)$$

Band densitometry revealed that the CRISPR-Cas9 nuclease cleaved approximately 71% of the amplified PCR product with an efficiency of 46%. Taken together, these findings suggest that the CRISPR nuclease vector was functionally expressed in control C2 iPSCs.

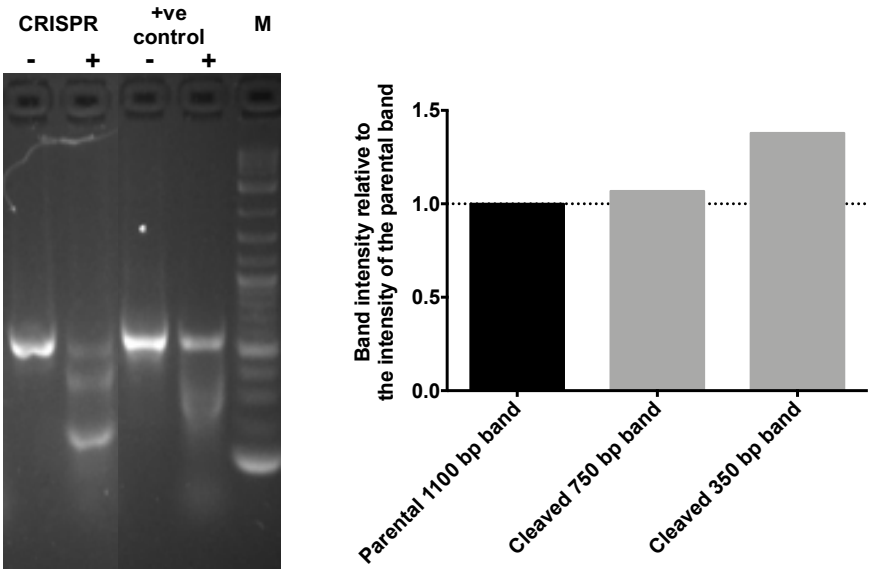

Figure 3.5. Analysis of CRISPR cleavage efficiency. The efficiency with which the CRISPR construct produced targeted double-strand breaks at the locus of interest after electroporation was determined using the GeneArt® Genomic Cleavage Detection Kit (Thermo Fisher Scientific). Loci at which CRISPR-Cas9 produced targeted double-strand breaks and resulted in insertions/deletions (indels) being created by cellular repair mechanisms were amplified by PCR. The PCR product was then denatured and re-annealed in order to enable strands with indels to re-anneal with strands without indels or with different indels, thus creating mismatches. These mismatches were subsequently detected and cleaved by Detection Enzyme, with the resultant bands being analysed on a 2% agarose gel. Band densitometry using ImageJ software revealed that the CRISPR-Cas9 nuclease cleaved approximately 71% of the amplified PCR product with an efficiency of 46%. The formulae used to calculate CRISPR cleavage efficiency are stated in the main body of the text. M: 2-log DNA ladder (0.1 – 10 kb).

3.1.5 – Introduction of *BMPR2* mutations into a control iPSC line

The W9X targeting DNA construct was designed in such a way that successful CRISPR-Cas9-mediated homologous recombination would confer neomycin resistance to the targeted iPSCs and result in the disruption of an endogenous *PstI* restriction enzyme site whilst creating a new *AatII* site within the targeted allele (**Figure 3.1**).

Having successfully generated the W9X targeting vector, I co-transfected wild-type C2 iPSCs with the linearised W9X targeting construct and the CRISPR vector. After 5 days of culturing the transfected cells in cell culture medium containing the neomycin sulphate analogue Geneticin (G418, 50 ng/ml), over fifty geneticin-resistant iPSC colonies emerged from a starting population of 2.4 x 10^6 transfected cells. Twenty-two of these colonies were picked and genotyped by PCR to amplify a 1.1 kb region containing the W9X site. When genotyped, three of these picked colonies gave rise to PCR products which were digested by *AatII* restriction enzyme but were not digested by *PstI*. If homologous recombination is successful, *AatII* should cut the DNA at a single site within the 1.1 kb homology region to produce 750 bp and 350 bp bands on an agarose gel, which is what I observed (**Figure 3.6 A**). Taken together, these results suggest that these three iPSC colonies were successfully and correctly targeted.

By contrast, successful CRISPR-Cas9-mediated homologous recombination of the ΔExon1 targeting construct would confer neomycin resistance and result in the introduction of a new *PvuI* restriction site within the targeted allele (see **Figure 3.3**). When genotyped, successfully targeted colonies gave rise to PCR products which were digested by *PvuI* to produce the expected 547 bp and 293 bp bands on an agarose gel (**Figure 3.6 B**).

In iPSCs targeted with the W9X targeting construct, one of the targeted colonies was heterozygous for the W9X mutation (C2 W9X$^{+/-}$), whereas the other two were homozygous (C2 W9X$^{-/-}$). By contrast, in iPSCs targeted with the ΔExon1 targeting construct, two heterozygous iPSC colonies (C2 ΔExon1) were obtained. Successful introduction of the W9X and ΔExon1 mutations into C2 iPSCs was confirmed by Sanger sequencing (performed by Source Bioscience, Cambridge, UK, and shown for the W9X mutation in **Figure 3.6 C**). qPCR analysis revealed that *BMPR2* mRNA expression was significantly lower in C2 W9X$^{+/-}$, C2 W9X$^{-/-}$ and C2 ΔExon1 iPSCs relative to the C2 control iPSC line (**Figures 3.6 D-E**), thus further suggesting that successful targeting had been achieved.

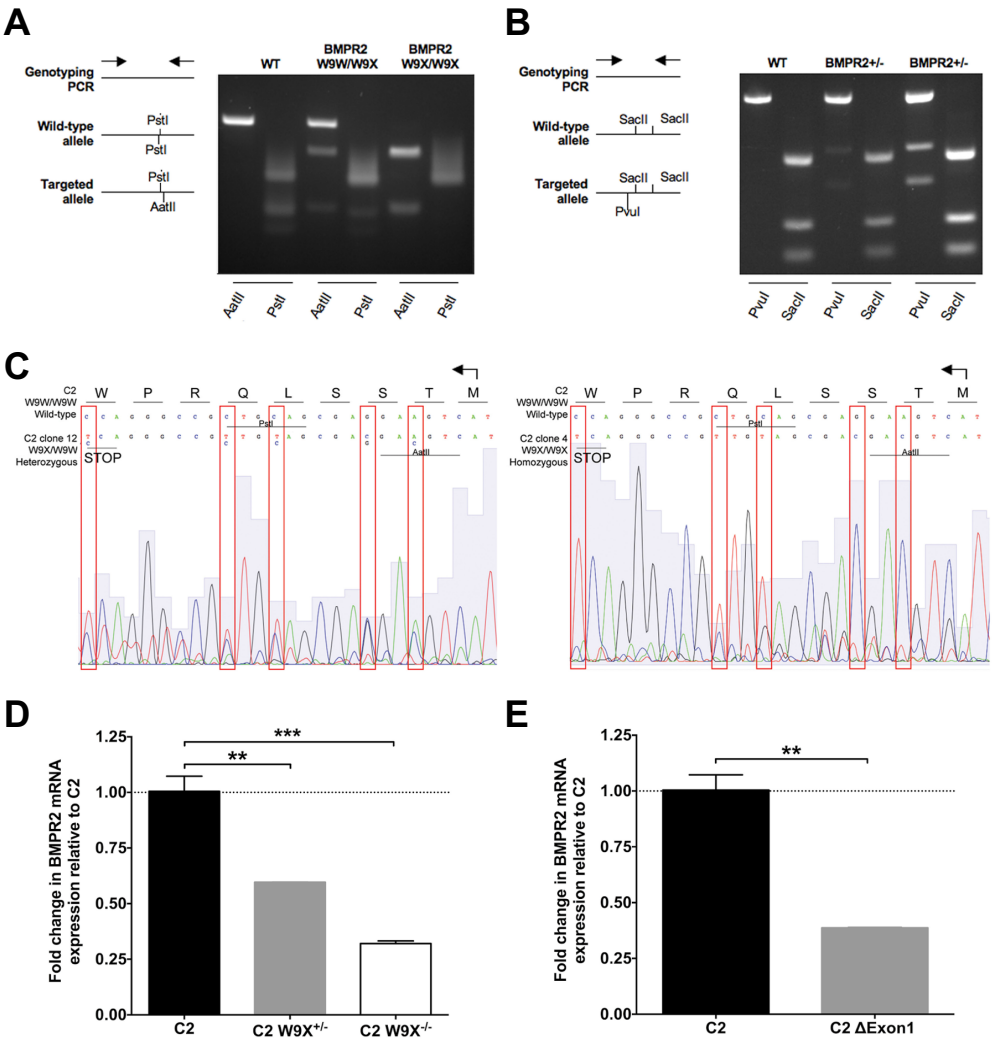

Figure 3.6. Generation of two types of *BMPR2* mutations in a human control iPSC line. (**A**) Genotyping to reveal W9X heterozygous and homozygous alleles. Geneticin-resistant iPSC colonies were picked and genotyped by PCR to amplify the 1.1 kb homology region containing the W9X site, giving rise to PCR products that were not digested by *PstI* restriction enzyme but were digested by *AatII* to produce the predicted 750 bp and 350 bp band sizes on a 2% agarose gel. (**B**) Genotyping to reveal the ΔExon1 heterozygous allele (performed by Dr C-Hong Chang). Geneticin-resistant iPSC colonies transfected with the ΔExon1 targeting construct gave rise to PCR products which were digested by *PvuI* to produce the predicted 547 bp and 293 bp band sizes on a 2% agarose gel. (**C**) Sanger sequencing confirmed the introduction of a heterozygous or homozygous W9X mutation into C2 iPSCs. The sequence is shown as a reverse complement, with start methionine indicated by an arrow showing the direction of the reading frame. (**D** and **E**) qPCR analysis showed that the newly generated heterozygous (C2 W9X$^{+/-}$ and C2 ΔExon1) and homozygous (C2 W9X$^{-/-}$) *BMPR2* mutant iPSC lines displayed reduced *BMPR2* mRNA expression relative to control C2 iPSCs. Data in **D** and **E** presented as mean ± s.e.m. of n=2-3 independent qPCR analyses performed on cells from the same differentiation (** $P <$ 0.01, *** $P < 0.001$, one-way ANOVA with Tukey's post hoc test (**D**) and unpaired two-tailed Student's t test (**E**)).

In addition, to check that transfection of the CRISPR vector did not have any confounding effects on cell phenotypes being studied, I also carried out a control transfection which involved transfecting C2 iPSCs with the CRISPR vector and a pmaxGFP control plasmid (Lonza) only. Successfully transfected cells were selected by fluorescence-activated cell sorting (FACS), with the resulting C2 pmaxGFP iPSC line displaying a similar proliferation rate compared to the wild-type C2 iPSC line (data not shown).

3.2 – Generation of lineage-specific iPSC-derived smooth muscle-like cells that can be used as surrogates for distal PASMCs

Previous work has shown that PAH patient-derived iPSCs can be differentiated into endothelial-like cells (iPSC-ECs) that recapitulate some PAH-associated cellular phenotypes and can be used as surrogates for PAECs (Sa et al., 2017). However, no iPSC-SMC model of PAH has yet been described and the derivation of iPSC-SMCs that perfectly represent adult PASMCs is yet to be achieved.

When developing protocols for differentiating iPSCs into vascular smooth muscle-like cells, it is important to ensure that the right types of cells are being produced and that these display functional responses akin to the specific type of primary cell they are trying to mimic. As it is the distal PASMCs that are predominantly affected in PAH, I therefore aimed to generate iPSC-derived smooth muscle-like cells (iPSC-SMCs) with functional responses to BMP4 signalling akin to those observed in distal PASMCs (Yang et al., 2005).

Distal PASMCs arise from lateral plate mesoderm, whereas the most proximal PASMCs arise from neural crest (Jiang et al., 2000). I thus used previously published lineage-specific, serum-free and chemically defined SMC differentiation protocols (Cheung et al., 2012) to generate iPSC-SMCs from the lateral plate mesoderm (LM-SMCs) and neural ectoderm (NE-SMCs) lineages. In addition, I also differentiated iPSCs from the paraxial mesoderm lineage as a further comparator, although this lineage is not thought to contribute to distal PASMCs (Wasteson et al., 2008).

3.2.1 – Lineage-specific iPSC-SMCs express several SMC markers

After differentiating wild-type and *BMPR2*$^{+/-}$ iPSCs into iPSC-SMCs from lateral plate mesoderm, paraxial mesoderm and neuroectoderm, I performed immunostaining to show that these cells expressed the smooth muscle markers calponin and smooth muscle actin (SMA) (**Figure 3.7**). Furthermore, I also differentiated isogenic C2 and C2 W9X$^{+/-}$ iPSCs into LM-iPSC-SMCs and showed that these cells stained positively for smooth muscle myosin heavy chain (MYH11) (**Figure 3.8**), which is considered to be the most robust marker of mature vascular smooth muscle cells (Owens et al., 2004). In addition, wild-type C2 LM-iPSC-SMCs displayed contractile responses to stimulation with carbachol (300 μM) (*see Section 4.3.2*). Taken together, these findings show that our iPSCs can be differentiated into SMCs using these lineage-specific differentiation protocols (Cheung et al., 2012).

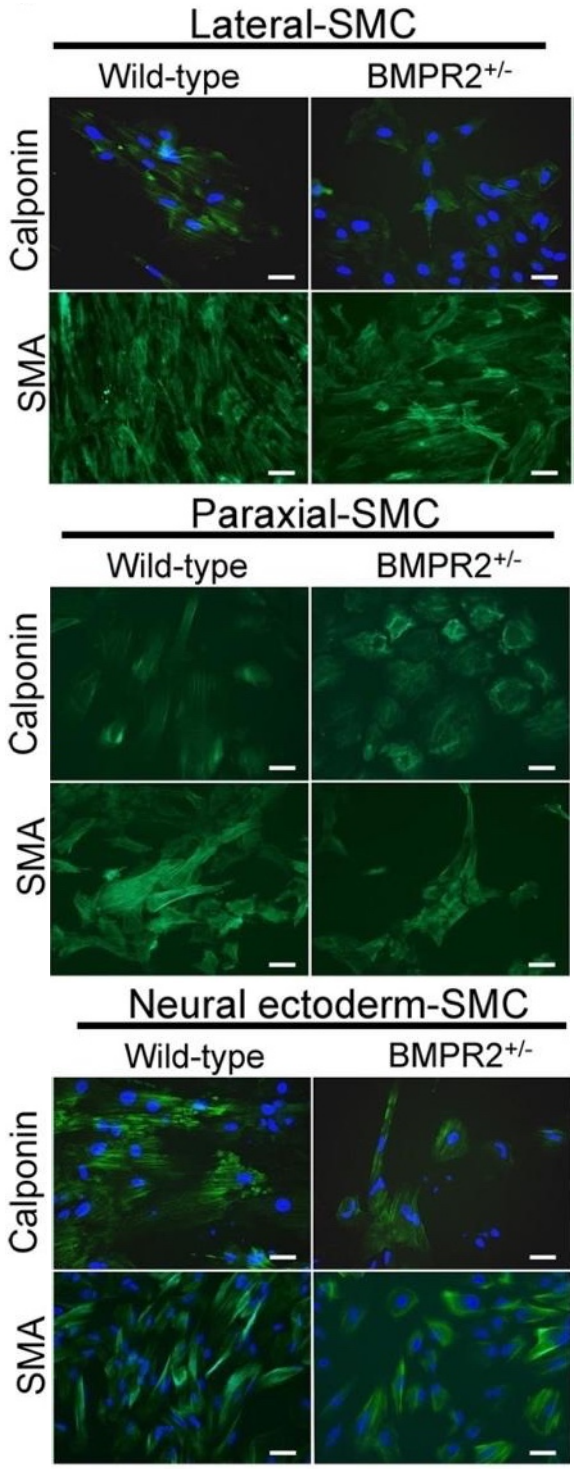

Figure 3.7. Lineage-specific iPSC-SMCs express the SMC markers smooth muscle actin and calponin. Representative immunofluorescence images of wild-type and *BMPR2*$^{+/-}$ iPSCs differentiated into iPSC-SMCs from lateral plate mesoderm (LM), paraxial mesoderm (PM) and neuroectoderm (NE), and immunostained for smooth muscle actin (SMA) and calponin (green). Nuclei were visualised using DAPI staining (blue). Scale bars are 20 μm.

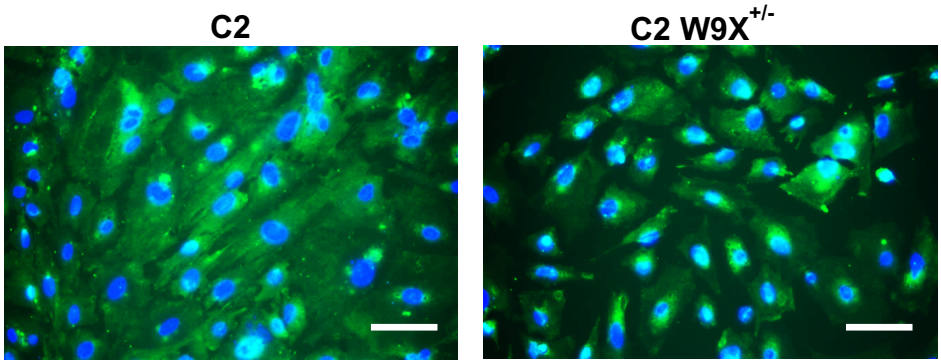

Figure 3.8. LM-iPSC-SMCs express the SMC marker smooth muscle myosin heavy chain. Representative immunofluorescence images of C2 wild-type and C2 W9X$^{+/-}$ LM-iPSC-SMCs immunostained for smooth muscle myosin heavy chain (MYH11, green). Nuclei were visualised using DAPI staining (blue). Scale bars are 100 μm.

3.2.2 – Lateral plate mesoderm-derived iPSC-SMCs most closely resemble the gene expression profile of distal PASMCs

Having successfully generated iPSC-SMCs from LM, PM and NE lineages, I collaborated with Dr Felipe Serrano from Dr Sanjay Sinha's group to determine which of the three iPSC-SMC lineages most closely resembles the gene expression profile of distal PASMCs. To achieve this, I also collaborated with Dr Benjamin Dunmore who isolated RNA from PASMCs and with Dr Christine Cheung who isolated RNA from LM-, PM- and NE-iPSC-SMCs. Dr Serrano and his colleagues then used Illumina Human HT-12 v4 Expression BeadChip microarrays to perform a global microarray gene expression analysis, comparing adult proximal and distal PASMCs to LM-SMCs, PM-SMCs and NE-SMCs. Since the neural crest is one of the origins of pulmonary artery SMCs, a two-dimensional principal component analysis based on differential gene expression restricted to 171 neural crest- and SMC-specific genes (Chi et al., 2007; Betancur et al., 2010) was also carried out.

In both of these analyses, distal PASMCs were more similar to LM-SMCs compared with NE-SMCs and PM-SMCs based on the first principal component (**Figure 3.9 A**). These results suggest that, among these three different lineages, LM-SMCs might be the most appropriate surrogate for distal PASMCs in terms of gene expression profile.

3.2.3 – Lateral plate mesoderm-derived iPSC-SMCs mimic the BMP4 responsiveness of distal PASMCs

To further characterise which lineage might serve as a surrogate for adult PASMCs, I examined the effect of BMP4 (50 ng/ml) on the growth responses of wild-type iPSC-SMCs from each lineage (**Figure 3.9 B**). After 1 week of exposure to 2% serum and BMP4 (50 ng/ml), SMCs from neural ectoderm and paraxial mesoderm origins were growth-inhibited by BMP4, consistent with the phenotype of adult-derived proximal PASMCs (Yang et al., 2005). By contrast, SMCs from the LM lineage were not growth-suppressed, consistent with responses reported in distal PASMCs derived from adults. Since iPSCs from different individuals varied in the absolute numbers of SMCs produced during the differentiation process, growth responses are presented as fold changes rather than absolute numbers of cells.

Furthermore, I also showed that BMP4-treated wild-type LM-iPSC-SMCs were significantly less apoptotic compared to untreated wild-type LM-iPSC-SMCs (**Figure 3.9 C**), which is in line with what has previously been observed using distal PASMCs (Yang et al., 2005).

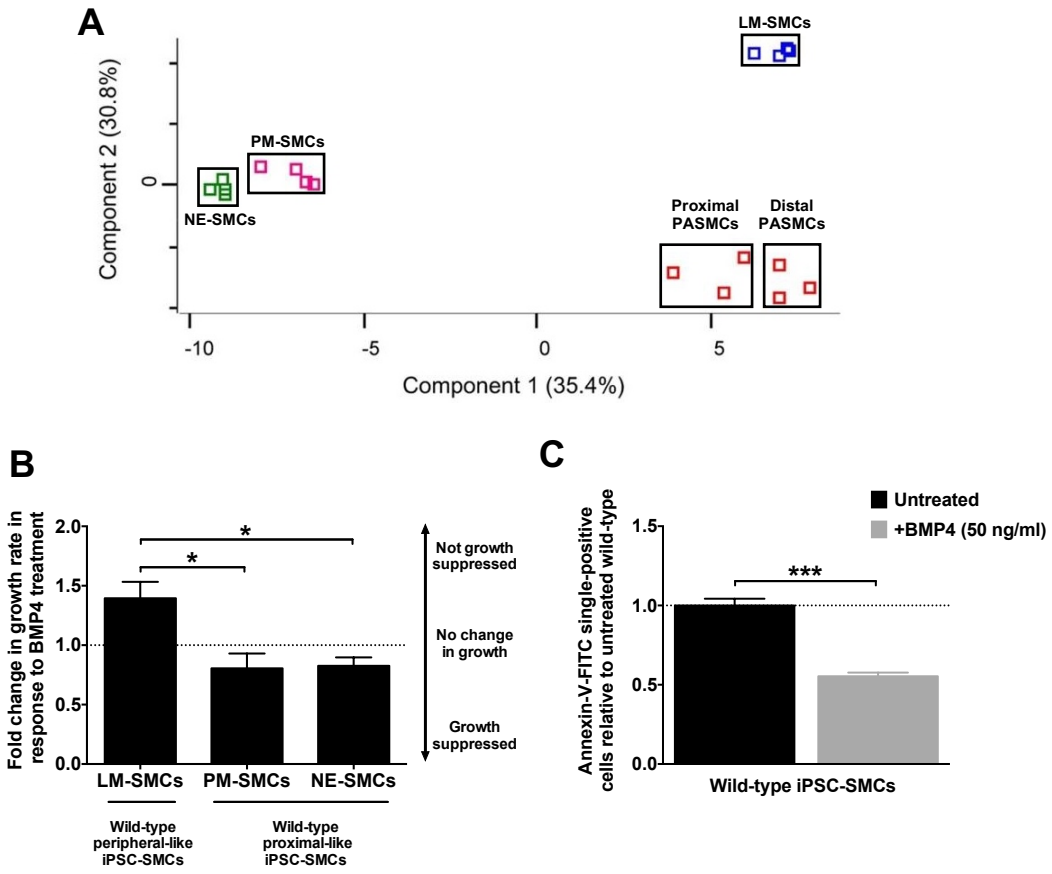

Figure 3.9. LM-iPSC-SMCs display a gene expression profile and responses to BMP4 stimulation akin to distal PASMCs. (**A**) Gene expression patterns of proximal and distal human PASMCs, as well as iPSC-SMCs derived from paraxial mesoderm (PM-SMCs), neuroectoderm (NE-SMCs), and lateral plate mesoderm (LM-SMCs), were analysed using Illumina HumanHT-12 v4 Expression BeadChip microarrays. Gene expression patterns of samples were sorted based on similarity by hierarchical clustering. For this analysis, 171 SMC-specific genes were selected based on the wikipathway database (WikiPathway WP2064 revision 47071) and were subjected to two-dimensional principal component analysis of differential gene expression. (**B**) LM-SMCs are not growth-suppressed after being cultured for one week in cell culture medium supplemented with 2% FBS and BMP4 (50 ng/ml), unlike PM- and NE-SMCs. (**C**) Serum starvation-induced apoptosis in wild-type LM-SMCs, assessed using flow cytometric analysis of cells stained with annexin-V-FITC and propidium iodide, is significantly reduced in the presence of exogenous BMP4 (50 ng/ml), as previously described for distal PASMCs. Data in (**B**) and (**C**) presented as mean ± s.e.m. of 3 different iPSC-SMC lines (biological replicates) per group (* $P < 0.05$, *** $P < 0.001$, one-way ANOVA with Dunnett's post hoc test (**B**) and unpaired two-tailed Student's *t* test (**C**)).

3.2.4 – *BMPR2*$^{+/-}$ lateral plate mesoderm-derived iPSC-SMCs display reduced BMP signalling relative to wild-type iPSC-SMCs

As further validation of the iPSC-SMC model of PAH, I performed qPCR analysis to confirm that the mRNA expression of *BMPR2* and its downstream target genes *ID1* and *ID2* was significantly reduced in C2 W9X$^{+/-}$ LM-iPSC-SMCs relative to isogenic wild-type C2 LM-iPSC-SMCs (**Figure 3.10 A-C**). In addition, similar to what has previously been described in adult distal PASMCs (Upton et al., 2013), previous work performed by Dr Liam Hurst in our group showed that PAH patient-derived *BMPR2*$^{+/-}$ LM-iPSC-SMCs display reduced Smad1/5 phosphorylation in response to BMP4 stimulation (**Figure 3.10 D-E**). Taken together, these findings suggest that lateral plate mesoderm-derived iPSC-SMCs might be suitable surrogates for distal PASMCs when developing an iPSC-based disease model of PAH.

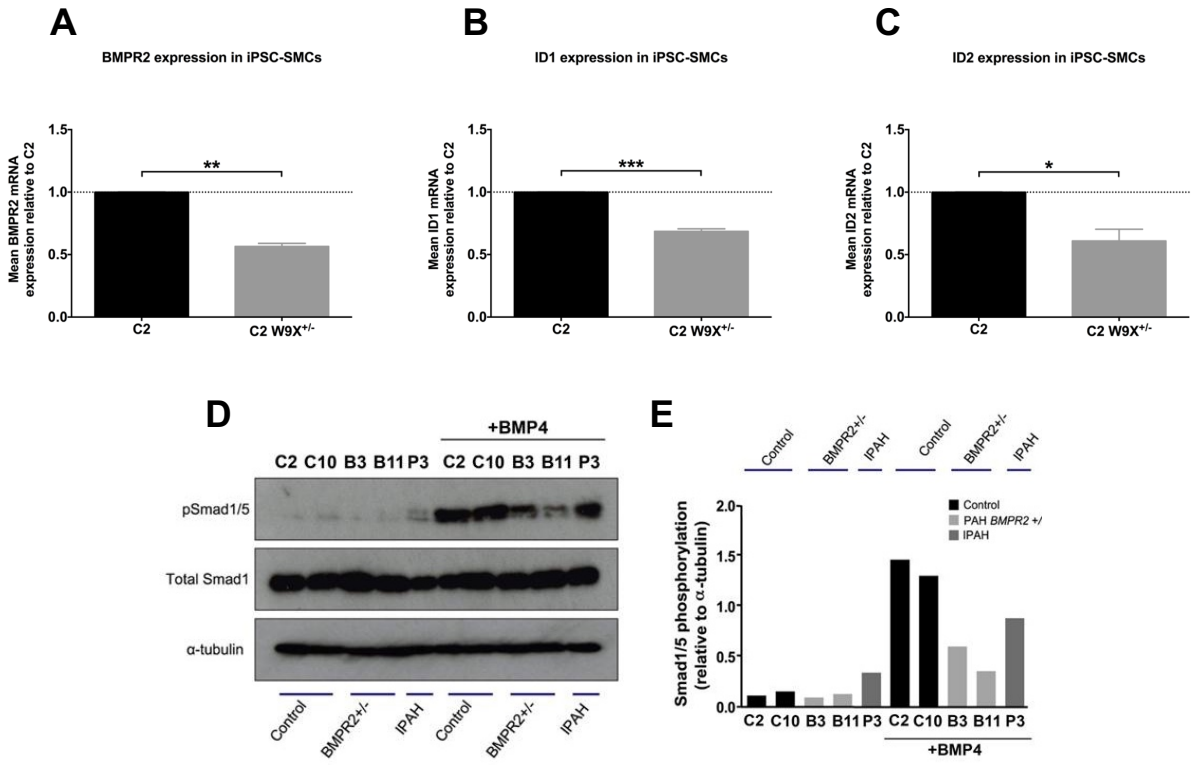

Figure 3.10. *BMPR2*$^{+/-}$ LM-iPSC-SMCs display reduced BMP signalling (**A-C**) qPCR analysis of *BMPR2* (**A**), *ID1* (**B**) and *ID2* (**C**) mRNA expression in isogenic C2 and C2 W9X$^{+/-}$ LM-iPSC-SMCs cultured for one week in 10% FBS post-differentiation. Data presented as mean ± s.e.m. of the results from two (**A**) or three (**B** and **C**) independent differentiations (* $P < 0.05$, ** $P < 0.01$, *** $P < 0.001$, unpaired two-tailed Student's *t* test). (**D**) PAH patient-derived LM-iPSC-SMCs display reduced Smad1/5 phosphorylation following BMP4 (10 ng/ml) treatment, shown by a representative Western blot for phospho-Smad1/5 and total Smad1 (loading control: α-tubulin) in untreated and BMP4-treated wild-type (C2 and C10), *BMPR2*$^{+/-}$ (B3 and B11) and non-*BMPR2*$^{+/-}$ idiopathic pulmonary arterial hypertension (IPAH) (P3) patient-derived iPSC-SMCs, with the corresponding densitometry analysis (*n*=1 per cell line) shown in (**E**).

3.3 – Discussion

In addition to developing the first iPSC-SMC model of PAH associated with mutations in *BMPR2*, one of the main aims of this study was to examine the impact of *BMPR2* mutation on the establishment of PAH-associated cellular phenotypes without the confounding effects of other genetic differences between cell lines. In this chapter, CRISPR-Cas9 genome editing was used to either introduce a known causal *BMPR2* mutation (W9X) or delete exon 1 of the *BMPR2* gene (ΔExon1) in a wild-type iPSC line from a healthy individual with no family history of PAH or cardiovascular disease. This approach resulted in the generation of wild-type and *BMPR2*$^{+/-}$ iPSCs with an otherwise isogenic background, thus removing the effects that different genetic modifiers (Gu et al., 2017) may have on the penetrance of cellular phenotypes. As a result, any difference in phenotype between the wild-type and genome-edited *BMPR2*$^{+/-}$ iPSC lines can then be attributed to the introduction of the *BMPR2* mutation. Although the possibility of CRISPR-mediated off-target effects cannot be excluded because these iPSC lines were not submitted to whole-genome sequencing, numerous studies have shown that such off-target effects are rare (Smith et al., 2014; Suzuki et al., 2014; Veres et al., 2014; Chang et al., 2015; Park et al., 2015; Li et al., 2016) and are thus unlikely to confound the phenotypes being studied.

Another important new finding presented in this chapter is that wild-type and *BMPR2*$^{+/-}$ iPSCs differentiated into iPSC-SMCs via lateral plate mesoderm (LM), but not via paraxial mesoderm (PM) or neuroectoderm (NE), display a gene expression profile and functional responses to BMP4 signalling akin to distal PASMCs. This suggests that LM-iPSC-SMCs might be suitable surrogates for distal PASMCs when developing a human iPSC model of PAH. By comparison, a recent study using these three lineage-specific iPSC-SMC differentiation protocols (Granata et al., 2017) showed that neural crest-derived iPSC-SMCs are the most suitable surrogates for SMCs of the aortic root, ascending aorta and arch for studying the development of aortic aneurysms in Marfan syndrome. Taken together, these observations highlight the importance of using appropriate lineage-specific differentiation protocols in iPSC disease modelling studies.

It is important to note that the LM-iPSC-SMCs described in this thesis do not perfectly represent adult PASMCs. For example, although the gene expression profile of LM-iPSC-SMCs was similar to that of PASMCs in terms of the first principal component, it differed in the second principal component. Furthermore, because the generation of iPSC-SMCs that distinctly represent pulmonary as opposed to systemic smooth muscle cells is yet to be achieved, phenotypes that are only present in pulmonary vascular cells cannot be directly studied in this model. Nevertheless, because phenotypes such as aberrant proliferation, apoptosis and mitochondrial membrane polarisation are not unique to the pulmonary vasculature, this does not preclude LM-iPSC-SMCs from being used to develop an iPSC model of PAH.

It is also worth noting that the iPSC-SMCs generated in this investigation might not be composed of a single homogenous SMC population. Due to a lack of definitive SMC subtype-specific cell surface markers, lineage-specific iPSC-SMCs cannot easily be purified by fluorescent or magnetic-activated cell sorting (Kumar et al., 2017). Alternative strategies to purify iPSC-SMCs could involve generating iPSC-SMCs in which an antibiotic resistance gene is expressed under the control of the *MYH11* promoter. This would allow iPSC-SMCs to be purified whilst still in the dish, as has been previously demonstrated with iPSC-derived cardiomyocytes (Kita-Matsuo et al., 2009; Ma et al., 2011).

Nevertheless, Cheung et al. (2012) showed that more than 86% of LM-iPSC-SMCs expressed smooth muscle myosin heavy chain (*MYH11*), which is considered to be the most robust marker of mature SMCs (Owens et al., 2004). The LM-iPSC-SMCs described in this chapter were differentiated by following the same protocol described by Cheung et al. (2012) and also stained positively for the SMC markers smooth muscle actin (SMA), calponin and MYH11. Together with the observation that wild-type C2 LM-iPSC-SMCs displayed contractile responses to stimulation with carbachol (300 μM) (*see Section 4.3.2*), these findings suggest that the majority of these cells were in fact SMCs.

CHAPTER 4 – RESULTS (II)

Contributions of *BMPR2* mutations and extrinsic factors to cellular phenotypes of pulmonary arterial hypertension

4.1 – *BMPR2* heterozygosity in iPSC-SMCs is necessary and sufficient to recapitulate several PAH-associated SMC phenotypes

Having generated wild-type and *BMPR2*$^{+/-}$ LM-iPSC-SMCs with an otherwise isogenic background and shown that these cells mimic the BMP4 responsiveness of distal PASMCs, my next aim was to address the controversial question of whether genetic reduction of *BMPR2* alone is necessary and/or sufficient to establish major PAH-associated PASMC phenotypes in these cells. Compared to PASMCs from unaffected donor controls, PASMCs isolated from PAH patients have previously been shown to be more proliferative, less susceptible to apoptosis, and display increased inner mitochondrial membrane polarisation (Paulin & Michelakis, 2014). I therefore investigated whether *BMPR2*$^{+/-}$ LM-iPSC-SMCs are able to recapitulate these PAH-associated cellular phenotypes under basal serum-free, chemically-defined conditions in the presence or absence of additional extrinsic growth and/or inflammatory stimuli such as serum, BMP4 and TNFα.

4.1.1 – *BMPR2*$^{+/-}$ iPSC-SMCs are more proliferative relative to isogenic wild-type iPSC-SMCs under serum-free, chemically-defined conditions

Since increased PASMC proliferation is one of the hallmarks of PAH, I first set out to determine whether *BMPR2* heterozygosity in iPSC-SMCs is sufficient to recapitulate this pro-proliferative PASMC phenotype. I initially differentiated C2 and C2 W9X$^{+/-}$ LM-iPSC-SMCs according to the standard LM protocol in serum-free, chemically-defined medium (CDM) supplemented with PDGF-BB (10 ng/ml) and TGF-β1 (2 ng/ml) (hereafter referred to as 'PT') (**Figure 4.1 A**). These cells were subsequently cultured for one week in CDM + PT prior to assessing cell proliferation by performing cell counts and by measuring cellular DNA content. Under these serum-free conditions, cell counts revealed that there was no significant difference ($P > 0.05$) in proliferation between C2 W9X$^{+/-}$ iPSC-SMCs and isogenic wild-type C2 iPSC-SMCs (**Figure 4.2 A**). By contrast, when proliferation in PT was assessed by measuring cellular double-stranded DNA content using Vybrant DyeCycle Ruby stain, C2 W9X$^{+/-}$ iPSC-SMCs became significantly (1.5-fold, $P < 0.001$) more proliferative relative to C2 iPSC-SMCs (**Figure 4.2 B**).

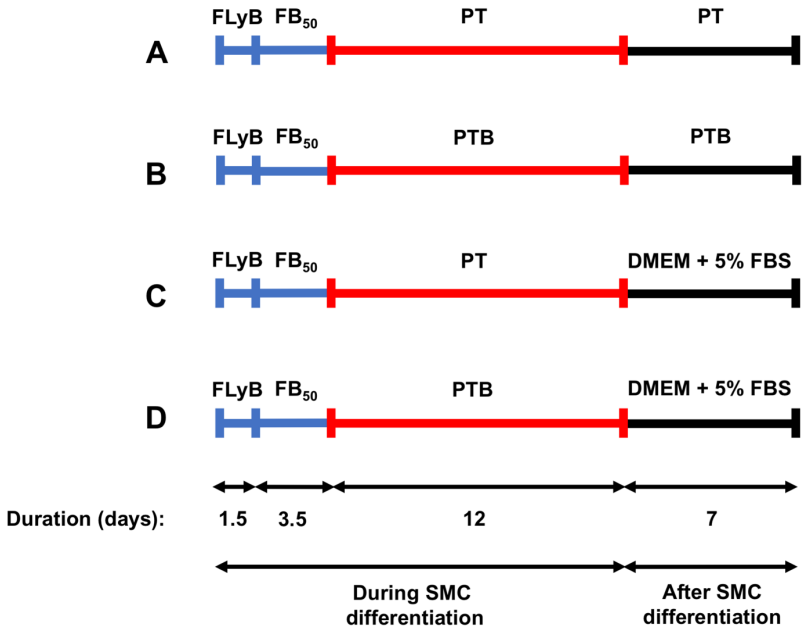

Figure 4.1. Outline of the iPSC-SMC differentiation and culture conditions used when assessing cell proliferation. (**A** and **C**) Wild-type and *BMPR2*$^{+/-}$ iPSC-SMCs were initially differentiated via lateral plate mesoderm (LM) according to the standard LM protocol (Cheung et al., 2012) in serum-free, chemically-defined medium (CDM) supplemented with PDGF-BB (10 ng/ml) and TGF-β1 (2 ng/ml) (referred to as 'PT'). After differentiation, LM-iPSC-SMCs were cultured for 7 days in either CDM + PT (**A**) or DMEM + 5% FBS (**C**) prior to assessing cell proliferation by measuring cellular DNA content and/or performing cell counts. (**B** and **D**) Cell proliferation was also assessed after differentiating wild-type and *BMPR2*$^{+/-}$ iPSC-SMCs in the presence of a high concentration (50 ng/ml) of exogenous BMP4 during the 12-day 'PT' SMC differentiation phase (referred to as 'PTB') and subsequently culturing the cells for 7 days in either CDM + PTB (**B**) or DMEM + 5% FBS (**D**). In all four protocols (**A-D**), lateral plate mesoderm formation was induced by culturing iPSCs for 1.5 days in CDM supplemented with FGF-2 (20 ng/ml), LY294002 (10 ng/ml) and BMP4 (10 ng/ml) (referred to as 'FLyB'), after which the cells were cultured for 3.5 days in CDM supplemented with FGF-2 (20 ng/ml) and BMP4 (50 ng/ml) (referred to as 'FB_{50}').

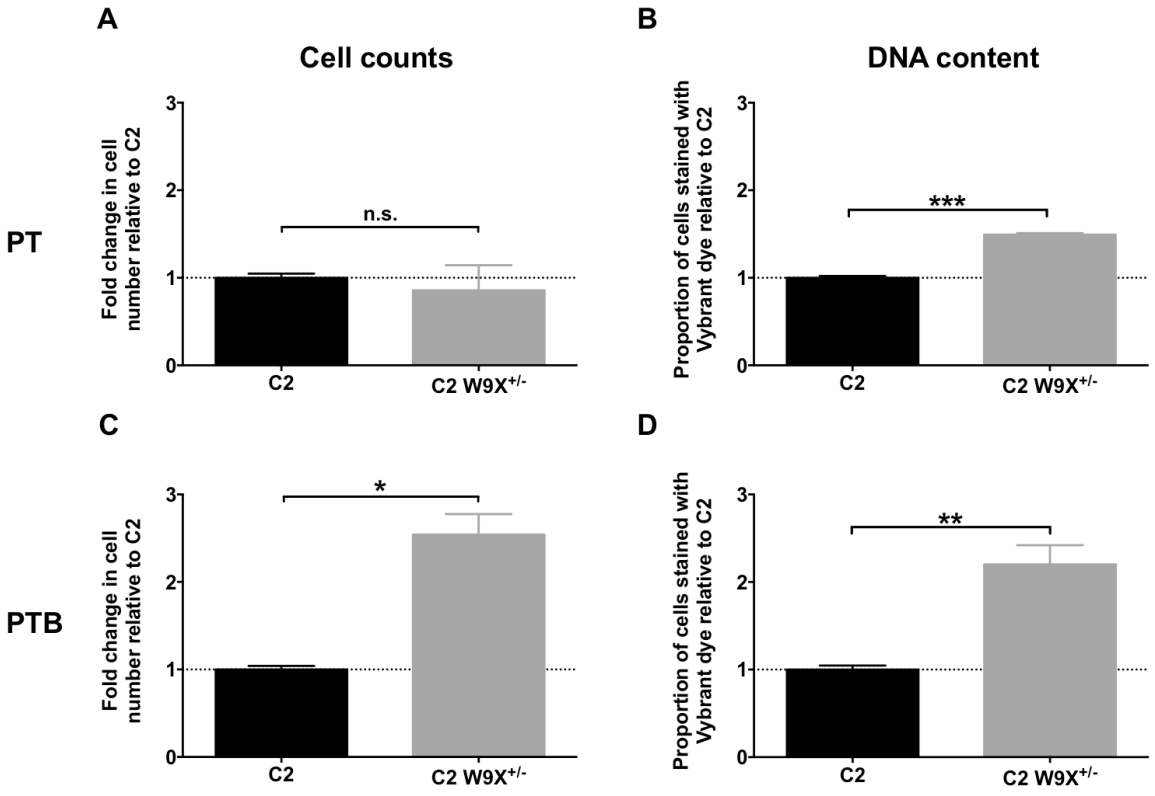

Figure 4.2. Proliferation of C2 and C2 W9X$^{+/-}$ iPSC-SMCs under serum-free conditions. Wild-type and *BMPR2*$^{+/-}$ iPSC-SMCs were differentiated under serum-free conditions in chemically-defined medium (CDM) supplemented with either PDGF-BB (10 ng/ml) and TGF-β1 (2 ng/ml) (hereafter referred to as 'PT') (**A** and **B**) or PDGF-BB (10 ng/ml), TGF-β1 (2 ng/ml) and BMP4 (50 ng/ml) (hereafter referred to as 'PTB') (**C** and **D**). iPSC-SMC proliferation was assessed by performing cell counts after culturing the differentiated cells for 7 days in CDM + PT (**A**) or CDM + PTB (**C**), or by measuring cellular DNA content via flow cytometric analysis of Vybrant DyeCycle Ruby staining (**B** and **D**). Data presented as mean ± s.e.m. of three technical replicates based on cells from the same differentiation (**A** and **C**), or based on the results from three independent differentiations (**B** and **D**) [n.s., not significant (P > 0.05), * $P < 0.05$, ** $P < 0.01$, *** $P < 0.001$, unpaired two-tailed Student's *t* test].

In view of the discrepancy between the findings obtained using these two complementary proliferation assays, I investigated whether the LM-iPSC-SMC differentiation protocol could be modified to better model distal PASMCs. Since BMP4 is highly expressed in the distal lung bud during development (Bellusci et al., 1996; Hogan, 1996), I repeated the iPSC-SMC proliferation assays after differentiating C2 and C2 W9X$^{+/-}$ LM-iPSC-SMCs in the presence of a high concentration (50 ng/ml) of exogenous BMP4 during the 12-day 'PT' SMC differentiation phase (hereafter referred to as 'PTB') (**Figure 4.1 B**).

After these cells were cultured for 7 days in serum-free PTB conditions, C2 W9X$^{+/-}$ iPSC-SMCs were significantly (2.5-fold, $P < 0.05$) more proliferative compared to isogenic C2 iPSC-SMCs (**Figure 4.2 C**). Consistent with these findings, C2 W9X$^{+/-}$ iPSC-SMCs were also significantly (2.2-fold, $P < 0.01$) more proliferative relative to C2 iPSC-SMCs when the proliferation of these cells was assessed by measuring cellular DNA content (**Figure 4.2 D**). Taken together, these results suggest that the pro-proliferative phenotype of C2 W9X$^{+/-}$ iPSC-SMCs was more pronounced after iPSC-SMCs were differentiated in PTB rather than in PT.

In support of these observations, after iPSC-SMCs were cultured for one week in DMEM + 5% FBS post-differentiation, C2 W9X$^{+/-}$ iPSC-SMCs were 1.4 times more proliferative compared to C2 iPSC-SMCs after being differentiated in PT (**Figure 4.1 C** and **Figure 4.3 A**) but became 2.4 times more proliferative after being differentiated in PTB (**Figure 4.1 D** and **Figure 4.3 B**).

Since adult PAH patient-derived PASMCs are frequently reported to be at least two times more proliferative compared to wild-type PASMCs (Courboulin et al., 2012; Wilson et al., 2015; Boucherat et al., 2017), these findings suggest that C2 W9X$^{+/-}$ iPSC-SMCs differentiated in PTB recapitulate the pro-proliferative phenotype of distal PASMCs from PAH patients more closely and robustly compared to C2 W9X$^{+/-}$ iPSC-SMCs differentiated in PT.

After serum-free differentiation in PTB, additional exposure to serum or other factors was not required for C2 W9X$^{+/-}$ iPSC-SMCs to be more proliferative relative to isogenic wild-type C2 iPSC-SMCs. This suggests that *BMPR2* heterozygosity in iPSC-SMCs differentiated in PTB is necessary and sufficient to recapitulate the pro-proliferative phenotype of distal PASMCs from PAH patients.

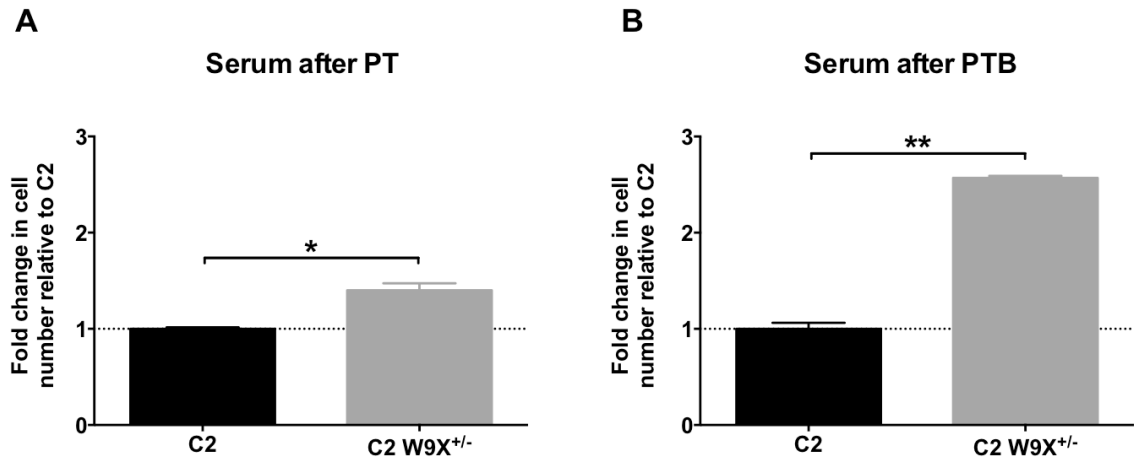

Figure 4.3. Proliferation of C2 and C2 W9X$^{+/-}$ iPSC-SMCs in serum. Proliferation of C2 and C2 W9X$^{+/-}$ iPSC-SMCs was assessed by differentiating the cells in CDM-PVA + PT (**A**) or CDM-PVA + PTB (**B**), after which all cells were cultured for 7 days in DMEM + 5% FBS, trypsinised and counted manually using disposable haemocytometer counting grids. Data presented as mean ± s.e.m. of three technical replicates based on cells from the same differentiation [n.s., not significant ($P > 0.05$), * $P < 0.05$, ** $P < 0.01$, unpaired two-tailed Student's *t* test].

Next, I performed cell counts to investigate whether the difference in proliferation between C2 and C2 W9X$^{+/-}$ iPSC-SMCs is representative of the relative levels of cell proliferation observed in LM-iPSC-SMCs differentiated from wild-type and patient-derived *BMPR2*$^{+/-}$ iPSC lines that were previously generated by our laboratory (Geti et al., 2012; see **Table 2.1** for characteristics).

Similar to the difference in proliferation between C2 and C2 W9X$^{+/-}$ iPSC-SMCs assessed by cell counts under serum-free PT conditions (**Figure 4.2 A**), cell counts revealed that patient-derived *BMPR2*$^{+/-}$ iPSC-SMCs assayed under serum-free PT conditions displayed a non-significant ($P > 0.05$) trend towards reduced proliferation compared to wild-type iPSC-SMCs (**Figure 4.4 A**). By contrast, patient-derived *BMPR2*$^{+/-}$ iPSC-SMCs became 1.8 times more proliferative compared to wild-type iPSC-SMCs when assayed under serum-free PTB conditions, although this difference was not statistically significant ($P > 0.05$) (**Figure 4.4 B**).

Furthermore, *BMPR2*$^{+/-}$ iPSC-SMCs differentiated in PT and subsequently cultured for one week in DMEM + 5% FBS displayed no significant difference in proliferation ($P > 0.05$) compared to wild-type iPSC-SMCs treated the same way (**Figure 4.4 C**) but became significantly (2.4-fold, $P < 0.01$) more proliferative in DMEM + 5% FBS after differentiation in PTB (**Figure 4.4 D**).

Taken together, these findings suggest that *BMPR2*$^{+/-}$ iPSC-SMCs differentiated in PTB recapitulate the pro-proliferative phenotype of distal PASMCs from PAH patients more robustly compared to *BMPR2*$^{+/-}$ iPSC-SMCs differentiated in PT, thus validating the findings observed in isogenic C2 and C2 W9X$^{+/-}$ iPSC-SMCs.

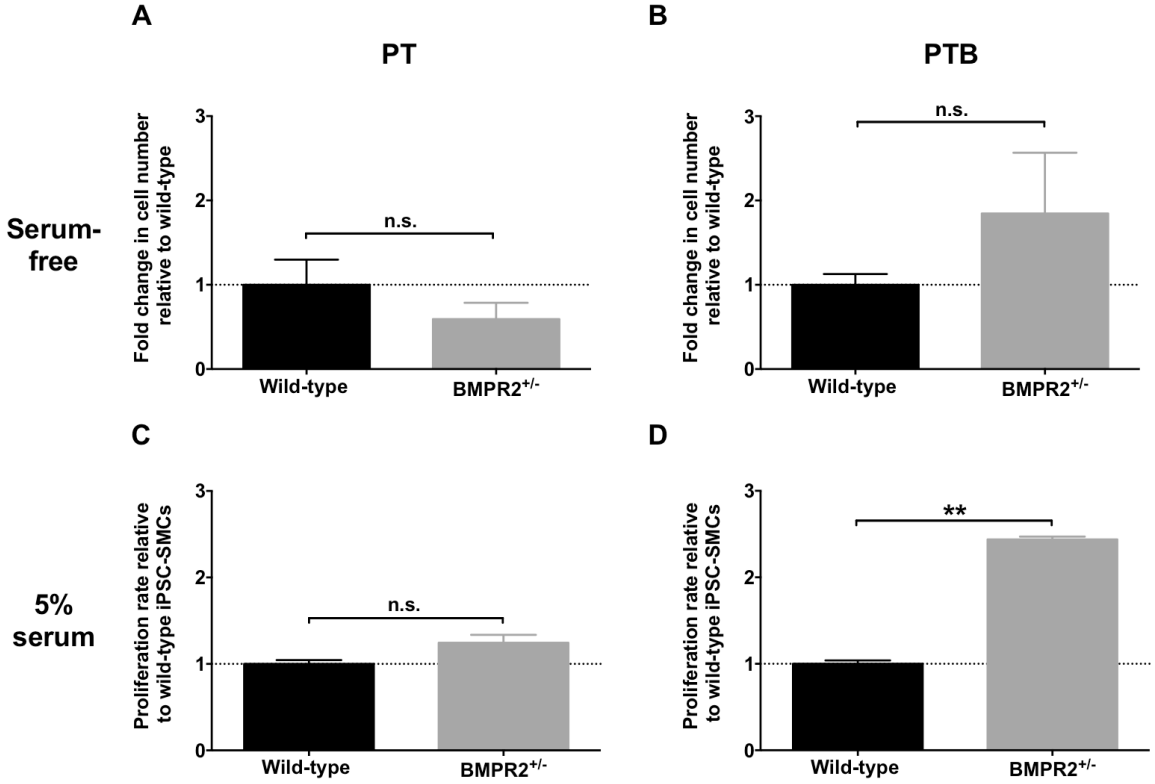

Figure 4.4. Proliferation of wild-type and PAH patient-derived *BMPR2*$^{+/-}$ iPSC-SMCs under serum-free and serum-containing conditions. Proliferation rates of wild-type and patient-derived *BMPR2*$^{+/-}$ iPSC-SMCs were assessed by differentiating cells in CDM-PVA + PT (**A** and **C**) or CDM-PVA + PTB (**B** and **D**), after which the cells were cultured for 7 days in CDM-PVA + PT (**A**), CDM-PVA + PTB (**B**) or in DMEM + 5% FBS (**C** and **D**). Subsequently, all iPSC-SMCs were trypsinised and counted manually using disposable haemocytometer counting grids. Data presented as mean ± s.e.m. of three wild-type and two patient-derived *BMPR2*$^{+/-}$ iPSC-SMC lines (**A** and **B**), or two wild-type and two patient-derived lines (**C** and **D**) based on cells from the same differentiation [n.s., not significant ($P > 0.05$), * $P < 0.05$, ** $P < 0.01$, unpaired two-tailed Student's *t* test].

4.1.2 – *BMPR2*$^{+/-}$ iPSC-SMCs are less apoptotic relative to isogenic wild-type iPSC-SMCs under serum-free, chemically-defined conditions

Next, I used two complementary apoptosis assays to determine whether *BMPR2* heterozygosity in iPSC-SMCs is sufficient to recapitulate the anti-apoptotic phenotype of PASMCs derived from PAH patients. First, I differentiated C2 and C2 W9X$^{+/-}$ iPSC-SMCs in PT or PTB and assessed apoptosis under basal serum-free conditions using the Caspase-Glo 3/7 Assay (Promega). This assay measures the activity of caspase-3 and caspase-7 in terms of their ability to cleave a pro-luminescent caspase-3/7 substrate. My analysis revealed that C2 W9X$^{+/-}$ iPSC-SMCs were significantly ($P < 0.01$) less apoptotic relative to C2 iPSC-SMCs, regardless of whether they were differentiated in PT or PTB (**Figures 4.5 A** and **C**). These results were confirmed by flow cytometric analysis of isogenic wild-type and *BMPR2*$^{+/-}$ iPSC-SMCs which were positive for annexin-V-FITC staining but negative for propidium iodide (PI) staining (**Figures 4.5 B** and **D**).

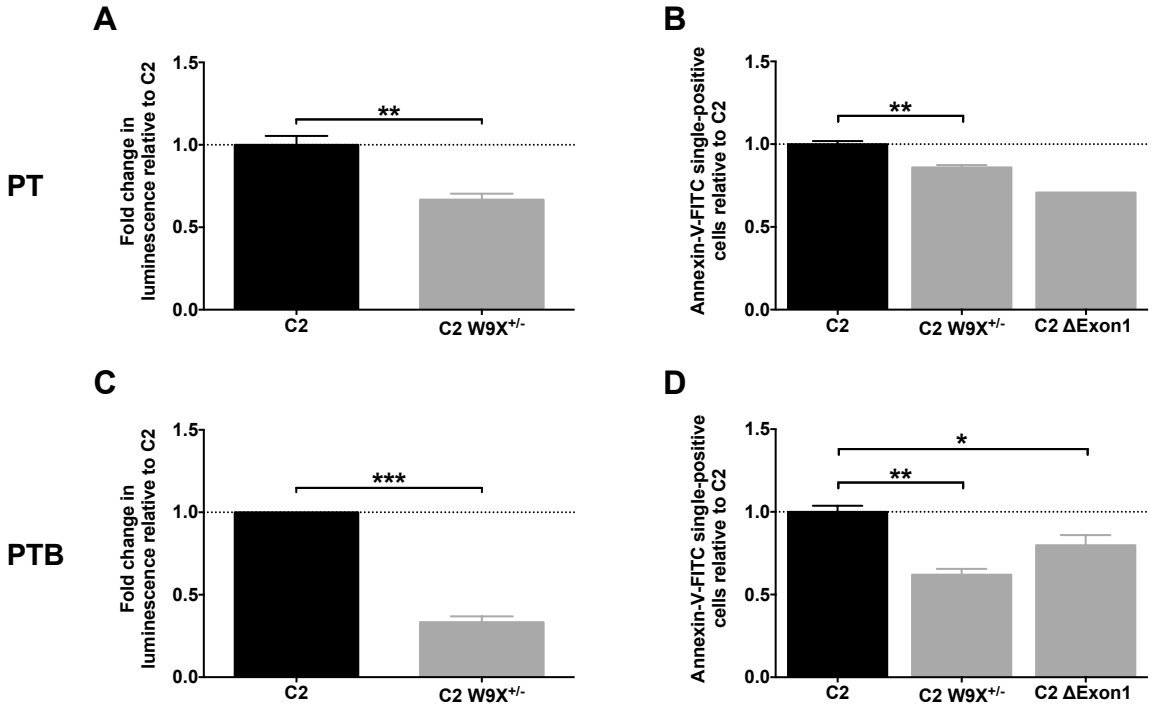

Figure 4.5. Serum-free *BMPR2*$^{+/-}$ iPSC-SMCs are less apoptotic relative to isogenic wild-type iPSC-SMCs. LM-iPSC-SMCs with isogenic backgrounds were differentiated in either PT (**A** and **B**) or PTB (**C** and **D**). (**A** and **C**): Basal apoptosis in serum-free PT (**A**) or PTB (**C**) conditions was assessed using the Caspase Glo-3/7 Assay which provides a luminescent readout of caspase-3/7 activity. (**B** and **D**): As a complementary assay, iPSC-SMC apoptosis in PT (**B**) or PTB (**D**) was also assessed by flow cytometric analysis of iPSC-SMCs positive for annexin-V-FITC staining but negative for propidium iodide (PI) staining. Data presented as mean ± s.e.m. of the results from three independent differentiations, except for annexin-V-FITC/PI staining of C2 ΔExon1 iPSC-SMCs differentiated in PT (**B**), which were only analysed in a single experiment. (* $P < 0.05$, ** $P < 0.01$, *** $P < 0.001$, unpaired two-tailed Student's *t* test (**A-C**), or one-way ANOVA with multiple comparisons being corrected for using Dunnett's post hoc test (**D**)).

Furthermore, similar to the pro-proliferative phenotype of *BMPR2*$^{+/-}$ iPSC-SMCs, the anti-apoptotic phenotype of C2 W9X$^{+/-}$ iPSC-SMCs was more pronounced after iPSC-SMCs were differentiated in PTB rather than in PT.

In addition to displaying reduced rates of basal apoptosis relative to wild-type PASMCs, patient-derived *BMPR2*$^{+/-}$ PASMCs are also more resistant to apoptosis induction in response to extrinsic stimuli (Zhang et al., 2003). Therefore, I also used the Caspase-Glo 3/7 Assay to investigate whether C2 W9X$^{+/-}$ iPSC-SMCs are more resistant to apoptosis induction compared to C2 iPSC-SMCs in response to treatment for 1 hour with the protein kinase inhibitor staurosporine (50 nM). Although the difference in staurosporine-induced apoptosis was not statistically significant ($P > 0.05$), C2 W9X$^{+/-}$ iPSC-SMCs tended to be almost two times more resistant to staurosporine-induced apoptosis relative to C2 iPSC-SMCs (**Figure 4.6**).

The level of apoptosis resistance observed in C2 W9X$^{+/-}$ iPSC-SMCs differentiated in PTB is in line with the level of apoptosis resistance observed in *BMPR2*$^{+/-}$ PASMCs derived from PAH patients (Courboulin et al., 2012; Boucherat et al., 2017). Furthermore, apoptosis resistance in C2 W9X$^{+/-}$ iPSC-SMCs was more pronounced after differentiation in PTB rather than in PT. Taken together, these findings further support the use of the PTB differentiation protocol for generating iPSC-SMCs that can be used to model distal PASMCs. In addition, these results also suggest that *BMPR2* heterozygosity in iPSC-SMCs is necessary and sufficient to recapitulate the anti-apoptotic phenotype of distal PASMCs from PAH patients.

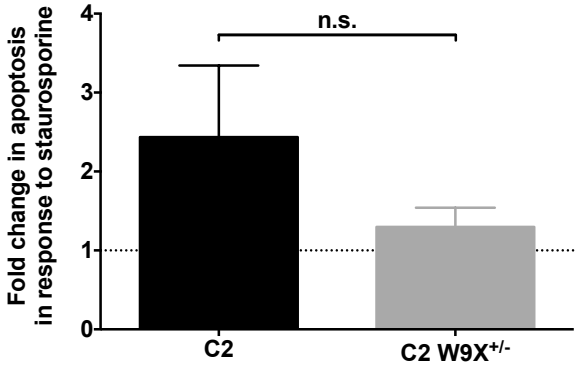

Figure 4.6. Staurosporine-induced apoptosis in serum-free C2 and C2 W9X$^{+/-}$ iPSC-SMCs. Isogenic C2 and C2 W9X$^{+/-}$ iPSC-SMCs were differentiated in PTB, after which apoptosis was induced by culturing the cells for 1 hour in serum-free DMEM in the presence or absence of staurosporine (50 nM), a broad-spectrum protein kinase inhibitor. Apoptosis was assessed using the Caspase Glo-3/7 Assay which provides a luminescent readout of caspase-3/7 activity. Data presented as mean ± s.e.m. of the results obtained from three independent differentiations and expressed as fold changes in apoptosis after 1 hour of exposure to DMEM + staurosporine relative to the level of apoptosis observed after exposure to DMEM only [n.s., not significant ($P > 0.05$), unpaired two-tailed Student's *t* test].

4.1.3 – Isogenic *BMPR2*$^{+/-}$ iPSC-SMCs display increased *IL-6* mRNA expression relative to wild-type iPSC-SMCs

In addition to increased proliferation and reduced apoptosis of PAH-derived PASMCs, serum levels of the pro-inflammatory cytokine IL-6 are significantly elevated in IPAH patients compared to controls (Humbert et al., 1995; Soon et al., 2010). Increased IL-6 expression has also been detected in PASMCs isolated from *Bmpr2*$^{+/-}$ mice with lipopolysaccharide (LPS)-induced pulmonary hypertension (Soon et al., 2015), as well as in *BMPR2*$^{+/-}$ PAECs (Diebold et al., 2015).

To test whether *BMPR2*$^{+/-}$ iPSC-SMCs also display increased IL-6 expression, I therefore performed qPCR analysis of *IL-6* mRNA expression levels in wild-type and isogenic *BMPR2*$^{+/-}$ iPSC-SMCs. C2 W9X$^{+/-}$ iPSC-SMCs differentiated in PT displayed a non-significant trend ($P > 0.05$) towards increased *IL-6* expression compared to wild-type C2 iPSC-SMCs (**Figure 4.7 A**). However, this difference became statistically significant ($P < 0.05$) and more pronounced after iPSC-SMCs were differentiated in PTB (**Figure 4.7 B**). Taken together, these findings suggest that *BMPR2* heterozygosity in iPSC-SMCs differentiated in PTB is sufficient to recapitulate the increased *IL-6* expression observed in PAH-derived PASMCs. In addition, these observations further suggest that iPSC-SMC differentiation in PTB instead of PT

generates cells that more strongly re-capitulate PAH-associated phenotypes observed in distal PASMCs.

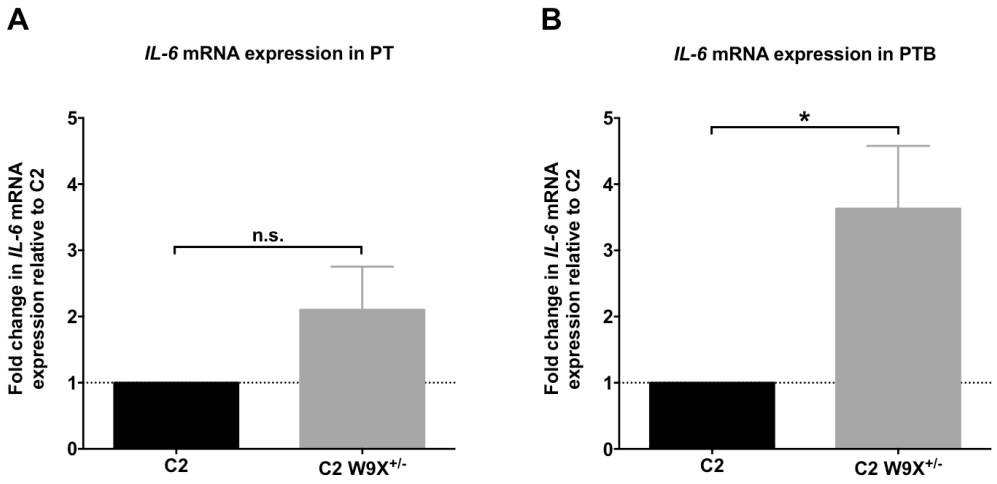

Figure 4.7. Isogenic *BMPR2*$^{+/-}$ iPSC-SMCs display increased *IL-6* mRNA expression compared to wild-type iPSC-SMCs after differentiation in PTB but not after differentiation in PT. Quantitative PCR analysis of *IL-6* mRNA expression in LM-iPSC-SMCs differentiated in PT (**A**) or PTB (**B**) during the last 12 days of the LM-iPSC-SMC differentiation protocol. Data presented as mean ± s.e.m. of the results from three independent differentiations [n.s., not significant ($P > 0.05$); * $P < 0.05$, unpaired two-tailed Student's *t* test]

4.2 – *BMPR2*$^{+/-}$ iPSC-SMCs only recapitulate the mitochondrial hyperpolarisation phenotype of patient-derived PASMCs under specific conditions

Although I have shown that the iPSC model is able to recapitulate certain PAH-associated cellular phenotypes under serum-free conditions, not all phenotypes could be recapitulated under these conditions, as described below.

4.2.1 – Inner mitochondrial membrane polarisation in isogenic iPSC-SMCs

Hyperpolarisation of the inner mitochondrial membrane (IMM) is a feature of PASMCs and pulmonary artery endothelial cells (PAECs) isolated from patients with end-stage PAH and is linked to increased rates of glycolysis, changes in reactive oxygen species (ROS) production and vascular remodeling (Pak et al., 2013; Paulin & Michelakis, 2014; Diebold et al., 2015).

First, I determined whether *BMPR2* heterozygosity in iPSC-SMCs is sufficient to recapitulate IMM hyperpolarisation by performing flow cytometric analysis of isogenic wild-type and *BMPR2*$^{+/-}$ iPSC-SMCs stained with tetramethylrhodamine ethyl ester (TMRE, 30 nM). TMRE is a red fluorescent dye that is taken up into mitochondria at a rate that is proportional to the charge difference across the IMM, with a higher level of TMRE fluorescence being indicative of increased IMM polarisation.

To confirm that changes in TMRE staining intensity in iPSC-SMCs and PASMCs reflect changes in mitochondrial membrane potential, I incubated C2 LM-iPSC-SMCs (n=1) and wild-type PASMCs (n=3) for 20 minutes in the presence or absence of carbonyl cyanide 4-trifluoromethoxyphenylhydrazone (FCCP, 5 μM), after which the cells were loaded for 30 minutes with TMRE (30 nM) in the continuing presence or absence of FCCP. FCCP is a protonophore which causes mitochondrial uncoupling by dissipating the electrochemical proton gradient across the IMM and should hence reduce TMRE fluorescence under non-quenching conditions (Brand & Nicholls, 2011). Indeed, FCCP treatment significantly ($P < 0.001$) reduced TMRE fluorescence in wild-type PASMCs (**Figure 4.8 A**) and also decreased TMRE fluorescence in C2 iPSC-SMCs to a similar extent (**Figure 4.8 B**), confirming that the TMRE assay was working as expected.

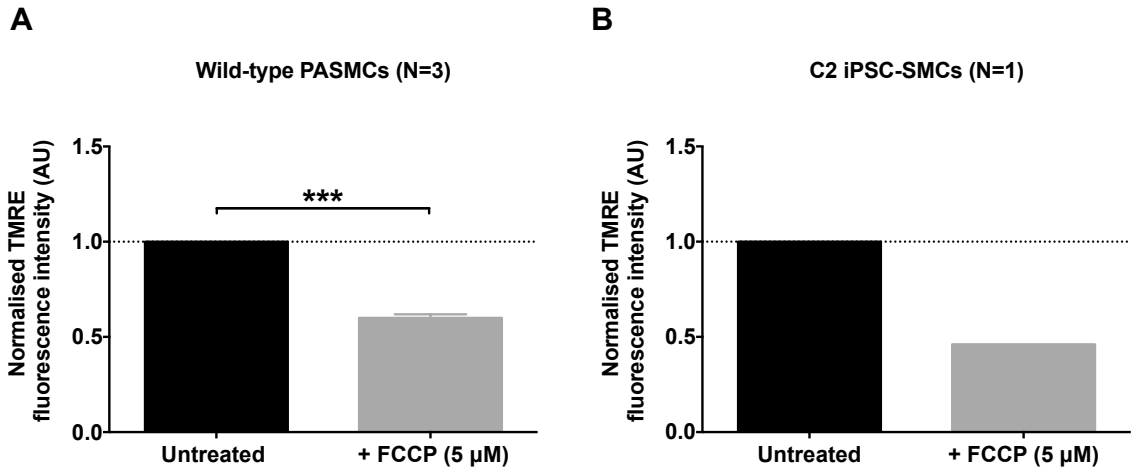

Figure 4.8. Effect of FCCP on inner mitochondrial membrane polarisation in C2 iPSC-SMCs and wild-type PASMCs. The mitochondrial uncoupling agent carbonyl cyanide 4-trifluoromethoxyphenylhydrazone (FCCP, 5 µM) reduced inner mitochondrial membrane (IMM) polarisation in wild-type PASMCs (*n*=3) (**A**) and C2 iPSC-SMCs (*n*=1) (**B**). IMM polarisation was assessed by flow cytometric analysis of cells stained with tetramethylrhodamine ethyl ester (TMRE, 30 nM), a red fluorescent dye that is taken up into mitochondria at a rate that is proportional to the charge difference across the IMM. Data in (**A**) presented as mean ± s.e.m. of the results obtained from three different PASMCs lines (*** $P < 0.001$, unpaired two-tailed Student's *t* test).

Having validated that changes in TMRE fluorescence reflected changes in mitochondrial membrane potential, I used TMRE staining to assess mitochondrial polarisation in isogenic iPSC-SMCs that were differentiated in PTB and assayed under serum-free conditions. Surprisingly, flow cytometric analysis of TMRE staining in these cells revealed that *BMPR2*$^{+/-}$ iPSC-SMCs had a significantly ($P < 0.001$) hypopolarised IMM state compared to their isogenic wild-type (**Figure 4.10 A**). I therefore investigated whether serum-free *BMPR2*$^{+/-}$ iPSC-SMCs might require exposure to extrinsic factors such as serum in order to acquire a hyperpolarised IMM state (see **Figure 4.9** for an outline of these experiments).

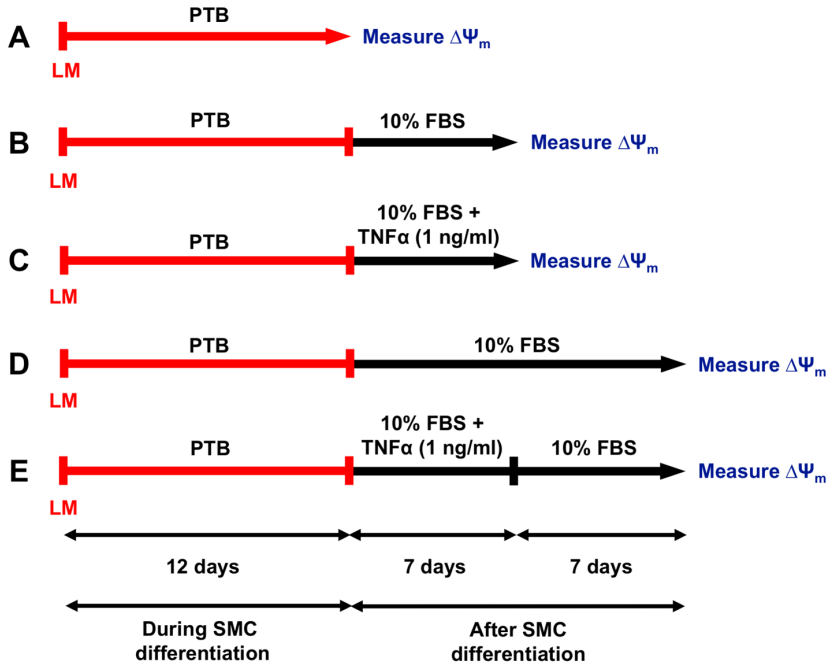

Figure 4.9. Schematic outline of the culture conditions used to assess inner mitochondrial membrane polarisation in iPSC-SMCs. Wild-type and *BMPR2*$^{+/-}$ iPSC-SMCs were differentiated via lateral plate mesoderm (LM) (Cheung et al., 2012) in serum-free, chemically-defined medium supplemented with PDGF-BB (10 ng/ml), TGF-β1 (2 ng/ml) and BMP4 (referred to as 'PTB'). The inner mitochondrial membrane polarisation state ($\Delta\Psi_m$) of iPSC-SMCs was assessed by flow cytometric analysis of tetramethylrhodamine ethyl ester (TMRE, 30 nM) staining under the following culture conditions: (**A**) under serum-free conditions after differentiation in PTB; (**B**) after being cultured for 1 week post-differentiation in DMEM + 10% FBS; (**C**) after being cultured for 1 week post-differentiation in DMEM + 10% FBS + TNFα (1 ng/ml); (**D**) after being cultured for 2 weeks post-differentiation in DMEM + 10% FBS; (**E**) after being cultured for 1 week post-differentiation in DMEM + 10% FBS + TNFα (1 ng/ml) and then for further week in DMEM + 10% FBS only.

Whilst isogenic *BMPR2*$^{+/-}$ iPSC-SMCs remained hypopolarised ($P < 0.01$) after one week of exposure to serum (10% FBS) post-PTB differentiation (**Figure 4.10 B**), C2 W9X$^{+/-}$ and C2 ΔExon1 iPSC-SMCs became significantly hyperpolarised ($P < 0.01$ and $P < 0.05$, respectively) relative to C2 iPSC-SMCs after two weeks of exposure to serum (**Figure 4.10 C**).

In addition, since TNFα has been shown to increase IMM polarisation (Sutendra et al., 2011) and is implicated in pulmonary vascular remodeling (Hurst et al., 2017), I also assessed IMM polarisation in isogenic wild-type and *BMPR2*$^{+/-}$ iPSC-SMCs treated for one week with either serum alone, or serum plus TNFα (1 ng/ml). As previously observed (**Figure 4.10 B**), *BMPR2*$^{+/-}$ iPSC-SMCs exposed to serum for one week maintained a hypopolarised IMM compared to isogenic wild-type cells ($P < 0.05$) (**Figure 4.10 D**). By contrast, C2 W9X$^{+/-}$ iPSC-SMCs exposed to serum plus TNFα for one week acquired a hyperpolarised IMM compared to C2 iPSC-SMCs ($P < 0.05$). Taken together, these findings suggest that *BMPR2* heterozygosity alone is not sufficient for increased IMM polarisation in *BMPR2*$^{+/-}$ iPSC-SMCs but lowers the threshold for hyperpolarisation in response to exogenous factors.

Inflammatory stimuli such as TNFα are one of the proposed "second hits" that are thought to be required to trigger PAH establishment and progression (Rabinovitch et al., 2014). However, it is unclear whether transient exposure to inflammatory stimuli in susceptible individuals is sufficient to drive disease progression, or whether PAH progression can be prevented or even reversed following cessation of inflammation. In a preliminary attempt to address this question, I therefore assessed whether the TNFα-induced hyperpolarised state in *BMPR2*$^{+/-}$ iPSC-SMCs was reversible following TNFα removal.

After one week of exposure to serum only or to serum plus TNFα (1 ng/ml), all cells were cultured for a further week in serum only (**Figures 4.9 D** and **E**). In isogenic wild-type cells, the trend towards hyperpolarisation after one week of exposure to serum plus TNFα was lost (**Figure 4.10 E** compared to **Figure 4.10 D**). By contrast, C2 W9X$^{+/-}$ iPSC-SMCs remained hyperpolarised ($P < 0.001$) compared to wild-type C2 iPSC-SMCs exposed to TNFα for one week (**Figure 4.10 E**). This suggests that transient exposure of iPSC-SMCs to inflammatory stimuli such as TNFα may be sufficient to drive the progression of disease in a *BMPR2* mutation carrier.

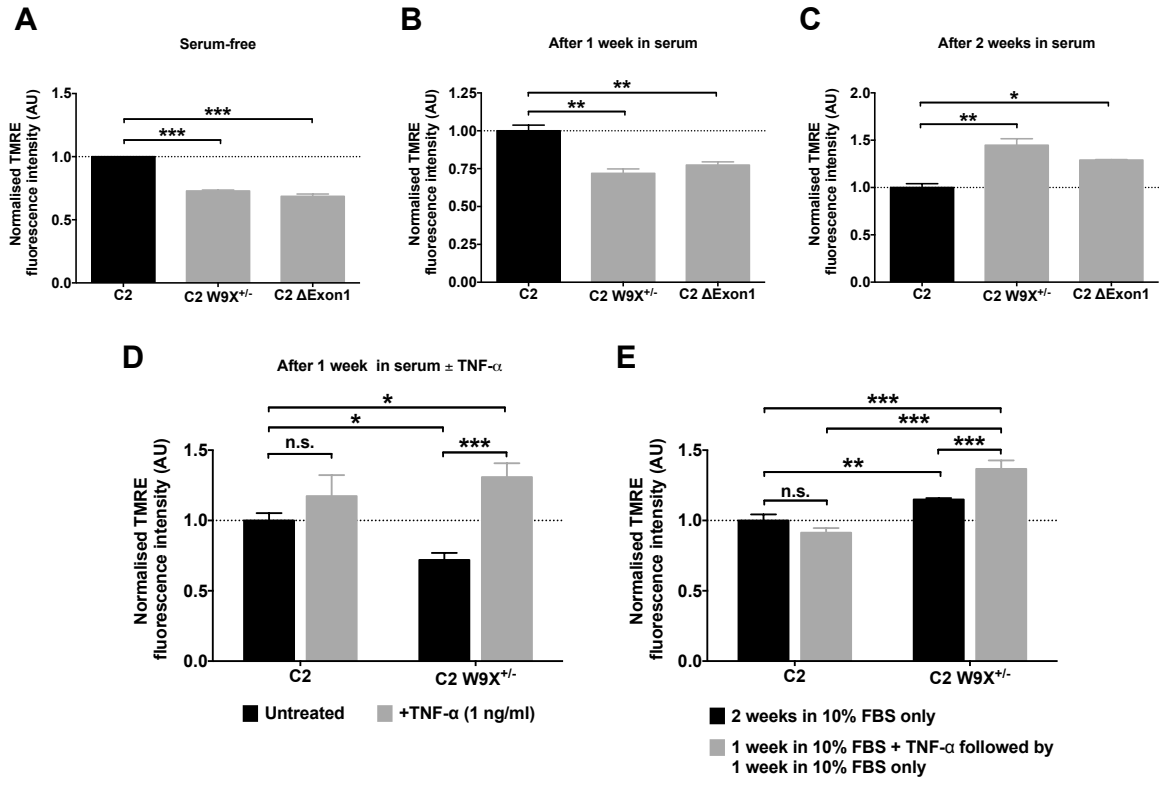

Figure 4.10. Inner mitochondrial membrane polarisation in isogenic wild-type and *BMPR2*$^{+/-}$ iPSC-SMCs assayed under serum-free and serum-containing conditions. Inner mitochondrial membrane polarisation in isogenic wild-type and *BMPR2*$^{+/-}$ iPSC-SMCs differentiated in PTB was assessed by flow cytometric analysis of cells stained for 30 minutes with tetramethylrhodamine ethyl ester (TMRE, 30 nM). (**A**) Serum-free *BMPR2*$^{+/-}$ iPSC-SMCs displayed a significantly hypopolarised IMM compared to isogenic wild-type cells. (**B**) After one week of exposure to serum (10% FBS), isogenic *BMPR2*$^{+/-}$ iPSC-SMCs remained hypopolarised compared to C2 iPSC-SMCs. However, *BMPR2*$^{+/-}$ iPSC-SMCs became hyperpolarised compared to isogenic wild-type cells after two weeks of exposure to serum (**C**) or after one week of exposure to serum and TNFα (1 ng/ml) (**D**). (**E**) After one week of exposure to serum + TNFα, TNFα was removed and all cells cultured for one further week in serum only to see if the polarisation state would recover. The polarisation state of *BMPR2*$^{+/-}$ iPSC-SMCs did not normalise after TNFα removal and was significantly higher compared to the polarisation state of *BMPR2*$^{+/-}$ iPSC-SMCs that were exposed to serum only for 2 weeks and was also significantly higher than in isogenic wild-type cells treated the same way. Data presented as mean ± s.e.m. of the results from two independent differentiations (**A**) or three technical replicates based on cells from the same differentiation (**B-E**) [n.s., not significant ($P > 0.05$), * $P < 0.05$, ** $P < 0.01$, *** $P < 0.001$, one-way ANOVA with Dunnett's post hoc test (**A-C**) or two-way ANOVA with Sidak's post hoc test (**D** and **E**)].

4.2.2 – Isogenic *BMPR2*$^{+/-}$ iPSC-SMCs are less glycolytic than wild-type iPSC-SMCs under serum-free conditions

As the reduced mitochondrial polarisation state of *BMPR2*$^{+/-}$ iPSC-SMCs compared to isogenic wild-type iPSC-SMCs assayed under serum-free conditions was such an unexpected result, I went on to assess phenotypes related to IMM polarisation to see if they were also affected in a way that is consistent with a hypopolarised IMM state.

For example, in addition to having a hyperpolarised inner mitochondrial membrane state, PAH patient-derived PASMCs have previously been shown to be more glycolytic compared to wild-type PASMCs (Paulin & Michelakis, 2014). I therefore investigated whether *BMPR2*$^{+/-}$ iPSC-SMCs assayed under serum-free conditions are less glycolytic compared to isogenic wild-type iPSC-SMCs. To achieve this, glucose-stimulated rates of glycolysis in serum-free isogenic wild-type and *BMPR2*$^{+/-}$ iPSC-SMCs were assessed using a Seahorse extracellular flux analyser which measures extracellular acidification rates (ECAR) in cells (**Figure 4.11**).

This assay revealed that C2 W9X$^{+/-}$ iPSC-SMCs were significantly ($P < 0.05$) less glycolytic compared to C2 iPSC-SMCs under serum-free conditions, with C2 ΔExon1 iPSC-SMCs also displaying a non-significant trend ($P > 0.05$) towards reduced glycolysis relative to the isogenic wild-type (**Figure 4.11 B**). These results therefore appear to be consistent with the reduced IMM polarisation state observed in serum-free isogenic *BMPR2*$^{+/-}$ iPSC-SMCs.

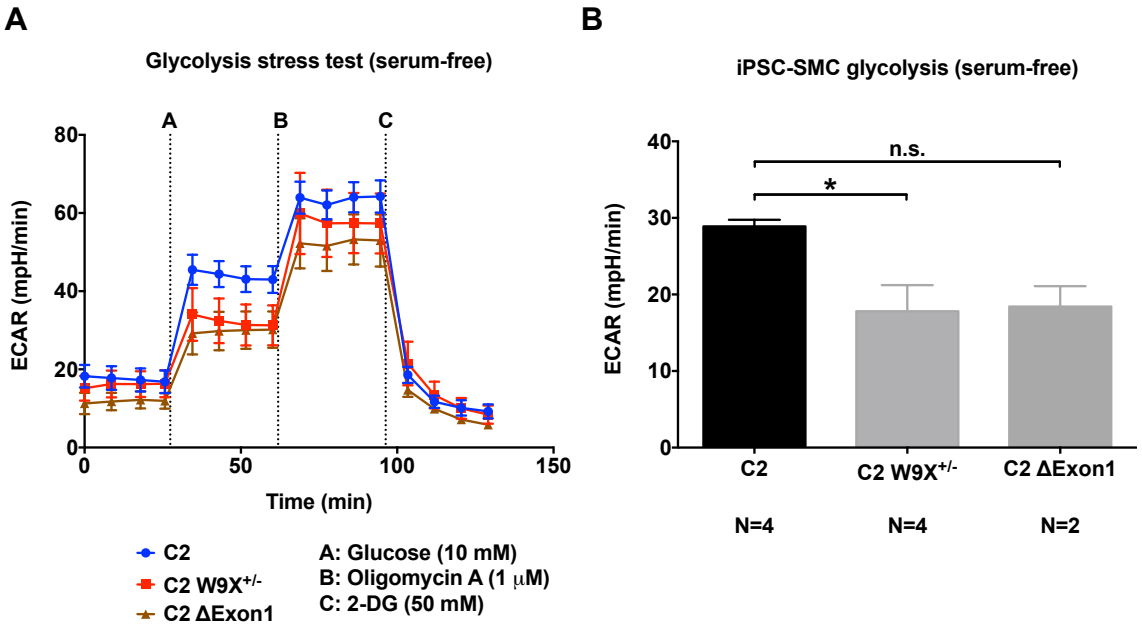

Figure 4.11. Serum-free isogenic *BMPR2*$^{+/-}$ iPSC-SMCs are less glycolytic than wild-type iPSC-SMCs. (**A**) Glucose-stimulated glycolytic rates in serum-free wild-type and isogenic *BMPR2*$^{+/-}$ iPSC-SMCs differentiated in PTB were assessed using the Seahorse XF Glycolysis Stress Test assay. Glycolysis was assessed by measuring the extracellular acidification rate (ECAR) four times for 3 minutes (with a 3-minute mixing step between each ECAR measurement) both before and after the injection of glucose (Port A, 10 mM final concentration) to stimulate glycolysis, oligomycin A (Port B, 1 μM final concentration) to maximise the glycolytic rate, and 2-deoxy-D-glucose (2-DG) (Port C, 50 mM final concentration) to inhibit glycolysis. (**B**) The glycolytic rate of serum-free wild-type and isogenic *BMPR2*$^{+/-}$ iPSC-SMCs was calculated from the ECAR measurements shown in (**A**) by subtracting the last ECAR measurement prior to the injection of glucose from the maximum ECAR measurement obtained prior to the injection of oligomycin A. C2 W9X$^{+/-}$ iPSC-SMCs were significantly less glycolytic compared to C2 iPSC-SMCs, with C2 ΔExon1 iPSC-SMCs also displaying a non-significant trend towards reduced glycolysis. Data presented as mean ± s.e.m. of the results from n=4 independent differentiations for C2 and C2 W9X$^{+/-}$ iPSC-SMCs and n=2 independent differentiations for C2 ΔExon1 iPSC-SMCs [n.s., not significant (P > 0.05), * P < 0.05, one-way ANOVA with Dunnett's post hoc test (**B**)].

4.2.3 – Isogenic *BMPR2*$^{+/-}$ iPSC-SMCs display reduced mitochondrial superoxide staining under serum-free conditions

In addition to being linked to increased glycolysis, increased IMM polarisation may under certain conditions drive an increase in reactive oxygen species (ROS) production and promote vascular remodeling (Pak et al., 2013; Paulin & Michelakis, 2014). I therefore performed a preliminary experiment to investigate whether the reduced IMM polarisation state in serum-free isogenic *BMPR2*$^{+/-}$ iPSC-SMCs might be associated with reduced ROS production in these cells. ROS production in serum-free wild-type and isogenic *BMPR2*$^{+/-}$ iPSC-SMCs was assessed by staining these cells with the mitochondrial superoxide indicator MitoSOX Red (5 μM) (**Figure 4.12**). Analysis of MitoSOX fluorescence intensities in these cells revealed that C2 W9X$^{+/-}$ iPSC-SMCs displayed less mitochondrial superoxide staining compared to C2 iPSC-SMCs. This observation therefore appears to be consistent with both reduced glycolysis and reduced IMM polarisation in serum-free isogenic *BMPR2*$^{+/-}$ iPSC-SMCs compared to wild-type iPSC-SMCs under serum-free conditions.

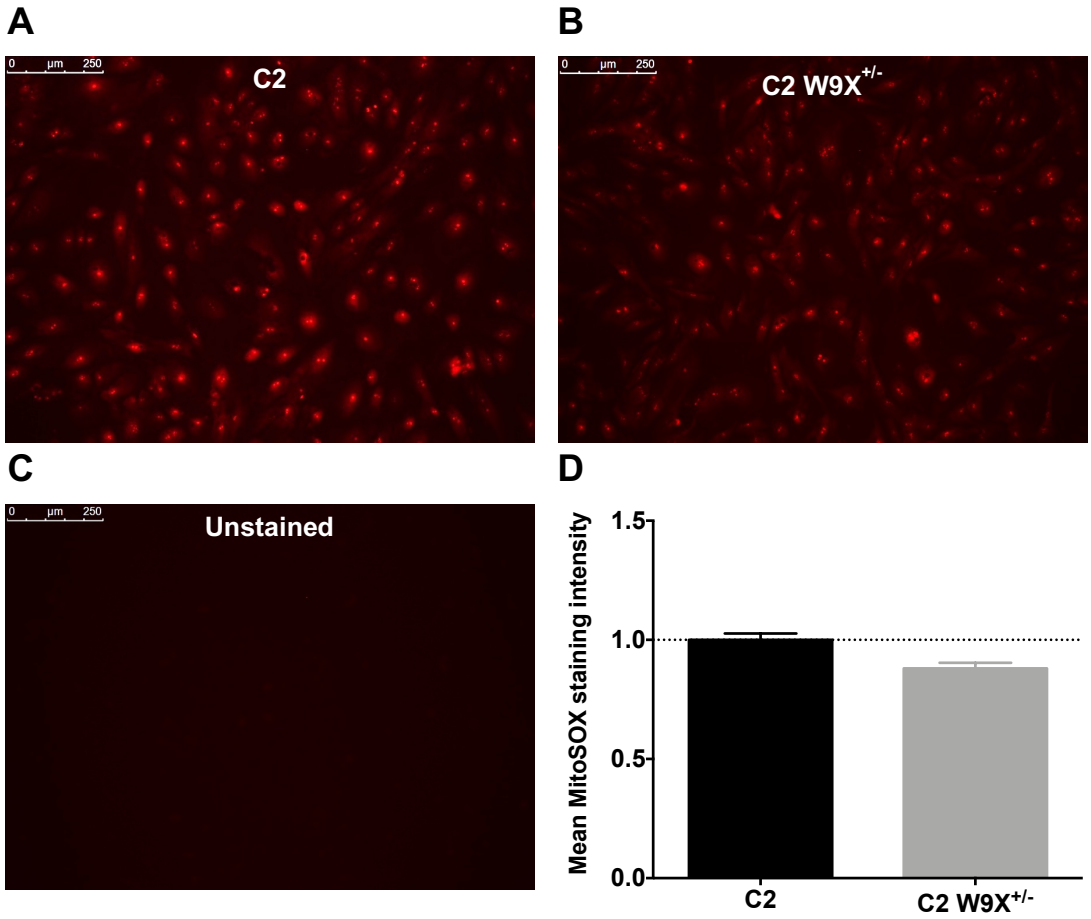

Figure 4.12. Serum-free isogenic *BMPR2*$^{+/-}$ iPSC-SMCs display reduced mitochondrial superoxide staining compared to wild-type iPSC-SMCs. Representative fluorescence microscope images of C2 iPSC-SMCs (**A**) and C2 W9X$^{+/-}$ iPSC-SMCs (**B**) incubated for 30 minutes at 37 ºC in HBSS/Ca^{2+}/Mg^{2+} buffer containing MitoSOX Red mitochondrial superoxide indicator (5 µM). (**C**) Immunofluorescence image of C2 iPSC-SMCs incubated in HBSS/Ca^{2+}/Mg^{2+} buffer only. Scale bars are 250 µm. (**D**) MitoSOX fluorescence intensities in C2 and C2 W9X$^{+/-}$ iPSC-SMCs, assessed by measuring average image intensities using ImageJ software. Data in (**D**) presented as mean ± s.e.m. of the intensities of three randomly-selected images for each cell line. All cells analysed originated from the same differentiation and the experiment was not repeated, hence no statistical analysis was performed.

4.3 – Novel cellular abnormalities in *BMPR2*$^{+/-}$ iPSC-SMCs

4.3.1 – *BMPR2*$^{+/-}$ iPSC-SMCs have an altered differentiation state that can be reversed by treatment with BMP4

In disease, including PAH, vascular SMCs exhibit phenotypic switching between differentiated and de-differentiated states. *In vitro*, differentiated SMCs are characterised by an elongated rather than rounded morphology, low proliferation rate, relatively higher expression of proteins required for contraction, and increased contractility compared to de-differentiated SMCs (Owens et al., 1997; Mam et al., 2010; Christou et al., 2012; Sahoo et al., 2016). It is also recognised in a developmental context that cells have to exit the cell cycle to become terminally differentiated. Conversely, for cells to enter a proliferative phase, they first need to de-differentiate (Owens & Wise, 1997; Owens et al., 2004). Given the increased level of proliferation observed in *BMPR2*$^{+/-}$ iPSC-SMCs, I therefore investigated whether *BMPR2*$^{+/-}$ iPSC-SMCs might have a more de-differentiated state compared to wild-type iPSC-SMCs.

Smooth muscle myosin heavy chain (MYH11) is a major contractile protein which is considered to be the most robust SMC-specific marker and is highly expressed in mature, fully differentiated SMCs (Owens et al., 2004). I therefore performed immunostaining to assess MYH11 expression in C2 and C2 W9X$^{+/-}$ iPSC-SMCs and found that MYH11 expression was reduced in C2 W9X$^{+/-}$ iPSC-SMCs compared to their isogenic wild-type (**Figure 4.13 A**). In support of this observation, qPCR analysis of *MYH11* mRNA expression revealed that *MYH11* was reduced in C2 W9X$^{+/-}$ iPSC-SMCs compared to C2 iPSC-SMCs (**Figure 4.13 B**). Taken together, these findings support the idea that *BMPR2*$^{+/-}$ iPSC-SMCs might be more de-differentiated relative to wild-type iPSC-SMCs.

Given that the only difference between wild-type and *BMPR2*$^{+/-}$ iPSC-SMCs in the system I am using is the presence of a deleterious mutation in the *BMPR2* gene, the de-differentiated phenotype of C2 W9X$^{+/-}$ iPSC-SMCs might be due to the reduced *BMPR2* expression in these cells. I therefore investigated whether treating C2 W9X$^{+/-}$ iPSC-SMCs with BMP4 might rescue the de-differentiated phenotype. Both immunostaining for MYH11 and qPCR analysis of *MYH11* mRNA expression revealed that exposure to BMP4 (50 ng/ml) increased MYH11 expression in C2 W9X$^{+/-}$ iPSC-SMCs to the level of MYH11 expression observed in C2 iPSC-SMCs (**Figures 4.13 A** and **B**). Furthermore, BMP4 treatment increased *BMPR2* mRNA expression in both C2 iPSC-SMCs and C2 W9X$^{+/-}$ iPSC-SMCs (**Figure 4.13 C**).

Taken together, these observations suggest that isogenic *BMPR2*$^{+/-}$ iPSC-SMCs have a de-differentiated phenotype compared to wild-type iPSC-SMCs and that this phenotype can be reversed by increasing the concentration of BMP4.

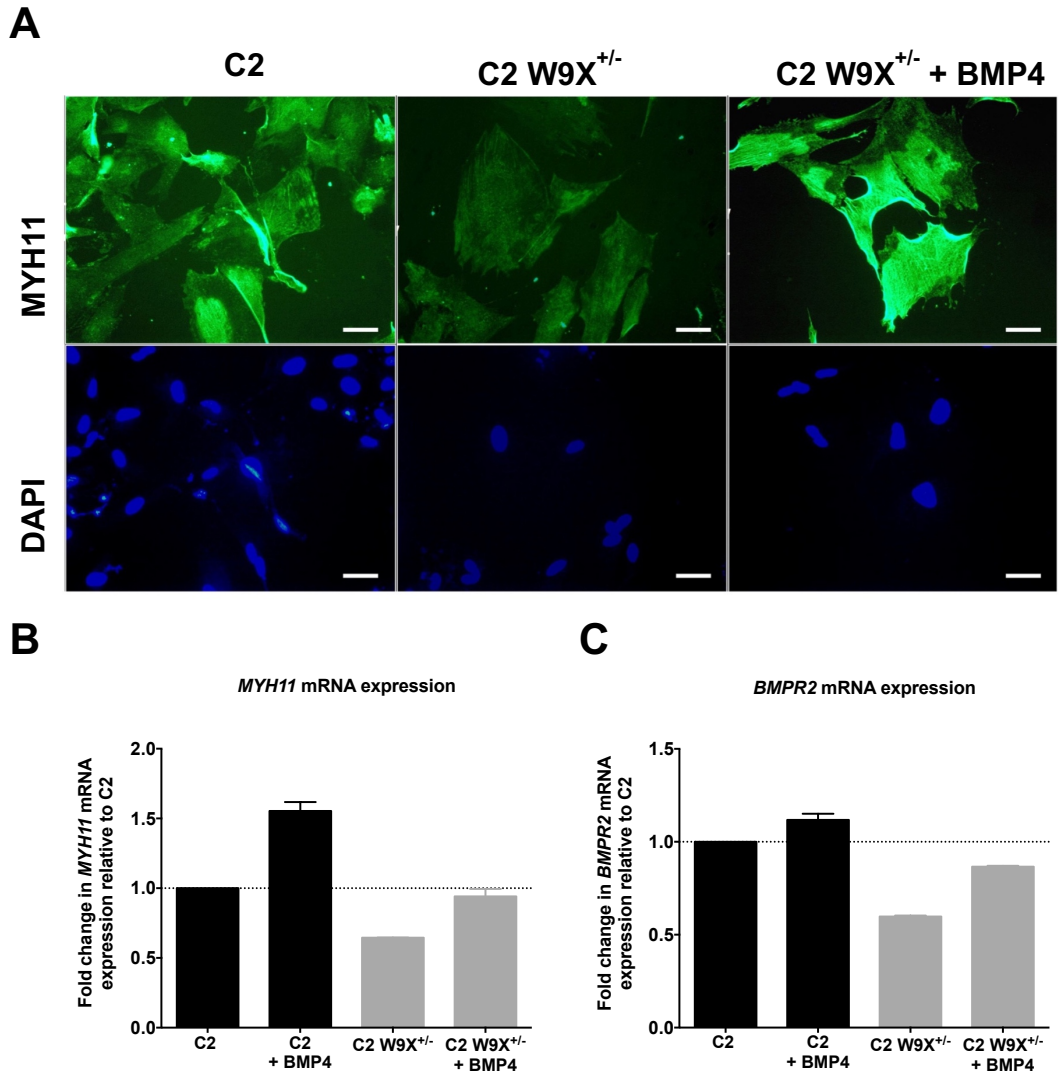

Figure 4.13. Isogenic *BMPR2*$^{+/-}$ iPSC-SMCs display reduced myosin heavy chain expression which can be reversed by treatment with BMP4. (**A**) Representative immunofluorescence images of C2 and C2 W9X$^{+/-}$ iPSC-SMCs cultured in the presence or absence of BMP4 (50 ng/ml) and immunostained for smooth muscle myosin heavy chain (MYH11, green). Nuclei were visualised using DAPI staining (blue). Scale bars are 10 µm. (**B** and **C**) qPCR analysis of *MYH11* (**B**) and *BMPR2* (**C**) mRNA expression in these cells showed that C2 W9X$^{+/-}$ iPSC-SMCs displayed reduced *MYH11* expression relative to C2 iPSC-SMCs. Treatment with BMP4 (50 ng/ml) increased both *BMPR2* and *MYH11* mRNA expression in both C2 and C2 W9X$^{+/-}$ iPSC-SMCs, restoring *MYH11* expression in C2 W9X$^{+/-}$ iPSC-SMCs to the level observed in isogenic wild-type C2 iPSC-SMCs. Data in (**B**) and (**C**) presented as mean ± s.e.m. of two independent differentiations.

4.3.2 – *BMPR2*$^{+/-}$ iPSC-SMCs and PASMCs are less contractile in response to carbachol stimulation

To functionally test the hypothesis that *BMPR2*$^{+/-}$ iPSC-SMCs are de-differentiated compared to wild-type iPSC-SMCs, I next went on to test the level of cell contractility in these cells. To achieve this, I stimulated wild-type and isogenic *BMPR2*$^{+/-}$ iPSC-SMCs with carbachol (300 μM), took time-lapse images of these cells over a 15-minute period and assessed cell contraction by calculating percentage changes in the cell surface areas of 10-11 randomly sampled cells per cell line between t = 0 and t = 15 minutes (**Figure 4.14 A**). Consistent with the results of a previous study (Cheung et al., 2012), the average cell surface area of wild-type C2 iPSC-SMCs decreased by 15% in response to carbachol stimulation. However, the average decrease in cell surface area was significantly ($P < 0.001$) lower in C2 W9X$^{+/-}$ iPSC-SMCs relative to C2 iPSC-SMCs (**Figure 4.14 B**), suggesting that *BMPR2*$^{+/-}$ iPSC-SMCs are less contractile compared to their isogenic wild-type. Since this phenotype has not been previously reported in PAH patient-derived PASMCs, I also assessed carbachol-induced contractility in PASMCs from PAH patients with *BMPR2* mutations and found that *BMPR2*$^{+/-}$ PASMCs were also significantly ($P < 0.01$) less contractile than wild-type PASMCs (**Figures 4.14 C** and **D**). Taken together, these data are consistent with the reduced MYH11 expression observed in isogenic *BMPR2*$^{+/-}$ iPSC-SMCs and further suggest that *BMPR2* heterozygosity leads to *BMPR2*$^{+/-}$ iPSC-SMCs having a more de-differentiated phenotype compared to wild-type iPSC-SMCs.

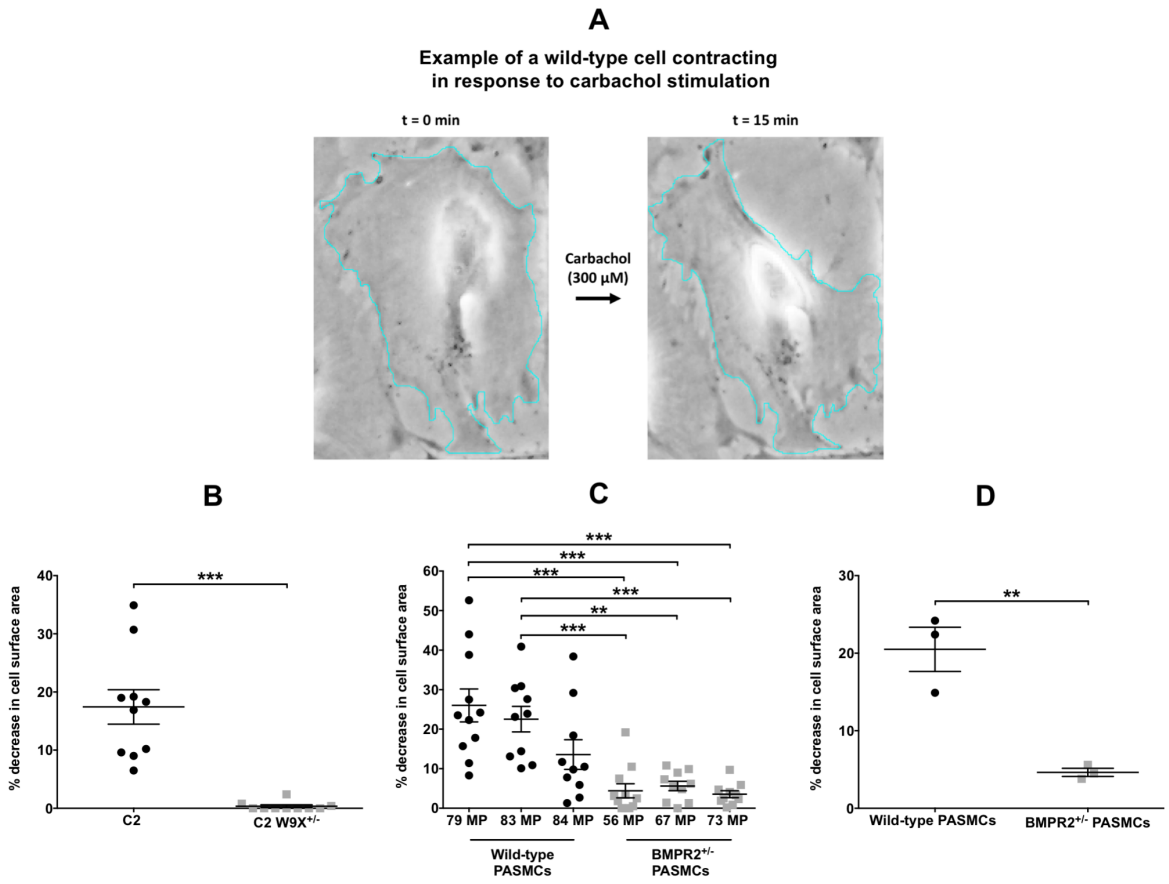

Figure 4.14. *BMPR2*$^{+/-}$ iPSC-SMCs and PASMCs are less contractile. (**A**) Representative bright field images of a wild-type C2 iPSC-derived smooth muscle cell taken immediately prior to and after 15 minutes of incubation in PBS supplemented with carbachol (300 µM) and bovine serum albumin (0.1 % w/v). Carbachol-induced cell contraction was assessed by using ImageJ software to measure percentage changes in cell surface area between t = 0 and t = 15 minutes. (**B-D**) Quantitative analysis of carbachol-induced contractility of n=10-11 randomly sampled cells per cell line revealed that C2 W9X$^{+/-}$ iPSC-SMCs were significantly less contractile than wild-type C2 iPSC-SMCs (**B**) and that *BMPR2*$^{+/-}$ PASMCs derived from PAH patients with *BMPR2* mutations were significantly less contractile than wild-type PASMCs (**C** and **D**). A breakdown of the results for individual wild-type and *BMPR2*$^{+/-}$ PASMC lines is shown in (**C**), with mean contractile responses of the three wild-type and three *BMPR2*$^{+/-}$ PASMC lines presented in (**D**). Data presented as mean ± s.e.m. [** $P < 0.01$, *** $P < 0.001$, unpaired two-tailed Student's t test (**B** and **D**), or one-way ANOVA with Tukey's post hoc test (**C**)].

4.4 – Discussion

4.4.1 – Contributions of *BMPR2* mutations and extrinsic factors to cellular phenotypes of pulmonary arterial hypertension

The results presented in this chapter suggest that *BMPR2* heterozygosity in iPSC-SMCs is necessary and sufficient to recapitulate the pro-proliferative and anti-apoptotic phenotype of PAH patient-derived PASMCs, but that additional exposure to serum and/or TNFα is required to recapitulate the mitochondrial hyperpolarisation phenotype of PAH-derived PASMCs. This highlights the utility of iPSC-SMCs with isogenic backgrounds for studying factors affecting disease penetrance and supports the hypothesis of this thesis that *BMPR2* heterozygosity in iPSC-SMCs is necessary and sufficient to recapitulate some but not all PAH-associated cellular phenotypes.

Furthermore, this chapter describes the establishment of the first iPSC-SMC model of PAH. Previous studies have focussed on using iPSC-derived mesenchymal stromal cells (iPSC-MSCs) (West et al., 2014) or iPSC-ECs (West et al., 2014; Sa et al., 2017; Gu et al., 2017) to study PAH. However, the *BMPR2*$^{+/-}$ iPSC-MSCs and iPSC-ECs used in these studies were not found to be more proliferative compared to their wild-type counterparts, and comparisons were predominantly confined to a limited number of patient-derived cell lines which had different genetic backgrounds (West et al., 2014; Sa et al., 2017; Gu et al., 2017). The variability between different patient-derived cell lines often means that a large number of lines from different patients need to be evaluated in order to detect robust differences in the phenotypes being studied. This was evident in this thesis investigation, with only non-significant trends usually being observed between wild-type and *BMPR2*$^{+/-}$ patient-derived iPSC lines, in contrast to the reduced variability that was present between cells with isogenic backgrounds.

However, it is important to note that whilst *BMPR2* heterozygosity in iPSC-SMCs was sufficient for the acquisition of a pro-proliferative and anti-apoptotic phenotype, these phenotypes might not be present in human *BMPR2* mutation carriers who do not have PAH. This discrepancy could be due to a lack of exposure of iPSC-SMCs to protective factors that might be provided by serum, endothelial cells or other cell types during differentiation (Budhiraja et al., 2004). Furthermore, endothelial cells secrete BMP4, pro-inflammatory cytokines and other paracrine signals which stimulate SMC proliferation and pulmonary

vascular remodelling in PAH (Frank et al., 2005; Eddahibi et al., 2006), and may therefore influence PAH-associated SMC phenotypes.

In addition, the results presented in this chapter argue that the acquisition of a hyperpolarised inner mitochondrial membrane state in *BMPR2*$^{+/-}$ iPSC-SMCs in response to serum and/or TNFα exposure might represent a transition from a pre-diseased to a diseased state. This is consistent with the notion that inflammation is thought to be a potential 'second hit' that is required for PAH establishment and progression (Rabinovitch et al., 2014) and is further supported by the finding that C2 W9X$^{+/-}$ iPSC-SMCs assayed under serum-free conditions were less glycolytic and displayed reduced mitochondrial membrane polarisation compared to C2 iPSC-SMCs.

Furthermore, C2 W9X$^{+/-}$ iPSC-SMCs also displayed slightly lower mitochondrial superoxide staining compared to isogenic wild-type cells when assayed under serum-free conditions. Whilst several studies suggest that increased IMM polarisation drives an increase in ROS production and promotes vascular remodeling (Pak et al., 2013; Paulin & Michelakis, 2014), there have also been conflicting reports of reduced ROS production in PAH (Aggarwal et al., 2013; Bonnet & Boucherat, 2018). This controversy is likely to be due to the existence of multiple cellular sources and types of ROS, their highly reactive nature and the different methods used to detect ROS production in cells (Bonnet & Boucherat, 2018). As a result, further work will be required to determine relative levels of ROS production between wild-type and *BMPR2*$^{+/-}$ iPSC-SMCs under serum-free and serum-containing conditions. Furthermore, future studies could focus on investigating the molecular mechanisms linking mitochondrial hyperpolarisation, ROS production, glycolysis and mitochondrial function in iPSC-SMCs.

The findings presented in this chapter also suggest that increased proliferation, reduced apoptosis and increased *IL-6* mRNA expression in *BMPR2*$^{+/-}$ LM-iPSC-SMCs were more pronounced when these cells were differentiated in the presence of a high concentration (50 ng/ml) of exogenous BMP4 during the 12-day 'PT' SMC differentiation phase (herein referred to as PTB). This suggests that differentiation in PTB represents a refinement of the LM-iPSC-SMC differentiation protocol in terms of its ability to generate cells that can be used as surrogates for distal PASMCs when studying PAH. Although the reason for this is unclear, the observation that BMP4 is highly expressed in the distal region of the lung bud during development (Bellusci et al., 1996) suggests that the addition of BMP4 during differentiation might promote the acquisition of a distal cell fate in LM-iPSC-SMCs.

4.4.2 – Comparisons with iPSC-derived endothelial cell models of PAH

As well as generating lineage-specific iPSC-SMCs which recapitulated key PAH-associated cellular phenotypes observed in distal PASMCs, I also contributed to work carried out by Mr Christopher JZ Huang and Dr C-Hong Chang in our group which involved generating an iPSC-derived endothelial cell (iPSC-EC) model of PAH (Kiskin et al., 2018). Using the same patient-derived and isogenic iPSC lines described in this thesis, wild-type and *BMPR2*$^{+/-}$ iPSCs were differentiated into iPSC-ECs which formed vascular networks and displayed an enhanced expression of arterial EC markers (Kiskin et al., 2018). Using these iPSC-ECs, we then investigated whether *BMPR2* heterozygosity in iPSC-ECs was necessary and/or sufficient to recapitulate key PAH-associated phenotypes observed in patient-derived PAECs (Kiskin et al., 2018). Interestingly, unlike in iPSC-SMCs, we found that *BMPR2* heterozygosity in iPSC-ECs required additional exposure to serum to manifest increased proliferation and apoptosis (Kiskin et al., 2018). Neither iPSC-SMCs or iPSC-ECs displayed hyperpolarised IMMs as they emerged from the serum-free iPSC differentiation protocols. However, in contrast to *BMPR2*$^{+/-}$ iPSC-SMCs which required two weeks of exposure to serum to become hyperpolarised, one week of exposure to serum was sufficient to induce IMM hyperpolarisation in *BMPR2*$^{+/-}$ iPSC-ECs (Kiskin et al., 2018).

Taken together, these findings demonstrate a clear difference in the contribution of *BMPR2* heterozygosity to establishing PAH-associated cellular phenotypes in SMCs and ECs, thus highlighting an important difference between these cell types. This suggests that tailored, cell type-specific approaches might be required when developing therapies aimed at reversing or preventing pulmonary vascular dysfunction in ECs and SMCs. In iPSC-ECs, potential therapeutic interventions might include BMP9 treatment which reverses PH in rodent models (Long et al., 2015) and prevented IMM hyperpolarisation in *BMPR2*$^{+/-}$ iPSC-ECs (Kiskin et al., 2018). In addition, these findings further support the view that therapies aimed at restoring BMPR2 signalling could be beneficial in the treatment of PAH. However, whether BMP ligands also reduce IMM polarisation in *BMPR2*$^{+/-}$ iPSC-SMCs is yet to be determined.

Previously, iPSC-ECs derived from PAH patients with *BMPR2* mutations did not recapitulate the hyperpolarised inner mitochondrial membrane state associated with end-stage PAH (Gu et al., 2017). This may have been due to the lack of exposure to an environmental stimulus such as TNFα or due to the mixed genetic background of the patient-derived iPSC lines used. Supporting the importance of environmental stimuli as modifiers of disease penetrance is the observation of discordance for disease in monozygotic twins with *BMPR2* mutations (Ormiston et al., 2013).

In addition to environmental factors, disease penetrance may also be affected by genetic modifiers. For example, the lack of response of some PAH-derived PAEC and iPSC-EC lines to the immunosuppressant FK506 and the neutrophil elastase inhibitor, elafin, was attributed to increased expression of split guidance ligand 3 (*SLIT3*) (Sa et al., 2017). In a separate study from the same group (Gu et al., 2017), baculoviral IAP repeat containing 3 (*BIRC3*) was identified as being responsible for the preserved cell survival in iPSC-ECs derived from unaffected *BMPR2* mutation carriers and may hence be a protective genetic modifier in PAH. However, the precise roles that putative genetic modifiers such as *SLIT3* and *BIRC3* play in the pathogenesis of PAH are yet to be determined.

4.4.3 – *BMPR2*$^{+/-}$ iPSC-SMCs have an altered differentiation state

Another interesting new finding presented in this chapter is that *BMPR2*$^{+/-}$ LM-iPSC-SMCs displayed reduced smooth muscle myosin heavy chain (MYH11) expression and carbachol-induced cell contractility compared to wild-type iPSC-SMCs. This dedifferentiated phenotype is consistent with the pro-proliferative, 'synthetic' phenotype that vascular smooth muscle cells acquire due to phenotypic switching in response to vascular injury (Stiemer et al., 1993; Kane et al., 2011; Chelladurai et al., 2012). BMP4 treatment of *BMPR2*$^{+/-}$ iPSC-SMCs restored smooth muscle myosin heavy chain expression in these cells to levels observed in wild-type iPSC-SMCs, and also increased *BMPR2* mRNA expression.

It remains unclear whether BMP4 treatment improves the SMC differentiation process, acts by reducing dedifferentiation, or whether BMP4 mediates both of these effects. Nevertheless, the observations described in this chapter suggest that isogenic *BMPR2*$^{+/-}$ iPSC-SMCs have an altered differentiation state compared to wild-type iPSC-SMCs and that this phenotype can be reversed by increasing the concentration of BMP4. In support of these findings, previous work has shown that BMP4 maintains the expression of smooth muscle actin in cultured PASMCs

and reduces the PDGF-BB-induced dedifferentiation of arterial SMCs (Lagna et al., 2007). BMP4 treatment has also been shown to promote a contractile phenotype in VSMCs by reducing the expression of small non-coding microRNAs such as miR-96 (Kim et al., 2014). It would therefore be interesting to test whether BMP4 treatment improves carbachol-induced contractility of *BMPR2*$^{+/-}$ iPSC-SMCs and PASMCs. Alternatively, future studies could also explore the effect of other BMP ligands on MYH11 expression in iPSC-SMCs.

A further question is whether the introduction of the *BMPR2* mutation impairs iPSC-SMC differentiation or promotes the dedifferentiation of mature, contractile iPSC-SMCs. It cannot be ruled out that iPSC-SMCs generated in this study might consist of cells with a mixture of differentiation states, since a subset of cells may have disproportionately contributed to the altered differentiation state of *BMPR2*$^{+/-}$ iPSC-SMCs. However, a similar state might be present *in vivo*, where both mature, fully differentiated SMCs as well as less terminally differentiated 'non-muscle-like' cells have been reported to exist in close proximity within the arterial media (Frid et al., 1997).

CHAPTER 5 – RESULTS (III)

RNA-Seq gene expression analysis of wild-type and *BMPR2*$^{+/-}$ iPSC-SMCs

5.1 – Differential RNA-Seq gene expression analysis of wild-type and *BMPR2*$^{+/-}$ iPSC-SMCs

Having demonstrated that the iPSC-SMC model could recapitulate known PASMC cellular phenotypes relevant to PAH, my next aim was to identify genes that are differentially expressed between wild-type and *BMPR2*$^{+/-}$ iPSC-SMCs and thus provide further insights into PAH pathobiology. I therefore isolated and purified RNA from wild-type and both genome-edited and patient-derived *BMPR2*$^{+/-}$ iPSC-SMCs and submitted these samples for RNA sequencing. RNA-Seq libraries were generated by Dr Mattia Frontini and Dr Frances Burden, with the resulting libraries being quantified, pooled and sequenced using paired-end sequencing. Subsequently, I enlisted the help of Dr Marta Bleda and Dr Matthias Haimel who processed and analysed the raw RNA-Seq data. A summary of the RNA-Seq workflow is presented in **Figure 5.1.**

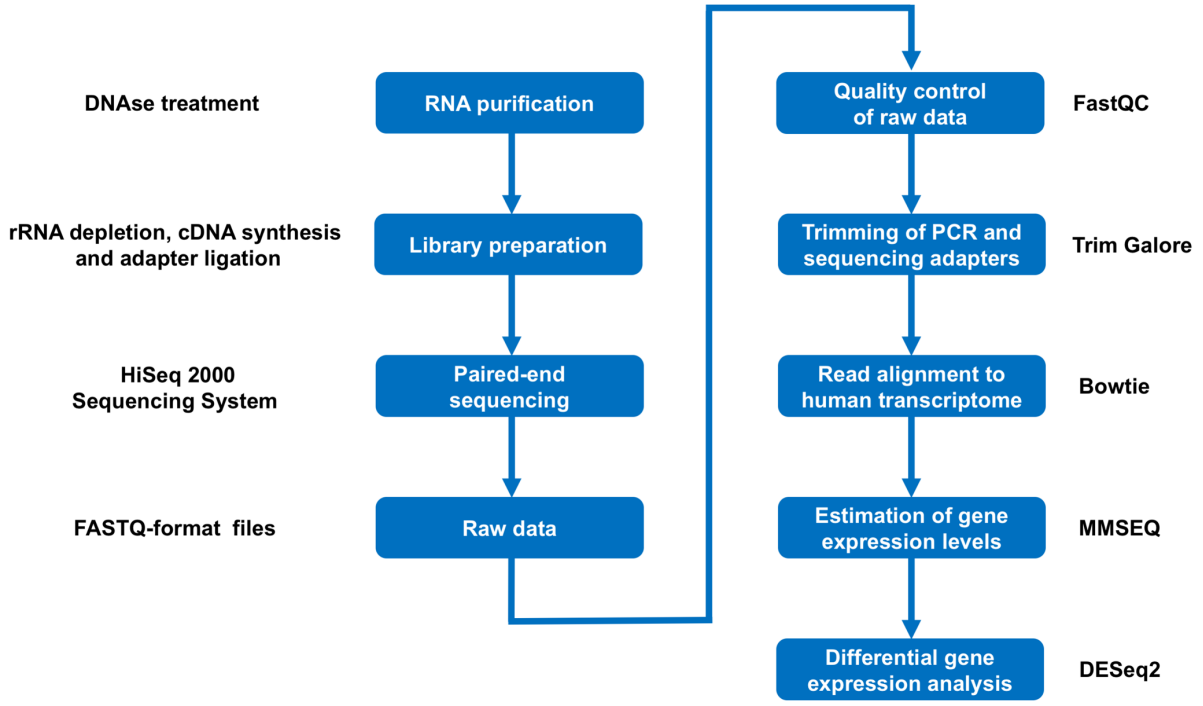

Figure 5.1. RNA-Seq workflow. After extracting and purifying RNA from wild-type and *BMPR2*$^{+/-}$ iPSC-SMCs, ribosomal RNA (rRNA)-depleted cDNA libraries were generated using a TruSeq Stranded Total RNA Library Prep Kit (Illumina). Libraries were quantified, pooled and sequenced using paired-end 76 bp sequencing on a HiSeq 2000 Sequencing System (Illumina). Raw RNA-Seq data was generated in FASTQ format and subjected to quality control using FastQC software before trimming PCR and sequencing adapters using Trim Galore. Trimmed reads were then aligned to the human transcriptome with Bowtie. MMSEQ was used with default parameters to calculate fragment counts and DESeq2 was applied with regularised log transformation to quantify gene expression.

Transcriptional differences between *BMPR2*$^{+/-}$ and wild-type iPSC-SMCs were analysed under serum-free PTB conditions because both apoptosis resistance and increased proliferation were caused by *BMPR2* heterozygosity alone and were enhanced after differentiation in PTB compared to PT. This analysis revealed that genes encoding somatostatin (*SST*), dual oxidase 2 (*DUOX2*) and mitochondrial uncoupling protein 2 (*UCP2*) were significantly ($P_{adj} < 0.05$) down-regulated in patient-derived (B3, B4 and B11) and genome-edited (C2 W9X$^{+/-}$ and C2 ΔExon1) *BMPR2*$^{+/-}$ iPSC-SMCs compared to wild-type (C2, C6 and C10) iPSC-SMCs. By contrast, cytokine receptor-like factor 1 (*CRLF1*) was significantly ($P_{adj} < 0.05$) upregulated in *BMPR2*$^{+/-}$ iPSC-SMCs compared to controls (**Figure 5.2**).

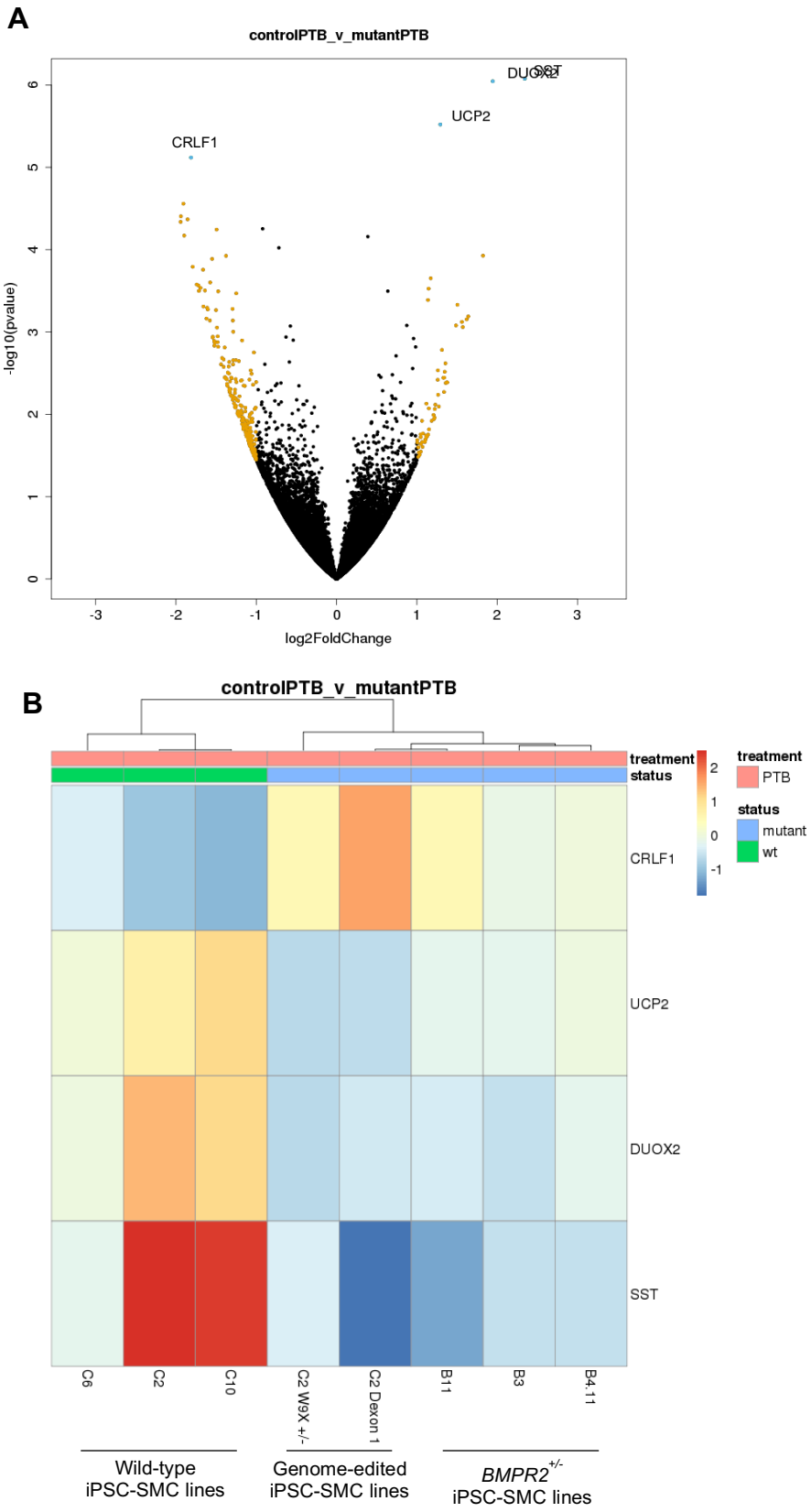
A
controlPTB_v_mutantPTB
DUOX2
SST
UCP2
CRLF1
-log10(pvalue)
log2FoldChange
B
controlPTB_v_mutantPTB
treatment
status
CRLF1
UCP2
DUOX2
SST
C6
C2
C10
C2 W9X +/-
C2 Dexon 1
B11
B3
B4.11
Wild-type iPSC-SMC lines
Genome-edited iPSC-SMC lines
BMPR2+/- iPSC-SMC lines
treatment
PTB
status
mutant
wt

Figure 5.2. Differential RNA-Seq gene expression analysis of wild-type and *BMPR2*$^{+/-}$ iPSC-SMCs reveals alterations in genes potentially involved in PAH. Volcano plot (**A**) and hierarchical clustering based on Pearson correlation (**B**) of differentially expressed genes comparing *BMPR2*$^{+/-}$ iPSC-SMC lines (B3, B4.11, B11, C2 ΔExon1, C2 W9X$^{+/-}$) with wild-type controls (C2, C6, C10) after serum-free differentiation in PTB. The heatmap in (**B**) shows the differentially expressed genes in rows and the iPSC-SMC samples in the columns. Samples are annotated according to their genotype at the top of the heatmap. Genes with a false discovery rate (FDR) adjusted *P* value < 0.05 were considered differentially expressed. Based on this analysis, somatostatin (*SST;* P_{adj} = 0.00780), dual oxidase 2 (*DUOX2;* P_{adj} = 0.00780), and mitochondrial uncoupling protein 2 (*UCP2;* P_{adj} = 0.0174) were significantly downregulated in *BMPR2*$^{+/-}$ relative to wild-type iPSC-SMCs, whereas cytokine receptor-like factor 1 (*CRLF1;* P_{adj} = 0.0329) was significantly upregulated.

To validate these results, I used quantitative PCR to analyse *SST*, *DUOX2*, *UCP2* and *CRLF1* mRNA expression in serum-free C2 and C2 W9X$^{+/-}$ iPSC-SMCs differentiated in PTB, which confirmed the differential expression of these genes between mutants and controls (**Figure 5.3**). However, after culturing PTB-differentiated iPSC-SMCs for one week in 10% FBS, *CRLF1* mRNA expression became significantly reduced rather than increased in C2 W9X$^{+/-}$ iPSC-SMCs relative to wild-type C2 iPSC-SMCs, whilst *SST*, *DUOX2* and *UCP2* expression remained reduced (**Figures 5.4 A-D**).

To determine whether these findings can be validated in a mouse model of PAH, I collaborated with Dr Xudong Yang and Dr Lu Long who isolated lung tissue from knock-in mice which harbour a heterozygous R899X mutation in exon 12 of the endogenous *Bmpr2* locus (*Bmpr2*$^{+/R899X}$) and develop increased RVSPs by 6 months of age (Long et al., 2015). qPCR analysis revealed that *Sst*, *Duox2*, *Ucp2* and *Crlf1* mRNA expression was reduced in the lungs of *Bmpr2*$^{+/R899X}$ mice compared with wild-type littermates (n=3 per group), although the difference in *Ucp2* expression between wild-type and *Bmpr2*$^{+/R899X}$ mouse lungs was not statistically significant ($P > 0.05$) (**Figures 5.4 E-H**). These findings are consistent with the reduced expression of these genes in C2 W9X$^{+/-}$ relative to wild-type C2 iPSC-SMCs after one week of serum exposure and suggest that exposure to serum may affect the relative expression levels of some genes between wild-type and *BMPR2*$^{+/-}$ iPSC-SMCs.

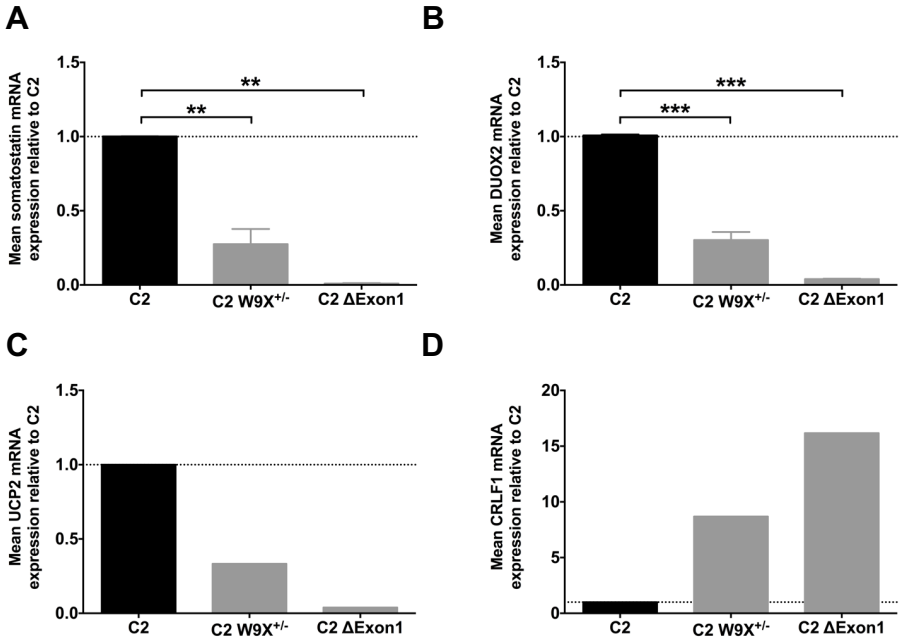

Figure 5.3. qPCR validation of genes that were differentially expressed between serum-free wild-type and *BMPR2*$^{+/-}$ iPSC-SMCs. qPCR analysis confirmed the reduced *SST* (**A**), *DUOX2* (**B**) and *UCP2* (**C**) mRNA expression, and increased *CRLF1* (**D**) mRNA expression observed in C2 W9X$^{+/-}$ relative to isogenic wild-type C2 iPSC-SMCs assayed under serum-free PTB conditions. Data in **A** and **B** presented as mean ± s.e.m. of the results from two independent qPCR analyses (technical replicates) performed on cells from the same differentiation (** $P < 0.01$, *** $P < 0.001$, one-way ANOVA with Dunnett's post hoc test). qPCR analysis of *UCP2* and *CRLF1* mRNA expression (**C** and **D**) was only performed once.

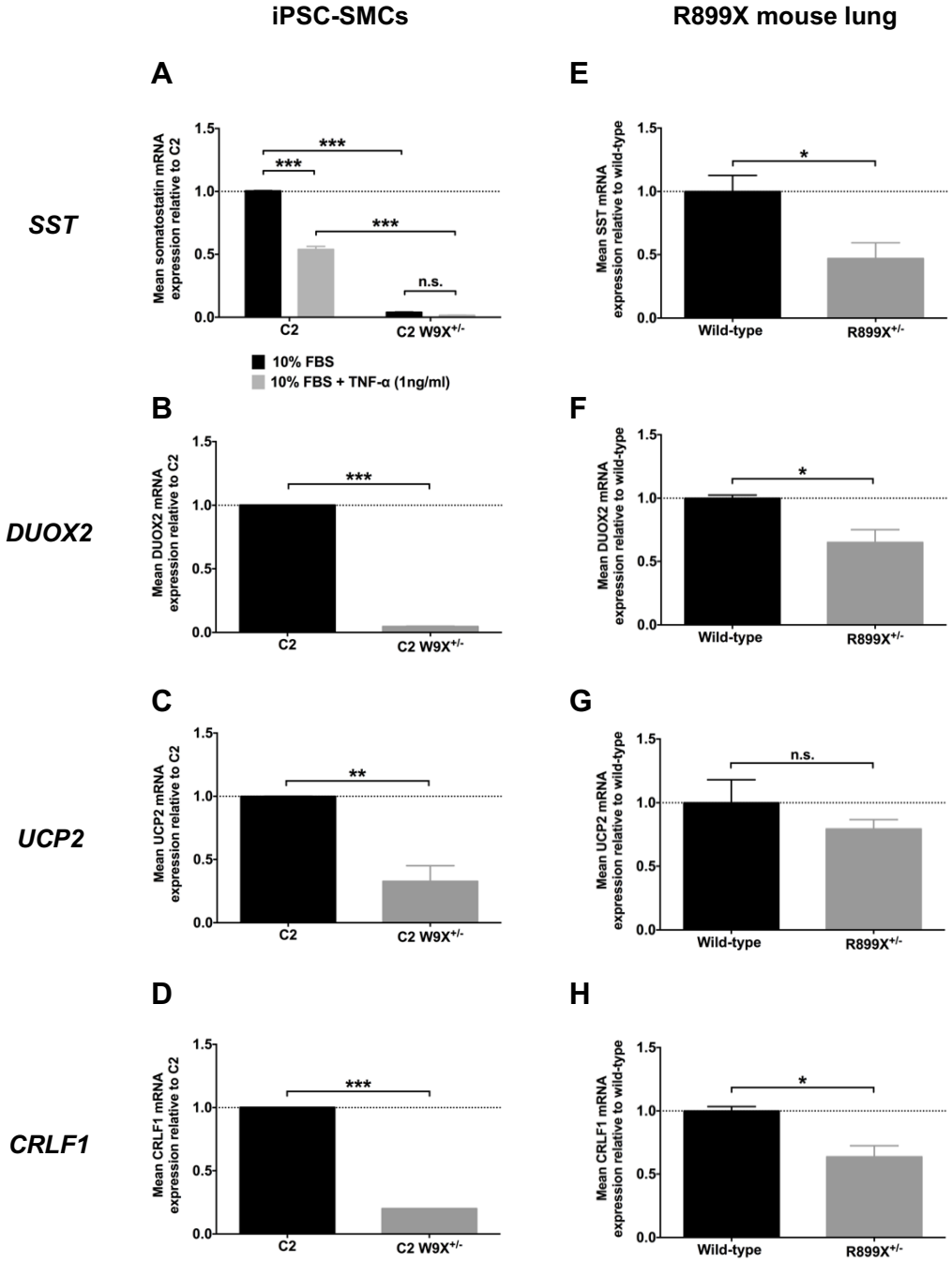
iPSC-SMCs
R899X mouse lung
A
B
C
D
E
F
G
H
SST
DUOX2
UCP2
CRLF1
Mean somatostatin mRNA expression relative to C2
Mean DUOX2 mRNA expression relative to C2
Mean UCP2 mRNA expression relative to C2
Mean CRLF1 mRNA expression relative to C2
Mean SST mRNA expression relative to wild-type
Mean DUOX2 mRNA expression relative to wild-type
Mean UCP2 mRNA expression relative to wild-type
Mean CRLF1 mRNA expression relative to wild-type
1.5
1.0
0.5
0.0
***
**
*
n.s.
C2
C2 W9X+/-
Wild-type
R899X+/-
10% FBS
10% FBS + TNF-α (1ng/ml)

Figure 5.4. qPCR analysis of *SST*, *DUOX2*, *UCP2* and *CRLF1* mRNA expression levels in serum-matured isogenic iPSC-SMCs and in *Bmpr2*$^{+/R899X}$ mouse lung tissue. (**A-D**): Somatostatin (*SST*) (**A**), dual oxidase 2 (*DUOX2*) (**B**), mitochondrial uncoupling protein 2 (*UCP2*) (**C**), and cytokine receptor like factor 1 (*CRLF1*) (**D**) mRNA expression was significantly reduced in C2 W9X$^{+/-}$ relative to wild-type C2 iPSC-SMCs cultured for one week in 10% FBS post-differentiation. Furthermore, exposure to serum + TNFα (1 ng/ml) for one week significantly decreased *SST* mRNA expression in C2 iPSC-SMCs (**A**). (**E-H**): Reduced *SST* (**E**), *DUOX2* (**F**) and *CRLF1* (**H**) mRNA expression in C2 W9X$^{+/-}$ iPSC-SMCs after one week of exposure to serum was further confirmed by qPCR in lung tissue samples from wild-type and heterozygous *Bmpr2* R899X knock-in (*Bmpr2*$^{+/R899X}$) mice (n=3 per group). *Ucp2* expression was also slightly lower in *Bmpr2*$^{+/R899X}$ mouse lungs compared to wild-type littermates (**G**), but this difference was not statistically significant ($P > 0.05$, n=3 per group). Data in **A-D** presented as mean ± s.e.m. of the results from three independent qPCR analyses (technical replicates) performed on cells from the same differentiation [n.s., not significant ($P > 0.05$), * $P < 0.05$, ** $P < 0.01$, *** $P < 0.001$, unpaired two-tailed Student's t test, or two-way ANOVA with Sidak's post hoc test].

5.2 – Investigating the effect of somatostatin on iPSC-SMC proliferation

Among the genes that were differentially expressed between wild-type and *BMPR2*$^{+/-}$ iPSC-SMCs under serum-free PTB conditions, somatostatin displayed the most significantly reduced expression in mutants relative to controls (P_{adj} = 0.0078). Furthermore, since TNFα has previously been shown to reduce somatostatin expression in human coronary endothelial cells (Yan et al., 2004), I investigated whether TNFα might also reduce *SST* expression in iPSC-SMCs. Indeed, I observed that exposure to TNFα (1 ng/ml) for one week significantly (P < 0.001) decreased *SST* mRNA expression in C2 iPSC-SMCs, and also reduced *SST* expression in C2 W9X$^{+/-}$ iPSC-SMCs (**Figure 5.4 A**), suggesting that inflammatory stimuli may reduce somatostatin expression.

Somatostatin is a cyclopeptide that broadly inhibits a number of hormones such as growth hormone, insulin and glucagon (Brazeau et al., 1973; Reichlin, 1983). In addition, somatostatin and its analogues have also been shown to inhibit smooth muscle cell proliferation (Leszczynski et al., 1993; Lauder et al., 1997; Zhao & Foegh, 1997), reduce medial pulmonary artery wall thickness in MCT rats (Takahashi et al., 1995) and ameliorate chronic hypoxia-induced pulmonary hypertension (Tjen et al., 1992), although the latter finding has been disputed (Sidney et al., 1996). Taken together, these observations raise the question of whether the reduced somatostatin expression observed in *BMPR2*$^{+/-}$ iPSC-SMCs might contribute to the pro-proliferative phenotype of these cells and thus play a role in the pathogenesis of PAH.

I therefore set out to determine whether somatostatin inhibits the proliferation of iPSC-SMCs and PASMCs by culturing isogenic C2 and C2 W9X$^{+/-}$ iPSC-SMCs and PAH patient-derived *BMPR2*$^{+/-}$ PASMCs for 7 days in the presence or absence of somatostatin-14 (1 μM), a bioactive form of somatostatin which binds with high affinity to all five somatostatin receptor subtypes (SSTR1-5) identified to date (Bruns et al., 1994). Cell counts after 7 days in culture revealed that somatostatin-14 had no significant effect (P > 0.05) on the proliferation of C2 W9X$^{+/-}$ iPSC-SMCs (**Figure 5.5 A**). Similarly, somatostatin-14 also did not affect the proliferation of *BMPR2*$^{+/-}$ PASMCs (**Figure 5.5 B**).

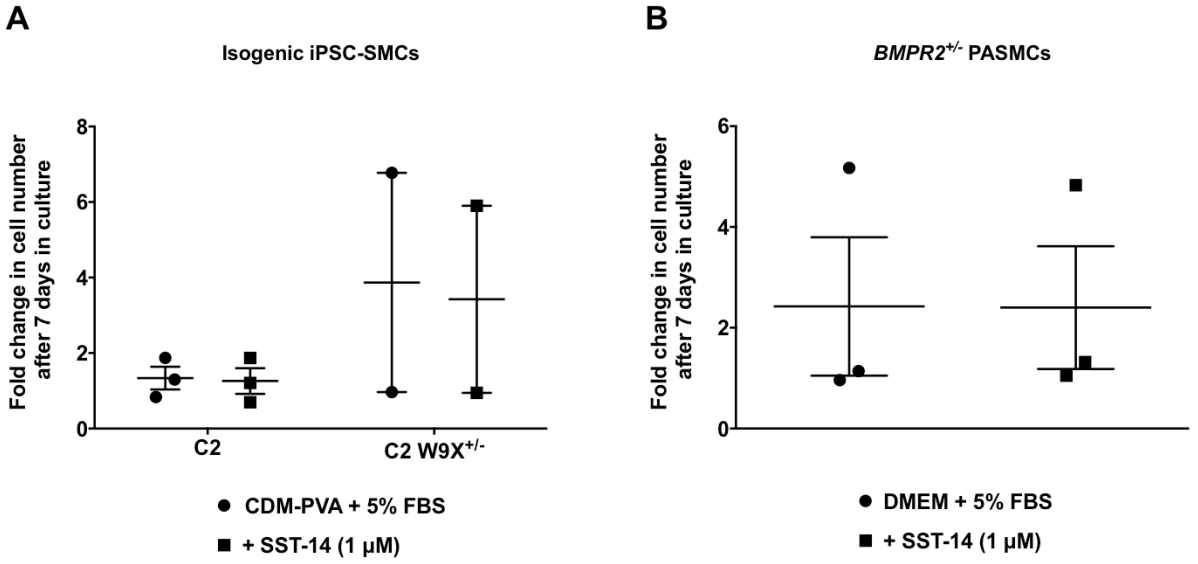

Figure 5.5. Somatostatin-14 does not significantly affect the proliferation of isogenic iPSC-SMCs and *BMPR2*$^{+/-}$ PASMCs. The effect of somatostatin on the proliferation of isogenic iPSC-SMCs (**A**) and *BMPR2*$^{+/-}$ PASMCs (**B**) was assessed by culturing the cells for seven days in CDM-PVA + 5% FBS (**A**) or DMEM + 5% FBS (**B**) in the presence or absence of somatostatin-14 (SST-14) (1 µM) and performing manual cell counts using disposable Haemocytometer counting grids. Data presented as mean ± s.e.m. of the results from 2-3 independent differentiations (**A**) or three different PAH patient-derived *BMPR2*$^{+/-}$ PASMC lines (**B**) and expressed as fold changes in cell number after seven days in culture. Statistical analysis was performed using two-way ANOVA with Sidak's post-hoc test (**A**) or unpaired two-tailed Student's *t* test (**B**). None of the differences in proliferation between treatment groups were deemed statistically significant ($P > 0.05$).

While somatostatin-14 may have failed to significantly decrease iPSC-SMC and PASMC proliferation due to the large variation in the experimental results and the low number of replicates, I wondered whether this lack of an anti-proliferative effect might also partly be due to low levels of somatostatin receptor expression in these cells. I therefore performed quantitative PCR analysis of *SSTR1-5* mRNA expression in isogenic iPSC-SMCs and wild-type and *BMPR2*$^{+/-}$ PASMCs, which revealed that the expression of *SSTR1, SSTR2, SSTR3* and *SSTR4* was significantly ($P < 0.01$) lower in C2 W9X$^{+/-}$ iPSC-SMCs compared to C2 iPSC-SMCs (**Figures 5.6 A-D**). Furthermore, C2 W9X$^{+/-}$ iPSC-SMCs displayed a non-significant trend ($P > 0.05$) towards reduced *SSTR5* expression (**Figure 5.6 E**) and *BMPR2*$^{+/-}$ PASMCs also displayed a non-significant trend ($P > 0.05$) towards reduced *SSTR1*, *SSTR3*, *SSTR4* and *SSTR5* expression compared to wild-type PASMCs (**Figures 5.6 F** and **H-J**). Taken together, these findings raise the possibility that somatostatin-14 may have failed to significantly reduce the proliferation of *BMPR2*$^{+/-}$ iPSC-SMCs and PASMCs due to reduced levels of somatostatin receptor expression in these cells.

Possible alternative reasons why somatostatin-14 did not display an anti-proliferative effect may be due to its short biological half-life (<3 min) (Patel & Wheatley, 1983) or because it might be necessary to target specific somatostatin receptor subtypes to reduce proliferation in iPSC-SMCs and PASMCs. I therefore also investigated whether the more stable somatostatin analogues octreotide and lanreotide, which preferentially bind to SSTR2 and are clinically approved for the treatment of neuroendocrine tumours (Bauer et al., 1982; Caron et al., 1997; Murphy et al., 1987; Weckbecker et al., 2003), might be more effective at reducing the proliferation of *BMPR2*$^{+/-}$ iPSC-SMCs and PASMCs. In addition, I also tested whether the proliferation of these cells can be reduced by treatment with CH-275, a somatostatin analogue that binds with high affinity to SSTR1 (Rivier et al., 2001). However, neither octreotide (100 nM – 1 μM), lanreotide (1 μM) or CH-275 (100 nM – 1 μM) significantly reduced the proliferation of *BMPR2*$^{+/-}$ iPSC-SMCs or PASMCs (**Figure 5.7**). Taken together, these findings suggest that somatostatin and its analogues do not affect the proliferation of iPSC-SMCs and PASMCs. Whether somatostatin might have potential other roles in the cellular pathogenesis of PAH is yet to be determined.

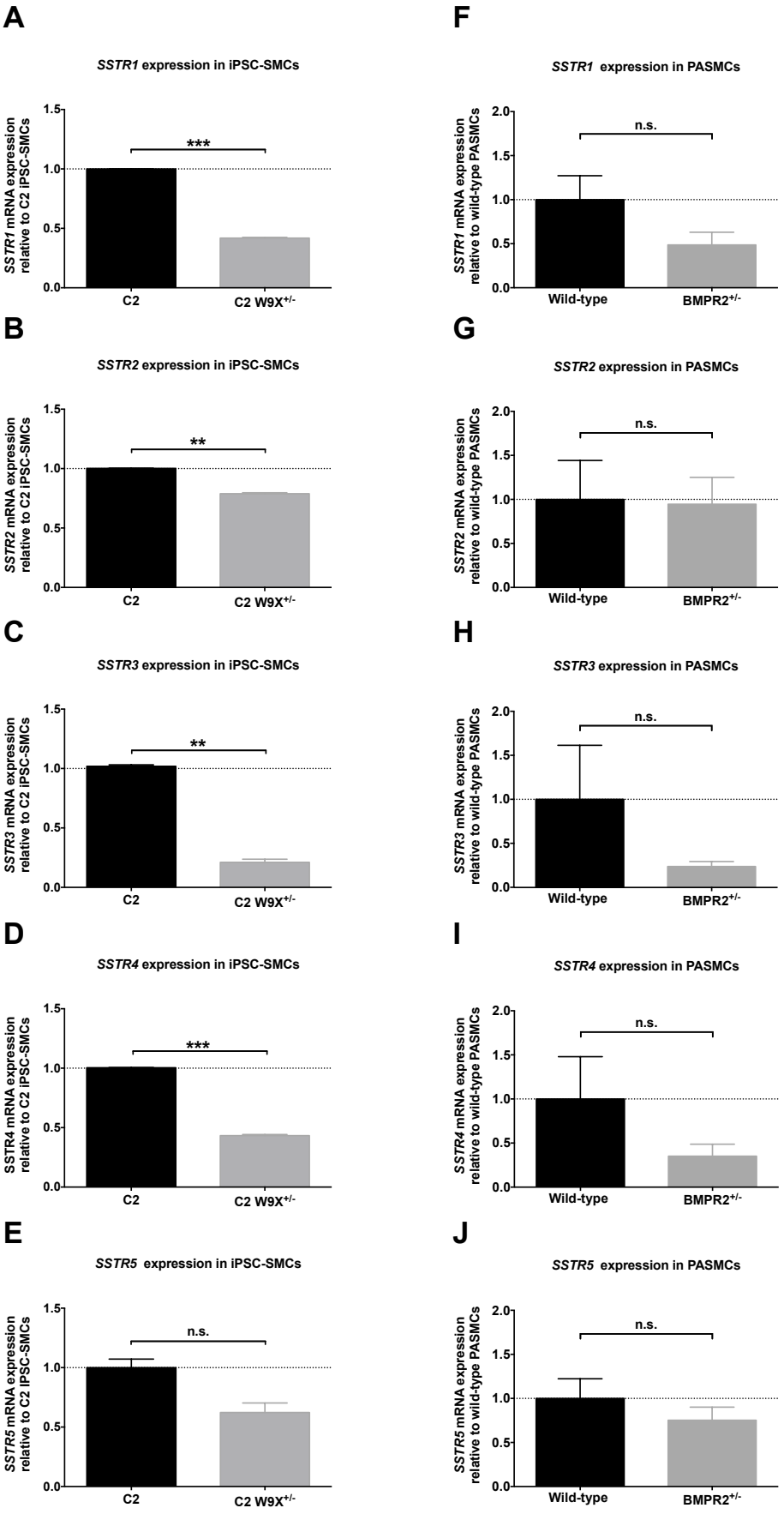
A
SSTR1 expression in iPSC-SMCs
SSTR1 mRNA expression relative to C2 iPSC-SMCs
1.5
1.0
0.5
0.0
***
C2
C2 W9X+/-
F
SSTR1 expression in PASMCs
SSTR1 mRNA expression relative to wild-type PASMCs
2.0
1.5
1.0
0.5
0.0
n.s.
Wild-type
BMPR2+/-
B
SSTR2 expression in iPSC-SMCs
SSTR2 mRNA expression relative to C2 iPSC-SMCs
**
G
SSTR2 expression in PASMCs
SSTR2 mRNA expression relative to wild-type PASMCs
C
SSTR3 expression in iPSC-SMCs
SSTR3 mRNA expression relative to C2 iPSC-SMCs
H
SSTR3 expression in PASMCs
SSTR3 mRNA expression relative to wild-type PASMCs
D
SSTR4 expression in iPSC-SMCs
SSTR4 mRNA expression relative to C2 iPSC-SMCs
I
SSTR4 expression in PASMCs
SSTR4 mRNA expression relative to wild-type PASMCs
E
SSTR5 expression in iPSC-SMCs
SSTR5 mRNA expression relative to C2 iPSC-SMCs
J
SSTR5 expression in PASMCs
SSTR5 mRNA expression relative to wild-type PASMCs

Figure 5.6. Somatostatin receptor mRNA expression levels in iPSC-SMCs and PASMCs. qPCR analysis of somatostatin receptor (*SSTR1-SSTR5*) mRNA expression in isogenic iPSC-SMCs cultured for one week in serum after differentiation in PTB (**A-E**), and in wild-type and *BMPR2*$^{+/-}$ PASMCs (**F-J**). Data presented as mean ± s.e.m. of two independent qPCR analyses performed on the cells from the same differentiation (**A-E**), or three different *BMPR2*$^{+/-}$ PASMC lines (**F-J**). [n.s., not significant ($P > 0.05$), ** $P < 0.01$, *** $P < 0.001$, unpaired two-tailed Student's *t* test].

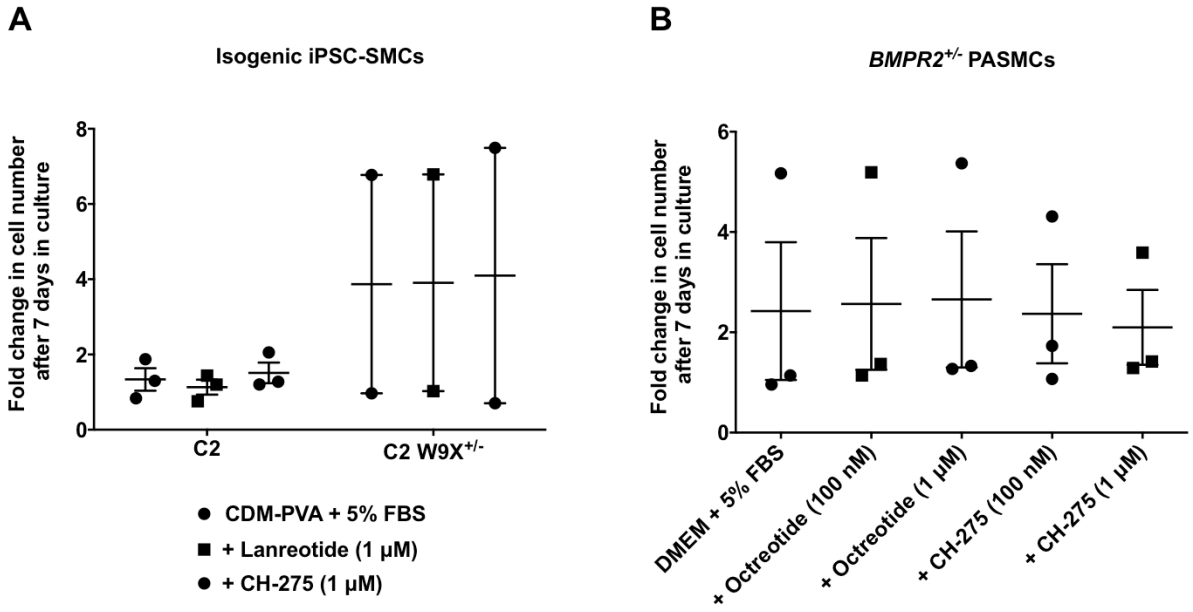

Figure 5.7. The somatostatin analogues lanreotide, octreotide and CH-275 have no significant effect on the proliferation of isogenic iPSC-SMCs and *BMPR2*$^{+/-}$ PASMCs. Isogenic iPSC-SMCs (**A**) and *BMPR2*$^{+}$ $^{-}$ PASMCs (**B**) were cultured for seven days in CDM-PVA + 5% FBS (**A**) or DMEM + 5% FBS (**B**) in the presence or absence of lanreotide (1 µM) (**A**), octreotide (100 nM – 1 µM) (**B**) or CH-275 (100 nM – 1 µM) (**A** and **B**). Proliferation was assessed by performing manual cell counts seven days after plating the cells. Data presented as mean ± s.e.m. of the results from 2-3 independent differentiations (**A**) or three different *BMPR2*$^{+/-}$ PASMC lines (**B**). Statistical analysis was performed using two-way ANOVA with Sidak's post-hoc test (**A**) or one-way ANOVA with Dunnett's post hoc test (**B**). None of the differences in proliferation between treatment groups were deemed statistically significant ($P > 0.05$).

5.3 – Discussion

The results presented in this chapter describe the identification of genes that were differentially expressed between serum-free wild-type and *BMPR2*$^{+/-}$ iPSC-SMCs and may hence provide further insights into PAH pathobiology. Genes encoding somatostatin (*SST*), dual oxidase 2 (*DUOX2*) and mitochondrial uncoupling protein 2 (*UCP2*) were significantly down-regulated in *BMPR2*$^{+/-}$ iPSC-SMCs compared to wild-type iPSC-SMCs under both serum-free conditions and after one week of exposure to serum. By contrast, whilst cytokine receptor-like factor 1 (*CRLF1*) expression was significantly upregulated in serum-free *BMPR2*$^{+/-}$ iPSC-SMCs compared to controls, *CRLF1* mRNA expression became significantly reduced in C2 W9X$^{+/-}$ iPSC-SMCs relative to the isogenic wild-type after one week of exposure to serum. Consistent with this, reduced *CRLF1* expression was also detected in the lungs of *Bmpr2*$^{+/R899X}$ mice compared with wild-type littermates.

Whilst several studies suggest that reduced *UCP2* and *SST* expression might be associated with PAH (Tjen et al., 1992; Takahashi et al., 1995; Dromparis et al., 2013; Pak et al. 2013; Michelakis et al., 2017), *DUOX2* and *CRLF1* have not previously been studied in the context of PAH. The following sections describe some of the known biological functions of *SST*, *UCP2, DUOX2* and *CRFL1* and discuss the possible roles that these genes may play in the pathogenesis of PAH.

5.3.1. – Somatostatin (SST)

Although somatostatin has previously been reported to inhibit smooth muscle cell proliferation (Leszczynski et al., 1993; Lauder et al., 1997; Zhao & Foegh, 1997), somatostatin-14 and the somatostatin analogues octreotide, lanreotide and CH-275 did not have any significant effect on the proliferation of *BMPR2*$^{+/-}$ iPSC-SMCs or PASMCs. The lack of a significant effect observed in this study may be due to the large variability in the data and the low number of experimental replicates (n=2-3) associated with the somatostatin proliferation assays. In some of the individual experiments, C2 W9X$^{+/-}$ iPSC-SMCs were not more proliferative compared to wild-type C2 iPSC-SMCs under basal conditions (see **Figure 5.5 A** and **Figure 5.7 A**), suggesting potential issues with cell viability or the iPSC-SMC differentiation process in those particular cases. Therefore, these experiments would need to be repeated to increase the number of replicates and clarify whether somatostatin and its analogues affect the proliferation of iPSC-SMCs and PASMCs.

Alternatively, it can not be ruled out that somatostatin might play a different yet unknown role in the cellular pathogenesis of PAH which might involve other cell types. For example, somatostatin and its analogues have been shown to reduce the production of pro-inflammatory cytokines in rats (Karalis et al., 2004) and in activated human monocytes (Peluso et al., 1996). Furthermore, somatostatin receptor subtype 2 (SSTR2) expression has been linked to apoptosis induction in mouse embryonic fibroblasts (Guillermet-Guibert et al., 2007). These observations raise the question of whether somatostatin reduces inflammation and promotes apoptosis in patient-derived PASMCs.

In addition, somatostatin also inhibits growth hormone, insulin, glucagon and thyroid hormone secretion (Brazeau et al., 1973; Burgus et al., 1973; Ahren et al., 1978). The reduced somatostatin expression observed in *BMPR2*$^{+/-}$ iPSC-SMCs might therefore contribute to insulin resistance and thyroid dysfunction in these cells. Since both insulin resistance and thyroid dysfunction been associated with pulmonary arterial hypertension (Chu et al., 2002; Zamanian et al., 2009; Scicchitano et al., 2016), it would therefore be interesting to investigate whether somatostatin affects inflammation, apoptosis, insulin signalling and thyroid function in PAH.

5.3.2. – Mitochondrial uncoupling protein 2 (UCP2)

UCP2 and other UCPs cause mild mitochondrial uncoupling by dissipating the electrochemical proton gradient across the inner mitochondrial membrane, which is generally thought to result in decreased production of mitochondrial reactive oxygen species (ROS), thus protecting against ROS-related cellular damage (Brand & Esteves, 2005). Consistent with this notion, increased mitochondrial ROS production has been reported in *Ucp3* knockout mice (Vidal-Puig et al., 2000; Brand et al., 2002). By contrast, *Ucp2* knockout mouse PASMCs display reduced ROS production, mitochondrial hyperpolarisation, normoxic HIF-1α activation, increased proliferation and resistance to apoptosis (Dromparis et al., 2013; Pak et al. 2013). In line with these findings, *BMPR2*$^{+/-}$ iPSC-SMCs displayed mitochondrial hyperpolarisation and reduced *UCP2* expression after exposure to serum and/or TNFα, and ROS production was reduced in serum-free *BMPR2*$^{+/-}$ iPSC-SMCs compared to controls. However, in contrast to IMM hyperpolarisation observed in PASMCs from PAH patients and *Ucp2*$^{-/-}$ mice (Pak et al., 2013; Paulin & Michelakis, 2014), *BMPR2*$^{+/-}$ iPSC-SMCs assayed under serum-free conditions displayed reduced IMM polarisation relative to controls. Although the reason for this

discrepancy is not known, it is tempting to speculate that reduced *UCP2* expression might precede the acquisition of a hyperpolarised IMM state in *BMPR2*$^{+/-}$ iPSC-SMCs.

Recently, further evidence supporting the role of *UCP2* in the pathogenesis PAH was provided by a phase I clinical trial in which IPAH patients were treated with the pyruvate dehydrogenase kinase inhibitor, dichloroacetate (DCA) (Michelakis et al., 2017). In most patients, DCA improved functional capacity and reduced both mean pulmonary arterial pressures and pulmonary vascular resistance. However, IPAH patients harbouring variants in *UCP2* and the mitochondrial deacetylase sirtuin-3 (*SIRT3*) which predicted reduced protein function did not respond to DCA treatment (Michelakis et al., 2017), suggesting that *UCP2* and *SIRT3* might act as genetic modifiers in PAH.

DCA has previously been shown to reverse the hyperglycolytic phenotype of PASMCs, stimulate mitochondria-dependent PASMC apoptosis, improve RV function and reverse PH in rat models (Michelakis et al., 2002; McMurtry et al., 2004, Zhao et al., 2013). Furthermore, *SIRT3* is thought to reduce mitochondrial membrane potential, inhibit ROS production and thus limit oxidative stress (Shi et al., 2005). *Sirt3* knockout (*Sirt3*$^{-/-}$) mice spontaneously develop PH, with *Sirt3*$^{-/-}$ mouse PASMCs displaying increased glycolysis compared to PASMCs isolated from wild-type littermates (Paulin et al., 2014). Given the reduced *UCP2* expression and IMM hyperpolarisation observed in serum-treated *BMPR2*$^{+/-}$ iPSC-SMCs, it would therefore be interesting to investigate *SIRT3* expression and the effect of DCA on glycolysis, mitochondrial polarisation and apoptosis in these cells.

Furthermore, reduced *UCP2* mRNA expression has been detected in adipose tissue of patients with hypothyroidism (Gjedde et al., 2010), suggesting that changes in *UCP2* expression might partially explain why PAH patients sometimes present with thyroid disorders (Scicchitano et al., 2016). The thyroid hormone triiodothyronine (T_3) has been reported to increase UCP2 and UCP3 expression in the heart and skeletal muscle of rats (Gong et al., 1997; Lanni et al., 1997; Lanni et al., 1999), and also stimulates *UCP2* and *UCP3* mRNA expression in human adipose tissue and skeletal muscle (Barbe et al., 2001). T_3 also reduced IMM polarisation, increased mitochondrial superoxide dismutase [SOD2, also known as manganese superoxide dismutase (MnSOD)] expression and improved mitochondrial Complex V activity in human fibroblasts with mitochondrial DNA mutations (Menzies et al., 2009). However, T_3 did not affect UCP2 expression in these cells. Whether thyroid hormone affects UCP2 expression in iPSC-SMCs or PASMCs is yet to be determined.

5.3.3. – Dual oxidase 2 (DUOX2)

DUOX2 belongs to the large family of NADPH-oxidase enzymes which regulate the synthesis of H_2O_2 and reactive oxygen species and play important roles in modulating immune responses, hormone synthesis, cell growth and differentiation (Lambeth, 2004; Sirokmany et al., 2016). Among the seven isoforms of NADPH oxidase (NOX), *NOX1*, *NOX2* and *NOX4* have been implicated in the development of PAH (Mittal et al., 2007; Nisbet et al., 2009; Veit et al., 2013; Goncharov et al., 2014; Liu et al., 2014). For example, Nox4 expression has been detected in human airways and in PASMCs (Djordjevic et al., 2005) and is upregulated in PASMCs in response to hypoxia (Diebold et al., 2010). Increased Nox4 expression has also been detected in the lungs of patients with idiopathic pulmonary arterial hypertension (Mittal et al., 2007; Goncharov et al., 2014). Furthermore, siRNA-mediated inhibition of Nox4 significantly reduced the proliferation of PH-derived PASMCs (Mittal et al., 2007) and decreased the expression of smooth muscle cell differentiation markers in rat VSMCs (Clempus et al., 2007).

In contrast to the other NADPH oxidase isoforms, relatively little is known about the functional role of DUOX2 (Konior et al., 2014). DUOX2 is required for thyroid hormone biosynthesis (Dupuy et al., 1999; De Deken et al., 2000), with *DUOX2* mutations being associated with congenital hypothyroidism and reduced ROS production (Kizys et al., 2017). Decreased ROS levels have been linked to mitochondrial hyperpolarisation and apoptosis resistance in PH PASMCs (Sutendra et al., 2011), whilst autoimmune thyroid disorders have also been detected in PAH patients (Scicchitano et al., 2016). Interestingly, Nox4 is also expressed in human thyrocytes and is thought to be upregulated in human thyroid tumours (Weyemi et al., 2010), thus suggesting that aberrant Nox4 expression might promote thyroid dysfunction in PAH. Furthermore, Duox2 dysfunction has been reported in inflammatory bowel disease (Hayes et al., 2015), suggesting that reduced *DUOX2* expression may promote inflammation. Taken together, these findings suggest that the reduced *DUOX2* expression observed in *BMPR2*$^{+/-}$ iPSC-SMCs in this thesis study may play an important but yet unknown role in the pathogenesis of PAH.

5.3.4 – Cytokine receptor-like factor 1 (CRLF1)

The *CRLF1* gene product cytokine-like factor 1 (CLF1) was originally identified as a protein that is secreted in a complex with the IL-6 family member cardiotrophin-like cytokine (CLC) (Elson et al., 2000), suggesting that CRLF1 plays a role in inflammatory signalling. *CRLF1* has also been linked to resistance to oxidative stress (Looyenga et al., 2013), making it tempting to speculate that the reduction in *CRLF1* expression in *BMPR2*$^{+/-}$ iPSC-SMCs following exposure to serum might correlate with the loss of resistance to oxidative stress in these cells. However, further work will be required to determine whether this is indeed the case.

Apart from the potential role of *CRLF1* in resistance to oxidative stress (Looyenga et al., 2013), increased *CRLF1* expression has been detected in a mouse model of idiopathic pulmonary fibrosis, where it promoted the accumulation of $CD4^+$ T lymphocytes and reduced pulmonary fibrosis (Kass et al., 2012). Increased *CLF1* gene expression has also been detected in patients with osteoarthritis (Tsuritani et al., 2010) and in a mouse model of cardiac fibrosis (Kim et al., 2016) where it might also play protective roles. For example, increased *CLF1* levels have been shown to reduce IL-6 expression in a mouse model of arthritis (Nishimoto, 2006; Chao et al., 2011). However, it is possible that increased *CRLF1* expression might also have detrimental effects. For example, increased *CRLF1* expression has recently been detected in papillary thyroid carcinoma (PTC), where it was associated with poor survival (Yu et al., 2018). However, the biological role of *CRLF1* in PASMCs is yet to be elucidated.

5.3.5 – Thyroid disorders and PAH

Thyroid disorders involving both increased and decreased thyroid function have been detected in PAH patients, but the relationship between thyroid function and PAH pathogenesis is poorly understood (Chu et al., 2002; Satoh et al., 2010; Scicchitano et al., 2016). The roles of *SST*, *UCP2*, *DUOX2* and *CRLF1* in thyroid function described above, together with their differential expression between wild-type and *BMPR2*$^{+/-}$ iPSC-SMCs, therefore raise the intriguing question of whether *BMPR2* mutations might promote thyroid dysfunction in PAH. Further work will be required to investigate whether this is indeed the case.

CHAPTER 6 – DISCUSSION

6.1 – Summary of findings

Reduced BMPR2 signalling is a central finding in PAH, both in patient samples and in preclinical models of the disease (Atkinson et al., 2002). However, given the reduced penetrance of *BMPR2* mutations in affected families (Newman et al., 2001), a major outstanding question is the identities of additional factors or pathways that are responsible for the manifestation of clinical disease. The use of vascular cell types derived from iPSCs provides a system to identify such factors. Patient-specific iPSC-ECs have previously been shown to recapitulate some PAH-associated cellular phenotypes observed in patient-derived PAECs (Gu et al., 2017; Sa et al., 2017). However, other PAH-associated phenotypes, such as inner mitochondrial membrane hyperpolarisation, could not be recapitulated. Furthermore, no iPSC-SMC model of PAH has previously been described. This thesis study addresses these issues.

This investigation describes the first iPSC-SMC model of PAH associated with *BMPR2* mutations and supports the hypothesis that the introduction of a single *BMPR2* mutation is necessary and sufficient to establish some but not all PAH-associated cellular phenotypes in iPSC-SMCs. By generating wild-type and *BMPR2*$^{+/-}$ iPSC-SMC lines with isogenic backgrounds that could be used as surrogates for distal PASMCs, it was possible to show that the introduction of a single *BMPR2* mutation in iPSC-SMCs was necessary and sufficient to recapitulate the pro-proliferative and anti-apoptotic phenotype of PAH patient-derived PASMCs. However, additional exposure to serum and/or TNFα was required to recapitulate the mitochondrial hyperpolarisation phenotype of PAH-derived PASMCs, thus suggesting a potential mechanism through which inflammatory stimuli such as TNFα might influence disease penetrance in *BMPR2* mutation carriers. Furthermore, *BMPR2*$^{+/-}$ iPSC-SMCs cultured in serum demonstrated prolonged hyperpolarisation despite withdrawal of TNFα, suggesting that transient exposure to an inflammatory stimulus may be sufficient to drive disease progression in a *BMPR2* mutation carrier.

Another important observation in this study was that increased proliferation, *IL-6* mRNA expression and reduced apoptosis were more pronounced in *BMPR2*$^{+/-}$ iPSC-SMCs differentiated in the presence of exogenous BMP4 (herein referred to as PTB) compared to iPSC-SMCs differentiated according to the protocol described by Cheung et al. (2012). These findings suggest that differentiation in PTB represents a refinement of the LM-iPSC-SMC differentiation protocol in terms of its ability to generate cells that can be used as surrogates for distal PASMCs when studying PAH. Although the reason for this is unclear, the observation

that BMP4 is highly expressed in the distal region of the lung bud during development (Bellusci et al., 1996) suggests that addition of BMP4 during differentiation might promote the acquisition of a distal cell fate in LM-iPSC-SMCs.

In addition, this study also revealed that *BMPR2*$^{+/-}$ iPSC-SMCs have an altered differentiation state and are less contractile compared to wild-type iPSC-SMCs – phenotypes which have not previously been observed in PAH-derived PASMCs. Finally, RNA-Seq analysis of wild-type and *BMPR2*$^{+/-}$ iPSC-SMCs identified that genes encoding somatostatin (*SST*), mitochondrial uncoupling protein 2 (*UCP2*), dual oxidase 2 (*DUOX2*) and cytokine receptor-like factor 1 (*CRLF1*) were differentially expressed between wild-type and *BMPR2*$^{+/-}$ iPSC-SMCs. Although somatostatin has previously been reported to reduce smooth muscle cell proliferation (Leszczynski et al., 1993; Lauder et al., 1997; Zhao & Foegh, 1997;), somatostatin and its analogues octreotide, lanreotide and CH-275 had no significant effect on the proliferation of iPSC-SMCs or PASMCs in this thesis study, possibly due to the large variation in the experimental results and the low number of experimental replicates.

6.2 – Advantages and limitations of the iPSC-SMC model to study PAH

An important observation in this study was the reduced variability between experiments in isogenic cell lines, which contrasted with the results obtained when comparing wild-type and patient-derived *BMPR2*$^{+/-}$ iPSC-SMCs. The variability between patient-derived cell lines is challenging and would require large numbers of lines from different patients to detect robust differences. This might be a possible reason why a previous study using patient-derived iPSC-ECs (Sa et al., 2017) could not recapitulate all PAH-associated phenotypes, thus highlighting a major advantage of using iPSC lines with an isogenic background to determine the impact of specific mutations.

Furthermore, the iPSC-SMC model described in this study raises a number of interesting questions. For example, we still do not know the precise molecular mechanism through which *BMPR2* mutations, either alone or via interaction with genetic, epigenetic or environmental factors, lead to the acquisition of PAH-associated cellular phenotypes. To this end, RNA-Seq differential gene expression analysis of iPSC-SMCs cultured under either serum-free or serum-containing conditions and in the presence or absence of TNFα may reveal genes and molecular pathways implicated in the acquisition of a hyperpolarised IMM state. This analysis, together

with RNA-Seq differential gene expression analysis of wild-type and *BMPR2*$^{+/-}$ PASMCs, is currently underway.

In addition, although this study showed that *BMPR2*$^{+/-}$ iPSC-SMCs display significantly increased *IL-6* mRNA expression compared to wild-type iPSC-SMCs differentiated in PTB, IL-6 expression was not analysed at the protein level. An enzyme-linked immunosorbent assay (ELISA) could therefore be performed to determine whether *BMPR2*$^{+/-}$ iPSC-SMCs also display significantly increased IL-6 expression at the protein level.

Similarly, whilst the differential expression of *SST*, *DUOX2*, *UCP2* and *CRLF1* was validated by qPCR in both iPSC-SMCs and in the lungs of *Bmpr2*$^{+/R899X}$ mice, this study did not determine whether the differential expression of these genes is reflected at the protein level. Furthermore, the low number of iPSC-SMC lines submitted for RNA sequencing meant that only a very limited number of genes were found to be differentially expressed after performing false discovery rate analysis to adjust for multiple comparisons. Analysis of a larger number of different wild-type and *BMPR2*$^{+/-}$ iPSC-SMCs lines might have uncovered additional differentially expressed genes.

Finally, the validity of the findings presented in this study could be strengthened by performing the reverse experiment in which genome editing is used to correct a *BMPR2* mutation to determine whether this reverses PAH-associated cellular phenotypes in iPSC-SMCs. It would also have been desirable to introduce the W9X mutation into an additional wild-type iPSC line to determine whether the contribution of *BMPR2* mutation to PAH-associated phenotypes can be replicated in an independent cell line. Alternatively, CRISPR-Cas9 gene editing could be used to repair the W9X mutation to determine whether this reverses the PAH-associated cellular phenotypes observed in this thesis study. In addition, whilst the W9X mutation results the insertion of a premature stop codon and hence the production of a truncated protein, missense mutations in *BMPR2* (eg C118W) which impair BMPR2 trafficking to the plasma membrane (Sobolewski et al., 2008) could be introduced in order to determine whether the findings presented in this study apply to different types of *BMPR2* mutation. Furthermore, screening for potential CRISPR-Cas9-mediated off-target effects or single nucleotide variations which may spontaneously occur in culture (reviewed in Musunuru et al., 2018) could also be performed to limit the possible number of confounders.

6.3 – Conclusions and future directions

In conclusion, this study characterises the first iPSC-SMC model of PAH and elucidates the role of *BMPR2* in establishing PAH-associated phenotypes in iPSC-derived SMCs. It also provides new insights into factors that might influence disease penetrance in *BMPR2* mutation carriers and the mechanisms by which these influence cell phenotypes, through alterations in mitochondrial membrane polarisation. This study also revealed that *BMPR2*$^{+/-}$ iPSC-SMCs have an altered differentiation state and are less contractile compared to wild-type iPSC-SMCs – phenotypes which have not previously been observed in PAH-derived PASMCs. Furthermore, RNA-Seq analysis of wild-type and *BMPR2*$^{+/-}$ iPSC-SMCs identified several novel genes that are differentially expressed between wild-type and *BMPR2*$^{+/-}$ iPSC-SMCs.

However, further work will be required to elucidate the precise molecular mechanisms through which *BMPR2* mutations interact with genetic, epigenetic or environmental factors to cause PAH establishment and progression. For example, this study could be extended to investigate whether any of the phenotypes described in this study are also present in iPSC-SMCs derived from unaffected *BMPR2* mutation carriers and idiopathic PAH patients. Furthermore, comparisons between male and female *BMPR2* mutation carriers with or without PAH could also be performed in an attempt to provide insights into why PAH predominantly affects women but is associated with reduced survival in male *BMPR2* mutation carriers (Hatton & Ryan, 2014; Jacobs et al., 2014). Future studies could also focus on developing iPSC-SMC and iPSC-EC models of other forms of pulmonary hypertension by examining the role of factors such as hypoxia. The importance of this is highlighted by the fact that whilst there are several clinically-approved therapies for the management of Group 1 PAH (Lau et al., 2017), there are currently no approved drugs for treating most other types of pulmonary hypertension, with Group 2 PH being the most common form of pulmonary hypertension worldwide (Lam et al., 2009; Strange et al., 2012).

Together with the iPSC-derived endothelial cells generated in our group (Kiskin et al., 2018), patient-derived iPSC-SMCs hold great promise for drug screening and precision medicine. For example, iPSC disease models might be able to identify drug-responsive patient subgroups which should improve the quality of clinical trials (Inoue et al., 2014). Furthermore, patient-derived iPSC-lines could be used to test the efficacy of several drugs, thus enabling the most appropriate medication to be chosen for a particular patient rather than determining the effectiveness of prescribed medications in patients by trial and error (Chen et al., 2016).

In addition, preclinical studies rely on prospective treatments being tested in animal models which do not fully recapitulate the disease pathology observed in humans. By contrast, iPSCs are genetically matched to the person from whom they were derived, whilst at the same time being stripped of epigenetic changes that are acquired during a person's lifetime and which might confound the phenotypes being studied. This makes iPSC-derived cells especially useful for modelling complex diseases such PAH which are caused by a combination of multiple genetic and environmental factors.

Wild-type and both patient-derived and isogenic *BMPR2*$^{+/-}$ iPSC-SMCs and iPSC-ECs could be used to test whether therapeutic interventions aimed at restoring BMPR2 signalling reverse the PAH-associated phenotypes described in this study. Such drug screening candidates could include (i) the immunosuppressant FK506 (tacrolimus), which activates *BMPR2* by binding to the BMP inhibitor FK506-binding protein-12 (FKBP12) (Spiekerkoetter et al., 2013), (ii) the lysosomal inhibitor hydroxychloroquine, which promotes BMPR2 trafficking to the cell surface (Dunmore et al., 2013), and (iii) ataluren, a drug that promotes ribosomal read-through of premature stop codons (Drake et al., 2013). The effect of metabolic modulators such as dichloroacetate or peroxisome proliferator-activated receptor gamma (PPAR-γ) agonists such as rosiglitazone, which reverse PAH in animal models (McMurtry et al., 2004; Nisbet et al., 2010), could also be tested. However, since PAH is associated with multiple metabolic abnormalities beyond aerobic glycolysis (referred to as the 'Warburg effect') (D'Alessandro et al., 2018), it is likely that multiple signalling pathways might need to be targeted at the same time in order to achieve a robust clinical response.

In future studies, iPSC-SMCs could also be generated from PAH patients with mutations in other PAH-associated genes, thus extending the study of PAH-associated phenotypes to a broader patient population. Furthermore, iPSC-SMCs could be co-cultured with iPSC-ECs or combined with adult pulmonary vascular cells in organoid or artery-on-a-chip setups for a more comprehensive evaluation of PAH-associated phenotypes in a setting that more closely resembles *in vivo* conditions. In summary, the iPSC-SMC model of PAH described in this study will be useful for identifying novel druggable targets that could be used to develop novel therapeutic interventions that are desperately needed to treat this devastating and deadly disease.

REFERENCES

Abe, K., Toba, M., Alzoubi, A., Ito, M., Fagan, K. A., Cool, C. D., Voelkel, N. F., McMurtry, I. F. and Oka, M. (2010) 'Formation of plexiform lesions in experimental severe pulmonary arterial hypertension', *Circulation,* 121(25), pp. 2747-54.

Abman, S. H., Shanley, P. F. and Accurso, F. J. (1989) 'Failure of postnatal adaptation of the pulmonary circulation after chronic intrauterine pulmonary hypertension in fetal lambs', *J Clin Invest,* 83(6), pp. 1849-58.

Adams, L. D., Geary, R. L., McManus, B. and Schwartz, S. M. (2000) 'A comparison of aorta and vena cava medial message expression by cDNA array analysis identifies a set of 68 consistently differentially expressed genes, all in aortic media', *Circ Res,* 87(7), pp. 623-31.

Aggarwal, S., Gross, C. M., Sharma, S., Fineman, J. R. and Black, S. M. (2013) 'Reactive oxygen species in pulmonary vascular remodeling', *Compr Physiol,* 3(3), pp. 1011-34.

Aguirre, J. I., Morrell, N. W., Long, L., Clift, P., Upton, P. D., Polak, J. M. and Wilkins, M. R. (2000) 'Vascular remodeling and ET-1 expression in rat strains with different responses to chronic hypoxia', *Am J Physiol Lung Cell Mol Physiol,* 278(5), pp. L981-7.

Ahmed, M. I., Mardaryev, A. N., Lewis, C. J., Sharov, A. A. and Botchkareva, N. V. (2011) 'MicroRNA-21 is an important downstream component of BMP signalling in epidermal keratinocytes', *J Cell Sci,* 124(Pt 20), pp. 3399-404.

Ahren, B., Ericsson, M., Hedner, P., Ingemansson, S. and Westgren, U. (1978) 'Somatostatin inhibits thyroid hormone secretion induced by exogenous TSH in man', J Clin Endocrinol Metab, 47(5), pp. 1156-9.

Alastalo, T. P., Li, M., Perez Vde, J., Pham, D., Sawada, H., Wang, J. K., Koskenvuo, M., Wang, L., Freeman, B. A., Chang, H. Y. and Rabinovitch, M. (2011) 'Disruption of PPARgamma/beta-catenin-mediated regulation of apelin impairs BMP-induced mouse and human pulmonary arterial EC survival', *J Clin Invest,* 121(9), pp. 3735-46.

Alt, A., Miguel-Romero, L., Donderis, J., Aristorena, M., Blanco, F. J., Round, A., Rubio, V., Bernabeu, C. and Marina, A. (2012) 'Structural and functional insights into endoglin ligand recognition and binding', *PLoS One,* 7(2), pp. e29948.

Alva, J. A. and Iruela-Arispe, M. L. (2004) 'Notch signaling in vascular morphogenesis', *Curr Opin Hematol,* 11(4), pp. 278-83.

Andersson, E. R., Sandberg, R. and Lendahl, U. (2011) 'Notch signaling: simplicity in design, versatility in function', *Development,* 138(17), pp. 3593-612.

Archer, S. L., Gomberg-Maitland, M., Maitland, M. L., Rich, S., Garcia, J. G. and Weir, E. K. (2008) 'Mitochondrial metabolism, redox signaling, and fusion: a mitochondria-ROS-HIF-1alpha-Kv1.5 O2-sensing pathway at the intersection of pulmonary hypertension and cancer', *Am J Physiol Heart Circ Physiol,* 294(2), pp. H570-8.

Archer, S. L., Weir, E. K. and Wilkins, M. R. (2010) 'Basic science of pulmonary arterial hypertension for clinicians: new concepts and experimental therapies', *Circulation,* 121(18), pp. 2045-66.

Archer, S. L., Will, J. A. and Weir, E. K. (1986) 'Redox status in the control of pulmonary vascular tone', *Herz,* 11(3), pp. 127-41.

Arias-Stella, J. and Saldana, M. (1963) 'The Terminal Portion of the Pulmonary Arterial Tree in People Native to High Altitudes', *Circulation,* 28, pp. 915-25.

Atkinson, C., Stewart, S., Upton, P. D., Machado, R., Thomson, J. R., Trembath, R. C. and Morrell, N. W. (2002) 'Primary pulmonary hypertension is associated with reduced pulmonary vascular expression of type II bone morphogenetic protein receptor', *Circulation,* 105(14), pp. 1672-8.

Attisano, L. and Labbe, E. (2004) 'TGFbeta and Wnt pathway cross-talk', *Cancer Metastasis Rev,* 23(1-2), pp. 53-61.

Austin, E. D., Ma, L., LeDuc, C., Berman Rosenzweig, E., Borczuk, A., Phillips, J. A., 3rd, Palomero, T., Sumazin, P., Kim, H. R., Talati, M. H., West, J., Loyd, J. E. and Chung, W. K. (2012) 'Whole exome sequencing to identify a novel gene (caveolin-1) associated with human pulmonary arterial hypertension', *Circ Cardiovasc Genet,* 5(3), pp. 336-43.

Badesch, D. B., Raskob, G. E., Elliott, C. G., Krichman, A. M., Farber, H. W., Frost, A. E., Barst, R. J., Benza, R. L., Liou, T. G., Turner, M., Giles, S., Feldkircher, K., Miller, D. P. and McGoon, M. D. (2010) 'Pulmonary arterial hypertension: baseline characteristics from the REVEAL Registry', *Chest,* 137(2), pp. 376-87.

Badri, K. R., Zhou, Y. and Schuger, L. (2008) 'Embryological origin of airway smooth muscle', *Proc Am Thorac Soc,* 5(1), pp. 4-10.

Ball, M. K., Waypa, G. B., Mungai, P. T., Nielsen, J. M., Czech, L., Dudley, V. J., Beussink, L., Dettman, R. W., Berkelhamer, S. K., Steinhorn, R. H., Shah, S. J. and Schumacker, P. T. (2014) 'Regulation of hypoxia-induced pulmonary hypertension by vascular smooth muscle hypoxia-inducible factor-1alpha', *Am J Respir Crit Care Med,* 189(3), pp. 314-24.

Barbe, P., Larrouy, D., Boulanger, C., Chevillotte, E., Viguerie, N., Thalamas, C., Oliva Trastoy, M., Roques, M., Vidal, H. and Langin, D. (2001) 'Triiodothyronine-mediated up-regulation of UCP2 and UCP3 mRNA expression in human skeletal muscle without coordinated induction of mitochondrial respiratory chain genes', *FASEB J,* 15(1), pp. 13-15.

Bauer, W., Briner, U., Doepfner, W., Haller, R., Huguenin, R., Marbach, P., Petcher, T. J. and Pless (1982) 'SMS 201-995: a very potent and selective octapeptide analogue of somatostatin with prolonged action', *Life Sci,* 31(11), pp. 1133-40.

Beall, C. M., Cavalleri, G. L., Deng, L., Elston, R. C., Gao, Y., Knight, J., Li, C., Li, J. C., Liang, Y., McCormack, M., Montgomery, H. E., Pan, H., Robbins, P. A., Shianna, K. V., Tam, S. C., Tsering, N., Veeramah, K. R., Wang, W., Wangdui, P., Weale, M. E., Xu, Y., Xu, Z., Yang, L., Zaman, M. J., Zeng, C., Zhang, L., Zhang, X., Zhaxi, P. and Zheng, Y. T. (2010) 'Natural selection on EPAS1 (HIF2alpha) associated with low hemoglobin concentration in Tibetan highlanders', *Proc Natl Acad Sci U S A,* 107(25), pp. 11459-64.

Belik, J., Halayko, A. J., Rao, K. and Stephens, N. L. (1993) 'Fetal ductus arteriosus ligation. Pulmonary vascular smooth muscle biochemical and mechanical changes', *Circ Res,* 72(3), pp. 588-96.

Bellusci, S., Henderson, R., Winnier, G., Oikawa, T. and Hogan, B. L. (1996) 'Evidence from normal expression and targeted misexpression that bone morphogenetic protein (Bmp-4) plays a role in mouse embryonic lung morphogenesis', *Development,* 122(6), pp. 1693-702.

Benza, R. L., Miller, D. P., Barst, R. J., Badesch, D. B., Frost, A. E. and McGoon, M. D. (2012) 'An evaluation of long-term survival from time of diagnosis in pulmonary arterial hypertension from the REVEAL Registry', *Chest,* 142(2), pp. 448-456.

Benza, R. L., Miller, D. P., Gomberg-Maitland, M., Frantz, R. P., Foreman, A. J., Coffey, C. S., Frost, A., Barst, R. J., Badesch, D. B., Elliott, C. G., Liou, T. G. and McGoon, M. D. (2010) 'Predicting survival in pulmonary arterial hypertension: insights from the Registry to Evaluate Early and Long-Term Pulmonary Arterial Hypertension Disease Management (REVEAL)', *Circulation,* 122(2), pp. 164-72.

Beppu, H., Lei, H., Bloch, K. D. and Li, E. (2005) 'Generation of a floxed allele of the mouse BMP type II receptor gene', *Genesis,* 41(3), pp. 133-7.

Best, D. H., Austin, E. D., Chung, W. K. and Elliott, C. G. (2014) 'Genetics of pulmonary hypertension', *Curr Opin Cardiol,* 29(6), pp. 520-7.

Best, D. H., Sumner, K. L., Smith, B. P., Damjanovich-Colmenares, K., Nakayama, I., Brown, L. M., Ha, Y., Paul, E., Morris, A., Jama, M. A., Dodson, M. W., Bayrak-Toydemir, P. and Elliott, C. G. (2017) 'EIF2AK4 Mutations in Patients Diagnosed With Pulmonary Arterial Hypertension', *Chest,* 151(4), pp. 821-828.

Betancur, P., Bronner-Fraser, M. and Sauka-Spengler, T. (2010) 'Assembling neural crest regulatory circuits into a gene regulatory network', *Annu Rev Cell Dev Biol,* 26, pp. 581-603.

Black, S. M., Johengen, M. J. and Soifer, S. J. (1998) 'Coordinated regulation of genes of the nitric oxide and endothelin pathways during the development of pulmonary hypertension in fetal lambs', *Pediatr Res,* 44(6), pp. 821-30.

Bogaard, H. J., Abe, K., Vonk Noordegraaf, A. and Voelkel, N. F. (2009) 'The right ventricle under pressure: cellular and molecular mechanisms of right-heart failure in pulmonary hypertension', *Chest,* 135(3), pp. 794-804.

Bonnet, S. and Boucherat, O. (2018) 'The ROS controversy in hypoxic pulmonary hypertension revisited', *Eur Respir J,* 51(3).

Bonnet, S., Michelakis, E. D., Porter, C. J., Andrade-Navarro, M. A., Thebaud, B., Bonnet, S., Haromy, A., Harry, G., Moudgil, R., McMurtry, M. S., Weir, E. K. and Archer, S. L. (2006) 'An abnormal mitochondrial-hypoxia inducible factor-1alpha-Kv channel pathway disrupts oxygen sensing and triggers pulmonary arterial hypertension in fawn hooded rats: similarities to human pulmonary arterial hypertension', *Circulation,* 113(22), pp. 2630-41.

Boucherat, O., Chabot, S., Paulin, R., Trinh, I., Bourgeois, A., Potus, F., Lampron, M. C., Lambert, C., Breuils-Bonnet, S., Nadeau, V., Paradis, R., Goncharova, E. A., Provencher, S. and Bonnet, S. (2017) 'HDAC6: A Novel Histone Deacetylase Implicated in Pulmonary Arterial Hypertension', *Sci Rep,* 7(1), pp. 4546.

Bragdon, B., Moseychuk, O., Saldanha, S., King, D., Julian, J. and Nohe, A. (2011) 'Bone morphogenetic proteins: a critical review', *Cell Signal,* 23(4), pp. 609-20.

Brand, M. D. and Esteves, T. C. (2005) 'Physiological functions of the mitochondrial uncoupling proteins UCP2 and UCP3', *Cell Metab,* 2(2), pp. 85-93.

Brand, M. D. and Nicholls, D. G. (2011) 'Assessing mitochondrial dysfunction in cells', *Biochem J,* 435(2), pp. 297-312.

Brand, M. D., Pamplona, R., Portero-Otin, M., Requena, J. R., Roebuck, S. J., Buckingham, J. A., Clapham, J. C. and Cadenas, S. (2002) 'Oxidative damage and phospholipid fatty acyl composition in skeletal muscle mitochondria from mice underexpressing or overexpressing uncoupling protein 3', *Biochem J,* 368(Pt 2), pp. 597-603.

Brazeau, P., Vale, W., Burgus, R., Ling, N., Butcher, M., Rivier, J. and Guillemin, R. (1973) 'Hypothalamic polypeptide that inhibits the secretion of immunoreactive pituitary growth hormone', *Science,* 179(4068), pp. 77-9.

Brons, I. G., Smithers, L. E., Trotter, M. W., Rugg-Gunn, P., Sun, B., Chuva de Sousa Lopes, S. M., Howlett, S. K., Clarkson, A., Ahrlund-Richter, L., Pedersen, R. A. and Vallier, L. (2007) 'Derivation of pluripotent epiblast stem cells from mammalian embryos', *Nature,* 448(7150), pp. 191-5.

Brown, M. A., Zhao, Q., Baker, K. A., Naik, C., Chen, C., Pukac, L., Singh, M., Tsareva, T., Parice, Y., Mahoney, A., Roschke, V., Sanyal, I. and Choe, S. (2005) 'Crystal structure of BMP-9 and functional interactions with pro-region and receptors', *J Biol Chem,* 280(26), pp. 25111-8.

Bruns, C., Weckbecker, G., Raulf, F., Kaupmann, K., Schoeffter, P., Hoyer, D. and Lubbert, H. (1994) 'Molecular pharmacology of somatostatin-receptor subtypes', *Ann NY Acad Sci,* 733, pp. 138-46.

Budhiraja, R., Tuder, R. M. and Hassoun, P. M. (2004) 'Endothelial dysfunction in pulmonary hypertension', *Circulation,* 109(2), pp. 159-65.

Burgus, R., Ling, N., Butcher, M. and Guillemin, R. (1973) 'Primary structure of somatostatin, a hypothalamic peptide that inhibits the secretion of pituitary growth hormone', *Proc Natl Acad Sci USA,* 70(3), pp. 684-8.

Camara, A. K., Lesnefsky, E. J. and Stowe, D. F. (2010) 'Potential therapeutic benefits of strategies directed to mitochondria', *Antioxid Redox Signal,* 13(3), pp. 279-347.

Caron, P., Morange-Ramos, I., Cogne, M. and Jaquet, P. (1997) 'Three year follow-up of acromegalic patients treated with intramuscular slow-release lanreotide', *J Clin Endocrinol Metab,* 82(1), pp. 18-22.

Chamley-Campbell, J., Campbell, G. R. and Ross, R. (1979) 'The smooth muscle cell in culture', *Physiol Rev,* 59(1), pp. 1-61.

Chan, E. M., Ratanasirintrawoot, S., Park, I. H., Manos, P. D., Loh, Y. H., Huo, H., Miller, J. D., Hartung, O., Rho, J., Ince, T. A., Daley, G. Q. and Schlaeger, T. M. (2009) 'Live cell imaging distinguishes bona fide human iPS cells from partially reprogrammed cells', *Nat Biotechnol,* 27(11), pp. 1033-7.

Chanakira, A., Dutta, R., Charboneau, R., Barke, R., Santilli, S. M. and Roy, S. (2012) 'Hypoxia differentially regulates arterial and venous smooth muscle cell proliferation via PDGFR-beta and VEGFR-2 expression', *Am J Physiol Heart Circ Physiol,* 302(5), pp. H1173-84.

Chang, C. W., Lai, Y. S., Westin, E., Khodadadi-Jamayran, A., Pawlik, K. M., Lamb, L. S., Jr., Goldman, F. D. and Townes, T. M. (2015) 'Modeling Human Severe Combined Immunodeficiency and Correction by CRISPR/Cas9-Enhanced Gene Targeting', *Cell Rep,* 12(10), pp. 1668-77.

Chao, C., Joyce-Shaikh, B., Grein, J., Moshrefi, M., Raoufi, F., Laface, D. M., McClanahan, T. K., Bourne, P. A., Pierce, R. H., Gorman, D. M. and Pflanz, S. (2011) 'C17 prevents inflammatory arthritis and associated joint destruction in mice', *PLoS One,* 6(7), pp. e22256.

Chaouat, A., Coulet, F., Favre, C., Simonneau, G., Weitzenblum, E., Soubrier, F. and Humbert, M. (2004) 'Endoglin germline mutation in a patient with hereditary haemorrhagic telangiectasia and dexfenfluramine associated pulmonary arterial hypertension', *Thorax,* 59(5), pp. 446-8.

Chelladurai, P., Seeger, W. and Pullamsetti, S. S. (2012) 'Matrix metalloproteinases and their inhibitors in pulmonary hypertension', *Eur Respir J,* 40(3), pp. 766-82.

Chen, H., Shi, S., Acosta, L., Li, W., Lu, J., Bao, S., Chen, Z., Yang, Z., Schneider, M. D., Chien, K. R., Conway, S. J., Yoder, M. C., Haneline, L. S., Franco, D. and Shou, W. (2004) 'BMP10 is essential for maintaining cardiac growth during murine cardiogenesis', *Development,* 131(9), pp. 2219-31.

Chen, I. Y., Matsa, E. and Wu, J. C. (2016) 'Induced pluripotent stem cells: at the heart of cardiovascular precision medicine', *Nat Rev Cardiol,* 13(6), pp. 333-49.

Cheung, C., Bernardo, A. S., Trotter, M. W., Pedersen, R. A. and Sinha, S. (2012) 'Generation of human vascular smooth muscle subtypes provides insight into embryological origin-dependent disease susceptibility', *Nat Biotechnol,* 30(2), pp. 165-73.

Chi, J. T., Rodriguez, E. H., Wang, Z., Nuyten, D. S., Mukherjee, S., van de Rijn, M., van de Vijver, M. J., Hastie, T. and Brown, P. O. (2007) 'Gene expression programs of human smooth muscle cells: tissue-specific differentiation and prognostic significance in breast cancers', *PLoS Genet,* 3(9), pp. 1770-84.

Chida, A., Shintani, M., Nakayama, T., Furutani, Y., Hayama, E., Inai, K., Saji, T., Nonoyama, S. and Nakanishi, T. (2012) 'Missense mutations of the BMPR1B (ALK6) gene in childhood idiopathic pulmonary arterial hypertension', *Circ J,* 76(6), pp. 1501-8.

Choi, K. D., Yu, J., Smuga-Otto, K., Salvagiotto, G., Rehrauer, W., Vodyanik, M., Thomson, J. and Slukvin, I. (2009) 'Hematopoietic and endothelial differentiation of human induced pluripotent stem cells', *Stem Cells,* 27(3), pp. 559-67.

Christian, M., Cermak, T., Doyle, E. L., Schmidt, C., Zhang, F., Hummel, A., Bogdanove, A. J. and Voytas, D. F. (2010) 'Targeting DNA double-strand breaks with TAL effector nucleases', *Genetics,* 186(2), pp. 757-61.

Chu, J. W., Kao, P. N., Faul, J. L. and Doyle, R. L. (2002) 'High prevalence of autoimmune thyroid disease in pulmonary arterial hypertension', *Chest,* 122(5), pp. 1668-73.

Clempus, R. E., Sorescu, D., Dikalova, A. E., Pounkova, L., Jo, P., Sorescu, G. P., Schmidt, H. H., Lassegue, B. and Griendling, K. K. (2007) 'Nox4 is required for maintenance of the differentiated vascular smooth muscle cell phenotype', *Arterioscler Thromb Vasc Biol,* 27(1), pp. 42-8.

Cong, L., Ran, F. A., Cox, D., Lin, S., Barretto, R., Habib, N., Hsu, P. D., Wu, X., Jiang, W., Marraffini, L. A. and Zhang, F. (2013) 'Multiplex genome engineering using CRISPR/Cas systems', *Science,* 339(6121), pp. 819-23.

Corada, M., Orsenigo, F., Morini, M. F., Pitulescu, M. E., Bhat, G., Nyqvist, D., Breviario, F., Conti, V., Briot, A., Iruela-Arispe, M. L., Adams, R. H. and Dejana, E. (2013) 'Sox17 is indispensable for acquisition and maintenance of arterial identity', *Nat Commun,* 4, pp. 2609.

Corcoran, S. E. and O'Neill, L. A. (2016) 'HIF1alpha and metabolic reprogramming in inflammation', *J Clin Invest,* 126(10), pp. 3699-3707.

Courboulin, A., Barrier, M., Perreault, T., Bonnet, P., Tremblay, V. L., Paulin, R., Tremblay, E., Lambert, C., Jacob, M. H., Bonnet, S. N., Provencher, S. and Bonnet, S. (2012) 'Plumbagin reverses proliferation and resistance to apoptosis in experimental PAH', *Eur Respir J,* 40(3), pp. 618-29.

Courboulin, A., Tremblay, V. L., Barrier, M., Meloche, J., Jacob, M. H., Chapolard, M., Bisserier, M., Paulin, R., Lambert, C., Provencher, S. and Bonnet, S. (2011) 'Kruppel-like factor 5 contributes to pulmonary artery smooth muscle proliferation and resistance to apoptosis in human pulmonary arterial hypertension', *Respir Res,* 12, pp. 128.

Cracowski, J. L., Chabot, F., Labarere, J., Faure, P., Degano, B., Schwebel, C., Chaouat, A., Reynaud-Gaubert, M., Cracowski, C., Sitbon, O., Yaici, A., Simonneau, G. and Humbert, M. (2014) 'Proinflammatory cytokine levels are linked to death in pulmonary arterial hypertension', *Eur Respir J,* 43(3), pp. 915-7.

Crosby, A., Jones, F. M., Kolosionek, E., Southwood, M., Purvis, I., Soon, E., Butrous, G., Dunne, D. E. and Morrell, N. W. (2011) 'Praziquantel reverses pulmonary hypertension and vascular remodeling in murine schistosomiasis', *Am J Respir Crit Care Med,* 184(4), pp. 467-73.

Crosby, A., Jones, F. M., Southwood, M., Stewart, S., Schermuly, R., Butrous, G., Dunne, D. W. and Morrell, N. W. (2010) 'Pulmonary vascular remodeling correlates with lung eggs and cytokines in murine schistosomiasis', *Am J Respir Crit Care Med,* 181(3), pp. 279-88.

Cummins, E. P., Keogh, C. E., Crean, D. and Taylor, C. T. (2016) 'The role of HIF in immunity and inflammation', *Mol Aspects Med,* 47-48, pp. 24-34.

D'Alessandro, A., El Kasmi, K. C., Plecita-Hlavata, L., Jezek, P., Li, M., Zhang, H., Gupte, S. A. and Stenmark, K. R. (2018) 'Hallmarks of Pulmonary Hypertension: Mesenchymal and Inflammatory Cell Metabolic Reprogramming', *Antioxid Redox Signal,* 28(3), pp. 230-250.

D'Alonzo, G. E., Barst, R. J., Ayres, S. M., Bergofsky, E. H., Brundage, B. H., Detre, K. M., Fishman, A. P., Goldring, R. M., Groves, B. M., Kernis, J. T. and et al. (1991) 'Survival in patients with primary pulmonary hypertension. Results from a national prospective registry', *Ann Intern Med,* 115(5), pp. 343-9.

Dai, Z., Li, M., Wharton, J., Zhu, M. M. and Zhao, Y. Y. (2016) 'Prolyl-4 Hydroxylase 2 (PHD2) Deficiency in Endothelial Cells and Hematopoietic Cells Induces Obliterative Vascular Remodeling and Severe Pulmonary Arterial Hypertension in Mice and Humans Through Hypoxia-Inducible Factor-2alpha', *Circulation,* 133(24), pp. 2447-58.

Daly, A. C., Randall, R. A. and Hill, C. S. (2008) 'Transforming growth factor beta-induced Smad1/5 phosphorylation in epithelial cells is mediated by novel receptor complexes and is essential for anchorage-independent growth', *Mol Cell Biol,* 28(22), pp. 6889-902.

David, L., Mallet, C., Mazerbourg, S., Feige, J. J. and Bailly, S. (2007) 'Identification of BMP9 and BMP10 as functional activators of the orphan activin receptor-like kinase 1 (ALK1) in endothelial cells', *Blood,* 109(5), pp. 1953-61.

de Caestecker, M. (2004) 'The transforming growth factor-beta superfamily of receptors', *Cytokine Growth Factor Rev,* 15(1), pp. 1-11.

De Deken, X., Wang, D., Many, M. C., Costagliola, S., Libert, F., Vassart, G., Dumont, J. E. and Miot, F. (2000) 'Cloning of two human thyroid cDNAs encoding new members of the NADPH oxidase family', *J Biol Chem,* 275(30), pp. 23227-33.

de Jesus Perez, V. A., Alastalo, T. P., Wu, J. C., Axelrod, J. D., Cooke, J. P., Amieva, M. and Rabinovitch, M. (2009) 'Bone morphogenetic protein 2 induces pulmonary angiogenesis via Wnt-beta-catenin and Wnt-RhoA-Rac1 pathways', *J Cell Biol,* 184(1), pp. 83-99.

de Jesus Perez, V. A., Yuan, K., Orcholski, M. E., Sawada, H., Zhao, M., Li, C. G., Tojais, N. F., Nickel, N., Rajagopalan, V., Spiekerkoetter, E., Wang, L., Dutta, R., Bernstein, D. and Rabinovitch, M. (2012) 'Loss of adenomatous poliposis coli-alpha3 integrin interaction promotes endothelial apoptosis in mice and humans', *Circ Res,* 111(12), pp. 1551-64.

Deleidi, M. and Yu, C. (2016) 'Genome editing in pluripotent stem cells: research and therapeutic applications', *Biochem Biophys Res Commun,* 473(3), pp. 665-74.

DeLeve, L. D., McCuskey, R. S., Wang, X., Hu, L., McCuskey, M. K., Epstein, R. B. and Kanel, G. C. (1999) 'Characterization of a reproducible rat model of hepatic veno-occlusive disease', *Hepatology,* 29(6), pp. 1779-91.

Deng, D. X., Spin, J. M., Tsalenko, A., Vailaya, A., Ben-Dor, A., Yakhini, Z., Tsao, P., Bruhn, L. and Quertermous, T. (2006) 'Molecular signatures determining coronary artery and saphenous vein smooth muscle cell phenotypes: distinct responses to stimuli', *Arterioscler Thromb Vasc Biol,* 26(5), pp. 1058-65.

Deng, Z., Morse, J. H., Slager, S. L., Cuervo, N., Moore, K. J., Venetos, G., Kalachikov, S., Cayanis, E., Fischer, S. G., Barst, R. J., Hodge, S. E. and Knowles, J. A. (2000) 'Familial primary pulmonary hypertension (gene PPH1) is caused by mutations in the bone morphogenetic protein receptor-II gene', *Am J Hum Genet,* 67(3), pp. 737-44.

Detar, R. (1980) 'Mechanism of physiological hypoxia-induced depression of vascular smooth muscle contraction', *Am J Physiol,* 238(6), pp. H761-9.

Dewachter, L., Adnot, S., Guignabert, C., Tu, L., Marcos, E., Fadel, E., Humbert, M., Dartevelle, P., Simonneau, G., Naeije, R. and Eddahibi, S. (2009) 'Bone morphogenetic protein signalling in heritable versus idiopathic pulmonary hypertension', *Eur Respir J,* 34(5), pp. 1100-10.

Diebold, I., Hennigs, J. K., Miyagawa, K., Li, C. G., Nickel, N. P., Kaschwich, M., Cao, A., Wang, L., Reddy, S., Chen, P. I., Nakahira, K., Alcazar, M. A., Hopper, R. K., Ji, L., Feldman, B. J. and Rabinovitch, M. (2015) 'BMPR2 preserves mitochondrial function and DNA during reoxygenation to promote endothelial cell survival and reverse pulmonary hypertension', *Cell Metab,* 21(4), pp. 596-608.

Diebold, I., Petry, A., Hess, J. and Gorlach, A. (2010) 'The NADPH oxidase subunit NOX4 is a new target gene of the hypoxia-inducible factor-1', *Mol Biol Cell,* 21(12), pp. 2087-96.

Dimos, J. T., Rodolfa, K. T., Niakan, K. K., Weisenthal, L. M., Mitsumoto, H., Chung, W., Croft, G. F., Saphier, G., Leibel, R., Goland, R., Wichterle, H., Henderson, C. E. and Eggan, K. (2008) 'Induced pluripotent stem cells generated from patients with ALS can be differentiated into motor neurons', *Science,* 321(5893), pp. 1218-21.

Djordjevic, T., BelAiba, R. S., Bonello, S., Pfeilschifter, J., Hess, J. and Gorlach, A. (2005) 'Human urotensin II is a novel activator of NADPH oxidase in human pulmonary artery smooth muscle cells', *Arterioscler Thromb Vasc Biol,* 25(3), pp. 519-25.

Domenga, V., Fardoux, P., Lacombe, P., Monet, M., Maciazek, J., Krebs, L. T., Klonjkowski, B., Berrou, E., Mericskay, M., Li, Z., Tournier-Lasserve, E., Gridley, T. and Joutel, A. (2004) 'Notch3 is required for arterial identity and maturation of vascular smooth muscle cells', *Genes Dev,* 18(22), pp. 2730-5.

Dosch, R., Gawantka, V., Delius, H., Blumenstock, C. and Niehrs, C. (1997) 'Bmp-4 acts as a morphogen in dorsoventral mesoderm patterning in Xenopus', *Development,* 124(12), pp. 2325-34.

Drake, K. M., Dunmore, B. J., McNelly, L. N., Morrell, N. W. and Aldred, M. A. (2013) 'Correction of nonsense BMPR2 and SMAD9 mutations by ataluren in pulmonary arterial hypertension', *Am J Respir Cell Mol Biol,* 49(3), pp. 403-9.

Dromparis, P., Paulin, R., Sutendra, G., Qi, A. C., Bonnet, S. and Michelakis, E. D. (2013) 'Uncoupling protein 2 deficiency mimics the effects of hypoxia and endoplasmic reticulum stress on mitochondria and triggers pseudohypoxic pulmonary vascular remodeling and pulmonary hypertension', *Circ Res,* 113(2), pp. 126-36.

Dunmore, B. J., Drake, K. M., Upton, P. D., Toshner, M. R., Aldred, M. A. and Morrell, N. W. (2013) 'The lysosomal inhibitor, chloroquine, increases cell surface BMPR-II levels and restores BMP9 signalling in endothelial cells harbouring BMPR-II mutations', *Hum Mol Genet,* 22(18), pp. 3667-79.

Dupuy, C., Ohayon, R., Valent, A., Noel-Hudson, M. S., Deme, D. and Virion, A. (1999) 'Purification of a novel flavoprotein involved in the thyroid NADPH oxidase. Cloning of the porcine and human cdnas', *J Biol Chem,* 274(52), pp. 37265-9.

Ebert, A. D., Yu, J., Rose, F. F., Jr., Mattis, V. B., Lorson, C. L., Thomson, J. A. and Svendsen, C. N. (2009) 'Induced pluripotent stem cells from a spinal muscular atrophy patient', *Nature,* 457(7227), pp. 277-80.

Ebisawa, T., Tada, K., Kitajima, I., Tojo, K., Sampath, T. K., Kawabata, M., Miyazono, K. and Imamura, T. (1999) 'Characterization of bone morphogenetic protein-6 signaling 'Cross talk between endothelial and smooth muscle cells in pulmonary hypertension: critical role for serotonin-induced smooth muscle hyperplasia', *Circulation,* 113(15), pp. 1857-64.

Eddahibi, S., Guignabert, C., Barlier-Mur, A. M., Dewachter, L., Fadel, E., Dartevelle, P., Humbert, M., Simonneau, G., Hanoun, N., Saurini, F., Hamon, M. and Adnot, S. (2006) 'Cross talk between endothelial and smooth muscle cells in pulmonary hypertension: critical role for serotonin-induced smooth muscle hyperplasia', *Circulation,* 113(15), pp. 1857-64.

Elson, G. C., Lelievre, E., Guillet, C., Chevalier, S., Plun-Favreau, H., Froger, J., Suard, I., de Coignac, A. B., Delneste, Y., Bonnefoy, J. Y., Gauchat, J. F. and Gascan, H. (2000) 'CLF associates with CLC to form a functional heteromeric ligand for the CNTF receptor complex', *Nat Neurosci,* 3(9), pp. 867-72.

Eltzschig, H. K. and Carmeliet, P. (2011) 'Hypoxia and inflammation', *N Engl J Med,* 364(7), pp. 656-65.

Evans, J. D., Girerd, B., Montani, D., Wang, X. J., Galie, N., Austin, E. D., Elliott, G., Asano, K., Grunig, E., Yan, Y., Jing, Z. C., Manes, A., Palazzini, M., Wheeler, L. A., Nakayama, I., Satoh, T., Eichstaedt, C., Hinderhofer, K., Wolf, M., Rosenzweig, E. B., Chung, W. K., Soubrier, F., Simonneau, G., Sitbon, O., Graf, S., Kaptoge, S., Di Angelantonio, E., Humbert, M. and Morrell, N. W. (2016) 'BMPR2 mutations and survival in pulmonary arterial hypertension: an individual participant data meta-analysis', *Lancet Respir Med,* 4(2), pp. 129-37.

Farber, H. W. and Loscalzo, J. (2004) 'Pulmonary arterial hypertension', *N Engl J Med,* 351(16), pp. 1655-65.

Farber, H. W. and Loscalzo, J. (2005) 'Mechanism of disease: Pulmonary hypertension', *Discov Med,* 5(25), pp. 80-7.

Fessel, J. P., Flynn, C. R., Robinson, L. J., Penner, N. L., Gladson, S., Kang, C. J., Wasserman, D. H., Hemnes, A. R. and West, J. D. (2013) 'Hyperoxia synergizes with mutant bone morphogenic protein receptor 2 to cause metabolic stress, oxidant injury, and pulmonary hypertension', *Am J Respir Cell Mol Biol,* 49(5), pp. 778-87.

Finsnes, F., Lyberg, T., Christensen, G. and Skjonsberg, O. H. (2001) 'Effect of endothelin antagonism on the production of cytokines in eosinophilic airway inflammation', *Am J Physiol Lung Cell Mol Physiol,* 280(4), pp. L659-65.

Fioravanti, A., Govoni, M., La Montagna, G., Perpignano, G., Tirri, G., Trotta, F., Bogliolo, A., Ciocci, A., Mauceri, M. T. and Marcolongo, R. (1995) 'Somatostatin 14 and joint inflammation: evidence for intraarticular efficacy of prolonged administration in rheumatoid arthritis', *Drugs Exp Clin Res,* 21(3), pp. 97-103.

Flicek, P., Ahmed, I., Amode, M. R., Barrell, D., Beal, K., Brent, S., Carvalho-Silva, D., Clapham, P., Coates, G., Fairley, S., Fitzgerald, S., Gil, L., Garcia-Giron, C., Gordon, L., Hourlier, T., Hunt, S., Juettemann, T., Kahari, A. K., Keenan, S., Komorowska, M., Kulesha, E., Longden, I., Maurel, T., McLaren, W. M., Muffato, M., Nag, R., Overduin, B., Pignatelli, M., Pritchard, B., Pritchard, E., Riat, H. S., Ritchie, G. R., Ruffier, M., Schuster, M., Sheppard, D., Sobral, D., Taylor, K., Thormann, A., Trevanion, S., White, S., Wilder, S. P., Aken, B. L., Birney, E., Cunningham, F., Dunham, I., Harrow, J., Herrero, J., Hubbard, T. J., Johnson, N., Kinsella, R., Parker, A., Spudich, G., Yates, A., Zadissa, A. and Searle, S. M. (2013) 'Ensembl 2013', *Nucleic Acids Res,* 41(Database issue), pp. D48-55.

Frank, D. B., Abtahi, A., Yamaguchi, D. J., Manning, S., Shyr, Y., Pozzi, A., Baldwin, H. S., Johnson, J. E. and de Caestecker, M. P. (2005) 'Bone morphogenetic protein 4 promotes pulmonary vascular remodeling in hypoxic pulmonary hypertension', *Circ Res,* 97(5), pp. 496-504.

Frank, D. B., Lowery, J., Anderson, L., Brink, M., Reese, J. and de Caestecker, M. (2008) 'Increased susceptibility to hypoxic pulmonary hypertension in Bmpr2 mutant mice is associated with endothelial dysfunction in the pulmonary vasculature', *Am J Physiol Lung Cell Mol Physiol,* 294(1), pp. L98-109.

Freund-Michel, V., Khoyrattee, N., Savineau, J. P., Muller, B. and Guibert, C. (2014) 'Mitochondria: roles in pulmonary hypertension', *Int J Biochem Cell Biol,* 55, pp. 93-7.

Frid, M. G., Aldashev, A. A., Dempsey, E. C. and Stenmark, K. R. (1997) 'Smooth muscle cells isolated from discrete compartments of the mature vascular media exhibit unique phenotypes and distinct growth capabilities', *Circ Res,* 81(6), pp. 940-52.

Frohlich, S., Boylan, J. and McLoughlin, P. (2013) 'Hypoxia-induced inflammation in the lung: a potential therapeutic target in acute lung injury?', *Am J Respir Cell Mol Biol,* 48(3), pp. 271-9.

Frost, A. E., Badesch, D. B., Barst, R. J., Benza, R. L., Elliott, C. G., Farber, H. W., Krichman, A., Liou, T. G., Raskob, G. E., Wason, P., Feldkircher, K., Turner, M. and McGoon, M. D. (2011) 'The changing picture of patients with pulmonary arterial hypertension in the United States: how REVEAL differs from historic and non-US Contemporary Registries', *Chest,* 139(1), pp. 128-37.

Fujita, M., Shannon, J. M., Irvin, C. G., Fagan, K. A., Cool, C., Augustin, A. and Mason, R. J. (2001) 'Overexpression of tumor necrosis factor-alpha produces an increase in lung volumes and pulmonary hypertension', *Am J Physiol Lung Cell Mol Physiol,* 280(1), pp. L39-49.

Gale, N. W., Baluk, P., Pan, L., Kwan, M., Holash, J., DeChiara, T. M., McDonald, D. M. and Yancopoulos, G. D. (2001) 'Ephrin-B2 selectively marks arterial vessels and neovascularization sites in the adult, with expression in both endothelial and smooth-muscle cells', *Dev Biol,* 230(2), pp. 151-60.

Galie, N., Ghofrani, H. A., Torbicki, A., Barst, R. J., Rubin, L. J., Badesch, D., Fleming, T., Parpia, T., Burgess, G., Branzi, A., Grimminger, F., Kurzyna, M., Simonneau, G. and Sildenafil Use in Pulmonary Arterial Hypertension Study, G. (2005) 'Sildenafil citrate therapy for pulmonary arterial hypertension', *N Engl J Med,* 353(20), pp. 2148-57.

Geti, I., Ormiston, M. L., Rouhani, F., Toshner, M., Movassagh, M., Nichols, J., Mansfield, W., Southwood, M., Bradley, A., Rana, A. A., Vallier, L. and Morrell, N. W. (2012) 'A practical and efficient cellular substrate for the generation of induced pluripotent stem cells from adults: blood-derived endothelial progenitor cells', *Stem Cells Transl Med,* 1(12), pp. 855-65.

Ghofrani, H. A., Galie, N., Grimminger, F., Grunig, E., Humbert, M., Jing, Z. C., Keogh, A. M., Langleben, D., Kilama, M. O., Fritsch, A., Neuser, D., Rubin, L. J. and Group, P.-S. (2013) 'Riociguat for the treatment of pulmonary arterial hypertension', *N Engl J Med,* 369(4), pp. 330-40.

Gjedde, S., Gormsen, L. C., Riis, A. L., Jorgensen, J. O., Rungby, J., Moller, N., Weeke, J. and Pedersen, S. B. (2010) 'Reduced expression of uncoupling protein 2 in adipose tissue in patients with hypothyroidism', *J Clin Endocrinol Metab,* 95(7), pp. 3537-41.

Goncharov, D. A., Kudryashova, T. V., Ziai, H., Ihida-Stansbury, K., DeLisser, H., Krymskaya, V. P., Tuder, R. M., Kawut, S. M. and Goncharova, E. A. (2014) 'Mammalian target of rapamycin complex 2 (mTORC2) coordinates pulmonary artery smooth muscle cell metabolism, proliferation, and survival in pulmonary arterial hypertension', *Circulation,* 129(8), pp. 864-74.

Gong, D. W., He, Y., Karas, M. and Reitman, M. (1997) 'Uncoupling protein-3 is a mediator of thermogenesis regulated by thyroid hormone, beta3-adrenergic agonists, and leptin', *J Biol Chem,* 272(39), pp. 24129-32.

Goumans, M. J., Valdimarsdottir, G., Itoh, S., Lebrin, F., Larsson, J., Mummery, C., Karlsson, S. and ten Dijke, P. (2003) 'Activin receptor-like kinase (ALK)1 is an antagonistic mediator of lateral TGFbeta/ALK5 signaling', *Mol Cell,* 12(4), pp. 817-28.

Graf, S., Haimel, M., Bleda, M., Hadinnapola, C., Southgate, L., Li, W., Hodgson, J., Liu, B., Salmon, R. M., Southwood, M., Machado, R. D., Martin, J. M., Treacy, C. M., Yates, K., Daugherty, L. C., Shamardina, O., Whitehorn, D., Holden, S., Aldred, M., Bogaard, H. J., Church, C., Coghlan, G., Condliffe, R., Corris, P. A., Danesino, C., Eyries, M., Gall, H., Ghio, S., Ghofrani, H. A., Gibbs, J. S. R., Girerd, B., Houweling, A. C., Howard, L., Humbert, M., Kiely, D. G., Kovacs, G., MacKenzie Ross, R. V., Moledina, S., Montani, D., Newnham, M., Olschewski, A., Olschewski, H., Peacock, A. J., Pepke-Zaba, J., Prokopenko, I., Rhodes, C. J., Scelsi, L., Seeger, W., Soubrier, F., Stein, D. F., Suntharalingam, J., Swietlik, E. M., Toshner, M. R., van Heel, D. A., Vonk Noordegraaf, A., Waisfisz, Q., Wharton, J., Wort, S. J., Ouwehand, W. H., Soranzo, N., Lawrie, A., Upton, P. D., Wilkins, M. R., Trembath, R. C. and Morrell, N. W. (2018) 'Identification of rare sequence variation underlying heritable pulmonary arterial hypertension', *Nat Commun,* 9(1), pp. 1416.

Graham, B. B., Bandeira, A. P., Morrell, N. W., Butrous, G. and Tuder, R. M. (2010) 'Schistosomiasis-associated pulmonary hypertension: pulmonary vascular disease: the global perspective', *Chest,* 137(6 Suppl), pp. 20S-29S.

Granata, A., Serrano, F., Bernard, W. G., McNamara, M., Low, L., Sastry, P. and Sinha, S. (2017) 'An iPSC-derived vascular model of Marfan syndrome identifies key mediators of smooth muscle cell death', *Nat Genet,* 49(1), pp. 97-109.

Grskovic, M., Javaherian, A., Strulovici, B. and Daley, G. Q. (2011) 'Induced pluripotent stem cells--opportunities for disease modelling and drug discovery', *Nat Rev Drug Discov,* 10(12), pp. 915-29.

Grunig, E., Mereles, D., Hildebrandt, W., Swenson, E. R., Kubler, W., Kuecherer, H. and Bartsch, P. (2000) 'Stress Doppler echocardiography for identification of susceptibility to high altitude pulmonary edema', *J Am Coll Cardiol,* 35(4), pp. 980-7.

Gu, M., Shao, N. Y., Sa, S., Li, D., Termglinchan, V., Ameen, M., Karakikes, I., Sosa, G., Grubert, F., Lee, J., Cao, A., Taylor, S., Ma, Y., Zhao, Z., Chappell, J., Hamid, R., Austin, E. D., Gold, J. D., Wu, J. C., Snyder, M. P. and Rabinovitch, M. (2017) 'Patient-Specific iPSC-Derived Endothelial Cells Uncover Pathways that Protect against Pulmonary Hypertension in BMPR2 Mutation Carriers', *Cell Stem Cell,* 20(4), pp. 490-504 e5.

Guignabert, C., Izikki, M., Tu, L. I., Li, Z., Zadigue, P., Barlier-Mur, A. M., Hanoun, N., Rodman, D., Hamon, M., Adnot, S. and Eddahibi, S. (2006) 'Transgenic mice overexpressing the 5-hydroxytryptamine transporter gene in smooth muscle develop pulmonary hypertension', *Circ Res,* 98(10), pp. 1323-30.

Guillermet-Guibert, J., Saint-Laurent, N., Davenne, L., Rochaix, P., Cuvillier, O., Culler, M. D., Pradayrol, L., Buscail, L., Susini, C. and Bousquet, C. (2007) 'Novel synergistic mechanism for sst2 somatostatin and TNFalpha receptors to induce apoptosis: crosstalk between NF-kappaB and JNK pathways', *Cell Death Differ,* 14(2), pp. 197-208.

Guo, X. and Wang, X. F. (2009) 'Signaling cross-talk between TGF-beta/BMP and other pathways', *Cell Res,* 19(1), pp. 71-88.

Gupte, S. A. and Wolin, M. S. (2008) 'Oxidant and redox signaling in vascular oxygen sensing: implications for systemic and pulmonary hypertension', *Antioxid Redox Signal,* 10(6), pp. 1137-52.

Guruli, G., Pflug, B. R., Pecher, S., Makarenkova, V., Shurin, M. R. and Nelson, J. B. (2004) 'Function and survival of dendritic cells depend on endothelin-1 and endothelin receptor autocrine loops', *Blood,* 104(7), pp. 2107-15.

Haimovici, H. and Maier, N. (1964) 'Fate of Aortic Homografts in Canine Atherosclerosis. 3. Study of Fresh Abdominal and Thoracic Aortic Implants into Thoracic Aorta: Role of Tissue Susceptibility in Atherogenesis', *Arch Surg,* 89, pp. 961-9.

Halbrooks, P. J., Ding, R., Wozney, J. M. and Bain, G. (2007) 'Role of RGM coreceptors in bone morphogenetic protein signaling', *J Mol Signal,* 2, pp. 4.

Hall, S. M., Hislop, A. A., Pierce, C. M. and Haworth, S. G. (2000) 'Prenatal origins of human intrapulmonary arteries: formation and smooth muscle maturation', *Am J Respir Cell Mol Biol,* 23(2), pp. 194-203.

Halligan, D. N., Murphy, S. J. and Taylor, C. T. (2016) 'The hypoxia-inducible factor (HIF) couples immunity with metabolism', *Semin Immunol,* 28(5), pp. 469-477.

Hao, H., Gabbiani, G. and Bochaton-Piallat, M. L. (2003) 'Arterial smooth muscle cell heterogeneity: implications for atherosclerosis and restenosis development', *Arterioscler Thromb Vasc Biol,* 23(9), pp. 1510-20.

Harrison, R. E., Flanagan, J. A., Sankelo, M., Abdalla, S. A., Rowell, J., Machado, R. D., Elliott, C. G., Robbins, I. M., Olschewski, H., McLaughlin, V., Gruenig, E., Kermeen, F., Halme, M., Raisanen-Sokolowski, A., Laitinen, T., Morrell, N. W. and Trembath, R. C. (2003) 'Molecular and functional analysis identifies ALK-1 as the predominant cause of pulmonary hypertension related to hereditary haemorrhagic telangiectasia', *J Med Genet,* 40(12), pp. 865-71.

Hatton, N. and Ryan, J. J. (2014) 'Sex differences in response to pulmonary arterial hypertension therapy: is what's good for the goose, good for the gander?', *Chest,* 145(6), pp. 1184-1186.

Hayes, P., Dhillon, S., O'Neill, K., Thoeni, C., Hui, K. Y., Elkadri, A., Guo, C. H., Kovacic, L., Aviello, G., Alvarez, L. A., Griffiths, A. M., Snapper, S. B., Brant, S. R., Doroshow, J. H., Silverberg, M. S., Peter, I., McGovern, D. P., Cho, J., Brumell, J. H., Uhlig, H. H., Bourke, B., Muise, A. A. and Knaus, U. G. (2015) 'Defects in NADPH Oxidase Genes NOX1 and DUOX2 in Very Early Onset Inflammatory Bowel Disease', *Cell Mol Gastroenterol Hepatol,* 1(5), pp. 489-502.

Heldin, C. H. and Moustakas, A. (2012) 'Role of Smads in TGFbeta signaling', *Cell Tissue Res,* 347(1), pp. 21-36.

Hill, N. S., Gillespie, M. N. and McMurtry, I. F. (2017) 'Fifty Years of Monocrotaline-Induced Pulmonary Hypertension: What Has It Meant to the Field?', *Chest,* 152(6), pp. 1106-1108.

Hislop, A. and Reid, L. (1976) 'New findings in pulmonary arteries of rats with hypoxia-induced pulmonary hypertension', *Br J Exp Pathol,* 57(5), pp. 542-54.

Hockemeyer, D. and Jaenisch, R. (2016) 'Induced Pluripotent Stem Cells Meet Genome Editing', *Cell Stem Cell,* 18(5), pp. 573-86.

Hockemeyer, D., Soldner, F., Beard, C., Gao, Q., Mitalipova, M., DeKelver, R. C., Katibah, G. E., Amora, R., Boydston, E. A., Zeitler, B., Meng, X., Miller, J. C., Zhang, L., Rebar, E. J., Gregory, P. D., Urnov, F. D. and Jaenisch, R. (2009) 'Efficient targeting of expressed and silent genes in human ESCs and iPSCs using zinc-finger nucleases', *Nat Biotechnol,* 27(9), pp. 851-7.

Hockemeyer, D., Soldner, F., Cook, E. G., Gao, Q., Mitalipova, M. and Jaenisch, R. (2008) 'A drug-inducible system for direct reprogramming of human somatic cells to pluripotency', *Cell Stem Cell,* 3(3), pp. 346-353.

Hockemeyer, D., Wang, H., Kiani, S., Lai, C. S., Gao, Q., Cassady, J. P., Cost, G. J., Zhang, L., Santiago, Y., Miller, J. C., Zeitler, B., Cherone, J. M., Meng, X., Hinkley, S. J., Rebar, E. J., Gregory, P. D., Urnov, F. D. and Jaenisch, R. (2011) 'Genetic engineering of human pluripotent cells using TALE nucleases', *Nat Biotechnol,* 29(8), pp. 731-4.

Hoeper, M. M., Bogaard, H. J., Condliffe, R., Frantz, R., Khanna, D., Kurzyna, M., Langleben, D., Manes, A., Satoh, T., Torres, F., Wilkins, M. R. and Badesch, D. B. (2013) 'Definitions and diagnosis of pulmonary hypertension', *J Am Coll Cardiol,* 62(25 Suppl), pp. D42-50.

Hoeper, M. M., Huscher, D., Ghofrani, H. A., Delcroix, M., Distler, O., Schweiger, C., Grunig, E., Staehler, G., Rosenkranz, S., Halank, M., Held, M., Grohe, C., Lange, T. J., Behr, J., Klose, H., Wilkens, H., Filusch, A., Germann, M., Ewert, R., Seyfarth, H. J., Olsson, K. M., Opitz, C. F., Gaine, S. P., Vizza, C. D., Vonk-Noordegraaf, A., Kaemmerer, H., Gibbs, J. S. and Pittrow, D. (2013) 'Elderly patients diagnosed with idiopathic pulmonary arterial hypertension: results from the COMPERA registry', *Int J Cardiol,* 168(2), pp. 871-80.

Hoeper, M. M. and Simon, R. G. J. (2014) 'The changing landscape of pulmonary arterial hypertension and implications for patient care', *Eur Respir Rev,* 23(134), pp. 450-7.

Hogan, B. L. (1996) 'Bone morphogenetic proteins: multifunctional regulators of vertebrate development', *Genes Dev,* 10(13), pp. 1580-94.

Hoshikawa, Y., Ono, S., Suzuki, S., Tanita, T., Chida, M., Song, C., Noda, M., Tabata, T., Voelkel, N. F. and Fujimura, S. (2001) 'Generation of oxidative stress contributes to the development of pulmonary hypertension induced by hypoxia', *J Appl Physiol (1985),* 90(4), pp. 1299-306.

Hotta, A. and Yamanaka, S. (2015) 'From Genomics to Gene Therapy: Induced Pluripotent Stem Cells Meet Genome Editing', *Annu Rev Genet,* 49, pp. 47-70.

Humbert, M. and Ghofrani, H. A. (2016) 'The molecular targets of approved treatments for pulmonary arterial hypertension', *Thorax,* 71(1), pp. 73-83.

Humbert, M., Lau, E. M., Montani, D., Jais, X., Sitbon, O. and Simonneau, G. (2014) 'Advances in therapeutic interventions for patients with pulmonary arterial hypertension', *Circulation,* 130(24), pp. 2189-208.

Humbert, M., Monti, G., Brenot, F., Sitbon, O., Portier, A., Grangeot-Keros, L., Duroux, P., Galanaud, P., Simonneau, G. and Emilie, D. (1995) 'Increased interleukin-1 and interleukin-6 serum concentrations in severe primary pulmonary hypertension', *Am J Respir Crit Care Med,* 151(5), pp. 1628-31.

Humbert, M., Morrell, N. W., Archer, S. L., Stenmark, K. R., MacLean, M. R., Lang, I. M., Christman, B. W., Weir, E. K., Eickelberg, O., Voelkel, N. F. and Rabinovitch, M. (2004) 'Cellular and molecular pathobiology of pulmonary arterial hypertension', *J Am Coll Cardiol,* 43(12 Suppl S), pp. 13S-24S.

Humbert, M., Sitbon, O., Chaouat, A., Bertocchi, M., Habib, G., Gressin, V., Yaici, A., Weitzenblum, E., Cordier, J. F., Chabot, F., Dromer, C., Pison, C., Reynaud-Gaubert, M., Haloun, A., Laurent, M., Hachulla, E. and Simonneau, G. (2006) 'Pulmonary arterial hypertension in France: results from a national registry', *Am J Respir Crit Care Med,* 173(9), pp. 1023-30.

Humbert, M., Sitbon, O., Yaici, A., Montani, D., O'Callaghan, D. S., Jais, X., Parent, F., Savale, L., Natali, D., Gunther, S., Chaouat, A., Chabot, F., Cordier, J. F., Habib, G., Gressin, V., Jing, Z. C., Souza, R., Simonneau, G. and French Pulmonary Arterial Hypertension, N. (2010) 'Survival in incident and prevalent cohorts of patients with pulmonary arterial hypertension', *Eur Respir J,* 36(3), pp. 549-55.

Hurst, L. A., Dunmore, B. J., Long, L., Crosby, A., Al-Lamki, R., Deighton, J., Southwood, M., Yang, X., Nikolic, M. Z., Herrera, B., Inman, G. J., Bradley, J. R., Rana, A. A., Upton, P. D. and Morrell, N. W. (2017) 'TNFalpha drives pulmonary arterial hypertension by suppressing the BMP type-II receptor and altering NOTCH signalling', *Nat Commun,* 8, pp. 14079.

Hussein, S. M., Batada, N. N., Vuoristo, S., Ching, R. W., Autio, R., Narva, E., Ng, S., Sourour, M., Hamalainen, R., Olsson, C., Lundin, K., Mikkola, M., Trokovic, R., Peitz, M., Brustle, O., Bazett-Jones, D. P., Alitalo, K., Lahesmaa, R., Nagy, A. and Otonkoski, T. (2011) 'Copy number variation and selection during reprogramming to pluripotency', *Nature,* 471(7336), pp. 58-62.

Imamura, T., Takase, M., Nishihara, A., Oeda, E., Hanai, J., Kawabata, M. and Miyazono, K. (1997) 'Smad6 inhibits signalling by the TGF-beta superfamily', *Nature,* 389(6651), pp. 622-6.

Inoue, H., Nagata, N., Kurokawa, H. and Yamanaka, S. (2014) 'iPS cells: a game changer for future medicine', *EMBO J,* 33(5), pp. 409-17.

Jacobs, W., van de Veerdonk, M. C., Trip, P., de Man, F., Heymans, M. W., Marcus, J. T., Kawut, S. M., Bogaard, H. J., Boonstra, A. and Vonk Noordegraaf, A. (2014) 'The right ventricle explains sex differences in survival in idiopathic pulmonary arterial hypertension', *Chest,* 145(6), pp. 1230-1236.

Jais, X., Launay, D., Yaici, A., Le Pavec, J., Tcherakian, C., Sitbon, O., Simonneau, G. and Humbert, M. (2008) 'Immunosuppressive therapy in lupus- and mixed connective tissue disease-associated pulmonary arterial hypertension: a retrospective analysis of twenty-three cases', *Arthritis Rheum,* 58(2), pp. 521-31.

Jansa, P., Jarkovsky, J., Al-Hiti, H., Popelova, J., Ambroz, D., Zatocil, T., Votavova, R., Polacek, P., Maresova, J., Aschermann, M., Brabec, P., Dusek, L. and Linhart, A. (2014) 'Epidemiology and long-term survival of pulmonary arterial hypertension in the Czech Republic: a retrospective analysis of a nationwide registry', *BMC Pulm Med,* 14, pp. 45.

Jasmin, J. F., Lucas, M., Cernacek, P. and Dupuis, J. (2001) 'Effectiveness of a nonselective ET(A/B) and a selective ET(A) antagonist in rats with monocrotaline-induced pulmonary hypertension', *Circulation,* 103(2), pp. 314-8.

Jiang, X., Rowitch, D. H., Soriano, P., McMahon, A. P. and Sucov, H. M. (2000) 'Fate of the mammalian cardiac neural crest', *Development,* 127(8), pp. 1607-16.

Jinek, M., Chylinski, K., Fonfara, I., Hauer, M., Doudna, J. A. and Charpentier, E. (2012) 'A programmable dual-RNA-guided DNA endonuclease in adaptive bacterial immunity', *Science,* 337(6096), pp. 816-21.

Kaebisch, C., Schipper, D., Babczyk, P. and Tobiasch, E. (2015) 'The role of purinergic receptors in stem cell differentiation', *Comput Struct Biotechnol J,* 13, pp. 75-84.

Kameda, T., Koike, C., Saitoh, K., Kuroiwa, A. and Iba, H. (1999) 'Developmental patterning in chondrocytic cultures by morphogenic gradients: BMP induces expression of indian hedgehog and noggin', *Genes Cells,* 4(3), pp. 175-84.

Kane, N. M., Xiao, Q., Baker, A. H., Luo, Z., Xu, Q. and Emanueli, C. (2011) 'Pluripotent stem cell differentiation into vascular cells: a novel technology with promises for vascular re(generation)', *Pharmacol Ther,* 129(1), pp. 29-49.

Kang, H., Louie, J., Weisman, A., Sheu-Gruttadauria, J., Davis-Dusenbery, B. N., Lagna, G. and Hata, A. (2012) 'Inhibition of microRNA-302 (miR-302) by bone morphogenetic protein 4 (BMP4) facilitates the BMP signaling pathway', *J Biol Chem,* 287(46), pp. 38656-64.

Karalis, K., Mastorakos, G., Chrousos, G. P. and Tolis, G. (1994) 'Somatostatin analogues suppress the inflammatory reaction in vivo', *J Clin Invest,* 93(5), pp. 2000-6.

Kass, D. J., Yu, G., Loh, K. S., Savir, A., Borczuk, A., Kahloon, R., Juan-Guardela, B., Deiuliis, G., Tedrow, J., Choi, J., Richards, T., Kaminski, N. and Greenberg, S. M. (2012) 'Cytokine-like factor 1 gene expression is enriched in idiopathic pulmonary fibrosis and drives the accumulation of CD4+ T cells in murine lungs: evidence for an antifibrotic role in bleomycin injury', *Am J Pathol,* 180(5), pp. 1963-78.

Katagiri, T. and Watabe, T. (2016) 'Bone Morphogenetic Proteins', *Cold Spring Harb Perspect Biol,* 8(6).

Kay, J. M., Harris, P. and Heath, D. (1967) 'Pulmonary hypertension produced in rats by ingestion of Crotalaria spectabilis seeds', *Thorax,* 22(2), pp. 176-9.

Kerstjens-Frederikse, W. S., Bongers, E. M., Roofthooft, M. T., Leter, E. M., Douwes, J. M., Van Dijk, A., Vonk-Noordegraaf, A., Dijk-Bos, K. K., Hoefsloot, L. H., Hoendermis, E. S., Gille, J. J., Sikkema-Raddatz, B., Hofstra, R. M. and Berger, R. M. (2013) 'TBX4 mutations (small patella syndrome) are associated with childhood-onset pulmonary arterial hypertension', *J Med Genet,* 50(8), pp. 500-6.

Kessler, E., Takahara, K., Biniaminov, L., Brusel, M. and Greenspan, D. S. (1996) 'Bone morphogenetic protein-1: the type I procollagen C-proteinase', *Science,* 271(5247), pp. 360-2.

Kim, H. O., Kim, H. S., Youn, J. C., Shin, E. C. and Park, S. (2011) 'Serum cytokine profiles in healthy young and elderly population assessed using multiplexed bead-based immunoassays', *J Transl Med,* 9, pp. 113.

Kim, J., Kim, J., Lee, S. H., Kepreotis, S. V., Yoo, J., Chun, J. S., Hajjar, R. J., Jeong, D. and Park, W. J. (2016) 'Cytokine-Like 1 Regulates Cardiac Fibrosis via Modulation of TGF-beta Signaling', *PLoS One,* 11(11), pp. e0166480.

Kim, S., Hata, A. and Kang, H. (2014) 'Down-regulation of miR-96 by bone morphogenetic protein signaling is critical for vascular smooth muscle cell phenotype modulation', *J Cell Biochem,* 115(5), pp. 889-95.

Kiskin, F. N., Chang, C. H., Huang, C. J. Z., Kwieder, B., Cheung, C., Dunmore, B. J., Serrano, F., Sinha, S., Morrell, N. W. and Rana, A. A. (2018) 'Contributions of BMPR2 Mutations and Extrinsic Factors to Cellular Phenotypes of Pulmonary Arterial Hypertension Revealed by Induced Pluripotent Stem Cell Modeling', *Am J Respir Crit Care Med*., 198(2), pp. 271-5

Kiskinis, E. and Eggan, K. (2010) 'Progress toward the clinical application of patient-specific pluripotent stem cells', *J Clin Invest,* 120(1), pp. 51-9.

Kita-Matsuo, H., Barcova, M., Prigozhina, N., Salomonis, N., Wei, K., Jacot, J. G., Nelson, B., Spiering, S., Haverslag, R., Kim, C., Talantova, M., Bajpai, R., Calzolari, D., Terskikh, A., McCulloch, A. D., Price, J. H., Conklin, B. R., Chen, H. S. and Mercola, M. (2009) 'Lentiviral vectors and protocols for creation of stable hESC lines for fluorescent tracking and drug resistance selection of cardiomyocytes', *PLoS One,* 4(4), pp. e5046.

Kizys, M. M. L., Louzada, R. A., Mitne-Neto, M., Jara, J. R., Furuzawa, G. K., de Carvalho, D. P., Dias-da-Silva, M. R., Nesi-Franca, S., Dupuy, C. and Maciel, R. M. B. (2017) 'DUOX2 Mutations Are Associated With Congenital Hypothyroidism With Ectopic Thyroid Gland', *J Clin Endocrinol Metab,* 102(11), pp. 4060-4071.

Kleiner, G., Marcuzzi, A., Zanin, V., Monasta, L. and Zauli, G. (2013) 'Cytokine levels in the serum of healthy subjects', *Mediators Inflamm,* 2013, pp. 434010.

Konior, A., Schramm, A., Czesnikiewicz-Guzik, M. and Guzik, T. J. (2014) 'NADPH oxidases in vascular pathology', *Antioxid Redox Signal,* 20(17), pp. 2794-814.

Korshunov, S. S., Skulachev, V. P. and Starkov, A. A. (1997) 'High protonic potential actuates a mechanism of production of reactive oxygen species in mitochondria', *FEBS Lett,* 416(1), pp. 15-8.

Kumar, A., D'Souza, S. S., Moskvin, O. V., Toh, H., Wang, B., Zhang, J., Swanson, S., Guo, L. W., Thomson, J. A. and Slukvin, II (2017) 'Specification and Diversification of Pericytes and Smooth Muscle Cells from Mesenchymoangioblasts', *Cell Rep,* 19(9), pp. 1902-1916.

Lagna, G., Ku, M. M., Nguyen, P. H., Neuman, N. A., Davis, B. N. and Hata, A. (2007) 'Control of phenotypic plasticity of smooth muscle cells by bone morphogenetic protein signaling through the myocardin-related transcription factors', *J Biol Chem,* 282(51), pp. 37244-55.

Lai, Y. C., Potoka, K. C., Champion, H. C., Mora, A. L. and Gladwin, M. T. (2014) 'Pulmonary arterial hypertension: the clinical syndrome', *Circ Res,* 115(1), pp. 115-30.

Lalich, J. J. and Merkow, L. (1961) 'Pulmonary arteritis produced in rat by feeding Crotalaria spectabilis', *Lab Invest,* 10, pp. 744-50.

Lam, C. S., Roger, V. L., Rodeheffer, R. J., Borlaug, B. A., Enders, F. T. and Redfield, M. M. (2009) 'Pulmonary hypertension in heart failure with preserved ejection fraction: a community-based study', *J Am Coll Cardiol,* 53(13), pp. 1119-26.

Lambeth, J. D. (2004) 'NOX enzymes and the biology of reactive oxygen', *Nat Rev Immunol,* 4(3), pp. 181-9.

Lane, K. B., Machado, R. D., Pauciulo, M. W., Thomson, J. R., Phillips, J. A., 3rd, Loyd, J. E., Nichols, W. C. and Trembath, R. C. (2000) 'Heterozygous germline mutations in BMPR2, encoding a TGF-beta receptor, cause familial primary pulmonary hypertension', *Nat Genet,* 26(1), pp. 81-4.

Langmead, B., Trapnell, C., Pop, M. and Salzberg, S. L. (2009) 'Ultrafast and memory-efficient alignment of short DNA sequences to the human genome', *Genome Biol,* 10(3), pp. R25.

Lannan, K. L., Phipps, R. P. and White, R. J. (2014) 'Thrombosis, platelets, microparticles and PAH: more than a clot', *Drug Discov Today,* 19(8), pp. 1230-5.

Lanni, A., Beneduce, L., Lombardi, A., Moreno, M., Boss, O., Muzzin, P., Giacobino, J. P. and Goglia, F. (1999) 'Expression of uncoupling protein-3 and mitochondrial activity in the transition from hypothyroid to hyperthyroid state in rat skeletal muscle', *FEBS Lett,* 444(2-3), pp. 250-4.

Lanni, A., De Felice, M., Lombardi, A., Moreno, M., Fleury, C., Ricquier, D. and Goglia, F. (1997) 'Induction of UCP2 mRNA by thyroid hormones in rat heart', *FEBS Lett,* 418(1-2), pp. 171-4.

Larkin, E. K., Newman, J. H., Austin, E. D., Hemnes, A. R., Wheeler, L., Robbins, I. M., West, J. D., Phillips, J. A., 3rd, Hamid, R. and Loyd, J. E. (2012) 'Longitudinal analysis casts doubt on the presence of genetic anticipation in heritable pulmonary arterial hypertension', *Am J Respir Crit Care Med,* 186(9), pp. 892-6.

Lau, E. M. T., Giannoulatou, E., Celermajer, D. S. and Humbert, M. (2017) 'Epidemiology and treatment of pulmonary arterial hypertension', *Nat Rev Cardiol,* 14(10), pp. 603-614.

Lauder, H., Sellers, L. A., Fan, T. P., Feniuk, W. and Humphrey, P. P. (1997) 'Somatostatin sst5 inhibition of receptor mediated regeneration of rat aortic vascular smooth muscle cells', *Br J Pharmacol,* 122(4), pp. 663-70.

Laumanns, I. P., Fink, L., Wilhelm, J., Wolff, J. C., Mitnacht-Kraus, R., Graef-Hoechst, S., Stein, M. M., Bohle, R. M., Klepetko, W., Hoda, M. A., Schermuly, R. T., Grimminger, F., Seeger, W. and Voswinckel, R. (2009) 'The noncanonical WNT pathway is operative in idiopathic pulmonary arterial hypertension', *Am J Respir Cell Mol Biol,* 40(6), pp. 683-91.

Lee, G., Papapetrou, E. P., Kim, H., Chambers, S. M., Tomishima, M. J., Fasano, C. A., Ganat, Y. M., Menon, J., Shimizu, F., Viale, A., Tabar, V., Sadelain, M. and Studer, L. (2009) 'Modelling pathogenesis and treatment of familial dysautonomia using patient-specific iPSCs', *Nature,* 461(7262), pp. 402-6.

Lensch, M. W., Schlaeger, T. M., Zon, L. I. and Daley, G. Q. (2007) 'Teratoma formation assays with human embryonic stem cells: a rationale for one type of human-animal chimera', *Cell Stem Cell,* 1(3), pp. 253-8.

Lepetit, H., Eddahibi, S., Fadel, E., Frisdal, E., Munaut, C., Noel, A., Humbert, M., Adnot, S., D'Ortho, M. P. and Lafuma, C. (2005) 'Smooth muscle cell matrix metalloproteinases in idiopathic pulmonary arterial hypertension', *Eur Respir J,* 25(5), pp. 834-42.

Leszczynski, D., Zhao, Y., Cathapermal, S., Nilsson, J. and Foegh, M. L. (1993) 'Rat heart smooth muscle cells express high and low affinity receptors for somatostatin-14, which are involved in regulation of cell proliferation', *Life Sci,* 53(22), pp. 1663-74.

Li, L., Blumenthal, D. K., Terry, C. M., He, Y., Carlson, M. L. and Cheung, A. K. (2011) 'PDGF-induced proliferation in human arterial and venous smooth muscle cells: molecular basis for differential effects of PDGF isoforms', *J Cell Biochem,* 112(1), pp. 289-98.

Li, M., Riddle, S. R., Frid, M. G., El Kasmi, K. C., McKinsey, T. A., Sokol, R. J., Strassheim, D., Meyrick, B., Yeager, M. E., Flockton, A. R., McKeon, B. A., Lemon, D. D., Horn, T. R., Anwar, A., Barajas, C. and Stenmark, K. R. (2011) 'Emergence of fibroblasts with a proinflammatory epigenetically altered phenotype in severe hypoxic pulmonary hypertension', *J Immunol,* 187(5), pp. 2711-22.

Li, S., Xue, H., Wu, J., Rao, M. S., Kim, D. H., Deng, W. and Liu, Y. (2015) 'Human Induced Pluripotent Stem Cell NEUROG2 Dual Knockin Reporter Lines Generated by the CRISPR/Cas9 System', *Stem Cells Dev,* 24(24), pp. 2925-42.

Li, X., Zhang, X., Leathers, R., Makino, A., Huang, C., Parsa, P., Macias, J., Yuan, J. X., Jamieson, S. W. and Thistlethwaite, P. A. (2009) 'Notch3 signaling promotes the development of pulmonary arterial hypertension', *Nat Med,* 15(11), pp. 1289-97.

Lin, Y., Weisdorf, D. J., Solovey, A. and Hebbel, R. P. (2000) 'Origins of circulating endothelial cells and endothelial outgrowth from blood', *J Clin Invest,* 105(1), pp. 71-7.

Ling, Y., Johnson, M. K., Kiely, D. G., Condliffe, R., Elliot, C. A., Gibbs, J. S., Howard, L. S., Pepke-Zaba, J., Sheares, K. K., Corris, P. A., Fisher, A. J., Lordan, J. L., Gaine, S., Coghlan, J. G., Wort, S. J., Gatzoulis, M. A. and Peacock, A. J. (2012) 'Changing demographics, epidemiology, and survival of incident pulmonary arterial hypertension: results from the pulmonary hypertension registry of the United Kingdom and Ireland', *Am J Respir Crit Care Med,* 186(8), pp. 790-6.

Liu, B., Luo, X. J., Yang, Z. B., Zhang, J. J., Li, T. B., Zhang, X. J., Ma, Q. L., Zhang, G. G., Hu, C. P. and Peng, J. (2014) 'Inhibition of NOX/VPO1 pathway and inflammatory reaction by trimethoxystilbene in prevention of cardiovascular remodeling in hypoxia-induced pulmonary hypertensive rats', *J Cardiovasc Pharmacol,* 63(6), pp. 567-76.

Liu, J. Q., Zelko, I. N., Erbynn, E. M., Sham, J. S. and Folz, R. J. (2006) 'Hypoxic pulmonary hypertension: role of superoxide and NADPH oxidase (gp91phox)', *Am J Physiol Lung Cell Mol Physiol,* 290(1), pp. L2-10.

Livak, K. J. and Schmittgen, T. D. (2001) 'Analysis of relative gene expression data using real-time quantitative PCR and the 2(-Delta Delta C(T)) Method', *Methods,* 25(4), pp. 402-8.

Loh, Y. H., Agarwal, S., Park, I. H., Urbach, A., Huo, H., Heffner, G. C., Kim, K., Miller, J. D., Ng, K. and Daley, G. Q. (2009) 'Generation of induced pluripotent stem cells from human blood', *Blood,* 113(22), pp. 5476-9.

Loh, Y. H., Hartung, O., Li, H., Guo, C., Sahalie, J. M., Manos, P. D., Urbach, A., Heffner, G. C., Grskovic, M., Vigneault, F., Lensch, M. W., Park, I. H., Agarwal, S., Church, G. M., Collins, J. J., Irion, S. and Daley, G. Q. (2010) 'Reprogramming of T cells from human peripheral blood', *Cell Stem Cell,* 7(1), pp. 15-9.

Long, L., MacLean, M. R., Jeffery, T. K., Morecroft, I., Yang, X., Rudarakanchana, N., Southwood, M., James, V., Trembath, R. C. and Morrell, N. W. (2006) 'Serotonin increases susceptibility to pulmonary hypertension in BMPR2-deficient mice', *Circ Res,* 98(6), pp. 818-27.

Long, L., Ormiston, M. L., Yang, X., Southwood, M., Graf, S., Machado, R. D., Mueller, M., Kinzel, B., Yung, L. M., Wilkinson, J. M., Moore, S. D., Drake, K. M., Aldred, M. A., Yu, P. B., Upton, P. D. and Morrell, N. W. (2015) 'Selective enhancement of endothelial BMPR-II with BMP9 reverses pulmonary arterial hypertension', *Nat Med,* 21(7), pp. 777-85.

Looyenga, B. D., Resau, J. and MacKeigan, J. P. (2013) 'Cytokine receptor-like factor 1 (CRLF1) protects against 6-hydroxydopamine toxicity independent of the gp130/JAK signaling pathway', *PLoS One,* 8(6), pp. e66548.

Love, M. I., Huber, W. and Anders, S. (2014) 'Moderated estimation of fold change and dispersion for RNA-seq data with DESeq2', *Genome Biol,* 15(12), pp. 550.

Lowry, W. E., Richter, L., Yachechko, R., Pyle, A. D., Tchieu, J., Sridharan, R., Clark, A. T. and Plath, K. (2008) 'Generation of human induced pluripotent stem cells from dermal fibroblasts', *Proc Natl Acad Sci U S A,* 105(8), pp. 2883-8.

Ma, J., Guo, L., Fiene, S. J., Anson, B. D., Thomson, J. A., Kamp, T. J., Kolaja, K. L., Swanson, B. J. and January, C. T. (2011) 'High purity human-induced pluripotent stem cell-derived cardiomyocytes: electrophysiological properties of action potentials and ionic currents', *Am J Physiol Heart Circ Physiol,* 301(5), pp. H2006-17.

Ma, L., Roman-Campos, D., Austin, E. D., Eyries, M., Sampson, K. S., Soubrier, F., Germain, M., Tregouet, D. A., Borczuk, A., Rosenzweig, E. B., Girerd, B., Montani, D., Humbert, M., Loyd, J. E., Kass, R. S. and Chung, W. K. (2013) 'A novel channelopathy in pulmonary arterial hypertension', *N Engl J Med,* 369(4), pp. 351-361.

Machado, R. D., Aldred, M. A., James, V., Harrison, R. E., Patel, B., Schwalbe, E. C., Gruenig, E., Janssen, B., Koehler, R., Seeger, W., Eickelberg, O., Olschewski, H., Elliott, C. G., Glissmeyer, E., Carlquist, J., Kim, M., Torbicki, A., Fijalkowska, A., Szewczyk, G., Parma, J., Abramowicz, M. J., Galie, N., Morisaki, H., Kyotani, S., Nakanishi, N., Morisaki, T., Humbert, M., Simonneau, G., Sitbon, O., Soubrier, F., Coulet, F., Morrell, N. W. and Trembath, R. C. (2006) 'Mutations of the TGF-beta type II receptor BMPR2 in pulmonary arterial hypertension', *Hum Mutat,* 27(2), pp. 121-32.

Machado, R. D., Eickelberg, O., Elliott, C. G., Geraci, M. W., Hanaoka, M., Loyd, J. E., Newman, J. H., Phillips, J. A., 3rd, Soubrier, F., Trembath, R. C. and Chung, W. K. (2009) 'Genetics and genomics of pulmonary arterial hypertension', *J Am Coll Cardiol,* 54(1 Suppl), pp. S32-42.

Machado, R. D., Southgate, L., Eichstaedt, C. A., Aldred, M. A., Austin, E. D., Best, D. H., Chung, W. K., Benjamin, N., Elliott, C. G., Eyries, M., Fischer, C., Graf, S., Hinderhofer, K., Humbert, M., Keiles, S. B., Loyd, J. E., Morrell, N. W., Newman, J. H., Soubrier, F., Trembath, R. C., Viales, R. R. and Grunig, E. (2015) 'Pulmonary Arterial Hypertension: A Current Perspective on Established and Emerging Molecular Genetic Defects', *Hum Mutat,* 36(12), pp. 1113-27.

Macias-Silva, M., Hoodless, P. A., Tang, S. J., Buchwald, M. and Wrana, J. L. (1998) 'Specific activation of Smad1 signaling pathways by the BMP7 type I receptor, ALK2', *J Biol Chem,* 273(40), pp. 25628-36.

Maherali, N., Ahfeldt, T., Rigamonti, A., Utikal, J., Cowan, C. and Hochedlinger, K. (2008) 'A high-efficiency system for the generation and study of human induced pluripotent stem cells', *Cell Stem Cell,* 3(3), pp. 340-5.

Majesky, M. W. (2007) 'Developmental basis of vascular smooth muscle diversity', *Arterioscler Thromb Vasc Biol,* 27(6), pp. 1248-58.

Marques, G., Musacchio, M., Shimell, M. J., Wunnenberg-Stapleton, K., Cho, K. W. and O'Connor, M. B. (1997) 'Production of a DPP activity gradient in the early Drosophila embryo through the opposing actions of the SOG and TLD proteins', *Cell,* 91(3), pp. 417-26.

Martins-Taylor, K. and Xu, R. H. (2012) 'Concise review: Genomic stability of human induced pluripotent stem cells', *Stem Cells,* 30(1), pp. 22-7.

Massague, J., Seoane, J. and Wotton, D. (2005) 'Smad transcription factors', *Genes Dev,* 19(23), pp. 2783-810.

Mazerbourg, S. and Hsueh, A. J. (2006) 'Genomic analyses facilitate identification of receptors and signalling pathways for growth differentiation factor 9 and related orphan bone morphogenetic protein/growth differentiation factor ligands', *Hum Reprod Update,* 12(4), pp. 373-83.

McMurtry, M. S., Bonnet, S., Wu, X., Dyck, J. R., Haromy, A., Hashimoto, K. and Michelakis, E. D. (2004) 'Dichloroacetate prevents and reverses pulmonary hypertension by inducing pulmonary artery smooth muscle cell apoptosis', *Circ Res,* 95(8), pp. 830-40.

Medina, R. J., O'Neill, C. L., Humphreys, M. W., Gardiner, T. A. and Stitt, A. W. (2010) 'Outgrowth endothelial cells: characterization and their potential for reversing ischemic retinopathy', *Invest Ophthalmol Vis Sci,* 51(11), pp. 5906-13.

Menzies, K. J., Robinson, B. H. and Hood, D. A. (2009) 'Effect of thyroid hormone on mitochondrial properties and oxidative stress in cells from patients with mtDNA defects', *Am J Physiol Cell Physiol,* 296(2), pp. C355-62.

Mercier, O. and Fadel, E. (2013) 'Chronic thromboembolic pulmonary hypertension: animal models', *Eur Respir J,* 41(5), pp. 1200-6.

Meyrick, B. and Reid, L. (1980) 'Hypoxia-induced structural changes in the media and adventitia of the rat hilar pulmonary artery and their regression', *Am J Pathol,* 100(1), pp. 151-78.

Michelakis, E. D., Gurtu, V., Webster, L., Barnes, G., Watson, G., Howard, L., Cupitt, J., Paterson, I., Thompson, R. B., Chow, K., O'Regan, D. P., Zhao, L., Wharton, J., Kiely, D. G., Kinnaird, A., Boukouris, A. E., White, C., Nagendran, J., Freed, D. H., Wort, S. J., Gibbs, J. S. R. and Wilkins, M. R. (2017) 'Inhibition of pyruvate dehydrogenase kinase improves pulmonary arterial hypertension in genetically susceptible patients', *Sci Transl Med,* 9(413).

Michelakis, E. D., McMurtry, M. S., Wu, X. C., Dyck, J. R., Moudgil, R., Hopkins, T. A., Lopaschuk, G. D., Puttagunta, L., Waite, R. and Archer, S. L. (2002) 'Dichloroacetate, a metabolic modulator, prevents and reverses chronic hypoxic pulmonary hypertension in rats: role of increased expression and activity of voltage-gated potassium channels', *Circulation,* 105(2), pp. 244-50.

Mittal, M., Roth, M., Konig, P., Hofmann, S., Dony, E., Goyal, P., Selbitz, A. C., Schermuly, R. T., Ghofrani, H. A., Kwapiszewska, G., Kummer, W., Klepetko, W., Hoda, M. A., Fink, L., Hanze, J., Seeger, W., Grimminger, F., Schmidt, H. H. and Weissmann, N. (2007) 'Hypoxia-dependent regulation of nonphagocytic NADPH oxidase subunit NOX4 in the pulmonary vasculature', *Circ Res,* 101(3), pp. 258-67.

Miyauchi, T., Yorikane, R., Sakai, S., Sakurai, T., Okada, M., Nishikibe, M., Yano, M., Yamaguchi, I., Sugishita, Y. and Goto, K. (1993) 'Contribution of endogenous endothelin-1 to the progression of cardiopulmonary alterations in rats with monocrotaline-induced pulmonary hypertension', *Circ Res,* 73(5), pp. 887-97.

Miyazono, K., Kamiya, Y. and Morikawa, M. (2010) 'Bone morphogenetic protein receptors and signal transduction', *J Biochem,* 147(1), pp. 35-51.

Morin, F. C., 3rd and Egan, E. A. (1989) 'The effect of closing the ductus arteriosus on the pulmonary circulation of the fetal sheep', *J Dev Physiol,* 11(5), pp. 283-7.

Morrell, N. W., Adnot, S., Archer, S. L., Dupuis, J., Jones, P. L., MacLean, M. R., McMurtry, I. F., Stenmark, K. R., Thistlethwaite, P. A., Weissmann, N., Yuan, J. X. and Weir, E. K. (2009) 'Cellular and molecular basis of pulmonary arterial hypertension', *J Am Coll Cardiol,* 54(1 Suppl), pp. S20-31.

Moser, M., Binder, O., Wu, Y., Aitsebaomo, J., Ren, R., Bode, C., Bautch, V. L., Conlon, F. L. and Patterson, C. (2003) 'BMPER, a novel endothelial cell precursor-derived protein, antagonizes bone morphogenetic protein signaling and endothelial cell differentiation', *Mol Cell Biol,* 23(16), pp. 5664-79.

Murai, K., Sun, G., Ye, P., Tian, E., Yang, S., Cui, Q., Sun, G., Trinh, D., Sun, O., Hong, T., Wen, Z., Kalkum, M., Riggs, A. D., Song, H., Ming, G. L. and Shi, Y. (2016) 'The TLX-miR-219 cascade regulates neural stem cell proliferation in neurodevelopment and schizophrenia iPSC model', *Nat Commun,* 7, pp. 10965.

Murakami, G., Watabe, T., Takaoka, K., Miyazono, K. and Imamura, T. (2003) 'Cooperative inhibition of bone morphogenetic protein signaling by Smurf1 and inhibitory Smads', *Mol Biol Cell,* 14(7), pp. 2809-17.

Murphy, W. A., Lance, V. A., Moreau, S., Moreau, J. P. and Coy, D. H. (1987) 'Inhibition of rat prostate tumor growth by an octapeptide analog of somatostatin', *Life Sci,* 40(26), pp. 2515-22.

Murray, K. J. (1990) 'Cyclic AMP and mechanisms of vasodilation', *Pharmacol Ther,* 47(3), pp. 329-45.

Murry, C. E. and Keller, G. (2008) 'Differentiation of embryonic stem cells to clinically relevant populations: lessons from embryonic development', *Cell,* 132(4), pp. 661-80.

Musunuru, K., Sheikh, F., Gupta, R. M., Houser, S. R., Maher, K. O., Milan, D. J., Terzic, A., Wu, J. C., American Heart Association Council on Functional, G., Translational, B., Council on Cardiovascular Disease in the, Y., Council on, C. and Stroke, N. (2018) 'Induced Pluripotent Stem Cells for Cardiovascular Disease Modeling and Precision Medicine: A Scientific Statement From the American Heart Association', *Circ Genom Precis Med,* 11(1), pp. e000043.

Nasim, M. T., Ogo, T., Ahmed, M., Randall, R., Chowdhury, H. M., Snape, K. M., Bradshaw, T. Y., Southgate, L., Lee, G. J., Jackson, I., Lord, G. M., Gibbs, J. S., Wilkins, M. R., Ohta-Ogo, K., Nakamura, K., Girerd, B., Coulet, F., Soubrier, F., Humbert, M., Morrell, N. W., Trembath, R. C. and Machado, R. D. (2011) 'Molecular genetic characterization of SMAD signaling molecules in pulmonary arterial hypertension', *Hum Mutat,* 32(12), pp. 1385-9.

Newman, J. H., Wheeler, L., Lane, K. B., Loyd, E., Gaddipati, R., Phillips, J. A., 3rd and Loyd, J. E. (2001) 'Mutation in the gene for bone morphogenetic protein receptor II as a cause of primary pulmonary hypertension in a large kindred', *N Engl J Med,* 345(5), pp. 319-24.

Nisbet, R. E., Bland, J. M., Kleinhenz, D. J., Mitchell, P. O., Walp, E. R., Sutliff, R. L. and Hart, C. M. (2010) 'Rosiglitazone attenuates chronic hypoxia-induced pulmonary hypertension in a mouse model', *Am J Respir Cell Mol Biol,* 42(4), pp. 482-90.

Nisbet, R. E., Graves, A. S., Kleinhenz, D. J., Rupnow, H. L., Reed, A. L., Fan, T. H., Mitchell, P. O., Sutliff, R. L. and Hart, C. M. (2009) 'The role of NADPH oxidase in chronic intermittent hypoxia-induced pulmonary hypertension in mice', *Am J Respir Cell Mol Biol,* 40(5), pp. 601-9.

Nishimoto, N. (2006) 'Interleukin-6 in rheumatoid arthritis', *Curr Opin Rheumatol,* 18(3), pp. 277-81.

Nozik-Grayck, E., Suliman, H. B., Majka, S., Albietz, J., Van Rheen, Z., Roush, K. and Stenmark, K. R. (2008) 'Lung EC-SOD overexpression attenuates hypoxic induction of Egr-1 and chronic hypoxic pulmonary vascular remodeling', *Am J Physiol Lung Cell Mol Physiol,* 295(3), pp. L422-30.

Oka, M., Homma, N., Taraseviciene-Stewart, L., Morris, K. G., Kraskauskas, D., Burns, N., Voelkel, N. F. and McMurtry, I. F. (2007) 'Rho kinase-mediated vasoconstriction is important in severe occlusive pulmonary arterial hypertension in rats', *Circ Res,* 100(6), pp. 923-9.

Olschewski, H., Simonneau, G., Galie, N., Higenbottam, T., Naeije, R., Rubin, L. J., Nikkho, S., Speich, R., Hoeper, M. M., Behr, J., Winkler, J., Sitbon, O., Popov, W., Ghofrani, H. A., Manes, A., Kiely, D. G., Ewert, R., Meyer, A., Corris, P. A., Delcroix, M., Gomez-Sanchez, M., Siedentop, H., Seeger, W. and Aerosolized Iloprost Randomized Study, G. (2002) 'Inhaled iloprost for severe pulmonary hypertension', *N Engl J Med,* 347(5), pp. 322-9.

Ormiston, M. L., Southgate, L., Treacy, C., Pepke-Zaba, J., Trembath, R. C., Machado, R. D. and Morrell, N. W. (2013) 'Assessment of a pulmonary origin for blood outgrowth endothelial cells by examination of identical twins harboring a BMPR2 mutation', *Am J Respir Crit Care Med,* 188(2), pp. 258-60.

Ormiston, M. L., Toshner, M. R., Kiskin, F. N., Huang, C. J., Groves, E., Morrell, N. W. and Rana, A. A. (2015) 'Generation and Culture of Blood Outgrowth Endothelial Cells from Human Peripheral Blood', *J Vis Exp,* (106), pp. e53384.

Orqueda, A. J., Gimenez, C. A. and Pereyra-Bonnet, F. (2016) 'iPSCs: A Minireview from Bench to Bed, including Organoids and the CRISPR System', *Stem Cells Int,* 2016, pp. 5934782.

Owens, G. K. (1995) 'Regulation of differentiation of vascular smooth muscle cells', *Physiol Rev,* 75(3), pp. 487-517.

Owens, G. K., Kumar, M. S. and Wamhoff, B. R. (2004) 'Molecular regulation of vascular smooth muscle cell differentiation in development and disease', *Physiol Rev,* 84(3), pp. 767-801.

Owens, G. K. and Wise, G. (1997) 'Regulation of differentiation/maturation in vascular smooth muscle cells by hormones and growth factors', *Agents Actions Suppl,* 48, pp. 3-24.

Pak, O., Sommer, N., Hoeres, T., Bakr, A., Waisbrod, S., Sydykov, A., Haag, D., Esfandiary, A., Kojonazarov, B., Veit, F., Fuchs, B., Weisel, F. C., Hecker, M., Schermuly, R. T., Grimminger, F., Ghofrani, H. A., Seeger, W. and Weissmann, N. (2013) 'Mitochondrial hyperpolarization in pulmonary vascular remodeling. Mitochondrial uncoupling protein deficiency as disease model', *Am J Respir Cell Mol Biol,* 49(3), pp. 358-67.

Pak O., J. W., Ghofrani H.A., Seeger W., Grimminger F., Schermuly R.T., Weissmann N. (2010) 'Animal models of pulmonary hypertension: role in translational research', *Drug Discov Today,* 7, pp. 89-97.

Papkoff, J., Rubinfeld, B., Schryver, B. and Polakis, P. (1996) 'Wnt-1 regulates free pools of catenins and stabilizes APC-catenin complexes', *Mol Cell Biol,* 16(5), pp. 2128-34.

Park, C. Y., Kim, D. H., Son, J. S., Sung, J. J., Lee, J., Bae, S., Kim, J. H., Kim, D. W. and Kim, J. S. (2015) 'Functional Correction of Large Factor VIII Gene Chromosomal Inversions in Hemophilia A Patient-Derived iPSCs Using CRISPR-Cas9', *Cell Stem Cell,* 17(2), pp. 213-20.

Park, I. H., Arora, N., Huo, H., Maherali, N., Ahfeldt, T., Shimamura, A., Lensch, M. W., Cowan, C., Hochedlinger, K. and Daley, G. Q. (2008) 'Disease-specific induced pluripotent stem cells', *Cell,* 134(5), pp. 877-86.

Pastorino, J. G., Hoek, J. B. and Shulga, N. (2005) 'Activation of glycogen synthase kinase 3beta disrupts the binding of hexokinase II to mitochondria by phosphorylating voltage-dependent anion channel and potentiates chemotherapy-induced cytotoxicity', *Cancer Res,* 65(22), pp. 10545-54.

Patel, Y. C. and Wheatley, T. (1983) 'In vivo and in vitro plasma disappearance and metabolism of somatostatin-28 and somatostatin-14 in the rat', *Endocrinology,* 112(1), pp. 220-5.

Patsch, C., Challet-Meylan, L., Thoma, E. C., Urich, E., Heckel, T., O'Sullivan, J. F., Grainger, S. J., Kapp, F. G., Sun, L., Christensen, K., Xia, Y., Florido, M. H., He, W., Pan, W., Prummer, M., Warren, C. R., Jakob-Roetne, R., Certa, U., Jagasia, R., Freskgard, P. O., Adatto, I., Kling, D., Huang, P., Zon, L. I., Chaikof, E. L., Gerszten, R. E., Graf, M., Iacone, R. and Cowan, C. A. (2015) 'Generation of vascular endothelial and smooth muscle cells from human pluripotent stem cells', *Nat Cell Biol,* 17(8), pp. 994-1003.

Paulin, R., Dromparis, P., Sutendra, G., Gurtu, V., Zervopoulos, S., Bowers, L., Haromy, A., Webster, L., Provencher, S., Bonnet, S. and Michelakis, E. D. (2014) 'Sirtuin 3 deficiency is associated with inhibited mitochondrial function and pulmonary arterial hypertension in rodents and humans', *Cell Metab,* 20(5), pp. 827-839.

Paulin, R. and Michelakis, E. D. (2014) 'The metabolic theory of pulmonary arterial hypertension', *Circ Res,* 115(1), pp. 148-64.

Peacock, A. J., Murphy, N. F., McMurray, J. J., Caballero, L. and Stewart, S. (2007) 'An epidemiological study of pulmonary arterial hypertension', *Eur Respir J,* 30(1), pp. 104-9.

Peluso, G., Petillo, O., Melone, M. A., Mazzarella, G., Ranieri, M. and Tajana, G. F. (1996) 'Modulation of cytokine production in activated human monocytes by somatostatin', *Neuropeptides,* 30(5), pp. 443-51.

Peng, T., Tian, Y., Boogerd, C. J., Lu, M. M., Kadzik, R. S., Stewart, K. M., Evans, S. M. and Morrisey, E. E. (2013) 'Coordination of heart and lung co-development by a multipotent cardiopulmonary progenitor', *Nature,* 500(7464), pp. 589-92.

Pereira, R. C., Economides, A. N. and Canalis, E. (2000) 'Bone morphogenetic proteins induce gremlin, a protein that limits their activity in osteoblasts', *Endocrinology,* 141(12), pp. 4558-63.

Perez-Pinera, P., Kocak, D. D., Vockley, C. M., Adler, A. F., Kabadi, A. M., Polstein, L. R., Thakore, P. I., Glass, K. A., Ousterout, D. G., Leong, K. W., Guilak, F., Crawford, G. E., Reddy, T. E. and Gersbach, C. A. (2013) 'RNA-guided gene activation by CRISPR-Cas9-based transcription factors', *Nat Methods,* 10(10), pp. 973-6.

Perl, A. K. and Whitsett, J. A. (1999) 'Molecular mechanisms controlling lung morphogenesis', *Clin Genet,* 56(1), pp. 14-27.

Petersen, R., Lambourne, J. J., Javierre, B. M., Grassi, L., Kreuzhuber, R., Ruklisa, D., Rosa, I. M., Tome, A. R., Elding, H., van Geffen, J. P., Jiang, T., Farrow, S., Cairns, J., Al-Subaie, A. M., Ashford, S., Attwood, A., Batista, J., Bouman, H., Burden, F., Choudry, F. A., Clarke, L., Flicek, P., Garner, S. F., Haimel, M., Kempster, C., Ladopoulos, V., Lenaerts, A. S., Materek, P. M., McKinney, H., Meacham, S., Mead, D., Nagy, M., Penkett, C. J., Rendon, A., Seyres, D., Sun, B., Tuna, S., van der Weide, M. E., Wingett, S. W., Martens, J. H., Stegle, O., Richardson, S., Vallier, L., Roberts, D. J., Freson, K., Wernisch, L., Stunnenberg, H. G., Danesh, J., Fraser, P., Soranzo, N., Butterworth, A. S., Heemskerk, J. W., Turro, E., Spivakov, M., Ouwehand, W. H., Astle, W. J., Downes, K., Kostadima, M. and Frontini, M. (2017) 'Platelet function is modified by common sequence variation in megakaryocyte super enhancers', *Nat Commun,* 8, pp. 16058.

Piccolo, S., Agius, E., Lu, B., Goodman, S., Dale, L. and De Robertis, E. M. (1997) 'Cleavage of Chordin by Xolloid metalloprotease suggests a role for proteolytic processing in the regulation of Spemann organizer activity', *Cell,* 91(3), pp. 407-16.

Pugliese, S. C., Poth, J. M., Fini, M. A., Olschewski, A., El Kasmi, K. C. and Stenmark, K. R. (2015) 'The role of inflammation in hypoxic pulmonary hypertension: from cellular mechanisms to clinical phenotypes', *Am J Physiol Lung Cell Mol Physiol,* 308(3), pp. L229-52.

Pullamsetti, S., Krick, S., Yilmaz, H., Ghofrani, H. A., Schudt, C., Weissmann, N., Fuchs, B., Seeger, W., Grimminger, F. and Schermuly, R. T. (2005) 'Inhaled tolafentrine reverses pulmonary vascular remodeling via inhibition of smooth muscle cell migration', *Respir Res,* 6, pp. 128.

Que, J., Wilm, B., Hasegawa, H., Wang, F., Bader, D. and Hogan, B. L. (2008) 'Mesothelium contributes to vascular smooth muscle and mesenchyme during lung development', *Proc Natl Acad Sci U S A,* 105(43), pp. 16626-30.

Rabinovitch, M. (2001) 'Pathobiology of pulmonary hypertension. Extracellular matrix', *Clin Chest Med,* 22(3), pp. 433-49, viii.

Rabinovitch, M. (2008) 'Molecular pathogenesis of pulmonary arterial hypertension', *J Clin Invest,* 118(7), pp. 2372-9.

Rabinovitch, M., Guignabert, C., Humbert, M. and Nicolls, M. R. (2014) 'Inflammation and immunity in the pathogenesis of pulmonary arterial hypertension', *Circ Res,* 115(1), pp. 165-75.

Rafikova, O., Meadows, M. L., Kinchen, J. M., Mohney, R. P., Maltepe, E., Desai, A. A., Yuan, J. X., Garcia, J. G., Fineman, J. R., Rafikov, R. and Black, S. M. (2016) 'Metabolic Changes Precede the Development of Pulmonary Hypertension in the Monocrotaline Exposed Rat Lung', *PLoS One,* 11(3), pp. e0150480.

Rajavashisth, T. B., Xu, X. P., Jovinge, S., Meisel, S., Xu, X. O., Chai, N. N., Fishbein, M. C., Kaul, S., Cercek, B., Sharifi, B. and Shah, P. K. (1999) 'Membrane type 1 matrix metalloproteinase expression in human atherosclerotic plaques: evidence for activation by proinflammatory mediators', *Circulation,* 99(24), pp. 3103-9.

Reeves, J. T., Wagner, W. W., Jr., McMurtry, I. F. and Grover, R. F. (1979) 'Physiological effects of high altitude on the pulmonary circulation', *Int Rev Physiol,* 20, pp. 289-310.

Reichlin, S. (1983) 'Somatostatin', *N Engl J Med,* 309(24), pp. 1495-501.

Reynolds, A. M., Xia, W., Holmes, M. D., Hodge, S. J., Danilov, S., Curiel, D. T., Morrell, N. W. and Reynolds, P. N. (2007) 'Bone morphogenetic protein type 2 receptor gene therapy attenuates hypoxic pulmonary hypertension', *Am J Physiol Lung Cell Mol Physiol,* 292(5), pp. L1182-92.

Rhodes, C. J., Im, H., Cao, A., Hennigs, J. K., Wang, L., Sa, S., Chen, P. I., Nickel, N. P., Miyagawa, K., Hopper, R. K., Tojais, N. F., Li, C. G., Gu, M., Spiekerkoetter, E., Xian, Z., Chen, R., Zhao, M., Kaschwich, M., Del Rosario, P. A., Bernstein, D., Zamanian, R. T., Wu, J. C., Snyder, M. P. and Rabinovitch, M. (2015) 'RNA Sequencing Analysis Detection of a Novel Pathway of Endothelial Dysfunction in Pulmonary Arterial Hypertension', *Am J Respir Crit Care Med,* 192(3), pp. 356-66.

Rhodes, J. (2005) 'Comparative physiology of hypoxic pulmonary hypertension: historical clues from brisket disease', *J Appl Physiol (1985),* 98(3), pp. 1092-100.

Rich, S., Dantzker, D. R., Ayres, S. M., Bergofsky, E. H., Brundage, B. H., Detre, K. M., Fishman, A. P., Goldring, R. M., Groves, B. M., Koerner, S. K. and et al. (1987) 'Primary pulmonary hypertension. A national prospective study', *Ann Intern Med,* 107(2), pp. 216-23.

Rivier, J. E., Hoeger, C., Erchegyi, J., Gulyas, J., DeBoard, R., Craig, A. G., Koerber, S. C., Wenger, S., Waser, B., Schaer, J. C. and Reubi, J. C. (2001) 'Potent somatostatin undecapeptide agonists selective for somatostatin receptor 1 (sst1)', *J Med Chem,* 44(13), pp. 2238-46.

Robinton, D. A. and Daley, G. Q. (2012) 'The promise of induced pluripotent stem cells in research and therapy', *Nature,* 481(7381), pp. 295-305.

Rosenquist, T. H., Kirby, M. L. and van Mierop, L. H. (1989) 'Solitary aortic arch artery. A result of surgical ablation of cardiac neural crest and nodose placode in the avian embryo', *Circulation,* 80(5), pp. 1469-75.

Rosenzweig, B. L., Imamura, T., Okadome, T., Cox, G. N., Yamashita, H., ten Dijke, P., Heldin, C. H. and Miyazono, K. (1995) 'Cloning and characterization of a human type II receptor for bone morphogenetic proteins', *Proc Natl Acad Sci U S A,* 92(17), pp. 7632-6.

Rosenzweig, E. B., Morse, J. H., Knowles, J. A., Chada, K. K., Khan, A. M., Roberts, K. E., McElroy, J. J., Juskiw, N. K., Mallory, N. C., Rich, S., Diamond, B. and Barst, R. J. (2008) 'Clinical implications of determining BMPR2 mutation status in a large cohort of children and adults with pulmonary arterial hypertension', *J Heart Lung Transplant,* 27(6), pp. 668-74.

Roth, R. A., Dotzlaf, L. A., Baranyi, B., Kuo, C. H. and Hook, J. B. (1981) 'Effect of monocrotaline ingestion on liver, kidney, and lung of rats', *Toxicol Appl Pharmacol,* 60(2), pp. 193-203.

Rubin, L. J., Badesch, D. B., Barst, R. J., Galie, N., Black, C. M., Keogh, A., Pulido, T., Frost, A., Roux, S., Leconte, I., Landzberg, M. and Simonneau, G. (2002) 'Bosentan therapy for pulmonary arterial hypertension', *N Engl J Med,* 346(12), pp. 896-903.

Ryan, J., Bloch, K. and Archer, S. L. (2011) 'Rodent models of pulmonary hypertension: harmonisation with the world health organisation's categorisation of human PH', *Int J Clin Pract Suppl,* (172), pp. 15-34.

Sa, S., Gu, M., Chappell, J., Shao, N. Y., Ameen, M., Elliott, K. A., Li, D., Grubert, F., Li, C. G., Taylor, S., Cao, A., Ma, Y., Fong, R., Nguyen, L., Wu, J. C., Snyder, M. P. and Rabinovitch, M. (2017) 'Induced Pluripotent Stem Cell Model of Pulmonary Arterial Hypertension Reveals Novel Gene Expression and Patient Specificity', *Am J Respir Crit Care Med,* 195(7), pp. 930-941.

Said, S. I., Hamidi, S. A., Dickman, K. G., Szema, A. M., Lyubsky, S., Lin, R. Z., Jiang, Y. P., Chen, J. J., Waschek, J. A. and Kort, S. (2007) 'Moderate pulmonary arterial hypertension in male mice lacking the vasoactive intestinal peptide gene', *Circulation,* 115(10), pp. 1260-8.

Sakao, S., Taraseviciene-Stewart, L., Lee, J. D., Wood, K., Cool, C. D. and Voelkel, N. F. (2005) 'Initial apoptosis is followed by increased proliferation of apoptosis-resistant endothelial cells', *FASEB J,* 19(9), pp. 1178-80.

Sanders, K. A. and Hoidal, J. R. (2007) 'The NOX on pulmonary hypertension', *Circ Res,* 101(3), pp. 224-6.

Sanjana, N. E., Cong, L., Zhou, Y., Cunniff, M. M., Feng, G. and Zhang, F. (2012) 'A transcription activator-like effector toolbox for genome engineering', *Nat Protoc,* 7(1), pp. 171-92.

Sato, K., Webb, S., Tucker, A., Rabinovitch, M., O'Brien, R. F., McMurtry, I. F. and Stelzner, T. J. (1992) 'Factors influencing the idiopathic development of pulmonary hypertension in the fawn hooded rat', *Am Rev Respir Dis,* 145(4 Pt 1), pp. 793-7.

Satoh, M., Aso, K., Nakayama, T., Naoi, K., Ikehara, S., Uchino, Y., Shimada, H., Takatsuki, S., Matsuura, H. and Saji, T. (2010) 'Autoimmune thyroid disease in children and adolescents with idiopathic pulmonary arterial hypertension', *Circ J,* 74(2), pp. 371-4.

Savale, L., Tu, L., Rideau, D., Izziki, M., Maitre, B., Adnot, S. and Eddahibi, S. (2009) 'Impact of interleukin-6 on hypoxia-induced pulmonary hypertension and lung inflammation in mice', *Respir Res,* 10, pp. 6.

Schermuly, R. T., Dony, E., Ghofrani, H. A., Pullamsetti, S., Savai, R., Roth, M., Sydykov, A., Lai, Y. J., Weissmann, N., Seeger, W. and Grimminger, F. (2005) 'Reversal of experimental pulmonary hypertension by PDGF inhibition', *J Clin Invest,* 115(10), pp. 2811-21.

Schermuly, R. T., Ghofrani, H. A., Wilkins, M. R. and Grimminger, F. (2011) 'Mechanisms of disease: pulmonary arterial hypertension', *Nat Rev Cardiol,* 8(8), pp. 443-55.

Scicchitano, P., Dentamaro, I., Tunzi, F., Ricci, G., Carbonara, S., Devito, F., Zito, A., Ciampolillo, A. and Ciccone, M. M. (2016) 'Pulmonary hypertension in thyroid diseases', *Endocrine,* 54(3), pp. 578-587.

Seah, Y. F., El Farran, C. A., Warrier, T., Xu, J. and Loh, Y. H. (2015) 'Induced Pluripotency and Gene Editing in Disease Modelling: Perspectives and Challenges', *Int J Mol Sci,* 16(12), pp. 28614-34.

Semenza, G. L. (2011) 'Oxygen sensing, homeostasis, and disease', *N Engl J Med,* 365(6), pp. 537-47.

Semenza, G. L., Roth, P. H., Fang, H. M. and Wang, G. L. (1994) 'Transcriptional regulation of genes encoding glycolytic enzymes by hypoxia-inducible factor 1', *J Biol Chem,* 269(38), pp. 23757-63.

Shalem, O., Sanjana, N. E., Hartenian, E., Shi, X., Scott, D. A., Mikkelson, T., Heckl, D., Ebert, B. L., Root, D. E., Doench, J. G. and Zhang, F. (2014) 'Genome-scale CRISPR-Cas9 knockout screening in human cells', *Science,* 343(6166), pp. 84-87.

Sheikh, A. Q., Misra, A., Rosas, I. O., Adams, R. H. and Greif, D. M. (2015) 'Smooth muscle cell progenitors are primed to muscularize in pulmonary hypertension', *Sci Transl Med,* 7(308), pp. 308ra159.

Shi, T., Wang, F., Stieren, E. and Tong, Q. (2005) 'SIRT3, a mitochondrial sirtuin deacetylase, regulates mitochondrial function and thermogenesis in brown adipocytes', *J Biol Chem,* 280(14), pp. 13560-7.

Shi, Y., Inoue, H., Wu, J. C. and Yamanaka, S. (2017) 'Induced pluripotent stem cell technology: a decade of progress', *Nat Rev Drug Discov,* 16(2), pp. 115-130.

Shi, Y. and Massague, J. (2003) 'Mechanisms of TGF-beta signaling from cell membrane to the nucleus', *Cell,* 113(6), pp. 685-700.

Shin, D., Garcia-Cardena, G., Hayashi, S., Gerety, S., Asahara, T., Stavrakis, G., Isner, J., Folkman, J., Gimbrone, M. A., Jr. and Anderson, D. J. (2001) 'Expression of ephrinB2 identifies a stable genetic difference between arterial and venous vascular smooth muscle as well as endothelial cells, and marks subsets of microvessels at sites of adult neovascularization', *Dev Biol,* 230(2), pp. 139-50.

Shulman, J. M., Perrimon, N. and Axelrod, J. D. (1998) 'Frizzled signaling and the developmental control of cell polarity', *Trends Genet,* 14(11), pp. 452-8.

Sidney, E. J., Hampl, V., Nelson, D. P., Archer, S. L., Foegh, M. L., Cathapermal, S. S. and Weir, E. K. (1996) 'The somatostatin analog angiopeptin does not reduce chronic hypoxic pulmonary hypertension in rats', *Proc Soc Exp Biol Med,* 213(1), pp. 43-9.

Simonneau, G., Gatzoulis, M. A., Adatia, I., Celermajer, D., Denton, C., Ghofrani, A., Gomez Sanchez, M. A., Krishna Kumar, R., Landzberg, M., Machado, R. F., Olschewski, H., Robbins, I. M. and Souza, R. (2013) 'Updated clinical classification of pulmonary hypertension', *J Am Coll Cardiol,* 62(25 Suppl), pp. D34-41.

Simonneau, G., Robbins, I. M., Beghetti, M., Channick, R. N., Delcroix, M., Denton, C. P., Elliott, C. G., Gaine, S. P., Gladwin, M. T., Jing, Z. C., Krowka, M. J., Langleben, D., Nakanishi, N. and Souza, R. (2009) 'Updated clinical classification of pulmonary hypertension', *J Am Coll Cardiol,* 54(1 Suppl), pp. S43-54.

Simonson, T. S., Yang, Y., Huff, C. D., Yun, H., Qin, G., Witherspoon, D. J., Bai, Z., Lorenzo, F. R., Xing, J., Jorde, L. B., Prchal, J. T. and Ge, R. (2010) 'Genetic evidence for high-altitude adaptation in Tibet', *Science,* 329(5987), pp. 72-5.

Sirokmany, G., Donko, A. and Geiszt, M. (2016) 'Nox/Duox Family of NADPH Oxidases: Lessons from Knockout Mouse Models', *Trends Pharmacol Sci,* 37(4), pp. 318-327.

Sitbon, O., Channick, R., Chin, K. M., Frey, A., Gaine, S., Galie, N., Ghofrani, H. A., Hoeper, M. M., Lang, I. M., Preiss, R., Rubin, L. J., Di Scala, L., Tapson, V., Adzerikho, I., Liu, J., Moiseeva, O., Zeng, X., Simonneau, G., McLaughlin, V. V. and Investigators, G. (2015) 'Selexipag for the Treatment of Pulmonary Arterial Hypertension', *N Engl J Med,* 373(26), pp. 2522-33.

Smith, C., Gore, A., Yan, W., Abalde-Atristain, L., Li, Z., He, C., Wang, Y., Brodsky, R. A., Zhang, K., Cheng, L. and Ye, Z. (2014) 'Whole-genome sequencing analysis reveals high specificity of CRISPR/Cas9 and TALEN-based genome editing in human iPSCs', *Cell Stem Cell,* 15(1), pp. 12-3.

Sobolewski, A., Rudarakanchana, N., Upton, P. D., Yang, J., Crilley, T. K., Trembath, R. C. and Morrell, N. W. (2008) 'Failure of bone morphogenetic protein receptor trafficking in pulmonary arterial hypertension: potential for rescue', *Hum Mol Genet,* 17(20), pp. 3180-90.

Sobue, K., Hayashi, K. and Nishida, W. (1999) 'Expressional regulation of smooth muscle cell-specific genes in association with phenotypic modulation', *Mol Cell Biochem,* 190(1-2), pp. 105-18.

Soldner, F., Hockemeyer, D., Beard, C., Gao, Q., Bell, G. W., Cook, E. G., Hargus, G., Blak, A., Cooper, O., Mitalipova, M., Isacson, O. and Jaenisch, R. (2009) 'Parkinson's disease patient-derived induced pluripotent stem cells free of viral reprogramming factors', *Cell,* 136(5), pp. 964-77.

Soon, E., Crosby, A., Southwood, M., Yang, P., Tajsic, T., Toshner, M., Appleby, S., Shanahan, C. M., Bloch, K. D., Pepke-Zaba, J., Upton, P. and Morrell, N. W. (2015) 'Bone morphogenetic protein receptor type II deficiency and increased inflammatory cytokine production. A gateway to pulmonary arterial hypertension', *Am J Respir Crit Care Med,* 192(7), pp. 859-72.

Soon, E., Holmes, A. M., Treacy, C. M., Doughty, N. J., Southgate, L., Machado, R. D., Trembath, R. C., Jennings, S., Barker, L., Nicklin, P., Walker, C., Budd, D. C., Pepke-Zaba, J. and Morrell, N. W. (2010) 'Elevated levels of inflammatory cytokines predict survival in idiopathic and familial pulmonary arterial hypertension', *Circulation,* 122(9), pp. 920-7.

Soubrier, F., Chung, W. K., Machado, R., Grunig, E., Aldred, M., Geraci, M., Loyd, J. E., Elliott, C. G., Trembath, R. C., Newman, J. H. and Humbert, M. (2013) 'Genetics and genomics of pulmonary arterial hypertension', *J Am Coll Cardiol,* 62(25 Suppl), pp. D13-21.

Spiekerkoetter, E., Tian, X., Cai, J., Hopper, R. K., Sudheendra, D., Li, C. G., El-Bizri, N., Sawada, H., Haghighat, R., Chan, R., Haghighat, L., de Jesus Perez, V., Wang, L., Reddy, S., Zhao, M., Bernstein, D., Solow-Cordero, D. E., Beachy, P. A., Wandless, T. J., Ten Dijke, P. and Rabinovitch, M. (2013) 'FK506 activates BMPR2, rescues endothelial dysfunction, and reverses pulmonary hypertension', *J Clin Invest,* 123(8), pp. 3600-13.

Stadtfeld, M., Nagaya, M., Utikal, J., Weir, G. and Hochedlinger, K. (2008) 'Induced pluripotent stem cells generated without viral integration', *Science,* 322(5903), pp. 945-9.

Steiner, M. K., Syrkina, O. L., Kolliputi, N., Mark, E. J., Hales, C. A. and Waxman, A. B. (2009) 'Interleukin-6 overexpression induces pulmonary hypertension', *Circ Res,* 104(2), pp. 236-44, 28p following 244.

Stenmark, K. R., Fagan, K. A. and Frid, M. G. (2006) 'Hypoxia-induced pulmonary vascular remodeling: cellular and molecular mechanisms', *Circ Res,* 99(7), pp. 675-91.

Stenmark, K. R. and Mecham, R. P. (1997) 'Cellular and molecular mechanisms of pulmonary vascular remodeling', *Annu Rev Physiol,* 59, pp. 89-144.

Stenmark, K. R., Meyrick, B., Galie, N., Mooi, W. J. and McMurtry, I. F. (2009) 'Animal models of pulmonary arterial hypertension: the hope for etiological discovery and pharmacological cure', *Am J Physiol Lung Cell Mol Physiol,* 297(6), pp. L1013-32.

Stenmark, K. R., Nozik-Grayck, E., Gerasimovskaya, E., Anwar, A., Li, M., Riddle, S. and Frid, M. (2011) 'The adventitia: Essential role in pulmonary vascular remodeling', *Compr Physiol,* 1(1), pp. 141-61.

Stiemer, B., Springmeier, G., el-Jarad, L. and Schroter-Kermani, C. (1993) 'Matrix production of smooth muscle cells from rat aorta in vitro', *Histol Histopathol,* 8(1), pp. 63-72.

Strange, G., Playford, D., Stewart, S., Deague, J. A., Nelson, H., Kent, A. and Gabbay, E. (2012) 'Pulmonary hypertension: prevalence and mortality in the Armadale echocardiography cohort', *Heart,* 98(24), pp. 1805-11.

Sumi, T., Tsuneyoshi, N., Nakatsuji, N. and Suemori, H. (2008) 'Defining early lineage specification of human embryonic stem cells by the orchestrated balance of canonical Wnt/beta-catenin, Activin/Nodal and BMP signaling', *Development,* 135(17), pp. 2969-79.

Sutendra, G., Dromparis, P., Bonnet, S., Haromy, A., McMurtry, M. S., Bleackley, R. C. and Michelakis, E. D. (2011) 'Pyruvate dehydrogenase inhibition by the inflammatory cytokine TNFalpha contributes to the pathogenesis of pulmonary arterial hypertension', *J Mol Med (Berl),* 89(8), pp. 771-83.

Suzuki, K., Yu, C., Qu, J., Li, M., Yao, X., Yuan, T., Goebl, A., Tang, S., Ren, R., Aizawa, E., Zhang, F., Xu, X., Soligalla, R. D., Chen, F., Kim, J., Kim, N. Y., Liao, H. K., Benner, C., Esteban, C. R., Jin, Y., Liu, G. H., Li, Y. and Izpisua Belmonte, J. C. (2014) 'Targeted gene correction minimally impacts whole-genome mutational load in human-disease-specific induced pluripotent stem cell clones', *Cell Stem Cell,* 15(1), pp. 31-6.

Swenson, E. R. (2013) 'Hypoxic pulmonary vasoconstriction', *High Alt Med Biol,* 14(2), pp. 101-10.

Swift, M. R. and Weinstein, B. M. (2009) 'Arterial-venous specification during development', *Circ Res,* 104(5), pp. 576-88.

Sztrymf, B., Coulet, F., Girerd, B., Yaici, A., Jais, X., Sitbon, O., Montani, D., Souza, R., Simonneau, G., Soubrier, F. and Humbert, M. (2008) 'Clinical outcomes of pulmonary arterial hypertension in carriers of BMPR2 mutation', *Am J Respir Crit Care Med,* 177(12), pp. 1377-83.

Sztuka, K. and Jasinska-Stroschein, M. (2017) 'Animal models of pulmonary arterial hypertension: A systematic review and meta-analysis of data from 6126 animals', *Pharmacol Res,* 125(Pt B), pp. 201-214.

Takahashi, H., Goto, N., Kojima, Y., Tsuda, Y., Morio, Y., Muramatsu, M. and Fukuchi, Y. (2006) 'Downregulation of type II bone morphogenetic protein receptor in hypoxic pulmonary hypertension', *Am J Physiol Lung Cell Mol Physiol,* 290(3), pp. L450-8.

Takahashi, J., Orcholski, M., Yuan, K. and de Jesus Perez, V. (2016) 'PDGF-dependent beta-catenin activation is associated with abnormal pulmonary artery smooth muscle cell proliferation in pulmonary arterial hypertension', *FEBS Lett,* 590(1), pp. 101-9.

Takahashi, K., Tanabe, K., Ohnuki, M., Narita, M., Ichisaka, T., Tomoda, K. and Yamanaka, S. (2007) 'Induction of pluripotent stem cells from adult human fibroblasts by defined factors', *Cell,* 131(5), pp. 861-72.

Takahashi, K. and Yamanaka, S. (2006) 'Induction of pluripotent stem cells from mouse embryonic and adult fibroblast cultures by defined factors', *Cell,* 126(4), pp. 663-76.

Takahashi, T., Kanda, T., Imai, S., Suzuki, T. and Murata, K. (1995) 'Sandostatin inhibits development of medial proliferation of pulmonary arteries in a rat model of pulmonary hypertension', *Life Sci,* 57(8), pp. PL91-5.

Taraseviciene-Stewart, L., Kasahara, Y., Alger, L., Hirth, P., Mc Mahon, G., Waltenberger, J., Voelkel, N. F. and Tuder, R. M. (2001) 'Inhibition of the VEGF receptor 2 combined with chronic hypoxia causes cell death-dependent pulmonary endothelial cell proliferation and severe pulmonary hypertension', *FASEB J,* 15(2), pp. 427-38.

Taura, D., Noguchi, M., Sone, M., Hosoda, K., Mori, E., Okada, Y., Takahashi, K., Homma, K., Oyamada, N., Inuzuka, M., Sonoyama, T., Ebihara, K., Tamura, N., Itoh, H., Suemori, H., Nakatsuji, N., Okano, H., Yamanaka, S. and Nakao, K. (2009) 'Adipogenic differentiation of human induced pluripotent stem cells: comparison with that of human embryonic stem cells', *FEBS Lett,* 583(6), pp. 1029-33.

Taylor, C. T. and Colgan, S. P. (2017) 'Regulation of immunity and inflammation by hypoxia in immunological niches', *Nat Rev Immunol,* 17(12), pp. 774-785.

ten Dijke, P., Yamashita, H., Ichijo, H., Franzen, P., Laiho, M., Miyazono, K. and Heldin, C. H. (1994) 'Characterization of type I receptors for transforming growth factor-beta and activin', *Science,* 264(5155), pp. 101-4.

Thenappan, T., Ormiston, M. L., Ryan, J. J. and Archer, S. L. (2018) 'Pulmonary arterial hypertension: pathogenesis and clinical management', *BMJ,* 360, pp. j5492.

Thenappan, T., Prins, K. W., Pritzker, M. R., Scandurra, J., Volmers, K. and Weir, E. K. (2016) 'The Critical Role of Pulmonary Arterial Compliance in Pulmonary Hypertension', *Ann Am Thorac Soc,* 13(2), pp. 276-84.

Thompson, K. and Rabinovitch, M. (1996) 'Exogenous leukocyte and endogenous elastases can mediate mitogenic activity in pulmonary artery smooth muscle cells by release of extracellular-matrix bound basic fibroblast growth factor', *J Cell Physiol,* 166(3), pp. 495-505.

Thomson, J. A., Itskovitz-Eldor, J., Shapiro, S. S., Waknitz, M. A., Swiergiel, J. J., Marshall, V. S. and Jones, J. M. (1998) 'Embryonic stem cell lines derived from human blastocysts', *Science,* 282(5391), pp. 1145-7.

Tjen, A. L. S., Ekman, R., Lippton, H., Cary, J. and Keith, I. (1992) 'CGRP and somatostatin modulate chronic hypoxic pulmonary hypertension', *Am J Physiol,* 263(3 Pt 2), pp. H681-90.

Topouzis, S. and Majesky, M. W. (1996) 'Smooth Muscle Lineage Diversity in the Chick Embryo', *Dev Biol,* 178(2), pp. 430-45.

Trembath, R. C., Thomson, J. R., Machado, R. D., Morgan, N. V., Atkinson, C., Winship, I., Simonneau, G., Galie, N., Loyd, J. E., Humbert, M., Nichols, W. C., Morrell, N. W., Berg, J., Manes, A., McGaughran, J., Pauciulo, M. and Wheeler, L. (2001) 'Clinical and molecular genetic features of pulmonary hypertension in patients with hereditary hemorrhagic telangiectasia', *N Engl J Med,* 345(5), pp. 325-34.

Tsuritani, K., Takeda, J., Sakagami, J., Ishii, A., Eriksson, T., Hara, T., Ishibashi, H., Koshihara, Y., Yamada, K. and Yoneda, Y. (2010) 'Cytokine receptor-like factor 1 is highly expressed in damaged human knee osteoarthritic cartilage and involved in osteoarthritis downstream of TGF-beta', *Calcif Tissue Int,* 86(1), pp. 47-57.

Tuder, R. M., Archer, S. L., Dorfmuller, P., Erzurum, S. C., Guignabert, C., Michelakis, E., Rabinovitch, M., Schermuly, R., Stenmark, K. R. and Morrell, N. W. (2013) 'Relevant issues in the pathology and pathobiology of pulmonary hypertension', *J Am Coll Cardiol,* 62(25 Suppl), pp. D4-12.

Tuder, R. M., Groves, B., Badesch, D. B. and Voelkel, N. F. (1994) 'Exuberant endothelial cell growth and elements of inflammation are present in plexiform lesions of pulmonary hypertension', *Am J Pathol,* 144(2), pp. 275-85.

Turro, E., Astle, W. J. and Tavare, S. (2014) 'Flexible analysis of RNA-seq data using mixed effects models', *Bioinformatics,* 30(2), pp. 180-8.

Turro, E., Su, S. Y., Goncalves, A., Coin, L. J., Richardson, S. and Lewin, A. (2011) 'Haplotype and isoform specific expression estimation using multi-mapping RNA-seq reads', *Genome Biol,* 12(2), pp. R13.

Upton, P. D., Davies, R. J., Tajsic, T. and Morrell, N. W. (2013) 'Transforming growth factor-beta(1) represses bone morphogenetic protein-mediated Smad signaling in pulmonary artery smooth muscle cells via Smad3', *Am J Respir Cell Mol Biol,* 49(6), pp. 1135-45.

Upton, P. D. and Morrell, N. W. (2009) 'TGF-beta and BMPR-II pharmacology--implications for pulmonary vascular diseases', *Curr Opin Pharmacol,* 9(3), pp. 274-80.

Urist, M. R. (1965) 'Bone: formation by autoinduction', *Science,* 150(3698), pp. 893-9.

Vallier, L., Touboul, T., Chng, Z., Brimpari, M., Hannan, N., Millan, E., Smithers, L. E., Trotter, M., Rugg-Gunn, P., Weber, A. and Pedersen, R. A. (2009) 'Early cell fate decisions of human embryonic stem cells and mouse epiblast stem cells are controlled by the same signalling pathways', *PLoS One,* 4(6), pp. e6082.

van der Bruggen, C. E., Happe, C. M., Dorfmuller, P., Trip, P., Spruijt, O. A., Rol, N., Hoevenaars, F. P., Houweling, A. C., Girerd, B., Marcus, J. T., Mercier, O., Humbert, M., Handoko, M. L., van der Velden, J., Vonk Noordegraaf, A., Bogaard, H. J., Goumans, M. J. and de Man, F. S. (2016) 'Bone Morphogenetic Protein Receptor Type 2 Mutation in Pulmonary Arterial Hypertension: A View on the Right Ventricle', *Circulation,* 133(18), pp. 1747-60.

Vander Heiden, M. G., Cantley, L. C. and Thompson, C. B. (2009) 'Understanding the Warburg effect: the metabolic requirements of cell proliferation', *Science,* 324(5930), pp. 1029-33.

VanderLaan, P. A., Reardon, C. A. and Getz, G. S. (2004) 'Site specificity of atherosclerosis: site-selective responses to atherosclerotic modulators', *Arterioscler Thromb Vasc Biol,* 24(1), pp. 12-22.

Veeman, M. T., Axelrod, J. D. and Moon, R. T. (2003) 'A second canon. Functions and mechanisms of beta-catenin-independent Wnt signaling', *Dev Cell,* 5(3), pp. 367-77.

Veit, F., Pak, O., Egemnazarov, B., Roth, M., Kosanovic, D., Seimetz, M., Sommer, N., Ghofrani, H. A., Seeger, W., Grimminger, F., Brandes, R. P., Schermuly, R. T. and Weissmann, N. (2013) 'Function of NADPH oxidase 1 in pulmonary arterial smooth muscle cells after monocrotaline-induced pulmonary vascular remodeling', *Antioxid Redox Signal,* 19(18), pp. 2213-31.

Vender, R. L. (1994) 'Chronic hypoxic pulmonary hypertension. Cell biology to pathophysiology', *Chest,* 106(1), pp. 236-43.

Veres, A., Gosis, B. S., Ding, Q., Collins, R., Ragavendran, A., Brand, H., Erdin, S., Cowan, C. A., Talkowski, M. E. and Musunuru, K. (2014) 'Low incidence of off-target mutations in individual CRISPR-Cas9 and TALEN targeted human stem cell clones detected by whole-genome sequencing', *Cell Stem Cell,* 15(1), pp. 27-30.

Verma, S., Arikawa, E., Lee, S., Dumont, A. S., Yao, L. and McNeill, J. H. (2002) 'Exaggerated coronary reactivity to endothelin-1 in diabetes: reversal with bosentan', *Can J Physiol Pharmacol,* 80(10), pp. 980-6.

Vidal-Puig, A. J., Grujic, D., Zhang, C. Y., Hagen, T., Boss, O., Ido, Y., Szczepanik, A., Wade, J., Mootha, V., Cortright, R., Muoio, D. M. and Lowell, B. B. (2000) 'Energy metabolism in uncoupling protein 3 gene knockout mice', *J Biol Chem,* 275(21), pp. 16258-66.

Vieillard-Baron, A., Frisdal, E., Raffestin, B., Baker, A. H., Eddahibi, S., Adnot, S. and D'Ortho, M. P. (2003) 'Inhibition of matrix metalloproteinases by lung TIMP-1 gene transfer limits monocrotaline-induced pulmonary vascular remodeling in rats', *Hum Gene Ther,* 14(9), pp. 861-9.

von Bubnoff, A. and Cho, K. W. (2001) 'Intracellular BMP signaling regulation in vertebrates: pathway or network?', *Dev Biol,* 239(1), pp. 1-14.

von Euler, U. S. and Liljestrand, G. (1946) 'Observations on the Pulmonary Arterial Blood Pressure in the Cat', *Acta Physiologica,* 12(4), pp. 301-320.

Wang, E. A., Rosen, V., Cordes, P., Hewick, R. M., Kriz, M. J., Luxenberg, D. P., Sibley, B. S. and Wozney, J. M. (1988) 'Purification and characterization of other distinct bone-inducing factors', *Proc Natl Acad Sci U S A,* 85(24), pp. 9484-8.

Wang, G., Fan, R., Ji, R., Zou, W., Penny, D. J., Varghese, N. P. and Fan, Y. (2016) 'Novel homozygous BMP9 nonsense mutation causes pulmonary arterial hypertension: a case report', *BMC Pulm Med,* 16, pp. 17.

Wasteson, P., Johansson, B. R., Jukkola, T., Breuer, S., Akyurek, L. M., Partanen, J. and Lindahl, P. (2008) 'Developmental origin of smooth muscle cells in the descending aorta in mice', *Development,* 135(10), pp. 1823-32.

Weaver, M., Yingling, J. M., Dunn, N. R., Bellusci, S. and Hogan, B. L. (1999) 'Bmp signaling regulates proximal-distal differentiation of endoderm in mouse lung development', *Development,* 126(18), pp. 4005-15.

Weckbecker, G., Lewis, I., Albert, R., Schmid, H. A., Hoyer, D. and Bruns, C. (2003) 'Opportunities in somatostatin research: biological, chemical and therapeutic aspects', *Nat Rev Drug Discov,* 2(12), pp. 999-1017.

Wen, Z., Nguyen, H. N., Guo, Z., Lalli, M. A., Wang, X., Su, Y., Kim, N. S., Yoon, K. J., Shin, J., Zhang, C., Makri, G., Nauen, D., Yu, H., Guzman, E., Chiang, C. H., Yoritomo, N., Kaibuchi, K., Zou, J., Christian, K. M., Cheng, L., Ross, C. A., Margolis, R. L., Chen, G., Kosik, K. S., Song, H. and Ming, G. L. (2014) 'Synaptic dysregulation in a human iPS cell model of mental disorders', *Nature,* 515(7527), pp. 414-8.

West, J. and Hemnes, A. (2011) 'Experimental and transgenic models of pulmonary hypertension', *Compr Physiol,* 1(2), pp. 769-82.

West, J. D., Austin, E. D., Gaskill, C., Marriott, S., Baskir, R., Bilousova, G., Jean, J. C., Hemnes, A. R., Menon, S., Bloodworth, N. C., Fessel, J. P., Kropski, J. A., Irwin, D., Ware, L. B., Wheeler, L., Hong, C. C., Meyrick, B., Loyd, J. E., Bowman, A. B., Ess, K. C., Klemm, D. J., Young, P. P., Merryman, W. D., Kotton, D. and Majka, S. M. (2014) 'Identification of a common Wnt-associated genetic signature across multiple cell types in pulmonary arterial hypertension', *Am J Physiol Cell Physiol,* 307(5), pp. C415-30.

West, J. D. and Carrier, E. J. (2018) 'Precision Modeling of Pulmonary Hypertension Pathology with iPSC-derived Cells', *Am J Respir Crit Care Med*., 198(2), pp. 154-5

Weyemi, U., Caillou, B., Talbot, M., Ameziane-El-Hassani, R., Lacroix, L., Lagent-Chevallier, O., Al Ghuzlan, A., Roos, D., Bidart, J. M., Virion, A., Schlumberger, M. and Dupuy, C. (2010) 'Intracellular expression of reactive oxygen species-generating NADPH oxidase NOX4 in normal and cancer thyroid tissues', *Endocr Relat Cancer,* 17(1), pp. 27-37.

Wilson, J. L., Yu, J., Taylor, L. and Polgar, P. (2015) 'Hyperplastic Growth of Pulmonary Artery Smooth Muscle Cells from Subjects with Pulmonary Arterial Hypertension Is Activated through JNK and p38 MAPK', *PLoS One,* 10(4), pp. e0123662.

Winnier, G., Blessing, M., Labosky, P. A. and Hogan, B. L. (1995) 'Bone morphogenetic protein-4 is required for mesoderm formation and patterning in the mouse', *Genes Dev,* 9(17), pp. 2105-16.

Wolf, D. and Goff, S. P. (2007) 'TRIM28 mediates primer binding site-targeted silencing of murine leukemia virus in embryonic cells', *Cell,* 131(1), pp. 46-57.

Wolinsky, H. and Glagov, S. (1967) 'Nature of species differences in the medial distribution of aortic vasa vasorum in mammals', *Circ Res,* 20(4), pp. 409-21.

Wong, A. P., Nili, N. and Strauss, B. H. (2005) 'In vitro differences between venous and arterial-derived smooth muscle cells: potential modulatory role of decorin', *Cardiovasc Res,* 65(3), pp. 702-10.

Wu, D., Talbot, C. C., Jr., Liu, Q., Jing, Z. C., Damico, R. L., Tuder, R., Barnes, K. C., Hassoun, P. M. and Gao, L. (2016) 'Identifying microRNAs targeting Wnt/beta-catenin pathway in end-stage idiopathic pulmonary arterial hypertension', *J Mol Med (Berl),* 94(8), pp. 875-85.

Xiao, Y., Gong, D. and Wang, W. (2013) 'Soluble JAGGED1 inhibits pulmonary hypertension by attenuating notch signaling', *Arterioscler Thromb Vasc Biol,* 33(12), pp. 2733-9.

Yamashita, H., ten Dijke, P., Huylebroeck, D., Sampath, T. K., Andries, M., Smith, J. C., Heldin, C. H. and Miyazono, K. (1995) 'Osteogenic protein-1 binds to activin type II receptors and induces certain activin-like effects', *J Cell Biol,* 130(1), pp. 217-26.

Yan, S., Li, M., Chai, H., Yang, H., Lin, P. H., Yao, Q. and Chen, C. (2005) 'TNF-alpha decreases expression of somatostatin, somatostatin receptors, and cortistatin in human coronary endothelial cells', *J Surg Res,* 123(2), pp. 294-301.

Yang, J., Li, X., Li, Y., Southwood, M., Ye, L., Long, L., Al-Lamki, R. S. and Morrell, N. W. (2013) 'Id proteins are critical downstream effectors of BMP signaling in human pulmonary arterial smooth muscle cells', *Am J Physiol Lung Cell Mol Physiol,* 305(4), pp. L312-21.

Yang, X., Long, L., Southwood, M., Rudarakanchana, N., Upton, P. D., Jeffery, T. K., Atkinson, C., Chen, H., Trembath, R. C. and Morrell, N. W. (2005) 'Dysfunctional Smad signaling contributes to abnormal smooth muscle cell proliferation in familial pulmonary arterial hypertension', *Circ Res,* 96(10), pp. 1053-63.

Yang, Z., Oemar, B. S., Carrel, T., Kipfer, B., Julmy, F. and Luscher, T. F. (1998) 'Different proliferative properties of smooth muscle cells of human arterial and venous bypass vessels: role of PDGF receptors, mitogen-activated protein kinase, and cyclin-dependent kinase inhibitors', *Circulation,* 97(2), pp. 181-7.

Ye, J. X., Wang, S. S., Ge, M. and Wang, D. J. (2016) 'Suppression of endothelial PGC-1alpha is associated with hypoxia-induced endothelial dysfunction and provides a new therapeutic target in pulmonary arterial hypertension', *Am J Physiol Lung Cell Mol Physiol,* 310(11), pp. L1233-42.

Ye, Z., Zhan, H., Mali, P., Dowey, S., Williams, D. M., Jang, Y. Y., Dang, C. V., Spivak, J. L., Moliterno, A. R. and Cheng, L. (2009) 'Human-induced pluripotent stem cells from blood cells of healthy donors and patients with acquired blood disorders', *Blood,* 114(27), pp. 5473-80.

Yi, E. S., Kim, H., Ahn, H., Strother, J., Morris, T., Masliah, E., Hansen, L. A., Park, K. and Friedman, P. J. (2000) 'Distribution of obstructive intimal lesions and their cellular phenotypes in chronic pulmonary hypertension. A morphometric and immunohistochemical study', *Am J Respir Crit Care Med,* 162(4 Pt 1), pp. 1577-86.

Yu, J., Vodyanik, M. A., Smuga-Otto, K., Antosiewicz-Bourget, J., Frane, J. L., Tian, S., Nie, J., Jonsdottir, G. A., Ruotti, V., Stewart, R., Slukvin, II and Thomson, J. A. (2007) 'Induced pluripotent stem cell lines derived from human somatic cells', *Science,* 318(5858), pp. 1917-20.

Yu, P. B., Beppu, H., Kawai, N., Li, E. and Bloch, K. D. (2005) 'Bone morphogenetic protein (BMP) type II receptor deletion reveals BMP ligand-specific gain of signaling in pulmonary artery smooth muscle cells', *J Biol Chem,* 280(26), pp. 24443-50.

Yu, S. T., Zhong, Q., Chen, R. H., Han, P., Li, S. B., Zhang, H., Yuan, L., Xia, T. L., Zeng, M. S. and Huang, X. M. (2018) 'CRLF1 promotes malignant phenotypes of papillary thyroid carcinoma by activating the MAPK/ERK and PI3K/AKT pathways', *Cell Death Dis,* 9(3), pp. 371.

Yu, Y. R., Mao, L., Piantadosi, C. A. and Gunn, M. D. (2013) 'CCR2 deficiency, dysregulation of Notch signaling, and spontaneous pulmonary arterial hypertension', *Am J Respir Cell Mol Biol,* 48(5), pp. 647-54.

Yusa, K., Rashid, S. T., Strick-Marchand, H., Varela, I., Liu, P. Q., Paschon, D. E., Miranda, E., Ordonez, A., Hannan, N. R., Rouhani, F. J., Darche, S., Alexander, G., Marciniak, S. J., Fusaki, N., Hasegawa, M., Holmes, M. C., Di Santo, J. P., Lomas, D. A., Bradley, A. and Vallier, L. (2011) 'Targeted gene correction of alpha1-antitrypsin deficiency in induced pluripotent stem cells', *Nature,* 478(7369), pp. 391-4.

Zaidi, S. H., You, X. M., Ciura, S., Husain, M. and Rabinovitch, M. (2002) 'Overexpression of the serine elastase inhibitor elafin protects transgenic mice from hypoxic pulmonary hypertension', *Circulation,* 105(4), pp. 516-21.

Zamanian, R. T., Hansmann, G., Snook, S., Lilienfeld, D., Rappaport, K. M., Reaven, G. M., Rabinovitch, M. and Doyle, R. L. (2009) 'Insulin resistance in pulmonary arterial hypertension', *Eur Respir J,* 33(2), pp. 318-24.

Zamzami, N. and Kroemer, G. (2001) 'The mitochondrion in apoptosis: how Pandora's box opens', *Nat Rev Mol Cell Biol,* 2(1), pp. 67-71.

Zamzami, N., Susin, S. A., Marchetti, P., Hirsch, T., Gomez-Monterrey, I., Castedo, M. and Kroemer, G. (1996) 'Mitochondrial control of nuclear apoptosis', *J Exp Med,* 183(4), pp. 1533-44.

Zardi, E. M., Zardi, D. M., Cacciapaglia, F., Dobrina, A., Amoroso, A., Picardi, A. and Afeltra, A. (2005) 'Endothelial dysfunction and activation as an expression of disease: role of prostacyclin analogs', *Int Immunopharmacol,* 5(3), pp. 437-59.

Zhang, H. and Bradley, A. (1996) 'Mice deficient for BMP2 are nonviable and have defects in amnion/chorion and cardiac development', *Development,* 122(10), pp. 2977-86.

Zhang, L. L., Lu, J., Li, M. T., Wang, Q. and Zeng, X. F. (2016) 'Preventive and remedial application of etanercept attenuate monocrotaline-induced pulmonary arterial hypertension', *Int J Rheum Dis,* 19(2), pp. 192-8.

Zhang, R., Dai, L. Z., Xie, W. P., Yu, Z. X., Wu, B. X., Pan, L., Yuan, P., Jiang, X., He, J., Humbert, M. and Jing, Z. C. (2011) 'Survival of Chinese patients with pulmonary arterial hypertension in the modern treatment era', *Chest,* 140(2), pp. 301-309.

Zhang, S., Fantozzi, I., Tigno, D. D., Yi, E. S., Platoshyn, O., Thistlethwaite, P. A., Kriett, J. M., Yung, G., Rubin, L. J. and Yuan, J. X. (2003) 'Bone morphogenetic proteins induce apoptosis in human pulmonary vascular smooth muscle cells', *Am J Physiol Lung Cell Mol Physiol,* 285(3), pp. L740-54.

Zhao, G. Q. and Hogan, B. L. (1996) 'Evidence that mouse Bmp8a (Op2) and Bmp8b are duplicated genes that play a role in spermatogenesis and placental development', *Mech Dev,* 57(2), pp. 159-68.

Zhao, L., Ashek, A., Wang, L., Fang, W., Dabral, S., Dubois, O., Cupitt, J., Pullamsetti, S. S., Cotroneo, E., Jones, H., Tomasi, G., Nguyen, Q. D., Aboagye, E. O., El-Bahrawy, M. A., Barnes, G., Howard, L. S., Gibbs, J. S., Gsell, W., He, J. G. and Wilkins, M. R. (2013) 'Heterogeneity in lung (18)FDG uptake in pulmonary arterial hypertension: potential of dynamic (18)FDG positron emission tomography with kinetic analysis as a bridging biomarker for pulmonary vascular remodeling targeted treatments', *Circulation,* 128(11), pp. 1214-24.

Zhao, L., Sebkhi, A., Nunez, D. J., Long, L., Haley, C. S., Szpirer, J., Szpirer, C., Williams, A. J. and Wilkins, M. R. (2001) 'Right ventricular hypertrophy secondary to pulmonary hypertension is linked to rat chromosome 17: evaluation of cardiac ryanodine Ryr2 receptor as a candidate', *Circulation,* 103(3), pp. 442-7.

Zhao, Y. and Foegh, M. L. (1997) 'Angiopeptin, a somatostatin analogue, inhibits rat coronary artery and aorta smooth muscle cell proliferation induced by the thromboxane A2 mimetic U46619', *Prostaglandins,* 54(5), pp. 781-93.

Zhou, W., Blackwell, T. S., Goleniewska, K., O'Neal, J. F., Fitzgerald, G. A., Lucitt, M., Breyer, R. M. and Peebles, R. S., Jr. (2007) 'Prostaglandin I2 analogs inhibit Th1 and Th2 effector cytokine production by CD4 T cells', *J Leukoc Biol,* 81(3), pp. 809-17.

Zhu, H., Kavsak, P., Abdollah, S., Wrana, J. L. and Thomsen, G. H. (1999) 'A SMAD ubiquitin ligase targets the BMP pathway and affects embryonic pattern formation', *Nature,* 400(6745), pp. 687-93.

Zou, J., Maeder, M. L., Mali, P., Pruett-Miller, S. M., Thibodeau-Beganny, S., Chou, B. K., Chen, G., Ye, Z., Park, I. H., Daley, G. Q., Porteus, M. H., Joung, J. K. and Cheng, L. (2009) 'Gene targeting of a disease-related gene in human induced pluripotent stem and embryonic stem cells', *Cell Stem Cell,* 5(1), pp. 97-110.